

THESIS ON NATURAL AND EXACT SCIENCES B227

Human Tropomyosin-Related Kinase A and B: from Transcript Diversity to Novel Inhibitors

KRISTI LUBERG

TUT
PRESS

TALLINN UNIVERSITY OF TECHNOLOGY
Faculty of Science
Department of Gene Technology

This dissertation was accepted for the defence of the degree of Doctor of Philosophy in Gene Technology on December 19, 2016.

Supervisors: Professor Tõnis Timmusk, PhD

Department of Gene Technology, Tallinn University of
Technology, Estonia

Professor Mati Karelson, PhD

Department of Chemistry, Tallinn University of Technology,
Estonia

Opponents: Associate Professor Tomi Rantamäki, PhD

Department of Biosciences, University of Helsinki, Finland

Professor Aleksandr Žarkovski, MD, PhD

Institute of Biomedicine and Translational Medicine,
University of Tartu, Estonia

Defence of the thesis: March 17, 2017.

Declaration:

Hereby I declare that this doctoral thesis, my original investigation and achievement, submitted for the doctoral degree at Tallinn University of Technology has not been submitted for doctoral or equivalent academic degree.

/Kristi Luberg/

Copyright: Kristi Luberg, 2017

ISSN 1406-4723

ISBN 978-9949-83-075-6 (publication)

ISBN 978-9949-83-076-3 (PDF)

LOODUS- JA TÄPPISTEADUSED B227

**Inimese tropomüosiin-seoselised
kinaasid A ja B: transkriptide
mitmekesisusest uudsete inhibiitoriteni**

KRISTI LUBERG

CONTENTS

List of publications	7
Author's Contribution to the Publications	8
Introduction	9
Abbreviations.....	10
Review of the literature	12
1. Trk receptors	12
1.1. Physiological role of Trk receptors.....	13
1.2. Signalling of Trk receptors	14
1.3. Organization of human <i>TrkA</i> and <i>TrkB</i> genes.....	18
1.4. TrkA and TrkB protein isoforms' characteristics	20
1.4.1. TrkA.....	20
1.4.2. TrkB	20
1.5. Gene expression patterns in space and time.....	21
1.5.1. <i>TrkA</i>	21
1.5.2. <i>TrkB</i>	22
2. Role of Trk receptors in disease.....	23
2.1. Pain, injury and inflammatory diseases	23
2.2. Neurodegeneration.....	25
2.3. Epilepsy and excitotoxicity.....	27
2.4. Cancer	28
2.5. Depression	29
2.6. Schizophrenia.....	31
2.7. Drug addiction	31
2.8. Chagas disease	32
3. Potential medical implementations of Trk kinase modulators	32
3.1. Trk agonists.....	33
3.2. Trk inhibitors	34
Aims of the study.....	40

Materials and methods.....	41
Results and discussion	42
4. An update to <i>TrkA</i> and <i>TrkB</i> gene structures (publications I and II)	42
5. Expression pattern of <i>TrkA</i> and <i>TrkB</i> mRNAs in human tissue samples (publications I and II).....	43
6. Developmental regulation of the levels of <i>TrkB</i> transcripts and TrkB proteins in human PFC (publication I).....	45
7. Properties of N- or C-terminally truncated Trk proteins (publications I and II).....	47
8. Identification and analysis of novel potent and selective Trk inhibitors (publication III).....	48
Conclusions	50
References	51
Acknowledgements.....	86
Abstract.....	87
Kokkuvõte	88
Publication I.....	89
Publication II	115
Publication III	145
<i>Curriculum vitae</i>	177
Elulookirjeldus.....	179

LIST OF PUBLICATIONS

I. **Luberg, K.**, Wong, J., Weickert, C.S., and Timmusk, T. (2010). Human TrkB gene: novel alternative transcripts, protein isoforms and expression pattern in the prefrontal cerebral cortex during postnatal development. *J. Neurochem.* 113, 952–964.

II. **Luberg, K.***, Park, R.* , Aleksejeva, E.* , and Timmusk, T. (2015). Novel transcripts reveal a complex structure of the human TRKA gene and imply the presence of multiple protein isoforms. *BMC Neurosci.* 16, 78.

III. Tammiku-Taul, J.* , Park, R.* , Jaanson, K., **Luberg, K.**, Dobchev, D.A., Kananovich, D., Noole, A., Mandel, M., Kaasik, A., Lopp, M., Timmusk, T., and Karelson, M. (2016). Indole-like Trk receptor antagonists. *Eur. J. Med. Chem.* 121, 541–552.

* Authors contributed equally

AUTHOR'S CONTRIBUTION TO THE PUBLICATIONS

I The author performed the in silico analysis of *TrkB* gene structure and transcripts, made RT-PCR, RPA, immunocytochemical analysis and immunoprecipitation-western blot experiments. The author also participated in RT-qPCR analysis and wrote the manuscript.

II The author wrote the manuscript and participated in analysing *TrkA* gene structure and in performing 5'-RACE and RT-PCR analyses.

III The author participated in the characterization of luciferase reporter cell-lines, in performing cell culture experiments, in western blot following ANOVA analysis, in the interpretation of the kinase panel results, and in the writing of the manuscript.

INTRODUCTION

The tropomyosin-related kinase (Trk) family of transmembrane proteins acts as receptors to neurotrophins (NTs). Trks are tyrosine kinases that are the starting point of many intracellular signalling pathways. They have an important role in the developmental guidance of neurons and neurites, and the delivery of pro-survival signals to neurons, but their role extends beyond the limits of development and the nervous system. For example, Trks are needed for the development and function of some peripheral tissues, TrkA governs proper pain sensation and TrkB is crucial for the development of long-term potentiation (LTP), which is the molecular equivalent of memory. It is no surprise therefore, that there are many diseases where Trk signalling plays a role in the induction, pathophysiology and/or treatment: neurodegenerative and psychiatric diseases, cancer, etc. For this reason, a considerable amount of effort by the international scientific community has been dedicated to the development of Trk modulatory drugs. However, to correctly understand the role of Trk receptors in these conditions, it is important to discriminate between alternative protein isoforms, as they have very different properties and physiological roles, due to specific expression patterns and signalling abilities.

This study is dedicated to the characterization of human *TrkA* and *TrkB* genes, including the description of their expression pattern and alternative transcripts. Also, characterization of novel putative Trk protein isoforms is given. Finally, novel inhibitors of Trk kinases are described.

ABBREVIATIONS

5'-RACE – 5' rapid amplification of cDNA ends
A β – amyloid- β peptide
AD – Alzheimer's disease
Alk – anaplastic lymphoma kinase
APP – amyloid precursor protein
BDNF – brain-derived neurotrophic factor
CIPA – congenital insensitivity to pain with anhidrosis
CNS – central nervous system
DRG – dorsal root ganglia
E – embryonic day number
EGF – epidermal growth factor
EGFR – epidermal growth factor receptor
ERK – extracellular signal-regulated kinase
Flt-3 – Fms related tyrosine kinase 3
Frs2 – fibroblast growth factor receptor substrate 2
GABA – γ -aminobutyric acid
GPCR – G protein-coupled receptors
HD – Huntington's disease
HPA – Human Protein Atlas
HSAN – hereditary sensory and autonomic neuropathy
Ig – immunoglobulin
INSRR – insulin receptor related receptor
IRES – internal ribosome entry site
Jak2 – Janus kinase 2
KCC2 – K-Cl cotransporter
LRP1 – low-density lipoprotein receptor-related protein 1
LTP – long-term potentiation
MAPK – mitogen-activated protein kinase
MPP⁺ – 1-methyl-4-phenylpyridinium
MRI – magnetic resonance imaging
NAc – nucleus accumbens
NGF – nerve growth factor
NMDA – N-methyl-D-aspartate
NT – neurotrophin
Ntrk – neurotrophic receptor tyrosine kinase
Oct4 – octamer-binding transcription factor 4
P – postnatal day number 60
p75^{NTR} – p75 neurotrophin receptor
PACAP – pituitary adenylate cyclase-activating polypeptide
PD – Parkinson's disease
PFC – prefrontal cortex
PI3K – phosphoinositide-3-kinase
PKB – protein kinase B

PKC – protein kinase C
PLC γ – phospholipase C- γ
PNS – peripheral nervous system
PSD – postsynaptic densities
PTP – protein tyrosine phosphatase
Rho – Ras homolog
Ros1 – Ros proto-oncogene 1
RPA – ribonuclease protection assay
SH2D2A – SH2 domain containing 2A
Shc – SH2 domain containing adaptor protein
SorCS2 – sortilin related VPS10 domain containing receptor 2
Src – Src proto-oncogene
Trk – tropomyosin-related kinase
TrkB-FL – full-length TrkB
TRPV1 – transient receptor potential cation channel subfamily V member 1
uORF – upstream open reading frame
UTR – untranslated region
VTA – ventral-tegmental area

REVIEW OF THE LITERATURE

1. Trk receptors

The infinitely intricate and, fascinatingly, conscious human brain has taken up, among other tasks, the quest to uncover its own building blocks and working mechanisms. One of the conclusions of the work done in molecular neurobiology is that among a huge array of other factors, neurotrophins (NTs) and their receptors represent proteins that are indispensable for the proper functioning of the brain.

The name of NT receptors – tropomyosin-related kinase (Trk; also known as tropomyosin receptor kinase) – reflects their discovery. An oncogene from human colon carcinoma was found in 1986 by the research group of Mariano Barbacid that was given the name *trk* oncogene, because this product of a somatic rearrangement was a fusion protein comprised of an extracellular part of N-terminal portion of tropomyosin, and transmembrane and intracellular sequences of an unknown kinase (Martin-Zanca et al., 1986). Three years later, the same laboratory described *TrkA* gene, officially known now as neurotrophic receptor tyrosine kinase 1 (*Ntrk1*) and formerly known as *trk* proto-oncogene, that was the source of *trk* oncogene tyrosine kinase-encoding sequences (Martin-Zanca et al., 1989). Shortly after that, the same group also discovered *TrkB* and *TrkC* genes, based on high sequence similarity to *TrkA* (Klein et al., 1989; Lamballe et al., 1991). At the protein level, Trk receptors are indeed very similar, with approximately 70 % sequence similarity between TrkA and TrkB that reaches 88 % in their tyrosine kinase domain (Klein et al., 1989).

Trks are a small family of transmembrane kinases that act as receptors for NTs – target-derived neurotrophic factors, and are the main mediators of NT-induced pro-survival and pro-differentiation signals for neurons innervating those targets (Klein et al., 1993; Smeyne et al., 1994). TrkA interacts mainly with nerve growth factor (NGF), TrkB with both brain-derived neurotrophic factor (BDNF) and NT4, and TrkC with NT3 (Ip et al., 1992; Klein et al., 1991a, 1991b, 1992; Lamballe et al., 1991; Soppet et al., 1991). A weaker interaction also takes place between NT3 and receptors TrkA and TrkB (Lamballe et al., 1991). In addition, NTs also use a low affinity p75 NT receptor (p75^{NTR}) which, using a co-receptor sortilin, usually opposes Trk signals by inducing apoptosis and/or axon pruning (Lee et al., 2001; Nykjaer et al., 2004; Singh et al., 2008). p75^{NTR} binds all NTs with higher affinity in their pro-form, which contain an N-terminal sequence that is proteolytically removed from mature NTs.

Remarkably, the discovery of NGF by Rita Levi-Montalcini and Stanley Cohen preceded the one of its receptors by more than three decades as it was one of the first growth factors to be identified. By the time Trks were found, a vast array of knowledge was already available on NGF protein and its functions in developmental neurobiology, neuroscience in general and even in the immune system (Levi-Montalcini, 1987). The second NT to be discovered was BDNF, which was purified in 1982 (Barde et al., 1982).

The first report of *TrkB* gene also described the structure of TrkB receptor which is very similar to other Trks. Namely, these proteins are approximately 800 aa long and are embedded in membrane. The extracellularly located N-terminal half of Trks is heavily glycosylated. During translation, its terminus contains a signal sequence which is cleaved from the protein in the endoplasmic reticulum. A major part of the C-terminally located intracellular portion of Trk receptors is a tyrosine kinase domain that ignites many intracellular signalling pathways (Klein et al., 1989; Lamballe et al., 1991; Martin-Zanca et al., 1989; Middlemas et al., 1991).

Genes encoding NTs and their receptors are evolutionally old, their orthologues can be found in many invertebrates, including sea urchins and molluscs (Bothwell, 2006). A lot of experiments studying Trk proteins are done in rodents. Protein sequence identity between human and rodent Trk orthologues is above 90 % (Nakagawara et al., 1995). This notion validates many results of Trk studies obtained in rodents also for human Trks.

1.1. Physiological role of Trk receptors

As demonstrated by knock-out mice, both TrkA and TrkB are important for the proper functioning and viability of mammals. *TrkA* knock-out animals have defects in the peripheral nervous system (PNS), that are manifested by a severe neuron loss in dorsal root, trigeminal and sympathetic ganglia (Smeyne et al., 1994). Approximately half of these animals die during first weeks after birth and the remaining have self-inflicted injuries due to severe deficiencies in perceiving pain and extreme temperatures. Adult animals have additionally a serious reduction in cholinergic fibre projections in striatal and basal forebrain (Smeyne et al., 1994).

TrkB knock-out mice die within the first postnatal week due to sensory deficits that manifest among other abnormalities as inability to eat, and are attributable mostly to neuron depletion in nodose and petrosal ganglia, but there is also a reduction in the number of neurons in trigeminal, geniculate, vestibular and dorsal root ganglia (DRG), and among motor neurons (Klein et al., 1993; Silos-Santiago et al., 1997; and reviewed in Barbacid, 1994). Although there are no gross abnormalities in the central nervous system (CNS) of *TrkB* knock-outs, activation of TrkB receptor by BDNF is required for the postnatal survival and maintenance of many types of neurons, e.g. cortical and hippocampal neurons (Alcántara et al., 1997; Ghosh et al., 1994; Martínez et al., 1998; Silos-Santiago et al., 1997; Xu et al., 2000).

In addition to regulating cell survival, NT-Trk signalling is also needed for neuronal differentiation. This can be illustrated in many aspects. First, NTs have chemotactic ability to promote and steer whole neuron or neurite growth cone movement (Campanot, 1977; Paves and Saarma, 1997). This effect is dependent on Trk receptors (Ming et al., 1999). For example, BDNF derived from preganglionic neurons in the spinal cord activates TrkB signal during development in sympathetic ganglia cells to guide the dorsal migration of these

discrete ganglia from their primary location so that they would localize in a correct pattern along both sides of the spinal cord (Kasemeier-Kulesa et al., 2015). TrkB acts here as a sensor on the plasma membrane. Later, sympathetic neuron cell bodies remain immobile, but their axons' growth is guided by NGF produced at the target organ, and the axon tip grows in the direction of higher NT concentration in response to TrkA activation. This NGF-TrkA signal is also needed to avoid the apoptosis of these neurons. However, there is not enough NGF produced to sustain all neurons that have reached the target and only half survive after initial competition (reviewed in Barford et al., 2016).

Second, Trk receptors influence synapse development and function on many levels. For example, a postnatal TrkB knock-out in the mouse forebrain reduces the level of dendritic spines – the postsynaptic storehouses (von Bohlen und Halbach et al., 2006). Also, TrkB-null mice have impaired γ -aminobutyric acid (GABA)-mediated neurotransmission and abnormal intrinsic synchronous activity in their hippocampi (Carmona et al., 2006), normal TrkB expression is needed for proper muscle function as reduced levels of TrkB affect the structure and functioning of neuromuscular synapse (Kulakowski et al., 2011), and NGF-TrkA retrogradely controls synapse assembly between spinal cord and sympathetic ganglia (Sharma et al., 2010).

Furthermore, a huge body of evidence indicates a highly important role of BDNF-TrkB signalling in memory formation: hippocampus-dependent learning and long-term potentiation (LTP), which are accompanied by structural enlargement of the dendritic spine, are dependent on postsynaptic BDNF release and TrkB activation (Harward et al., 2016; Kovalchuk et al., 2002; Minichiello et al., 1999; Monteggia et al., 2004).

TrkB regulates the function of neurons also indirectly: in oligodendrocytes, it promotes proper myelination, guaranteeing a suitable environment for electrical impulse propagation in neurons (Wong et al., 2013a).

Additionally, Trk receptors have functions outside of the nervous system. For example, they affect vascularization, bone growth and the development and/or functioning of heart, kidney, lung and some types of immune cells (Coppola et al., 2004; Feng et al., 2015; García-Suárez et al., 2009; Hepburn et al., 2014; Hutchison, 2013; Kermani et al., 2005; Sariola et al., 1991; and reviewed in Bracci-Laudiero and De Stefano, 2016). BDNF-TrkB activity is even implicated in the development of high blood pressure after chronic intake of very salty food (Choe et al., 2015).

1.2. Signalling of Trk receptors

All functions of Trk receptors are dependent on their ability to ignite downstream signalling pathways. The high-affinity interaction between two Trk receptor molecules with one NT homodimer brings about receptor dimerization and subsequent trans-auto-phosphorylation of receptor's intracellular tyrosine residues (Jing et al., 1992). The latter serve as docking sites and triggers for downstream signalling cascades (Schlessinger and Ullrich, 1992). It has been

postulated that a simultaneous interaction between NGF and both TrkA and p75^{NTR} is needed to create high-affinity binding sites for NGF (Esposito et al., 2001). However, evidence in this direction is questionable and it has been hypothesized that Trk and p75^{NTR} interact indirectly through common downstream pathways (Wehrman et al., 2007). Recently, however, a novel model was proposed, which assumes that a dimer of NGF dimers is formed, establishing a protein complex consisting of two TrkA, two p75^{NTR} and four NGF molecules (Covaceuszach et al., 2015).

Interestingly, TrkA and TrkB can be activated in the absence of neurotrophins, for example by the neurosteroid dehydroepiandrosterone, or via G protein-coupled receptors (GPCR), such as the receptors of neuropeptide pituitary adenylate cyclase-activating polypeptide (PACAP), serotonin or adenosine (Kruk et al., 2013; Lazaridis et al., 2011; Lee and Chao, 2001; Lee et al., 2002). It has been proposed that this transactivation by GPCRs is non-specific to tyrosine kinases, and occurs via phospholipase C- γ (PLC γ) and reactive oxygen species (Kruk et al., 2013). TrkB is also activated by epidermal growth factor (EGF) via its receptor (EGFR), a process that regulates the migration of mouse embryonic cortical neurons (Puehringer et al., 2013). Other transactivating mechanisms of Trks are triggered by zinc ions and low-density lipoprotein receptor-related protein 1 (LRP1; Huang et al., 2008; Shi et al., 2009). These transactivation events are often mediated via a Src proto-oncogene (Src) kinase. However, the role of zinc as an agonist of Trk receptors has been disputed, because it does not activate TrkB receptor *in vivo* (Helgager et al., 2014).

The main pathways activated by Trks (Figure 1) are typical to receptor tyrosine kinases in general and involve monomeric GTPases Ras and Ras homolog (Rho), phosphoinositide-3-kinase (PI3K) and PLC γ (Sandhya et al., 2013). Two tyrosines outside the kinase domain of Trks are the major sites for incorporating downstream signalling molecules – phospho-Y496 (Trk numbering here is based on TrkA) binds adaptor proteins SH2 domain containing adaptor protein (Shc) and fibroblast growth factor receptor substrate 2 (Frs2), making it the initiating point for Ras and PI3K pathways; and phospho-Y791 binds PLC γ (Meakin et al., 1999; Obermeier et al., 1993).

The interplay of different signalling pathways starting from Trk receptors is elaborate, culminating in various outcomes. However, a simplified picture highlighting only a few important components of these processes is the following. PLC γ activates the inositol phospholipid signalling pathway leading to activated protein kinase C (PKC) and increased cytosolic Ca²⁺ concentration. This way, activity and/or expression of many proteins is controlled, guaranteeing e.g. BDNF-TrkB induced synaptic plasticity (Minichiello et al., 2002). Ras, on the other hand, is involved in relaying the NT signal to the nucleus to alter gene expression so that it would favour survival and neuronal differentiation, or non-neuronal proliferation. To do so, Ras activates the mitogen-activated protein kinase (MAPK, originally called ERK, extracellular signal-regulated kinase) cascade which in turn phosphorylates gene expression regulating proteins (Marshall, 1995; Meakin et al., 1999). Trk signal reaches Rho GTPases through

different proteins and leads to changes in the cytoskeleton, a requirement for neurite extension (Lai et al., 2012; Miyamoto et al., 2006; Nakamura et al., 2002). Finally, PI3K creates lipid docking sites for downstream signalling molecules, such as the protein kinase B (PKB, also known as Akt), thus transmitting cell survival and growth signals of NTs (Crowder and Freeman, 1998). These four signal pathways are not separate, however, and often function in concert by relaying signal from one to another (Sandhya et al., 2013).

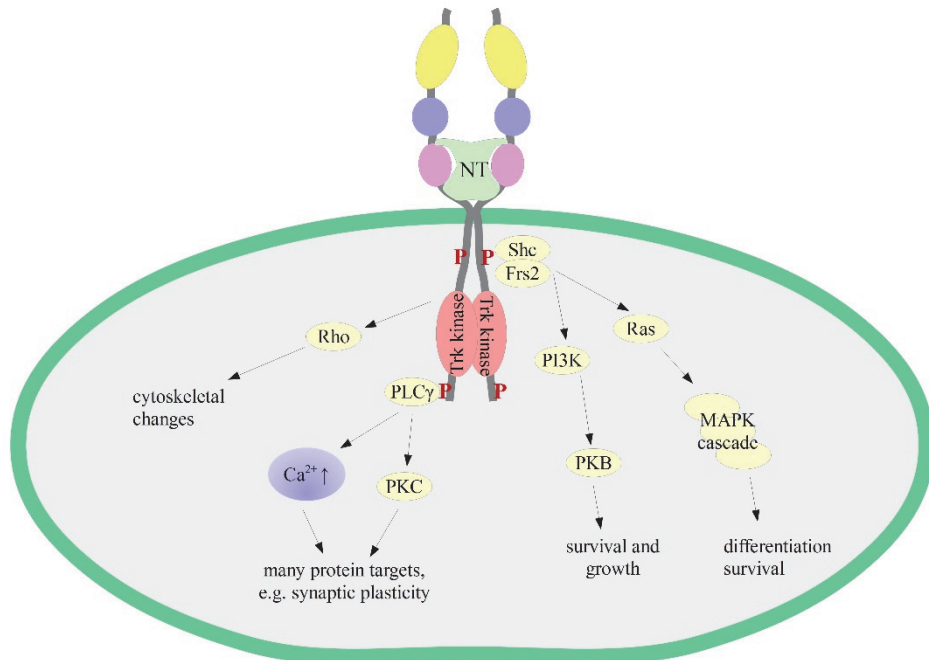


Figure 1. A simplified view of the signalling pathways initiated during the Trk-NT interaction. One neurotrophin dimer causes two Trk receptors to dimerise and transphosphorylate, creating docking sites for downstream signal transducers, which activate intracellular signalling pathways.

A crucial difference between TrkA and TrkB signalling was proposed by Yves-Alain Barde and co-workers. Namely, TrkA along with TrkC, but not TrkB are dependence receptors: in the absence of their ligand NTs, TrkA and TrkC transmits death signal via p75^{NTR} receptor (Nikoletopoulou et al., 2010).

Although this aspect of Trk biology is not very well studied, the kinases are unsurprisingly modulated by protein tyrosine phosphatases (PTPs). The PTPs that regulate either negatively or positively Trk-induced signalling are numerous, but one study found that a PTP named PTPN12 is the most important for regulating TrkB phosphorylation and, hence, signalling (Ambjørn et al., 2013).

The location of Trk receptors inside the cell is crucial for signal ignition and relay. Trk receptors are transported in an anterograde fashion from the cell soma

inside neurites using the help of sortilin (Vaegter et al., 2011). Even in the tips of neurites, Trks cannot be activated by NTs if the receptor is located in intracellular vesicles and is not accessible from the plasma membrane. This property is effectively used to regulate Trk signalling. For example, LTP induction is dependent on the insertion of TrkB into the postsynaptic densities (PSD) in response to neuron high-frequency stimulation. A sortilin related VPS10 domain containing receptor 2 (SorCS2) has been shown to be responsible for recruiting TrkB from intracellular stores into the activated synapse and thus guarantee its activation and signalling potential (Glerup et al., 2016).

The properties of the activated kinase are also dependent on intracellular logistics. It has been known already since the 1970s that NGF is internalized and retrogradely transported inside the axons to the cell soma in membranous vesicles (extensively reviewed in Thoenen and Barde, 1980). This effect was described in more detail during the last decade of the 20th century using compartmented chambers where axon terminals and cell bodies are grown in different conditions. Namely, for nuclear responses of NTs to take place, that is the induction of immediate-early genes, the NGF-TrkA or BDNF-TrkB receptor complex on the tips of neurites must be rapidly translocated to the cell soma inside an endosome along microtubules using retrograde vesicular transport (Riccio et al., 1997; Watson et al., 1999). In line with this finding, NGF-TrkA complexes and many associated downstream signalling proteins were detected in the retrograde trafficking of endosomes in DRG neurons (Delcroix et al., 2003). It is also known that dynein motor proteins are responsible for the relocation of endosomes containing activated Trk kinases (Heerssen et al., 2004). As an example of the importance of this process, one of the symptoms of Down syndrome – the loss of sympathetic neurons, takes place because of impaired endocytosis of TrkA (Patel et al., 2015).

TrkA endosomes of rat sympathetic neurons can escape lysosomal fusion and degradation for up to 25 hours (Suo et al., 2014). This feat is achieved via recycling of endocytic vesicles and is probably needed to guarantee a sufficiently long signalling in the cell soma. However, the regulation of Trk receptor activity also includes ubiquitination and proteolysis that is needed for proper protein levels and hence, a correct level of signalling from Trks (Arévalo et al., 2006; Geetha et al., 2005; Jadhav et al., 2008; Yu et al., 2014). In response to PKC activation and NGF treatment, TrkA is also subject to endoproteolysis that generates soluble ectodomain and membrane-bound kinase that is highly phosphorylated (Cabrera et al., 1996).

Trks also signal locally, for example, inside the synapse to directly modulate its activity. This can be achieved via changing the activity or localization of various receptors, channels and neurotransmitters (Blum et al., 2002; Melo et al., 2013; Narisawa-Saito et al., 2002).

Interestingly, TrkA endosomes are able to transition into retrograde-competent endosomes only if TrkA is bound to NGF, but not in the case of NT3. This is most probably because TrkA-NT3 complexes are more labile in the acidic environment of the early endosomes, restricting TrkA-NT3 signalling to synapses

(Harrington et al., 2011). It was uncovered recently that BDNF and NT4 also activate TrkB endocytosis differently: BDNF induces TrkB phosphorylation, ubiquitination and degradation more rapidly than NT4, while the latter guarantees a longer duration of TrkB signalling (Proenca et al., 2016).

1.3. Organization of human *TrkA* and *TrkB* genes

TrkA and *TrkB* genes are, at a first glance, very different – *TrkA* that is located on chromosome 1 spans 23 kb and has been described to contain 17 exons, while *TrkB* stretches to 350 kb on chromosome 9 and contains, according to a detailed investigation by Stoilov and co-workers, 24 exons (Nakagawara et al., 1995; Stoilov et al., 2002; Valent et al., 1997). The divergence in size is mainly attributable to large intron sizes in the case of *TrkB* (Nakagawara et al., 1995). Another difference between *TrkA* and *TrkB* lies in their 5' untranslated region (UTR) which is contained in the first exon of *TrkA*, but is produced using alternative initiation sites and splicing of exons 1-5 in the case of *TrkB* (Stoilov et al., 2002). This long 5' UTR has been shown to fold into an internal ribosome entry site (IRES) that provides cap-independent translation initiation (Dobson et al., 2005). Also, the 3' UTR of *TrkB* can reach a substantially greater length than *TrkA* 3' UTR (Klein et al., 1989).

Protein-coding exons of *TrkA* and *TrkB* are much more similar between the two genes (Figure 2). First, a signal sequence for membrane localization is encoded after translation initiation site in both *TrkA* and *TrkB* sequences (Klein et al., 1989; Martin-Zanca et al., 1989). Second, exons 1-5 of *TrkA* and 5-9 of *TrkB* encode three leucine-rich repeats flanked by cysteine-rich clusters and these amino acid residues together fold into a single physical domain (Wehrman et al., 2007). Third, the extracellular portion of Trks has additionally two more distinct domains, both of which are immunoglobulin (Ig)-like domains (Schneider and Schweiger, 1991). The first Ig-like domain is encoded by two separate exons and the second Ig-like domain by a single exon in the case of both *TrkA* and *TrkB* (Wehrman et al., 2007).

The biggest variation among protein-coding sequences between *TrkA* and *TrkB* is in the exons that encode the unstructured juxta-membrane parts of Trks, that is exons 9-12 of *TrkA* and 13-19 of *TrkB*. The transmembrane portion is encoded by exon 11 of *TrkA* and by exon 15 of *TrkB*. Exons 13-17 of *TrkA* and 20-24 of *TrkB* encode the tyrosine kinase domain (Klein et al., 1989; Martin-Zanca et al., 1989).

Alternative splicing has been described for human *TrkA* gene for cassette exon 9 that contains only 18 nucleotides, generating transcripts either without exon 9 that encode for TrkAI isoform, or transcripts with exon 9 from which TrkAII is translated (Barker et al., 1993). Additionally, TrkAIII isoform that was first found in neuroblastomas, is produced from transcripts where exons 6, 7 and 9 are spliced out (Tacconelli et al., 2004).

For human *TrkB*, a bigger variety of alternative transcripts is known: exons 13 and 17, which encode parts of juxta-membrane sequences, are cassette exons, and

exons 16 and 19 serve as alternative 3' exons generating TrkB-T1 and TrkB-T-Sch protein isoforms that lack the kinase domain (Hackett et al., 1998; Klein et al., 1990a; Middlemas et al., 1991; Stoilov et al., 2002).

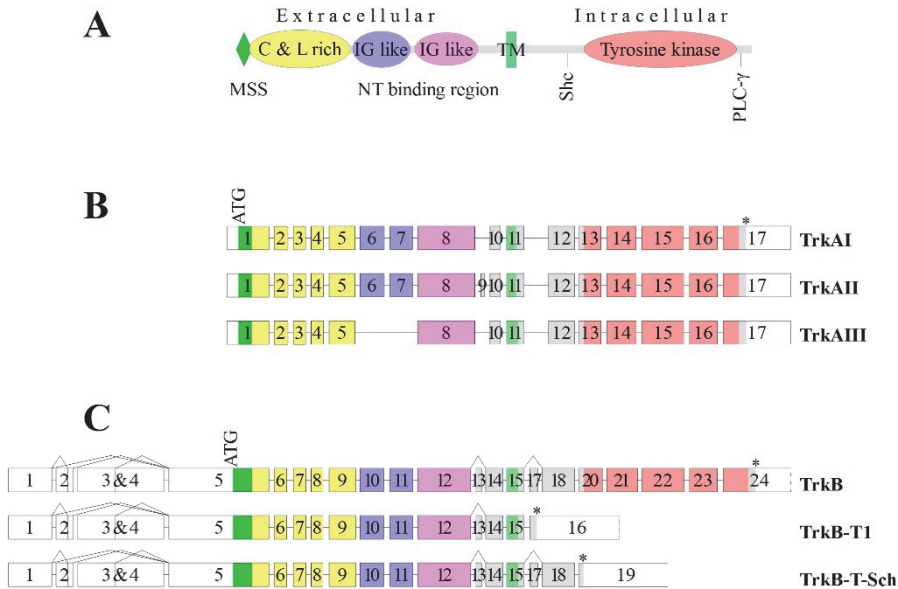


Figure 2. Simplified schematic representation of TrkA and TrkB receptor proteins, and transcripts of *TrkA* and *TrkB*. (A) a general structure of a Trk kinase. N-terminus is depicted on the left and C-terminus on the right. Shc and PLCγ binding sites are indicated. (B) and (C): known transcripts of *TrkA* (B) and *TrkB* (C). Boxes represent exons and are drawn to scale. Coloured boxes symbolize protein-encoding exons. Lines indicate possible junctions between exons. ATG – translation start-site; * - translation termination site; MSS – membrane signal sequence; C & L rich – cysteine and leucine rich sequence; IG like – immunoglobulin-like domain; TM – transmembrane.

TrkA mRNA has two in-frame AUG codons in the 3' part of exon 1, of which the second has been shown to be the main translation-initiation site, although the first can also be used (Martin-Zanca et al., 1989).

In other vertebrates, more alternative transcripts for both *TrkA* and *TrkB* have been described that encode alternative protein isoforms. This includes TrkB proteins that don't bind NTs, because they lack some or all of the leucine-rich repeats; deletions and insertions in the juxta-membrane region; and different truncated isoforms with unique intracellular tails (Garner et al., 1996; Middlemas et al., 1991; Ninkina et al., 1997). For *TrkA*, evidence of isoforms without some or all of the leucine-rich repeats in thymus has come from the detection of transcripts lacking exons 2-3 or 2-4 (Dubus et al., 2000). There is also one publication describing *TrkA* transcripts with 5' end inside exon 8 (Forrest et al., 2006).

As a side note, it can be mentioned that similarly to *TrkB* transcripts, *TrkC* mRNAs have been detected which encode receptors with or without the kinase

domain, but additionally some *TrkC* transcripts contain insertions in the region encoding the kinase domain (Lamballe et al., 1991; Tsoulfas et al., 1993; Valenzuela et al., 1993).

1.4. TrkA and TrkB protein isoforms' characteristics

The full-length TrkB (TrkB-FL), TrkAI and TrkAII have a calculated molecular weight of approximately 90 kDa, but due to glycosylation, the proteins are detected mainly in a fully-glycosylated 140...145 kDa form and, to a lesser extent, as partially-glycosylated 110 kDa protein (Klein et al., 1989; Martin-Zanca et al., 1989).

As a common property, both TrkA and TrkB isoforms which lack the extracellular juxta-membrane region encoded by exon 9 of *TrkA* and exon 13 of *TrkB*, namely TrkAI and TrkB Δ 13, are more specific for their main ligands – NGF or BDNF, and give weaker responses to NT3 and NT4 than the full-length receptors (Clary and Reichardt, 1994; Strohmaier et al., 1996). Thus, although the main ligand-binding region of Trk receptors is the second Ig-like domain, the proximally located juxta-membrane region also plays a role (Wiesmann et al., 1999).

1.4.1. TrkA

The lab of Andrew Reay Mackay in Italy discovered TrkAIII and it has been one of the few to study this protein isoform. Their results demonstrate some specific functionalities that Trk isoforms can have. TrkAIII, lacking the first Ig-like domain compared to TrkAI, has been shown to be incompletely glycosylated and is expressed on internal membranes – it is not transported to the plasma membrane, because it is continuously shuffled back from early Golgi network to the endoplasmic reticulum, where it starts to accumulate (Farina et al., 2009, 2015). TrkAIII is thus unable to bind NGF, but it is auto-activated and signals constitutively via PI3K but not via MAPK cascade, hence steering the cell away from differentiated phenotype and leading to tumorigenicity (Tacconelli et al., 2004).

Additional mechanisms contribute to TrkAIII-induced malignancy. TrkAIII is recruited to the centrosome, induces centrosome amplification and thus generates genetic instability (Farina et al., 2009). Furthermore, TrkAIII opposes mitochondrial free-radical mediated death in neuroblastomas (Ruggeri et al., 2014). In agreement with this, it has been shown that lab-generated TrkA mutants, which lack either one or both Ig-like domains, are prone to auto-activation and are tumorigenic in mouse models (Arevalo et al., 2000).

1.4.2. TrkB

TrkB isoform levels must be balanced to guarantee a normal number of cortical and hippocampal neurons – excess of TrkB-T1 induces apoptosis and

restoration of physiological levels of TrkB-T1 rescues neuronal cell numbers (Dorsey et al., 2006). On the other hand, TrkB-T1 knock-down animals have neurite abnormalities and shorter dendrites in amygdala, and show increased anxiety (Carim-Todd et al., 2009).

The exact mechanism of TrkB-T1 function has been a topic of hot discussion. For a long time it was believed that TrkB-T1 only serves as a dominant negative regulator of BDNF effects. This was because TrkB-T1 inhibits TrkB-FL dimerization, thus hindering the activation of downstream signalling cascades (Eide et al., 1996). Furthermore, TrkB-T1 expressed by non-neuronal cells reduces the ability of nearby neurons to grow neurites in response to BDNF (Fryer et al., 1997). This is probably due to BDNF sequestration by TrkB-T1, which is internalized after BDNF binding, and thus limits BDNF effects spatially by avoiding its diffusion (Biffo et al., 1995).

However, it was shown later that TrkB-T1 also has signalling properties. Namely, TrkB-T1 in glial cells is capable of initiating Ca^{2+} release from intracellular stores, and to modulate Rho activity to regulate cell morphology (Ohira et al., 2005; Rose et al., 2003). TrkB-T1 also induces neuronal dendrite elongation that is distinguishable from TrkB-FL-dependent neurite growth (Yacoubian and Lo, 2000). Furthermore, TrkB-T1 dictates cortical neural stem cells to become glial cells via activating an intracellular signalling pathway that includes PKC (Cheng et al., 2007).

TrkB-T1 has also been noted to regulate heart contraction force in a manner that is independent of the nervous system. TrkB-T1 is expressed in cardiomyocytes, and BDNF activates this receptor in an auto- or paracrine manner and induces Ca^{2+} signalling, leading to enhanced contraction force (Fulgenzi et al., 2015).

A fascinating example of the relevance of TrkB isoforms can be seen in the case of sexually dimorphic development of the mammary gland. More specifically, in response to testosterone, a shift occurs in the alternative splicing pattern of *TrkB* transcripts inside the sensory neurons innervating the developing mammary gland, leading to the production of TrkB-T1 proteins instead of TrkB kinases. This, in turn, results in axon pruning and termination of the mammary gland development in males as a response to the loss of innervation (Liu et al., 2012).

TrkB-T-Shc isoform is much less characterized, but it is known that it localizes to the plasma membrane, although it is not phosphorylated by TrkB-FL (Stoilov et al., 2002). Its precise function is unknown.

1.5. Gene expression patterns in space and time

1.5.1. *TrkA*

TrkA was first described in mice as a specific marker for some types of sensory ganglia, e.g. DRG and trigeminal ganglia (Martin-Zanca et al., 1990). *TrkA* is also expressed in high levels in sympathetic ganglia and in some parts of the CNS, namely in cholinergic neurons of the basal forebrain, and in caudate-putamen

(Holtzman et al., 1992; Schecterson and Bothwell, 1992). Some types of immune system cells also express *TrkA* (Ehrhard et al., 1993a, 1993b).

It was first described that *TrkA* expression in mouse coincides with major developmental processes of the nervous system, beginning at embryonic day number 9 (E9) and remaining stable after E13 (Martin-Zanca et al., 1990). It is believed that this expression is first needed in a brief window of time to guarantee the survival of neurons, and later to ensure proper pain functionalities. Interestingly, *TrkA* is expressed also much earlier in mouse embryos at blastocyst stage, although in human embryonic stem cells it is not (Moscatelli et al., 2009; Pyle et al., 2006). NGF stimulates the growth of mouse embryonic stem cell lines while retaining the expression of pluripotency markers, e.g. octamer-binding transcription factor 4 (Oct4) and Nanog (Moscatelli et al., 2009).

In the nervous tissue, mainly transcripts encoding TrkAII have been observed, and TrkAI-encoding transcripts have been detected in non-neuronal tissues, such as the kidney (Barker et al., 1993). TrkAIII mRNAs are produced in response to hypoxia in neuroblastoma cells and are also present in undifferentiated early neural progenitors, murine and human thymus and a subset of other neural crest-derived tumours (Tacconelli et al., 2004, 2007).

1.5.2. *TrkB*

TrkB has a higher and spatially wider expression in rodents than *TrkA*. In mouse, *TrkB* mRNA was first detected mostly in many regions of the central and peripheral nervous systems, but, to a lower level, also in lung, muscle, heart, kidney, testis and ovary (Klein et al., 1989). *TrkB* expression starts in mouse similarly to *TrkA* from E9, when the major events of the nervous system development take place (Klein et al., 1990b). However, these preliminary studies used riboprobes against *TrkB* mRNA regions that encode for the extracellular domain of TrkB, thus combining information of both the full-length and truncated receptors.

The same study that described the discovery of TrkB-T1 also made a first step in characterizing the variation in mouse TrkB-FL and TrkB-T1 transcripts' expression and concluded that the differences are major (Klein et al., 1990a). In many animal species, TrkB-FL-encoding mRNA expression is mainly limited to neurons, while TrkB-T1 mRNA is also expressed by non-neuronal cells (Biffo et al., 1995; Frisé et al., 1993; Ylikoski et al., 1993). It has been observed in human that transcripts encoding TrkB-FL and TrkB-T-Shc are primarily expressed in the brain, while *TrkB* mRNAs containing exon 16, from which TrkB-T1 is produced, are present at high levels at least in brain, pancreas, heart and kidney (Stoilov et al., 2002). In human brain, TrkB-FL-encoding transcripts are the most abundant in the cerebellum, the cerebral cortex and the hippocampus (Benisty et al., 1998; Romanczyk et al., 2002). *TrkB* transcripts without exon 13 have been detected in the human retinal pigmented epithelial cells (Hackett et al., 1998).

In rat, the expression of *TrkB* mRNAs encoding TrkB-FL peaks around birth and decreases with age in many brain regions, including the hippocampus and the

frontal cortex (Croll et al., 1998; Fryer et al., 1996). In contrast, TrkB-T1-encoding transcripts are more abundant in the brains of aged rats as compared to new-borns (Fryer et al., 1996; Silhol et al., 2005). TrkB expression pattern is more complex in humans. TrkB-FL mRNAs decrease after human neonatal period both in the hippocampus and in the temporal cortex, however, TrkB-T1-encoding transcripts are expressed at the same level throughout the lifespan in human temporal cortex and even decline in the hippocampus in higher age (Webster et al., 2006). Human prefrontal cortex (PFC) displays an additional pattern: TrkB-FL mRNA levels peak in early adulthood and decline in elderly, while no statistically significant changes in TrkB-T1-encoding transcripts were detected (Romanczyk et al., 2002). It is possible that the exceptionally late maturation of human PFC requires a delayed expression of TrkB-FL (Johnson et al., 2009).

The same tendency as described for rat mRNAs was seen for rat proteins: TrkB-FL is detectable in rat at E13 and its levels are the highest at or shortly after birth and decrease slowly with age, while TrkB-T1 increases continuously (Fryer et al., 1996; Fukumitsu et al., 1998; Silhol et al., 2005). Similarly, TrkB-FL levels peak during intermediate foetal period in most CNS regions of macaque monkey and stay relatively constant into adulthood, albeit TrkB-T1 levels reaching a maximum much later, in postnatal period (Ohira et al., 1999).

2. Role of Trk receptors in disease

Trk receptors regulate a vast array of physiological and anatomical functions in mammals, therefore, as can be expected, their dysregulation leads to multiple types of diseases. For example, the loss of one allele of either *BDNF* or *TrkB* leads to mental retardation, obesity and cognitive deficits (Gray et al., 2006; Yeo et al., 2004). This chapter should be taken as a list of examples, which names only some of the best known conditions that are connected to Trk expression and function, and is by no means exhaustive in its depth. The main emphasis here is on conditions where Trk agonist or antagonist implementation is currently considered and/or which accidental induction as a side-effect of Trk-modulatory compounds needs to be taken seriously into account before the start of the treatment.

2.1. Pain, injury and inflammatory diseases

NGF-TrkA and BDNF-TrkB activity modulates pain perception and inflammation in fascinatingly many ways that often intersect and, therefore, are here discussed together.

First, nociceptors depend on TrkA expression. Almost all nociceptors are lost in *TrkA* knock-out animals, leading to the lack of pain perception (Smeyne et al., 1994). Similarly, in human, different mutations in *TrkA* gene that affect the functioning or expression of TrkA cause congenital insensitivity to pain with anhidrosis (CIPA, also known as hereditary sensory and autonomic neuropathy type IV, HSAN4), which is an autosomal recessive disorder (Shaikh et al., 2016;

and reviewed in Indo, 2010). Unmyelinated and thinly myelinated peripheral nociceptive fibres, and eccrine sweat glands are lost in CIPA patients. These individuals have episodic fevers, are unable to sweat, fail to react to noxious stimuli, have self-mutilating behaviour and, typically, are intellectually disabled (reviewed in Indo, 2010). A closely related condition to HSAN4 is HSAN5, which is caused due to mutations in the *NGF* gene and has many common symptoms with HSAN4 (Yozu et al., 2016). Therefore, the ability to sense pain is crucially dependent on NGF-TrkA signalling.

Second, in response to injury or inflammation, many immune system cells are able to produce NGF (Leon et al., 1994; Lindholm et al., 1987; Shutov et al., 2016). In a murine model of asthma, NGF is upregulated in response to allergen challenge, and NGF in return leads to increased levels of IgE and interleukins 4 and 5, thereby augmenting the local inflammatory response (Braun et al., 1998). Also in human asthma patients, NGF levels are greatly increased (Bonini et al., 1996). Furthermore, allergen provocation in allergic asthma patients caused upregulation of all Trk receptors and the p75^{NTR} receptor in eosinophils from the lung but not in eosinophils from the peripheral blood – an effect which leads to an NT-dependent increase in the survival and activation of these allergy-promoting cells specifically in asthmatic lungs (Nassenstein et al., 2003).

Also, BDNF levels are increased in a mouse asthma model (Hahn et al., 2006). BDNF-TrkB activity has been noted to be involved in asthma by contributing to airway narrowing and limited airflow via promoting the proliferation of airway smooth muscles (Aravamudan et al., 2012).

NGF is also increased in inflamed skin, and in return contributes to inflammation (Donnerer et al., 1992). Thus, a vicious cycle of signal amplification is formed in inflammation: NGF can activate e.g. mast cells which start to produce pain mediators: serotonin, histamine and, again, NGF (Kawamoto et al., 2002). However, a contradictory result was found recently: NGF acting through TrkA reduces monocyte-mediated inflammation (Prencipe et al., 2014). Therefore, the role of NGF-TrkA in inflammation is most probably very complex.

Third, these elevated levels of NGF that are produced after injury or inflammation, also augment pain. Intradermal or intramuscular administration of NGF increases pain perception (Gerber et al., 2011; Rukwied et al., 2010). NGF-activated TrkA signals through PLC γ to induce nociceptor hypersensitivity by lowering the opening threshold of the cation channel named transient receptor potential cation channel subfamily V member 1 (TRPV1), that responds to mechanical, thermal and chemical stimuli (Chuang et al., 2001). TrkA signalling via different pathways enhances nociceptor firing also because it increases TRPV1 expression and enhances its trafficking to the plasma membrane, and up-regulates other genes that also lead to nociceptor sensitization (Ji et al., 2002; Kerr et al., 2001; Lindsay and Harmar, 1989; Stein et al., 2006).

Fourth, NGF-TrkA can induce nerve sprouting in cancerous tissue and thus, markedly increase cancer pain (Mantyh et al., 2010).

Fifth, BDNF-TrkB axis is also involved in some pathological pain states, for example, in neuropathic pain. This is a severe and debilitating chronic illness, where injury, pathology or infection have caused lesions to the somatosensory nervous system. Neuropathic pain is not simply a long-lasting acute pain warning the organism of potentially threatening circumstances, but rather a pathological condition with no benefits for survival. Neuropathic pain manifests because of a shift in inhibitory and excitatory control into and from the spinal cord leading to exaggerated and spontaneous pain that often doesn't respond to currently available treatments (reviewed in Beggs et al., 2012). Neuropathic pain arises because damaged nerves activate microglia, which start to secrete BDNF, among other factors (Inoue et al., 2007). BDNF from microglia activates TrkB in spinal lamina I neurons and this decreases the levels of K-Cl cotransporter KCC2, a process that causes an increase in intracellular Cl⁻ concentration and hence leads to weaker or even reversed GABA-elicited currents (Coull et al., 2003, 2005). In this way, signals that are normally inhibitory, are weaker or even become excitatory, causing aberrantly high pain perception. A similar mechanism is taking place in inflammation-induced pain (Zhang et al., 2008), because inflammation increases the levels of both BDNF and TrkB (Lin et al., 2011).

TrkB-T1 has also been implicated in the development of neuropathic pain. Specifically, after spinal cord injury, TrkB-T1 is upregulated and via modulating cell cycle pathways, it induces neuropathic pain (Wu et al., 2013).

2.2. Neurodegeneration

Taking into account that NT-Trk signalling contributes to the survival and maintenance of many types of neurons, it is only logical to assume that decreased strength of this signal would lead to reduced cellular viability. Indeed, dysregulation of Trks has been implicated in many types of neurodegeneration, of which Alzheimer's disease (AD), Huntington's disease (HD) and Parkinson's disease (PD) are here discussed in more detail.

The first of these, AD, is the most common form of dementia and has symptoms such as severe memory loss, changes in mood, confusion, motor problems and behavioural issues. Extensive loss of neurons and synapses is seen in cerebral cortex and some other brain regions in AD patients (reviewed in Bekris et al., 2010).

Cholinergic neurons form a dominant part of the forebrain circuitry involved in short-term memory and cognition, or more specifically – attention (reviewed in Everitt and Robbins, 1997; Parikh et al., 2007). NGF affects the survival, differentiation and function of cholinergic neurons (Hartikka and Hefti, 1988). TrkA, TrkB, TrkC and BDNF but not p75^{NTR} levels are significantly reduced in AD patients (Counts et al., 2004; Ginsberg et al., 2006; Peng et al., 2005). Additionally, suppression of TrkA in cholinergic neurons of rats simulates symptoms of AD: it leads to cognitive decline accompanied with a lower level of acetylcholine release, and decreased density of cholinergic processes in the cortex

of aged rats, even though the number and size of neurons is not affected (Parikh et al., 2013).

AD is a somewhat cryptic disease and it has turned out to be difficult to discriminate cause from effect. However, on the molecular level, two major types of changes are apparent: accumulation of extracellular amyloid- β peptides ($A\beta$) into amyloid plaques and increased level of intracellular tangles of tau protein. According to one popular view, extracellular $A\beta$ accumulation is the driving force of the development of AD (Jack Jr et al., 2010; McLean et al., 1999; Näslund J et al., 2000). Elevated levels of $A\beta$ and reduced signalling of BDNF through TrkB both impair hippocampal LTP and learning, mimicking some aspects of AD (Cleary et al., 2005; Korte et al., 1995; Minichiello et al., 1999; Patterson et al., 1996; Walsh et al., 2002). Furthermore, $A\beta$ oligomers decrease BDNF levels in human SH-SY5Y neuroblastoma cell line, decrease TrkB-FL and increase truncated TrkB levels, reduce the signal strength from TrkA and TrkB in response to their ligands, and hinder the retrograde transport of Trk-NT complex by disrupting the ubiquitination of Trk kinase (Garzon and Fahnstock, 2007; Kemppainen et al., 2012; Poon et al., 2011, 2013; Tong et al., 2004; Zheng et al., 2015). Also, BDNF was seen being accumulated around amyloid plaques, a process that can sequester BDNF and make it less accessible to TrkB (Rantamäki et al., 2013).

One of the competing hypotheses for AD inception is that the main culprit in this disease is abnormally elevated level of intracellular tangles of microtubule-associated protein tau (Gray et al., 1987). According to this view, a high level of intracellular tangles leads to a gradual disintegration of microtubules and, eventually, to the death of the affected cell (Goedert et al., 1991). Although BDNF levels are not changed in tau transgenic mice who have AD-like tau pathology (Burnouf et al., 2012), synaptic plasticity evoked by exogenous BDNF is lost in these animals (Burnouf et al., 2013). Apparently, tauopathy disturbs BDNF-TrkB signalling, because of excessive TrkB accumulation in the cell soma and in tau-affected dendrites (Mazzaro et al., 2016).

In conclusion, many aspects of AD still remain to be discovered, yet it is clear that functioning of Trk receptors is severely impaired in the development of AD. For this reason, Trk-agonistic treatment has been proposed for AD (Rafii et al., 2014). A recent finding supported this view from an interesting angle: apparently, NGF acting through TrkA reduces the cleavage of amyloid precursor protein (APP) and therefore, less $A\beta$ is formed (Triaca et al., 2016). These results also suggest that disruption of the NGF control over APP might be lost in AD, which could have a causative role in the pathogenesis of this disease.

Also in HD, a severe inherited neurodegenerative disorder with a major loss of striatal neurons, BDNF-TrkB signalling is attenuated. HD is a rare disease that is caused by a dominant mutation in the gene *Huntingtin* and first manifests as minor problems with mood and cognitive abilities. Later, coordination becomes increasingly more difficult, until speaking becomes impossible. Decline in mental abilities finally leads to dementia. No treatment for HD is available (reviewed in Roos, 2010). The levels of BDNF and TrkB protein have been reported to be

reduced in HD (Ginés et al., 2006; Zuccato et al., 2008). However, in the early stages of a mouse model of HD, BDNF and TrkB levels are not changed, albeit signalling of TrkB after BDNF treatment is compromised (Nguyen et al., 2016; Plotkin et al., 2014). In older HD mice and patients, TrkB expression is significantly reduced, accompanied with a marked increase in p75^{NTR} levels (Brito et al., 2013). This elevated p75^{NTR} expression has been reported to be responsible for counteracting TrkB signalling and for inhibiting synaptic potentiation in response to BDNF already in early stages of the disease in a mouse model (Plotkin et al., 2014). Nevertheless, a recent report stated that p75^{NTR} signals in early stages of HD to guarantee neuronal survival, and removing p75^{NTR} augments HD symptoms (Wehner et al., 2016). Problems with TrkB signalling in HD are also underlined with a finding that the mutated *Huntingtin* impairs TrkB retrograde transport, thus contributing to signal interference (Liot et al., 2013).

Neurodegeneration of the PD is also accompanied with reduced levels of BDNF mRNA and protein in substantia nigra (Howells et al., 2000; Mogi et al., 1999; Parain et al., 1999). The latter is the brain region producing dopamine where a massive cellular death occurs in PD. The symptoms of PD mainly include motor problems. In the beginning of the disease, slow, rigid and shaking movements can be observed, in the later stages, cognitive decline often follows. The cause of PD is unknown and there is no cure for this disease, even though there are medications that can relieve the symptoms to some degree (Jankovic, 2008). The neurons that degenerate in PD are dependent on BDNF for survival, furthermore, BDNF can counter dopaminergic cellular death induced by 1-methyl-4-phenylpyridinium (MPP+) – a chemical used to generate animal models of PD (Hyman et al., 1991).

2.3. Epilepsy and excitotoxicity

BDNF is upregulated in response to neuronal activity (Zafra et al., 1990). Therefore, it is no surprise that epileptic seizures drive BDNF upregulation. Indeed, after status epilepticus both BDNF levels and phosphorylated portion of TrkB protein are elevated (Danelon et al., 2016; Liu et al., 2013; Nawa et al., 1995). BDNF-TrkB signalling has been shown to be aggravating the effects of epilepsy (Heinrich et al., 2011; Scharfman et al., 2002). In agreement with this, a conditional knock-out of TrkB in mouse hippocampus hindered epileptogenesis, i.e. normal brain becoming epileptic, in a kindling model (He et al., 2004). Additionally, inhibiting TrkB kinase after status epilepticus prevented the development of epilepsy, reduced anxiety-like behaviour and avoided excessive cell death in the hippocampi of mice (Liu et al., 2013).

One possible mechanism by which BDNF-TrkB signalling augments epileptic activity is downregulating K⁺-Cl⁻ cotransporter KCC2 in the hippocampus, which manifests as a higher intracellular Cl⁻ concentration and leads to a reduced GABA-mediated neuronal inhibition potential (Rivera et al., 2002, 2004). Because this change in homeostasis puts neurons in a state where they are less

prone to inhibition, this might lead to the induction of excess neuronal activity and the establishment of epileptic status.

However, the involvement of BDNF-TrkB signalling in regulating epileptogenesis is complex, as some studies have also observed that elevating BDNF or TrkB-FL levels or downregulation of TrkB-T1 is protective against epileptogenesis and against the cell loss accompanying it (Kuramoto et al., 2011; Reibel et al., 2000; Vidaurre et al., 2012).

The latter effect is in accordance with recent findings about the fate of TrkB proteins in neurodegeneration due to excitotoxicity. Namely, based on in vitro experimental models, a number of papers have indicated that there might be a common mechanism by which TrkB-FL receptor is downregulated and TrkB-T1 upregulated in response to excitotoxicity occurring during brain ischemia, epileptiform discharges and A β accumulation (Danelon et al., 2016; Gomes et al., 2012; Jerónimo-Santos et al., 2014; Vidaurre et al., 2012; Xie et al., 2014). It is apparent from these studies that this happens because of two reasons. First, *TrkB* mRNAs encoding TrkB-FL receptors are downregulated and mRNAs encoding TrkB-T1 are upregulated. Second, TrkB-FL receptor is subject to calpain proteolysis in these disease states and the cleavage produces a membrane-bound ectodomain and intracellular soluble kinase domain.

Although some publications report that also in animal models of epilepsy TrkB-FL is downregulated after status epilepticus, others disagree and see no change in the levels of this receptor kinase (Unsain et al., 2008; versus Danzer et al., 2004). It is possible, that these discrepancies are due to the use of different types of epilepsy models, which impact neuronal viability in different degrees. Possibly, higher level of post-seizure cell death correlates with more pronounced decreases in TrkB-FL levels (Unsain et al., 2008).

2.4. Cancer

Abnormally high activity of Trk receptors has been shown to be involved in the progression and maintenance of multiple types of cancerous states, including neuroblastomas (Kaplan et al., 1993; Kogner et al., 1993; Nakagawara et al., 1993, 1994), breast (Davidson et al., 2003; Descamps et al., 1998, 2001), prostate (Djakiew et al., 1991) and pancreatic cancer (Sclabas et al., 2005). However, there is no simple correlation of the expression level of Trk proteins and outcome prognosis for cancer patients. For example, on the topic of breast cancer, some reports conclude that TrkA is correlated with a good prognosis while others have documented its high activity specifically in progressed and metastatic states (Davidson et al., 2003; Descamps et al., 2001). This contradiction may be in part due to different properties of alternative Trk isoforms – it has been shown in neuroblastoma-derived cells that while TrkAI signal is responsible for differentiation and growth arrest, TrkAIII promotes tumorigenic cell behaviour by rendering the kinase constitutively active and capable of signalling through the PI3K/PKB pathway, but not via the Ras/MAPK signal transduction cascade (Tacconelli et al., 2004). In case of Wilms' tumour, the expression of TrkB-FL is

associated with poor prognosis, but truncated isoforms lacking the kinase domain suggest a better outcome (reviewed in Thiele et al., 2009). This notion seems to agree with many other reports of different cancers, for the active kinase of TrkB seems to confer malignant and multidrug-resistant phenotype, as illustrated in the case of neuroblastomas (Matsumoto et al., 1995; Nakagawara et al., 1994), ovarian cancer (Yu et al., 2008), nasopharyngeal carcinoma (Li et al., 2014), etc. Nevertheless, there is a publication that announces the active role of TrkB-T1 in pancreatic cancer metastasis through a RhoA-activating manner (Li et al., 2009).

The crucial role of TrkB kinase in tumour development is underlined by two further aspects. First, its ability to suppress anoikis. This term refers to a type of programmed cell death, specifically to the one which extracellular matrix-detached cells undergo. Some cancer cells can resist anoikis and travel via lymphatic or blood vessels to other regions of the body where they can reattach and form metastases. It has been shown that TrkB is responsible for anoikis's suppression in at least some types of tumours with its kinase activity required for cell survival and therefore promotes the establishment of metastases (Douma et al., 2004; Geiger and Peeper, 2007; Yu et al., 2008). Second, the active kinase domain of TrkB stimulates neovascularization and angiogenesis (Hu et al., 2007; Kermani et al., 2005; Nakamura et al., 2006), processes essential for tumour and metastasis growth.

Oncogenic TrkA rearrangements have been observed in a small subset of lung cancer (Vaishnavi et al., 2013) and papillary thyroid tumours (reviewed in Pierotti et al., 1996). These rearrangements produce proteins with a constitutively active TrkA kinase domain. Indeed, TrkA was first characterized from human colon carcinomas as a fusion of its transmembrane and kinase domains to tropomyosin formed due to somatic rearrangement of the corresponding genes (Martin-Zanca et al., 1986). However, the percentage of tumours containing Trk-rearrangements is considered relatively low even in the abovementioned groups (reviewed in Thiele et al., 2009).

2.5. Depression

Major depressive disorder is a debilitating and life-threatening disease, which is a big public health problem with a high lifetime prevalence of 12-20 % in western countries (Jacobi et al., 2005). Although the true cause and developmental mechanisms of depression are unknown, it seems that neuronal connectivity problems might be to blame. Research has pinpointed the BDNF-TrkB signalling axis to be important in the development and especially in the treatment of depression, most probably due to modulation of neuronal plasticity (Castrén and Kojima, 2016; Rantamäki and Yalcin, 2016).

The conventional antidepressants used clinically promote the action of serotonin or noradrenaline in the brain. In response to antidepressant use, the levels of these monoamines rise rather quickly, however, the behavioural antidepressant effect typically comes only after weeks of treatment (Trivedi et al., 2006). For this reason, mechanisms downstream of monoamine

neurotransmission are thought to exhibit the main effect in fighting depression. One of the hypotheses in this field has been that the activation of TrkB signalling is responsible for the true antidepressant effect, presumably via increasing synaptic plasticity and/or affecting hippocampal neurogenesis. Evidence for this conclusion comes from studies which show that BDNF and TrkB levels in the serum, hippocampus and cortex of depressed patients are lower than in healthy control subjects, but rise to normal levels after antidepressant treatment (Chen et al., 2001; Gonul et al., 2005; and reviewed in Castrén and Kojima, 2016). Even though the role of TrkB signalling as a cause of depression is controversial, it seems to be imperative for antidepressant action. Namely, TrkB-T1 overexpression and full or partial knock-out of BDNF or TrkB does not seem to be affecting the depression-related behaviour in rodents, it is critically obstructing the function of antidepressants according to behavioural tests (Adachi et al., 2008; Li et al., 2008; Monteggia et al., 2004; Saarelainen et al., 2003). This effect is most probably caused by the induction of phosphorylation and activation of TrkB by antidepressants in animal models (Saarelainen et al., 2003).

All classes of antidepressants have been shown to increase the levels of both BDNF and TrkB mRNA (Nibuya et al., 1995). Antidepressants are also effective in preventing stress-induced reduction in BDNF levels (Castrén, 2014). In addition, all types of antidepressants have been shown to rapidly increase the level of TrkB phosphorylation and activation of the PLC γ signalling pathway. However, this effect has been shown to be independent of BDNF and monoamines (Rantamäki et al., 2007, 2011; Saarelainen et al., 2003). Which molecular route activates TrkB in response to conventional antidepressants is currently unclear.

Also, potential candidates for antidepressants increase TrkB activity (Ren et al., 2016). Recently, a lot of excitement has risen from the discovery that ketamine, a non-competitive N-methyl-D-aspartate (NMDA) receptor antagonist, triggers antidepressant effects rapidly, in only 2 hours, even in patients who have been unresponsive to conventional antidepressants (Berman et al., 2000; DiazGranados et al., 2010; Zarate et al., 2006). Ketamine rapidly increases the levels of BDNF and phosphorylation of TrkB in the hippocampus, and mice with conditional TrkB or inducible BDNF knock-out respond poorly to ketamine regarding the antidepressant effect (Autry et al., 2011).

Neuronal plasticity in the cortex and hippocampus evoked by TrkB signalling is offered as an explanation for the role of TrkB in antidepressant actions. This plasticity stimulated by antidepressants can be seen as enhanced neurogenesis in the dentate gyrus of hippocampus, promoted neurite growth and sprouting, changes in transcription of neuronal plasticity genes, and also elevated synaptogenesis and increased synaptic strength (reviewed in Castrén and Kojima, 2016; Rantamäki and Yalcin, 2016). Thus, antidepressants increase neuronal plasticity, which then leads to the rewiring of neuronal networks so that the physiological outcomes would fit better with the environment.

In accordance with these findings, a direct infusion of BDNF into hippocampus or posterior midbrain nuclei in rodents induces antidepressant-like

effect, mediated by TrkB (Shirayama et al., 2002; Siuciak et al., 1997). Also, it was recently discovered that a *TrkB* knockdown in dorsal raphe nucleus (a brainstem region that sends serotonergic input into the dentate gyrus of the hippocampus) removes antidepressant effect (Adachi et al., 2016). In contrast, opposite effects have been observed in the brain mesolimbic dopamine system, also known as the reward pathway that is composed of ventral-tegmental area (VTA) and nucleus accumbens (NAc). BDNF administration into VTA of rats resulted in a depressive behaviour, while blocking BDNF signalling by TrkB-T1 overexpression in NAc, the brain area which receives dopaminergic input from VTA induced antidepressant-like outcome (Eisch et al., 2003). Therefore, the result of the BDNF-TrkB signalling cascade on depressive behaviour seems to be dependent on a particular brain network.

As depression and anxiety are often co-occurring and antidepressants are effectively used in the management of anxiety, it is possible that the underlying molecular pathways are similar. Indeed, BDNF-TrkB signalling is also implicated in anxiety (Castrén, 2014).

2.6. Schizophrenia

Schizophrenia is a neurological disorder that usually manifests in late adolescence or early adulthood when psychosis, problems in cognition, perception and emotional responsiveness lead to disconnection from reality and disruptions in social behaviour (reviewed in Dimitrelis and Shankar, 2016).

As a clinical marker, peripheral BDNF levels are reduced in schizophrenia (Green et al., 2011). Also in the brain, both BDNF and TrkB levels are altered in this disease – for example, BDNF and TrkB-FL levels are reduced in the PFC, while TrkB-T1 and TrkB-Shc levels are increased (Weickert et al., 2003, 2005; Wong et al., 2013b). However, in some parts of the brain, rise in BDNF levels has been noticed (Pandya et al., 2013). The exact mechanism of action of schizophrenia is still unknown, and therefore also the role of BDNF-TrkB signalling is hard to pinpoint. Still, modern antipsychotic drugs restore BDNF levels, indicating a possibility that the shift in concentration of this important neural function modulator might be partly responsible for the development and sustenance of schizophrenia (Pandya et al., 2013).

2.7. Drug addiction

The stubbornly persistent effects of addiction that bring about careless behaviour can be seen as the implementation of a type of memory, and drugs that cause addiction do this by altering neuronal physiology in the brain (reviewed in Hyman, 2005). As can be expected based on BDNF-TrkB signalling's importance in LTP, shifts in this molecular pathway are among the mechanisms behind the changes in addiction pathology.

Levels of BDNF rise in the brain reward pathway after repeated cocaine administration in a time-dependent fashion due to the epigenetic changes of *bdnf*

promoters (Grimm et al., 2003; White et al., 2016) and lead to the activation of TrkB-mediated signalling (Graham et al., 2007). BDNF administered into VTA or NAc of rats enhances cocaine seeking after withdrawal, and BDNF produced in NAc is required for escalated cocaine self-administration (Graham et al., 2007; Lu et al., 2004). However, a different effect was observed if BDNF was administered into PFC, the brain region responsible for making decisions and assigning goals, which is therefore important in addiction-related behaviour (Hyman, 2005). In the PFC, BDNF suppressed cocaine seeking after withdrawal of the drug (Berglund et al., 2007). In agreement with this, the reduction of BDNF levels in the PFC leads to an increased demand for cocaine in rats who have been trained to self-administer the drug (Sadri-Vakili et al., 2010). Thus, the effect of BDNF on cocaine administration-dependent neuronal and behavioural plasticity vary depending on the brain region. Nevertheless, it seems that BDNF is responsible for changes in synaptic plasticity and diminished associative learning following cocaine administration in a mouse model (Zhong et al., 2015). Therefore, treating cocaine addiction with TrkB inhibitors has been proposed (Verheij et al., 2016).

Fascinating observations have come from epigenetic inheritance of cocaine addiction: male offspring of male rats who had been self-administering cocaine were less addicted to the drug when compared to control animals. This effect was shown to be mediated by histone acetylation in *bdnf* promoter regions in the neurons of PFC that decreased in response to TrkB inhibitor ANA-12 (Vassoler et al., 2013).

NT-Trk signalling effects have been noticed in the development of other addictions as well, e.g. alcohol and methamphetamine (Briones and Woods, 2013; Ren et al., 2015).

2.8. Chagas disease

Chagas disease is prevalent in Latin America and is caused by a protozoan *Trypanosoma cruzi*. Not only does the parasite use TrkA as a cell membrane receptor to enter neurons, epithelial or phagocytic cells, it additionally activates TrkA and its signalling pathways to promote host cell survival (Chuenkova and PereiraPerrin, 2004; de Melo-Jorge and PereiraPerrin, 2007). *T. cruzi* infects also cardiac fibroblasts via TrkA and triggers the production of NGF, rendering cardiac myocytes that express TrkA resistant to oxidative stress in a paracrine fashion (Aridgides et al., 2013).

3. Potential medical implementations of Trk kinase modulators

To summarise the previous paragraph, two types of diseases can be in theory targeted by Trk modulators. Trk agonists can be useful in cases where the cause of the disease lies in the reduced level of NTs or where additional activation of Trks can lead to alleviated symptoms, e.g. neural damage, neurodegeneration or depression. On the other hand, Trk antagonists or inhibitors are helpful in

conditions with excess Trk kinase activity. Examples can be seen in pain, inflammation or cancer.

NTs or artificial Trk agonists have been tested as therapeutics for AD, amyotrophic lateral sclerosis and neuropathies, although with poor results or limiting and negative side-effects (reviewed in Longo and Massa, 2013). Also in Rett syndrome, where extensive decrease in BDNF levels occurs, agonists of TrkB would give advantage to combating the symptoms (Chang et al., 2006).

On the top spot of promising Trk-inhibitor applications is their use in pain management. The prevalence of chronic pain is above 15 % and yet, many patients do not get relief of existing drugs due to low efficacy or serious side-effects, and have to suffer a great impairment to their quality of life (reviewed in McKelvey et al., 2013). For example, morphine use in chronic pain states is limited, because it causes both mechanical hypersensitivity (thus amplifying pain) and tolerance to morphine itself, in part due to augmenting the increase of BDNF expression following trauma in the spinal cord (Sahbaie et al., 2016). Therefore, novel pain remedies are badly needed. As a proof of principle, blocking NGF with antibodies or with TrkA extracellular portions has shown remarkable alleviation of irritant-caused pain in animal models (McMahon et al., 1995; Woolf et al., 1994).

The idea to use Trk inhibitors in cancer treatment is meaningful only in the context of personalized medicine, because overactive Trk signalling is implicated in only some types of tumours, and in some, Trk signalling may even give a favourable outcome.

In the case of neurodegeneration, depending on the specific disease, NT-treatment or the use of Trk agonists might not have the desired results. This is exemplified with HD, where processes downstream of TrkB activation are severely disturbed, leaving little room for the effect of TrkB activity modulation (Plotkin et al., 2014).

Drugs that adjust Trk activity need to pass a severe safety testing. Potential concerns that may arise include induction of pain and/or epilepsy, neurodegeneration, effects on mood and memory, improper reactions to injury, and problems with wound healing. In the case of Trk inhibition, not only effects of TrkA and TrkB have to be considered, but also pathways starting from TrkC, as almost all current candidates of commercial Trk inhibitors are nonselective among the Trk kinase family. While some of these potential side-effects can be overcome by limiting the chemical's bioavailability, e.g. restricting its access to the CNS, there might be some that we can only acknowledge.

3.1. Trk agonists

Clinical trials conducted for the treatment of different neuropathies with NTs were a big disappointment: biological responses failed to meet expectations, in part because NTs have a poor blood-brain-barrier penetration ability and extremely low half-life in serum (Poduslo and Curran, 1996; The BDNF Study

Group, 1999). In the case of NGF, a marked increase in pain perception was a major negative side-effect (Gerber et al., 2011; Rukwied et al., 2010).

Trk-activating antibodies have been a line of investigation and good results have been obtained in this field (Todd et al., 2014). Also, small synthetic peptides have been developed for Trk activation based on similarity to NT 3D structures (reviewed in Longo and Massa, 2013). Nevertheless, small peptides are not as active as NTs and Trk agonist antibodies, and all peptides have drawbacks in drug development, including bioavailability and stability.

A tempting approach for many laboratories both in big pharma and universities was for many years to generate low molecular weight chemicals that would activate Trk receptors. These compounds would be easier and cheaper to produce than activating antibodies. Indeed, there have been many papers reporting such compounds, e.g. 7,8-dihydroxyflavone, N-acetylserotonin and amitriptyline (Jang et al., 2009, 2010; Massa et al., 2010; Sompol et al., 2011; and thoroughly reviewed in Longo and Massa, 2013).

Sadly, experiments trying to reproduce the Trk-agonistic properties of these small molecules have failed (Todd et al., 2014, and my unpublished data). Even though 7,8-dihydroxyflavone has been shown in a vast number of in vivo studies as TrkB activator, most probably the phosphorylation of TrkB kinase induced by 7,8-dihydroxyflavone treatment in animal models is a secondary effect, which may be driven from 7,8-dihydroxyflavone's antioxidant activity (reviewed in Longo and Massa, 2013). At the moment it seems that maybe it is not possible to create allosteric changes for Trk kinase activation with low-molecular weight compounds, and that a true Trk agonist has to be bivalent and big enough to bind two receptor molecules to generate Trk trans-activation via proximity. Therefore, activating antibodies might be the best choice. A potential possibility is also to activate Trks via an indirect route – e.g. increasing the level of NT expression or modulating the activity of some other protein that would consequently activate Trk receptor without NTs.

Currently the safest method, however, to increase BDNF levels is physical exercise. Exercise gives thus many favourable outcomes of TrkB activation, for example, it offers antidepressant effects, improves memory, counters learning impairment induced by brain inflammation, and increases synaptic plasticity and recovery after spinal cord injury – all of that without the induction of negative side effects, such as pain or hyperreflexia (Bechara et al., 2014; Heyman et al., 2012; Kim et al., 2013; Ying et al., 2005; and reviewed in Weishaupt et al., 2012).

3.2. Trk inhibitors

Many anti-NGF monoclonal antibodies that neutralize NGF have been in clinical trials. As an example, one of them, Tanezumab by Pfizer, has shown alleviation of pain in all trials (Brown et al., 2012; Evans et al., 2011; Katz et al., 2011; Schnitzer et al., 2011). Adverse effects were also recorded in low incidence: 'abnormal sensation', e.g. paresthesia, was the most common type. However, some patients in a phase III clinical trial for the management of

osteoarthritis-related pain developed progressively worse osteoarthritis following Tanezumab administration (Brown et al., 2012). For this reason, these clinical trials were temporarily halted. There is also an anti-TrkA antibody currently in clinical trials for the treatment of pain (Khan and Smith, 2015).

Additionally, there are peptide mimetics of NT surface motifs that bind Trk receptors without induction of kinase activation, and thus disrupt the interaction between NT and Trk receptor. An example of these is cyclotraxin-b that is an antagonist of BDNF that inhibits TrkB in very low nanomolar concentrations (Cazorla et al., 2010).

Small molecules of NT antagonists have also been generated. Examples are depicted on Figure 3 and are named ALE-0540 and ANA-12 (Cazorla et al., 2011; Owolabi et al., 1999). These NT antagonists are highly specific and therefore, especially ANA-12 has been used widely as a proof of principle tool to study the effects of TrkB inhibition under different conditions. For example, ANA-12 treatment has shown moderate effects in preventing morphine-induced hyperalgesia and analgesic tolerance (Sahbaie et al., 2016). However, as the extracellular domains of Trks and NTs themselves are not very well druggable, i.e. the protein surface is relatively “flat”, a high dose reaching micromolar concentrations of such molecules is needed to achieve the inhibitory effect (Buchwald, 2010). Negative side-effects are a big concern at these concentrations when considering medical applications.

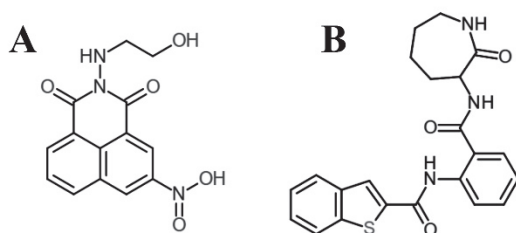


Figure 3. Chemical structures of small molecules that antagonize the NT-Trk interaction. (A) NGF antagonist ALE-0540 and (B) BDNF antagonist ANA-12.

An alternative effective strategy is to inhibit the Trk enzyme directly by blocking the binding of ATP via targeting deep “clefts” or “pockets” within the kinase domain that lie at or near the ATP-binding site. The druggability of these sites is extremely good from both steric and kinase-modulatory aspects. Therefore it is relatively easy to find and design compounds that bind into this region and inhibit Trk enzymatic activity, but developing inhibitors that are selective for a given kinase is more difficult, because this region is conserved among kinases. This is important, as a wider field of protein targets leads potentially to more numerous and severe side-effects.

In laboratory practice, a natural alkaloid K252a (Figure 4A) was used widely for some time with many scientific studies using this as a Trk-specific inhibitor. However, this assumption was false, as K252a has an extremely broad selection of target kinases (Gao et al., 2013; Martin et al., 2011). Based on similarity to K252a and a related natural compound, staurosporine, Cephalon designed

chemicals CEP-751 and CEP-701, a.k.a. lestaurtinib (Figure 4B). Lestaurtinib has shown promising results in preclinical studies and for this reason it has been tested in clinical trials as anticancer agent, but similarly to K252a, it is a multikinase inhibitor targeting e.g. Janus kinase 2 (Jak2) and Fms related tyrosine kinase 3 (Flt-3) in addition to Trks (Minturn et al., 2011; Wang et al., 2009). Possibly, the wide target field of lestaurtinib is responsible for the disappointing results of these trials, although a mechanism of drug tolerance in tumour cells has also been proposed, that relies on the signal induction from CD44 glycoprotein by NGF-bound Trk in the absence of Trk kinase activity, contributing to tumour aggressiveness (Aubert et al., 2015; Hexner et al., 2014).

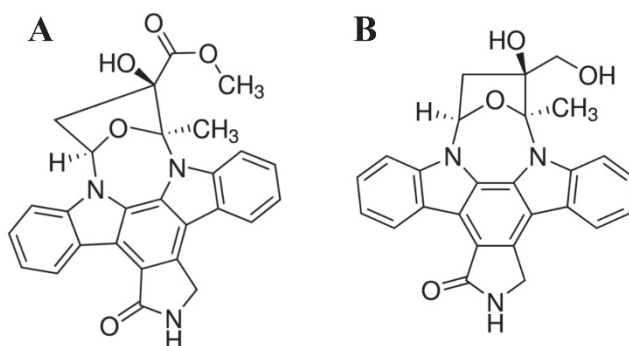


Figure 4. Representations of K252a and lestaurtinib chemical structures. (A) K252a and (B) lestaurtinib (CEP-701).

Creabilis has tested a Trk inhibitor CT327 topical applications in clinical trials to treat chronic pruritus in psoriasis and atopic dermatitis (McCarthy and Walker, 2014). The results have not completely met expectations (Roblin et al., 2015). Although the chemical structure of CT327 has not been reported, based on patents filed it can be assumed that CT327 is a derivative of K252a (Traversa et al., 2014). The selectivity of CT327 is also not reported, but it is likely that this compound is, similarly to K252a, capable of inhibiting a rather wide array of tyrosine kinases. Overall though, Trk kinase inhibitor design has developed in the direction of increasing selectivity and the following discussion describes mainly compounds for which good selectivity data is available.

In recent years, a new player named entrectinib (Figure 5A) has entered clinical trials as anticancer compound of Ignyta because it has shown low nanomolar inhibitory activity against Trks, Ros proto-oncogene 1 (Ros1) and anaplastic lymphoma kinase (Alk) in preclinical studies (Rolfo et al., 2015). The drug has given promising results and is relatively well tolerated. The main adverse effects were temporary cognitive impairment and fatigue (Passiglia et al., 2016). Entrectinib is currently in phase II trials. Entrectinib enters the CNS and was therefore able to reduce metastases from the brain of a patient (Rolfo et al., 2015). Resistance to entrectinib has emerged in clinical trials of a patient whose colorectal tumour cells acquired two point mutations in *TrkA* gene (Russo et al., 2016).

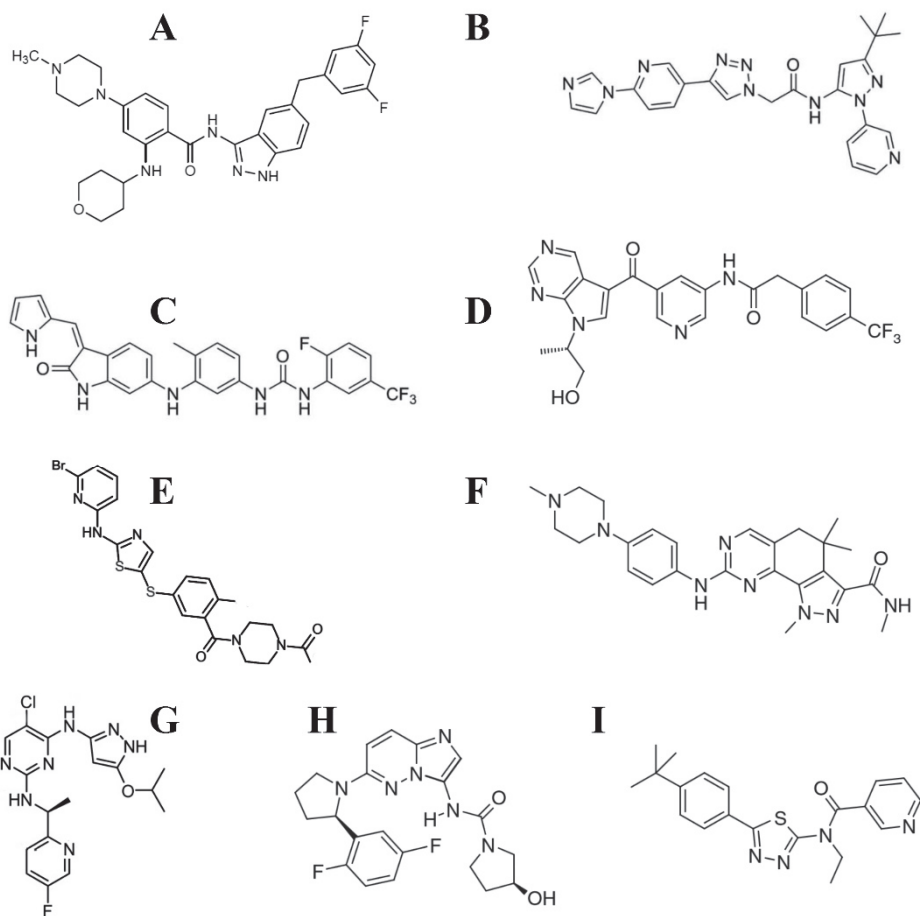


Figure 5. 2D chemical structures of a selection of relatively Trk-selective potent tyrosine kinase inhibitors. (A) entrectinib from Ignyta, (B) a Merck's triazole compound, (C) GNF-5835 from Novartis, (D) Pfizer's compound 9, (E) Bristol-Myers Squibb's compound 20h, (F) PHA-848125AC by Nerviano Medical Sciences, (G) AZ-23 from AstraZeneca, (H) Array Biopharma's ARRY-470, and (I) ADDN-1351 from Buck Institute for Research on Aging.

Other companies have also been developing Trk inhibitors for potential anti-pain or anti-cancer treatment. For example, a triazole compound from Merck (Figure 5B) inhibits TrkA in low nanomolar concentration and is Trk-selective (Stachel et al., 2014); an oxindole GNF-5835 derivative (Figure 5C) and imidazopyridazines by Novartis were validated in xenograft models as Trk-selective inhibitors (Albaugh et al., 2012; Choi et al., 2015). Pfizer has filed many patents claiming that e.g. pyrrolopyrimidine derivatives are potent TrkA inhibitors. One of these compounds also reached clinical trials, where side-effects from CNS penetration were obvious, commencing lead optimization to increase active efflux from the brain and leading to the creation of Compound 9 that is

depicted on Figure 5D (McCarthy and Walker, 2014). Bristol-Myers Squibb has conducted the development of Trk inhibitors for quite a while with good results, e.g. an aminothiazole-based compound 20h (Figure 5E) blocks TrkA in 1 nM concentration (Kim et al., 2008; McCarthy and Walker, 2014; Wang et al., 2009). Nerviano Medical Sciences has patented a compound named PHA-848125AC (Figure 5F), that has been tested in phase I clinical trials for treating patients who have advanced solid malignancies (Weiss et al., 2012). AstraZeneca has developed mainly pyrazolopyrimidines as Trk inhibitors (Wang et al., 2009). One of these, a compound named AZ-23 (Figure 5G), is a potent and selective Trk inhibitor that has been tested preclinically in a Trk-expressing xenograft tumour model (Thress et al., 2009). However, a phase I clinical trial with AZ-23 was halted due to poor pharmacodynamics (Thiele et al., 2009). Recently, a novel aminopyrazole from AstraZeneca named AZD6918 was tested in neuroblastoma xenograft models (Li et al., 2015).

Array Biopharma has been developing Trk inhibitors with good results: e.g. a compound named ARRY-470 (Figure 5H) has effectively attenuated bone cancer pain and reduced abnormal nerve sprouting in a mouse model because it inhibits selectively Trk kinases in low nanomolar concentration (Ghilardi et al., 2010). The hydrogen sulfate salt of ARRY-470 is named LOXO-101 and it produced a rapid tumor regression in a patient of a phase I clinical trial who had a *LMNA-TrkA* gene fusion (Doebele et al., 2015). LOXO-101 is relatively well tolerated, with the most common side-effects being fatigue, anemia, nausea and dizziness (Passiglia et al., 2016). Interestingly, Array seems to be the only company or institution currently developing allosteric TrkA kinase inhibitors, which bind to a site on the kinase domain further from the ATP pocket, being thus highly selective even among the Trk family of kinases. Of these compounds, AR786 is highly TrkA-selective and has shown promising results in preclinical models of arthritic pain and inflammation by alleviating the symptoms after oral dosing (Ashraf et al., 2016; Nwosu et al., 2016). Array is not very keen on reporting publicly the specific structures of their Trk inhibitors or binding sites on the protein, but from the patents it has filed, it can be concluded that the allosteric Trk inhibitors belong to a class of pyrrolidinyl(thio)ureas that is represented in Figure 6 (McCarthy and Walker, 2014).

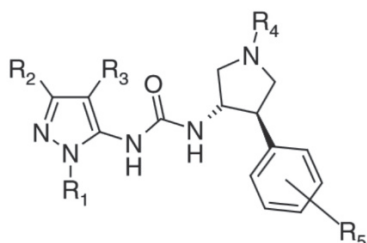


Figure 6. Markush structure of patented chemicals by Array Biopharma. This group represents the most probable candidate for allosteric TrkA inhibitors.

Quite surprisingly, Buck Institute for Research on Aging claims that some of the compounds they are developing are effective against AD because these are inhibitors of TrkA (Zhang et al., 2014). This is not in agreement with most of the research on AD, according to which active TrkA is protective against AD (see above, paragraph 2.2 Neurodegeneration). These compounds belong to the group of thiadiazoles and a representative, ADDN-1351 (Figure 5I) inhibits TrkA in very high nanomolar concentrations (McCarthy and Walker, 2014).

There are many more compounds that have been reported of being Trk inhibitors, but there is not much information available on these compounds. With some, selectivity data or even chemical structure has not been presented.

In conclusion, recent years have seen a fast increase in the development of Trk inhibitors with many clinical studies under way. The potential benefit of these drugs is huge, although many potential adverse effects have to be taken under strict consideration.

AIMS OF THE STUDY

The main focus of this thesis is on *TrkA* and *TrkB* genes and the proteins encoded by them: TrkA and TrkB. Specifically, the aims were set as follows:

- 1) to characterize different *TrkA* and *TrkB* transcripts and their expression patterns in human tissue samples,
- 2) to characterize putative Trk protein isoforms, which are predicted based on transcriptome analysis,
- 3) to identify novel Trk kinase inhibitors.

MATERIALS AND METHODS

Computer analysis and RT-PCR – publications I and II

Quantitative PCR – publication I

Western blotting – publications I, II and III

Ribonuclease protection assay (RPA) – publication I

Cloning of DNA plasmids – publications I and II

Immunofluorescence and confocal microscopy – publications I and II

Immunoprecipitation – publication I

5' rapid amplification of cDNA ends (5'-RACE) – publication II

Live imaging microscopy – publication II

Determination of IC₅₀ of compounds in cellular context – publication III

Cell viability assessment – publication III

RESULTS AND DISCUSSION

4. An update to *TrkA* and *TrkB* gene structures (publications I and II)

By 2007, when we first started this project, the gene structures, main exons and a few alternative transcripts of both *TrkA* and *TrkB* were already known for some time (Barker et al., 1993; Stoilov et al., 2002; Tacconelli et al., 2004). However, a preliminary examination of the information available in public databases indicated that this picture was not complete, because many ESTs containing thus far undescribed exon sequences or splicing patterns had been annotated. For this reason, the first part of my study and therefore, also of this thesis, is dedicated to the characterization of *TrkA* and *TrkB* transcripts, their expression patterns in different human tissues, and thus, a better understanding of these genes and their regulation can also be obtained.

Analysis of ESTs that map into *TrkA* and also our results of 5'-RACE analysis of this gene revealed that *TrkA* is intricately more complex than previously thought (publication II). Firstly, the gene has at least 7 alternative and mutually exclusive 5' exons and, in addition to the conventional transcription initiation exon, exon 1, these can be considered in three groups:

- 1) exon A that lies approximately 45 kb upstream of exon 1;
- 2) exons E and G that are located close to exon 1 (in a range of a few kb up- or downstream of exon 1);
- 3) exons 8b, 8c, 10a, and 11a in a 1 kb region that maps between the 5' ends of exon 8 and 11.

Therefore, secondly, due to the existence of numerous exons upstream of exon 1, *TrkA* gene length is almost three times larger than was previously considered (67 kb instead of 23 kb), it contains multiple promoters and engulfs another gene, insulin receptor related receptor (*INSRR*), which is transcribed in the opposite direction from *TrkA*. Of note, *INSRR* encodes another receptor tyrosine kinase, which was for a long time considered an orphan receptor with unknown function. Recently it was discovered that it senses pH and helps to regulate acid-base balance (Petrenko et al., 2013). *TrkA* also partially overlaps one more gene, namely SH2 domain containing 2A (*SH2D2A*), which is in a head-to-head orientation with *TrkA*: exon A of *TrkA* lies within the second intron of *SH2D2A* gene. Although the relative physical localization of these three genes on the chromosome is the same in human as compared to mouse and rat, we did not find any evidence of *TrkA* exon A in either of these rodents despite our efforts.

We also discovered that the splicing pattern of *TrkA* exons 2-9 is highly elaborate, generating a vast array of different transcripts. We did not observe any alternative splicing among exons 11-17 or any use of different polyadenylation signals, although the potential existence of alternative 3' exons of *TrkA* cannot be ruled out, because we did not specifically look for these.

For *TrkB* we performed bioinformatic analysis of ESTs that map into the gene. We didn't perform 5'-RACE for *TrkB*, because Stoilov and co-workers had

already made a similar analysis (Stoilov et al., 2002). We discovered that the splicing pattern among *TrkB* 5'-UTR exons is more intricate than previously thought (publication I). Furthermore, a novel 5' exon, exon 5c, was identified in the databases. It lies 1 kb downstream of exon 5. *TrkB* exons 12 and 22 turned out to be cassette exons, because in rare occasions these can be spliced out. Even though transcripts where exon 13 is spliced out have been described (Hackett et al., 1998), we did not observe such mRNAs. Lastly, exon 22 can be extended in the 3' direction and serve as an alternative 3' exon.

Thus, the structures of *TrkA* and *TrkB* genes and their splicing patterns are highly different, although they encode very similar kinases. First, *TrkB* gene is more than 5 times larger than *TrkA* (350 kb versus 67 kb, respectively). Second, the variability of 5' UTR regions arises mainly from the use of alternative splicing in the case of *TrkB*, while for *TrkA* alternative 5' exon usage from many distant regions on the chromosome also plays an important role. Third, the production of isoform diversity is achieved mainly by the use of multiple alternative 3' exons in the case of *TrkB*, while *TrkA* appears to have only one single 3' exon. Fourth, the elaborate alternative splicing pattern of human *TrkA* exons encoding the receptor's extracellular domain is not paralleled in *TrkB* mRNAs. Therefore, *TrkB* isoforms differ from each other mainly C-terminally, while *TrkA* isoforms have alternative extracellular domains and potentially also different N-termini.

5. Expression pattern of *TrkA* and *TrkB* mRNAs in human tissue samples (publications I and II)

We noticed very specific expression patterns for many of the novel exons of *TrkA* among different human tissue samples (publication II). However, the physiological relevance behind these differences is hard to predict, as many of these alternative forms encode multiple upstream open reading frames (uORFs) in addition to the main ORF and it is difficult to pinpoint which of these, if any, are translated into functional proteins. The same problem arises in interpreting the results which indicate multiple forms of alternative splicing among exons 2-8, which often interrupts the ORF.

We confirmed the predominantly neural-tissue specific expression of human *TrkA* transcripts with exon 9, while other tissues had *TrkA* mRNAs where this exon is spliced out, as has already been shown before (Barker et al., 1993). It has been postulated previously that TrkAI which is translated from mRNAs without exon 9, is as effective in binding NGF as is TrkAII (the full-length receptor), however, TrkAI is less sensitive to NT3 (Clary and Reichardt, 1994). It can be hypothesized that in peripheral tissues, NT3 binding is less important for *TrkA* functions than in the brain. Interestingly, even though the same expression pattern of TrkAI- and TrkAII-encoding mRNAs was detected in rat, we observed a different pattern in mouse, where all tested samples from both peripheral tissues and the CNS had *TrkA* transcripts that predominantly contained exon 9.

As can be expected from their chromosomal location relative to each other, *TrkA* and *INSRR* expression is highly synchronized in rat (Reinhardt et al., 1994).

These two genes do not overlap in rat (publication II), but their transcriptional start-sites are in close proximity and therefore, these genes might share a common bidirectional promoter. In human, there is additionally a partial overlap of *TrkA* exon D and the coding region of *INSRR* gene, therefore some mutual expression inhibition via RNA interference can occur. Nevertheless, it seems that these two genes share a common expression pattern in human as well: for example, both are expressed at relatively high levels in kidney and thymus, while in many other regions of the body their expression level is very low (publication II and Mathi et al., 1995). These findings are confirmed by modern RNA sequencing studies, for example the Human Protein Atlas (HPA) transcriptome data (Fagerberg et al., 2014). It is an interesting and unanswered question whether the simultaneous expression of *TrkA* and *INSRR* kinases that have such different functions is always needed or if at least in some tissues and under some conditions this happens as superfluous expression. HPA RNA sequencing data indicates that the expression pattern of *SH2D2A* gene, which overlaps only with a minor number of *TrkA* transcripts and is further away from the rest of *TrkA* exons, is more different from both *TrkA* and *INSRR*.

For *TrkB* transcripts, we confirmed previous findings that transcripts encoding TrkB-FL and TrkB-T-Shc (with exons 24 and 19, respectively) are mainly expressed in the nervous system and TrkB-T1-encoding mRNAs (with exon 16) have a ubiquitous expression pattern (publication I and Stoilov et al., 2002). The novel 5' exon 5c and 3' exon variant 22b were also mainly detected in neural samples, with the highest expression seen for both in the cerebellum. However, based on RPA, *TrkB* transcripts with exons 5c and 22b are expressed in minute amounts. The same is true for transcripts where exons 12 or 22 are spliced out. In contrast, the cassette exon 17 is included in *TrkB* transcripts with a 50 % probability, a result that is in agreement with previous findings (Stoilov et al., 2002).

It has been known before that there is a very complex splicing pattern among *TrkB* 5' exons that form an IRES (Dobson et al., 2005; Stoilov et al., 2002). It has also been shown that the translation of dendritically localized mRNAs is, in addition to cap-dependent initiation, induced via IRES (Pinkstaff et al., 2001). The advantages of having an IRES are not completely understood, but it might increase translation efficiency specifically in neurites as compared to soma (Pinkstaff et al., 2001). For *TrkB* mRNAs, Dobson and co-workers demonstrated that some regions of the 5' UTR can augment while others promote the translational capacity of *TrkB* mRNAs (Dobson et al., 2005). Considering all this, we hypothesised that alternative splicing in this region could account for the distinct regulation of *TrkB* expression in different tissues. However, the expression pattern among *TrkB* exons 1-5 was essentially the same in all tissue samples studied (publication II), indicating that this mechanism is probably not used to regulate the level of TrkB proteins in different tissues. Thus, it remains a mystery why the alternative splicing among *TrkB* 5' UTR exons is this complex. It is one possibility that the IRES is required for *TrkB* expression independent of cellular conditions, including stress, inflammation and hypoxia, and perhaps the

cell generates *TrkB* mRNAs with so many different 5' UTRs to guarantee that at least some of these are effective independent of external stimuli and environmental conditions.

It is not known if *TrkB* mRNAs that start with exon 5c fold into an IRES. If not, it would mean that these transcripts can be translated under different conditions as compared to mRNAs with conventional translation start-site in exon 5.

No IRES elements have been described for *TrkA*, even though TrkA kinase requires expression in neurites similarly to TrkB kinase. The 5' UTR of *TrkA* exon 1 is much shorter than the 5' UTR of TrkB: the difference is approximately 10 fold (up to 120 nt in the case of *TrkA* and up to 1100 nt for *TrkB*; publications I and II). This suggests that most of the transcripts of *TrkA* starting with exon 1 don't have 5' UTR that would be long enough to accommodate an IRES.

6. Developmental regulation of the levels of *TrkB* transcripts and TrkB proteins in human PFC (publication I)

The importance of PFC in regulating many aspects of human social behaviour, higher-order cognition and short-term memory is well known. Human PFC matures unusually late – only after early twenties (Johnson et al., 2009). *TrkB* is expressed in high levels in human cortex (Fagerberg et al., 2014), and TrkB kinase activity is important for the maturation, maintenance and function of cortical neurons (see paragraph 1.1 Physiological role). Decreased levels of TrkB-FL and transcripts encoding this kinase have been detected in the PFC of both suicide victims and schizophrenia patients (Dwivedi et al., 2003; Hashimoto et al., 2005). TrkB functioning in the PFC also plays a role in drug addiction (see paragraph 2.7. Drug addiction). For this reason, it was of interest to determine the temporal expression pattern of different *TrkB* transcripts and TrkB isoforms to find out if there are any age-related differences in the levels of these mRNAs and/or proteins.

We used 50 post-mortem samples from individuals of various age groups to detect *TrkB* mRNA and TrkB protein isoform levels. Our results indicated that the expression of TrkB-FL kinase-encoding *TrkB* mRNAs (containing exon 24) drops significantly in adults, as compared to toddler samples, where the expression level of these transcripts is the highest. The levels of transcripts with exon 16 that encode the TrkB-T1 protein isoform, however, are the lowest in toddler and school age children, and rise back to neonate levels in adulthood. One previous work has used *in situ* hybridization to describe the expression of these same mRNA isoforms in human PFC throughout the lifespan (Romanczyk et al., 2002). No statistically significant changes were detected in the expression levels of transcripts with exon 16 as the 3'-terminus, but mRNAs with exon 24 in cortical layer III were described to be considerably more abundant in young adult age group as compared to infants. The expression of these TrkB-FL-encoding transcripts plummeted in aged subjects' samples to approximately half of the level seen in young adults (Romanczyk et al., 2002).

Clearly, there are discrepancies between our results and the results obtained by Romanczyk et al. However, a common characteristic is a statistically significant reduction of the mRNAs that encode full-length TrkB kinase in older as compared to younger people. The same mRNAs have also been observed to decrease in the cortex of schizophrenia patients (Hashimoto et al., 2005; Weickert et al., 2005). As another similarity in PFC between aging and schizophrenia symptoms, the levels of *TrkB* transcripts with exons 16 (encoding TrkB-T1) increase significantly (publication I and Wong et al., 2013b). The latter study also found that the same effect can be seen at protein level: there is a reduction of TrkB-FL and an increase in TrkB-T1 quantity in schizophrenia patients as compared to healthy controls. Interestingly, it has been demonstrated, using magnetic resonance imaging (MRI), that the brains of schizophrenia patients age more rapidly than those of control individuals (Schnack et al., 2016). The authors found that among other changes, big reductions of grey matter density in the frontal lobe appear in schizophrenia. Thus, the reduction of TrkB-FL-encoding mRNA levels seen in schizophrenia patients is probably linked to the general aging of the brain in this disease.

Cognitive decline often accompanies aging and this is thought to be caused in part by decreased neuroplasticity. In fact, many genes, which products are involved in neurotrophic actions and synaptic integrity (including BDNF and NGF), are expressed at reduced levels in the PFC of aged humans (Primiani et al., 2014). TrkB-FL also fits into this category. In spite of that, it is not clear what the causative relationship of brain aging and reductions in the levels of NTs and TrkB-FL (or its transcripts) is. Still, if the PFC contains less TrkB kinase and more truncated forms of TrkB, signal transduction from TrkB-FL is hindered, because TrkB-T1 acts dominant negatively by forming a heterocomplex with the TrkB receptor kinase. TrkB-T1 dimers on the surface of either neurons or accompanying cells can also sequester BDNF, further reducing the possibility of kinase activation. Moreover, a decline of BDNF's and its mRNA levels has been repeatedly detected in human PFC in association with both aging and schizophrenia (Hashimoto et al., 2005; Primiani et al., 2014; Weickert et al., 2003; Wong et al., 2009). The lower levels of activating ligand must additionally augment TrkB-FL signalling deficiencies in both of these cohorts.

Our results of TrkB protein levels did not coincide with the experiments using mRNAs, even though an increase in TrkB-T1 protein's expression level with age was clearly evident. Specifically, we detected a significant rise of TrkB-FL levels in infants as compared to neonates, but there was no drop of TrkB-FL levels in adults. It is possible that this discrepancy (the lack of observed reduction of TrkB-FL expression level in the PFC of older subjects) was due to the small size of our cohort used for TrkB protein analysis, but alternatively, it is possible that TrkB kinase expression is regulated post-transcriptionally so that its levels do not coincide with mRNA levels. Therefore, it would be of interest to compare our results with some other study. Sadly, I have found no reliable reports that use good quality antibodies to detect TrkB kinase levels in human PFC dependent on age. It is possible instead to draw a parallel from our close relative: TrkB-FL is

expressed in the PFC of the macaque monkey at the highest levels in young animals (postnatal day number 60, P60) and displays a slight reduction in adults, while TrkB-T1 levels increase sharply in P60 from very low levels of newborns and rise even further in adults (Ohira et al., 1999). Therefore, at least in macaque monkey, the shift from higher levels of TrkB-FL to lower in adults can be seen. Further studies are needed to confirm or invalidate the result that in human PFC the level of TrkB-FL does not decrease in high age.

Our analysis of the differences in the expression levels of TrkB protein isoforms in different age groups of subjects was hindered by the lack of efficient and selective antibodies that would recognize all TrkB isoforms at low endogenous level. The antibody that we used did not recognize TrkB proteins with a putative alternative N terminus (named as TrkB-N and encoded by mRNAs starting with exon 5c). We registered a weak signal from presumably TrkB-T-Shc, which did not have age-dependent significant fluctuations.

Among other *TrkB* mRNAs that we tested, the transcripts with cassette exon 17 showed significantly higher levels in school age children as compared to neonates. Thus, the expression seems to have an opposite trend to mRNAs with *TrkB* exon 16. Indeed, we detected a statistically significant negative correlation of the expression levels between these two types of transcripts in our samples. We did not detect any statistically significant differences in the age-related fluctuation of the expression levels of transcripts with exon 5 (where the conventional start-codon lies), exon 5c (encoding TrkB proteins with unique N-termini), exon 19 (encoding TrkB-T-Shc) or exon 22b (encoding TrkB-T-TK), and transcripts lacking exon 17. It is possible that our sample size was too small to detect more subtle changes, because the individual differences between subjects were considerable.

7. Properties of N- or C-terminally truncated Trk proteins (publications I and II)

One of the results of our studies with *TrkA* and *TrkB* transcripts was a hint that there might be many more alternative protein isoforms of both TrkA and TrkB than was known. Even though we failed to demonstrate the existence of these protein isoforms at endogenous level due to technical difficulties, we decided to study the properties of a selection of these proteins, because under certain conditions these isoforms might play an important role, as demonstrated for TrkAIII (Farina et al., 2009). This is of importance, because while TrkB-T1 and TrkAIII have been a focus of research for some time, other TrkB and TrkA alternative isoforms, including TrkB-T-Shc have been overlooked.

We noticed that when overexpressed in cells, none of the TrkA and TrkB isoforms with novel N-termini is localized in the plasma membrane, even though a membrane signal sequence was predicted for one TrkA isoform, named as TrkA γ II (publication II). This isoform is not glycosylated even though it contains the same regions that are glycosylated in TrkAII. Therefore, this predicted signal sequence is not functional, omitting TrkA γ II from the endoplasmic reticulum and

Golgi network, where it could be glycosylated and later transported to the plasma membrane. Surprisingly, we discovered that an isoform named TrkA ζ II acts similarly to TrkAIII, in the aspect that it is glycosylated, but is not transported to the plasma membrane. Both TrkA ζ II and TrkAIII lack the first Ig-like domain. This underlines the importance of Trk domains in the extracellular part that are not specifically required for NT binding, but guarantee proper glycosylation and protein transport and insertion into the plasma membrane.

Our preliminary examination did not reveal any differences between TrkB receptors with or without the amino acid sequences encoded by exon 17 (publication I). However, there might still be some crucial differences in, for example, the induction of alternative signal cascades, the kinetics of kinase activation, or the endocytosis of the receptor following activation. Further studies are needed to determine these aspects.

Quite surprisingly, we discovered that the shortest TrkA isoform tested, TrkA κ , localizes to both the cell soma and the nucleus (publication II). TrkA κ consists of only the intracellular part of the conventional TrkAII receptor, which is mainly the kinase domain. Because there have been reports according to which TrkB-FL can be proteolytically cleaved by calpain to produce a fragment that is similar to TrkA κ (Jerónimo-Santos et al., 2014), we also tested if this TrkB protein fragment could enter the nucleus, and the results of immunocytochemistry indicated that it can (data not shown). The physiological role and functions of Trk kinases in the cell nucleus are at the moment unknown.

We also discovered that the TrkB-T-TK isoform, which has a truncated kinase domain, can be phosphorylated by TrkB-FL, even though it itself lacks the kinase activity (publication I). This is in contrast to TrkB-T-Shc, which is not phosphorylated by TrkB-FL (Stoilov et al., 2002).

The levels of auto-activated overexpressed TrkA isoforms were very variable: being the lowest for TrkAII (the full-length receptor) and TrkA κ , but significantly higher for TrkA proteins that contain some domains of the extracellular region, but have a cytosolic localization (publication II). This indicates that there might be other isoforms of TrkA besides TrkAIII that can become aberrantly active in cancer.

8. Identification and analysis of novel potent and selective Trk inhibitors (publication III)

Overexpression and/or activation of Trk kinases has been associated with many diseases, such as some types of cancer and neuropathic pain (see paragraph 2. Role of Trk receptors in disease). Even though many Trk inhibitors have been developed, none have reached patient bedside (see paragraph 3.2. Trk inhibitors). Therefore, it was our goal to design novel Trk inhibitors that could be further developed as painkillers or anti-cancer agents.

Using computer calculations and predictions based on known Trk inhibitors, we identified novel inhibitors of Trk kinases from the group of 2-oxindoles. Of these, (Z)-3-((5-methoxy-1-methyl-1H-indol-3-yl)methylene)-N-methyl-2-

oxindole-5-sulfonamide (compound 4a22) had the lowest IC_{50} against TrkA in both biochemical and cellular assays, 3.7 nM and 10.0 nM, respectively. Unsurprisingly, these compounds have similar profiles inhibiting all members of the Trk family, because they dock inside the kinase pocket, which is identical among this group of kinases. Representatives of these compounds also effectively inhibit the activation of downstream signalling cascades by Trks, as shown by MAPK (Erk) and PKB (Akt) phosphorylation levels.

These novel Trk inhibitors have a good selectivity: from a panel of 48 kinases, which represent a wide range of human kinases, a 50 % or greater inhibition by 100 nM 4a22 can be seen for only one kinase besides Trks. At 1 μ M concentration of 4a22, the number of off-target kinases rose to 4.

Therefore, these compounds can be considered as potential therapeutics for the treatment of pain or some cancer states, where Trk over-activation is the driving force behind malignancy. Nevertheless, preclinical studies involving pharmacokinetics, pharmacodynamics and disease model studies are needed before considering these compounds as candidates for clinical trials.

CONCLUSIONS

- Human *TrkA* gene is much larger than previously thought and it overlaps with two genes.
- Mouse and rat orthologues are shorter and have less complicated splicing patterns compared to human *TrkA*.
- Transcript diversity of *TrkA* is generated via usage of alternative promoters and an intricate splicing pattern among exons encoding the extracellular domain of TrkA.
- For *TrkB*, physiologically the most important variability among mRNAs is produced using alternative 3' exons, although alternative splicing of a few exons and the usage of one novel 5' exon also plays a part.
- There is a good agreement between data published before our study and our results about the expression pattern in different human tissue samples of the major transcripts of both *TrkA* and *TrkB*, namely mRNAs encoding proteins TrkAI, TrkAII, TrkB-FL, TrkB-T1 and TrkB-T-Shc.
- *TrkB* transcripts with novel 5' and 3' exons (5c and 22b) are mainly expressed in neural tissues and potentially encode novel protein isoforms with a truncated N-terminus and alternative C-terminus, respectively.
- TrkB-FL-encoding transcripts are expressed at lower levels in aged human PFC, as compared to younger age groups – a finding that correlates with a previous study.
- mRNAs encoding TrkB-T1 have the lowest levels in the PFC of toddler and school age children.
- TrkB-FL and TrkB-T1 protein levels in the PFC did not correlate with the expression level of mRNAs that encode these proteins: TrkB-T1 levels display a continuous rise from neonates to teenagers, and TrkB-FL levels rise in infants as compared to neonates, but do not decrease in older people.
- A preliminary characterization of putative novel Trk protein isoforms revealed that:
 - 1) there were no functional differences detected between TrkB isoforms with or without amino acids encoded by exon 17,
 - 2) TrkB-T-TK isoform, which lacks a part of the kinase domain, can be phosphorylated by TrkB-FL,
 - 3) all the tested TrkA and TrkB isoforms with alternative N-termini, as compared to the N-terminus of the conventional protein isoforms, are omitted from the plasma membrane, but often have very high level of auto-phosphorylation,
 - 4) Trk isoforms or proteolysis products that consist of only the intracellular part of the full-length receptor are able to localize in the cell nucleus.
- We identified novel highly selective Trk inhibitors among 2-oxindoles, with low nanomolar inhibitory activity against Trk family of kinases.

REFERENCES

- Adachi, M., Barrot, M., Autry, A.E., Theobald, D., and Monteggia, L.M. (2008). Selective loss of brain-derived neurotrophic factor in the dentate gyrus attenuates antidepressant efficacy. *Biol. Psychiatry* *63*, 642–649.
- Adachi, M., Autry, A.E., Mahgoub, M., Suzuki, K., and Monteggia, L.M. (2016). TrkB Signaling in Dorsal Raphe Nucleus is Essential for Antidepressant Efficacy and Normal Aggression Behavior. *Neuropsychopharmacol. Off. Publ. Am. Coll. Neuropsychopharmacol.*
- Albaugh, P., Fan, Y., Mi, Y., Sun, F., Adrian, F., Li, N., Jia, Y., Sarkisova, Y., Kreusch, A., Hood, T., et al. (2012). Discovery of GNF-5837, a Selective TRK Inhibitor with Efficacy in Rodent Cancer Tumor Models. *ACS Med. Chem. Lett.* *3*, 140–145.
- Alcántara, S., Frisén, J., Río, J.A. del, Soriano, E., Barbacid, M., and Silos-Santiago, I. (1997). TrkB Signaling Is Required for Postnatal Survival of CNS Neurons and Protects Hippocampal and Motor Neurons from Axotomy-Induced Cell Death. *J. Neurosci.* *17*, 3623–3633.
- Ambjørn, M., Dubreuil, V., Miozzo, F., Nigon, F., Møller, B., Issazadeh-Navikas, S., Berg, J., Lees, M., and Sap, J. (2013). A Loss-of-Function Screen for Phosphatases that Regulate Neurite Outgrowth Identifies PTPN12 as a Negative Regulator of TrkB Tyrosine Phosphorylation. *PLoS ONE* *8*.
- Aravamudan, B., Thompson, M., Pabelick, C., and Prakash, Y.S. (2012). Brain-derived neurotrophic factor induces proliferation of human airway smooth muscle cells. *J. Cell. Mol. Med.* *16*, 812–823.
- Arevalo, J.C., Conde, B., Hempstead, B.L., Chao, M.V., Martin-Zanca, D., and Perez, P. (2000). TrkA Immunoglobulin-Like Ligand Binding Domains Inhibit Spontaneous Activation of the Receptor. *Mol. Cell. Biol.* *20*, 5908–5916.
- Arévalo, J.C., Waite, J., Rajagopal, R., Beyna, M., Chen, Z.-Y., Lee, F.S., and Chao, M.V. (2006). Cell Survival through Trk Neurotrophin Receptors Is Differentially Regulated by Ubiquitination. *Neuron* *50*, 549–559.
- Aridgides, D., Salvador, R., and PereiraPerrin, M. (2013). Trypanosoma cruzi coaxes cardiac fibroblasts into preventing cardiomyocyte death by activating nerve growth factor receptor TrkA. *PLoS One* *8*, e57450.
- Ashraf, S., Bouhana, K.S., Pheneger, J., Andrews, S.W., and Walsh, D.A. (2016). Selective inhibition of tropomyosin-receptor-kinase A (TrkA) reduces

pain and joint damage in two rat models of inflammatory arthritis. *Arthritis Res. Ther.* *18*, 97.

Aubert, L., Guilbert, M., Corbet, C., Génot, E., Adriaenssens, E., Chassat, T., Bertucci, F., Daubon, T., Magné, N., Le Bourhis, X., et al. (2015). NGF-induced TrkA/CD44 association is involved in tumor aggressiveness and resistance to lestaurtinib. *Oncotarget* *6*, 9807–9819.

Autry, A.E., Adachi, M., Nosyreva, E., Na, E.S., Los, M.F., Cheng, P., Kavalali, E.T., and Monteggia, L.M. (2011). NMDA receptor blockade at rest triggers rapid behavioural antidepressant responses. *Nature* *475*, 91–95.

Barbacid, M. (1994). The Trk family of neurotrophin receptors. *J. Neurobiol.* *25*, 1386–1403.

Barde, Y.A., Edgar, D., and Thoenen, H. (1982). Purification of a new neurotrophic factor from mammalian brain. *EMBO J.* *1*, 549–553.

Barford, K., Deppmann, C., and Winckler, B. (2016). The neurotrophin receptor signaling endosome: where trafficking meets signaling. *Dev. Neurobiol.*

Barker, P.A., Lomen-Hoerth, C., Gensch, E.M., Meakin, S.O., Glass, D.J., and Shooter, E.M. (1993). Tissue-specific alternative splicing generates two isoforms of the trkA receptor. *J. Biol. Chem.* *268*, 15150–15157.

Bechara, R.G., Lyne, R., and Kelly, Á.M. (2014). BDNF-stimulated intracellular signalling mechanisms underlie exercise-induced improvement in spatial memory in the male Wistar rat. *Behav. Brain Res.* *275*, 297–306.

Beggs, S., Trang, T., and Salter, M.W. (2012). P2X4R+ microglia drive neuropathic pain. *Nat. Neurosci.* *15*, 1068–1073.

Bekris, L.M., Yu, C.-E., Bird, T.D., and Tsuang, D.W. (2010). Genetics of Alzheimer Disease. *J. Geriatr. Psychiatry Neurol.* *23*, 213–227.

Benisty, S., Boissiere, F., Faucheux, B., Agid, Y., and Hirsch, E.C. (1998). trkB messenger RNA expression in normal human brain and in the substantia nigra of parkinsonian patients: an in situ hybridization study. *Neuroscience* *86*, 813–826.

Berglind, W.J., See, R.E., Fuchs, R.A., Ghee, S.M., Whitfield, T.W., Miller, S.W., and McGinty, J.F. (2007). A BDNF infusion into the medial prefrontal cortex suppresses cocaine seeking in rats. *Eur. J. Neurosci.* *26*, 757–766.

Berman, R.M., Cappiello, A., Anand, A., Oren, D.A., Heninger, G.R., Charney, D.S., and Krystal, J.H. (2000). Antidepressant effects of ketamine in depressed patients. *Biol. Psychiatry* 47, 351–354.

Biffo, S., Offenhäuser, N., Carter, B.D., and Barde, Y.A. (1995). Selective binding and internalisation by truncated receptors restrict the availability of BDNF during development. *Dev. Camb. Engl.* 121, 2461–2470.

Blum, R., Kafitz, K.W., and Konnerth, A. (2002). Neurotrophin-evoked depolarization requires the sodium channel NaV1.9. *Nature* 419, 687–693.

von Bohlen und Halbach, O., Krause, S., Medina, D., Sciarretta, C., Minichiello, L., and Unsicker, K. (2006). Regional- and age-dependent reduction in trkB receptor expression in the hippocampus is associated with altered spine morphologies. *Biol. Psychiatry* 59, 793–800.

Bonini, S., Lambiase, A., Bonini, S., Angelucci, F., Magrini, L., Manni, L., and Aloe, L. (1996). Circulating nerve growth factor levels are increased in humans with allergic diseases and asthma. *Proc. Natl. Acad. Sci. U. S. A.* 93, 10955–10960.

Bothwell, M. (2006). Evolution of the neurotrophin signaling system in invertebrates. *Brain. Behav. Evol.* 68, 124–132.

Bracci-Laudiero, L., and De Stefano, M. (2016). NGF in Early Embryogenesis, Differentiation, and Pathology in the Nervous and Immune Systems. In *Neurotoxin Modeling of Brain Disorders — Life-Long Outcomes in Behavioral Teratology*, R.M. Kostrzewa, and T. Archer, eds. (Springer International Publishing), pp. 125–152.

Braun, A., Appel, E., Baruch, R., Herz, U., Botchkarev, V., Paus, R., Brodie, C., and Renz, H. (1998). Role of nerve growth factor in a mouse model of allergic airway inflammation and asthma. *Eur. J. Immunol.* 28, 3240–3251.

Briones, T.L., and Woods, J. (2013). Chronic binge-like alcohol consumption in adolescence causes depression-like symptoms possibly mediated by the effects of BDNF on neurogenesis. *Neuroscience* 254, 324–334.

Brito, V., Puigdemívol, M., Giral, A., del Toro, D., Alberch, J., and Ginés, S. (2013). Imbalance of p75(NTR)/TrkB protein expression in Huntington's disease: implication for neuroprotective therapies. *Cell Death Dis.* 4, e595.

Brown, M.T., Murphy, F.T., Radin, D.M., Davignon, I., Smith, M.D., and West, C.R. (2012). Tanezumab reduces osteoarthritic knee pain: results of a randomized, double-blind, placebo-controlled phase III trial. *J. Pain Off. J. Am. Pain Soc.* 13, 790–798.

Buchwald, P. (2010). Small-molecule protein–protein interaction inhibitors: Therapeutic potential in light of molecular size, chemical space, and ligand binding efficiency considerations. *IUBMB Life* *62*, 724–731.

Burnouf, S., Belarbi, K., Troquier, L., Derisbourg, M., Demeyer, D., Leboucher, A., Laurent, C., Hamdane, M., Buee, L., and Blum, D. (2012). Hippocampal BDNF Expression in a Tau Transgenic Mouse Model. *Curr. Alzheimer Res.* *9*, 406–410.

Burnouf, S., Martire, A., Derisbourg, M., Laurent, C., Belarbi, K., Leboucher, A., Fernandez-Gomez, F.J., Troquier, L., Eddarkaoui, S., Grosjean, M.-E., et al. (2013). NMDA receptor dysfunction contributes to impaired brain-derived neurotrophic factor-induced facilitation of hippocampal synaptic transmission in a Tau transgenic model. *Aging Cell* *12*, 11–23.

Cabrera, N., Díaz-Rodríguez, E., Becker, E., Martín-Zanca, D., and Pandiella, A. (1996). TrkA receptor ectodomain cleavage generates a tyrosine-phosphorylated cell-associated fragment. *J. Cell Biol.* *132*, 427–436.

Campenot, R.B. (1977). Local control of neurite development by nerve growth factor. *Proc. Natl. Acad. Sci. U. S. A.* *74*, 4516–4519.

Carim-Todd, L., Bath, K.G., Fulgenzi, G., Yanpallewar, S., Jing, D., Barrick, C.A., Becker, J., Buckley, H., Dorsey, S.G., Lee, F.S., et al. (2009). Endogenous Truncated TrkB.T1 Receptor Regulates Neuronal Complexity and TrkB Kinase Receptor Function in vivo. *J. Neurosci. Off. J. Soc. Neurosci.* *29*, 678–685.

Carmona, M.A., Pozas, E., Martínez, A., Espinosa-Parrilla, J.F., Soriano, E., and Aguado, F. (2006). Age-dependent Spontaneous Hyperexcitability and Impairment of GABAergic Function in the Hippocampus of Mice Lacking trkB. *Cereb. Cortex* *16*, 47–63.

Castrén, E. (2014). Neurotrophins and psychiatric disorders. *Handb. Exp. Pharmacol.* *220*, 461–479.

Castrén, E., and Kojima, M. (2016). Brain-derived neurotrophic factor in mood disorders and antidepressant treatments. *Neurobiol. Dis.*

Cazorla, M., Jouvenceau, A., Rose, C., Guilloux, J.-P., Pilon, C., Dranovsky, A., and Prémont, J. (2010). Cyclothiazin-B, the first highly potent and selective TrkB inhibitor, has anxiolytic properties in mice. *PloS One* *5*, e9777.

Cazorla, M., Prémont, J., Mann, A., Girard, N., Kellendonk, C., and Rognan, D. (2011). Identification of a low-molecular weight TrkB antagonist with anxiolytic and antidepressant activity in mice. *J. Clin. Invest.* *121*, 1846–1857.

Chang, Q., Khare, G., Dani, V., Nelson, S., and Jaenisch, R. (2006). The Disease Progression of *Mecp2* Mutant Mice Is Affected by the Level of BDNF Expression. *Neuron* *49*, 341–348.

Chen, B., Dowlatshahi, D., MacQueen, G.M., Wang, J.-F., and Young, L.T. (2001). Increased hippocampal *bdnf* immunoreactivity in subjects treated with antidepressant medication. *Biol. Psychiatry* *50*, 260–265.

Cheng, A., Coksaygan, T., Tang, H., Khatri, R., Balice-Gordon, R.J., Rao, M.S., and Mattson, M.P. (2007). Truncated tyrosine kinase B brain-derived neurotrophic factor receptor directs cortical neural stem cells to a glial cell fate by a novel signaling mechanism. *J. Neurochem.* *100*, 1515–1530.

Choe, K.Y., Han, S.Y., Gaub, P., Shell, B., Voisin, D.L., Knapp, B.A., Barker, P.A., Brown, C.H., Cunningham, J.T., and Bourque, C.W. (2015). High salt intake increases blood pressure via BDNF-mediated downregulation of KCC2 and impaired baroreflex inhibition of vasopressin neurons. *Neuron* *85*, 549–560.

Choi, H.-S., Rucker, P.V., Wang, Z., Fan, Y., Albaugh, P., Chopiuk, G., Gessier, F., Sun, F., Adrian, F., Liu, G., et al. (2015). (R)-2-Phenylpyrrolidine Substituted Imidazopyridazines: A New Class of Potent and Selective Pan-TRK Inhibitors. *ACS Med. Chem. Lett.* *6*, 562–567.

Chuang, H., Prescott, E.D., Kong, H., Shields, S., Jordt, S.-E., Basbaum, A.I., Chao, M.V., and Julius, D. (2001). Bradykinin and nerve growth factor release the capsaicin receptor from PtdIns(4,5)P₂-mediated inhibition. *Nature* *411*, 957–962.

Chuenkova, M.V., and PereiraPerrin, M. (2004). Chagas' disease parasite promotes neuron survival and differentiation through TrkA nerve growth factor receptor. *J. Neurochem.* *91*, 385–394.

Clary, D.O., and Reichardt, L.F. (1994). An alternatively spliced form of the nerve growth factor receptor TrkA confers an enhanced response to neurotrophin 3. *Proc. Natl. Acad. Sci. U. S. A.* *91*, 11133–11137.

Cleary, J.P., Walsh, D.M., Hofmeister, J.J., Shankar, G.M., Kuskowski, M.A., Selkoe, D.J., and Ashe, K.H. (2005). Natural oligomers of the amyloid- β protein specifically disrupt cognitive function. *Nat. Neurosci.* *8*, 79–84.

Coppola, V., Barrick, C.A., Southon, E.A., Celeste, A., Wang, K., Chen, B., Haddad, E.-B., Yin, J., Nussenzweig, A., Subramaniam, A., et al. (2004). Ablation of TrkA function in the immune system causes B cell abnormalities. *Development* *131*, 5185–5195.

Coull, J.A.M., Boudreau, D., Bachand, K., Prescott, S.A., Nault, F., Sk, A., De Koninck, P., and De Koninck, Y. (2003). Trans-synaptic shift in anion gradient in spinal lamina I neurons as a mechanism of neuropathic pain. *Nature* 424, 938–942.

Coull, J.A.M., Beggs, S., Boudreau, D., Boivin, D., Tsuda, M., Inoue, K., Gravel, C., Salter, M.W., and De Koninck, Y. (2005). BDNF from microglia causes the shift in neuronal anion gradient underlying neuropathic pain. *Nature* 438, 1017–1021.

Counts, S.E., Nadeem, M., Wu, J., Ginsberg, S.D., Saragovi, H.U., and Mufson, E.J. (2004). Reduction of cortical TrkA but not p75(NTR) protein in early-stage Alzheimer’s disease. *Ann. Neurol.* 56, 520–531.

Covaceuszach, S., Konarev, P.V., Cassetta, A., Paoletti, F., Svergun, D.I., Lamba, D., and Cattaneo, A. (2015). The Conundrum of the High-Affinity NGF Binding Site Formation Unveiled? *Biophys. J.* 108, 687–697.

Croll, S.D., Ip, N.Y., Lindsay, R.M., and Wiegand, S.J. (1998). Expression of BDNF and trkB as a function of age and cognitive performance. *Brain Res.* 812, 200–208.

Crowder, R.J., and Freeman, R.S. (1998). Phosphatidylinositol 3-Kinase and Akt Protein Kinase Are Necessary and Sufficient for the Survival of Nerve Growth Factor-Dependent Sympathetic Neurons. *J. Neurosci.* 18, 2933–2943.

Danelon, V., Montroull, L.E., Unsain, N., Barker, P.A., and Masc, D.H. (2016). Calpain-dependent truncated form of TrkB-FL increases in neurodegenerative processes. *Mol. Cell. Neurosci.* 75, 81–92.

Danzer, S.C., He, X., and McNamara, J.O. (2004). Ontogeny of seizure-induced increases in BDNF immunoreactivity and TrkB receptor activation in rat hippocampus. *Hippocampus* 14, 345–355.

Davidson, B., Reich, R., Lazarovici, P., Nesland, J.M., Skrede, M., Risberg, B., Trop, C.G., and Flrenes, V.A. (2003). Expression and activation of the nerve growth factor receptor TrkA in serous ovarian carcinoma. *Clin. Cancer Res. Off. J. Am. Assoc. Cancer Res.* 9, 2248–2259.

Delcroix, J.-D., Valletta, J.S., Wu, C., Hunt, S.J., Kowal, A.S., and Mobley, W.C. (2003). NGF Signaling in Sensory Neurons: Evidence that Early Endosomes Carry NGF Retrograde Signals. *Neuron* 39, 69–84.

Descamps, S., Lebourhis, X., Delehedde, M., Boilly, B., and Hondermarck, H. (1998). Nerve growth factor is mitogenic for cancerous but not normal human breast epithelial cells. *J. Biol. Chem.* 273, 16659–16662.

Descamps, S., Pawlowski, V., Révillion, F., Hornez, L., Hebbar, M., Boilly, B., Hondermarck, H., and Peyrat, J.-P. (2001). Expression of Nerve Growth Factor Receptors and Their Prognostic Value in Human Breast Cancer. *Cancer Res.* *61*, 4337–4340.

DiazGranados, N., Ibrahim, L.A., Brutsche, N.E., Ameli, R., Henter, I.D., Luckenbaugh, D.A., Machado-Vieira, R., and Zarate, C.A. (2010). Rapid resolution of suicidal ideation after a single infusion of an N-methyl-D-aspartate antagonist in patients with treatment-resistant major depressive disorder. *J. Clin. Psychiatry* *71*, 1605–1611.

Dimitrelis, K., and Shankar, R. (2016). Pharmacological treatment of schizophrenia – a review of progress. *Prog. Neurol. Psychiatry* *20*, 28–35.

Djakiew, D., Delsite, R., Pflug, B., Wrathall, J., Lynch, J.H., and Onoda, M. (1991). Regulation of growth by a nerve growth factor-like protein which modulates paracrine interactions between a neoplastic epithelial cell line and stromal cells of the human prostate. *Cancer Res.* *51*, 3304–3310.

Dobson, T., Minic, A., Nielsen, K., Amiott, E., and Krushel, L. (2005). Internal initiation of translation of the TrkB mRNA is mediated by multiple regions within the 5' leader. *Nucleic Acids Res.* *33*, 2929–2941.

Doebele, R.C., Davis, L.E., Vaishnavi, A., Le, A.T., Estrada-Bernal, A., Keysar, S., Jimeno, A., Varella-Garcia, M., Aisner, D.L., Li, Y., et al. (2015). An Oncogenic NTRK Fusion in a Patient with Soft-Tissue Sarcoma with Response to the Tropomyosin-Related Kinase Inhibitor LOXO-101. *Cancer Discov.* *5*, 1049–1057.

Donnerer, J., Schuligoi, R., and Stein, C. (1992). Increased content and transport of substance P and calcitonin gene-related peptide in sensory nerves innervating inflamed tissue: Evidence for a regulatory function of nerve growth factor in vivo. *Neuroscience* *49*, 693–698.

Dorsey, S.G., Renn, C.L., Carim-Todd, L., Barrick, C.A., Bambrick, L., Krueger, B.K., Ward, C.W., and Tessarollo, L. (2006). In Vivo Restoration of Physiological Levels of Truncated TrkB.T1 Receptor Rescues Neuronal Cell Death in a Trisomic Mouse Model. *Neuron* *51*, 21–28.

Douma, S., van Laar, T., Zevenhoven, J., Meuwissen, R., van Garderen, E., and Peeper, D.S. (2004). Suppression of anoikis and induction of metastasis by the neurotrophic receptor TrkB. *Nature* *430*, 1034–1039.

Dubus, P., Parrens, M., El-Mokhtari, Y., Ferrer, J., Groppi, A., and Merlio, J.P. (2000). Identification of novel trkA variants with deletions in leucine-rich motifs of the extracellular domain. *J. Neuroimmunol.* *107*, 42–49.

Dwivedi, Y., Rizavi, H.S., Conley, R.R., Roberts, R.C., Tamminga, C.A., and Pandey, G.N. (2003). Altered gene expression of brain-derived neurotrophic factor and receptor tyrosine kinase B in postmortem brain of suicide subjects. *Arch. Gen. Psychiatry* *60*, 804–815.

Ehrhard, P.B., Ganter, U., Stalder, A., Bauer, J., and Otten, U. (1993a). Expression of functional trk protooncogene in human monocytes. *Proc. Natl. Acad. Sci. U. S. A.* *90*, 5423–5427.

Ehrhard, P.B., Erb, P., Graumann, U., and Otten, U. (1993b). Expression of nerve growth factor and nerve growth factor receptor tyrosine kinase Trk in activated CD4-positive T-cell clones. *Proc. Natl. Acad. Sci. U. S. A.* *90*, 10984–10988.

Eide, F.F., Vining, E.R., Eide, B.L., Zang, K., Wang, X.Y., and Reichardt, L.F. (1996). Naturally occurring truncated trkB receptors have dominant inhibitory effects on brain-derived neurotrophic factor signaling. *J. Neurosci. Off. J. Soc. Neurosci.* *16*, 3123–3129.

Eisch, A.J., Bolaños, C.A., de Wit, J., Simonak, R.D., Pudiak, C.M., Barrot, M., Verhaagen, J., and Nestler, E.J. (2003). Brain-derived neurotrophic factor in the ventral midbrain–nucleus accumbens pathway: a role in depression. *Biol. Psychiatry* *54*, 994–1005.

Esposito, D., Patel, P., Stephens, R.M., Perez, P., Chao, M.V., Kaplan, D.R., and Hempstead, B.L. (2001). The Cytoplasmic and Transmembrane Domains of the p75 and Trk A Receptors Regulate High Affinity Binding to Nerve Growth Factor. *J. Biol. Chem.* *276*, 32687–32695.

Evans, R.J., Moldwin, R.M., Cossons, N., Darekar, A., Mills, I.W., and Scholfield, D. (2011). Proof of concept trial of tanezumab for the treatment of symptoms associated with interstitial cystitis. *J. Urol.* *185*, 1716–1721.

Everitt, B.J., and Robbins, and T.W. (1997). Central Cholinergic Systems and Cognition. *Annu. Rev. Psychol.* *48*, 649–684.

Fagerberg, L., Hallström, B.M., Oksvold, P., Kampf, C., Djureinovic, D., Odeberg, J., Habuka, M., Tahmasebpour, S., Danielsson, A., Edlund, K., et al. (2014). Analysis of the human tissue-specific expression by genome-wide integration of transcriptomics and antibody-based proteomics. *Mol. Cell. Proteomics MCP* *13*, 397–406.

Farina, A.R., Tacconelli, A., Cappabianca, L., Cea, G., Panella, S., Chioda, A., Romanelli, A., Pedone, C., Gulino, A., and Mackay, A.R. (2009). The alternative TrkAIII splice variant targets the centrosome and promotes genetic instability. *Mol. Cell. Biol.* *29*, 4812–4830.

Farina, A.R., Cappabianca, L., Ruggeri, P., Gneo, L., Maccarone, R., and Mackay, A.R. (2015). Retrograde TrkAIII transport from ERGIC to ER: a re-localisation mechanism for oncogenic activity. *Oncotarget* 6, 35636–35651.

Feng, N., Huke, S., Zhu, G., Tocchetti, C.G., Shi, S., Aiba, T., Kaludercic, N., Hoover, D.B., Beck, S.E., Mankowski, J.L., et al. (2015). Constitutive BDNF/TrkB signaling is required for normal cardiac contraction and relaxation. *Proc. Natl. Acad. Sci. U. S. A.* 112, 1880–1885.

Forrest, A.R.R., Taylor, D.F., Crowe, M.L., Chalk, A.M., Waddell, N.J., Kolle, G., Faulkner, G.J., Kodzius, R., Katayama, S., Wells, C., et al. (2006). Genome-wide review of transcriptional complexity in mouse protein kinases and phosphatases. *Genome Biol.* 7, R5.

Frisén, J., Verge, V.M., Fried, K., Risling, M., Persson, H., Trotter, J., Hökfelt, T., and Lindholm, D. (1993). Characterization of glial trkB receptors: differential response to injury in the central and peripheral nervous systems. *Proc. Natl. Acad. Sci. U. S. A.* 90, 4971–4975.

Fryer, R.H., Kaplan, D.R., Feinstein, S.C., Radeke, M.J., Grayson, D.R., and Kromer, L.F. (1996). Developmental and mature expression of full-length and truncated TrkB, receptors in the rat forebrain. *J. Comp. Neurol.* 374, 21–40.

Fryer, R.H., Kaplan, D.R., and Kromer, L.F. (1997). Truncated trkB Receptors on Nonneuronal Cells Inhibit BDNF-Induced Neurite Outgrowth in Vitro. *Exp. Neurol.* 148, 616–627.

Fukumitsu, H., Furukawa, Y., Tsusaka, M., Kinukawa, H., Nitta, A., Nomoto, H., Mima, T., and Furukawa, S. (1998). Simultaneous expression of brain-derived neurotrophic factor and neurotrophin-3 in Cajal–Retzius, subplate and ventricular progenitor cells during early development stages of the rat cerebral cortex. *Neuroscience* 84, 115–127.

Fulgenzi, G., Tomassoni-Ardori, F., Babini, L., Becker, J., Barrick, C., Puverel, S., and Tessarollo, L. (2015). BDNF modulates heart contraction force and long-term homeostasis through truncated TrkB.T1 receptor activation. *J Cell Biol* 210, 1003–1012.

Gao, Y., Davies, S.P., Augustin, M., Woodward, A., Patel, U.A., Kovelman, R., and Harvey, K.J. (2013). A broad activity screen in support of a chemogenomic map for kinase signalling research and drug discovery. *Biochem. J.* 451, 313–328.

García-Suárez, O., Pérez-Pinera, P., Laurà, R., Germana, A., Esteban, I., Cabo, R., Silos-Santiago, I., Cobo, J.L., and Vega, J.A. (2009). TrkB is necessary

for the normal development of the lung. *Respir. Physiol. Neurobiol.* *167*, 281–291.

Garner, A.S., Menegay, H.J., Boeshore, K.L., Xie, X.Y., Voci, J.M., Johnson, J.E., and Large, T.H. (1996). Expression of TrkB receptor isoforms in the developing avian visual system. *J. Neurosci. Off. J. Soc. Neurosci.* *16*, 1740–1752.

Garzon, D.J., and Fahnstock, M. (2007). Oligomeric Amyloid Decreases Basal Levels of Brain-Derived Neurotrophic factor (BDNF) mRNA via Specific Downregulation of BDNF Transcripts IV and V in Differentiated Human Neuroblastoma Cells. *J. Neurosci.* *27*, 2628–2635.

Geetha, T., Jiang, J., and Wooten, M.W. (2005). Lysine 63 Polyubiquitination of the Nerve Growth Factor Receptor TrkA Directs Internalization and Signaling. *Mol. Cell* *20*, 301–312.

Geiger, T.R., and Peeper, D.S. (2007). Critical Role for TrkB Kinase Function in Anoikis Suppression, Tumorigenesis, and Metastasis. *Cancer Res.* *67*, 6221–6229.

Gerber, R.K.H., Nie, H., Arendt-Nielsen, L., Curatolo, M., and Graven-Nielsen, T. (2011). Local pain and spreading hyperalgesia induced by intramuscular injection of nerve growth factor are not reduced by local anesthesia of the muscle. *Clin. J. Pain* *27*, 240–247.

Ghilardi, J.R., Freeman, K.T., Jimenez-Andrade, J.M., Mantyh, W.G., Bloom, A.P., Kuskowski, M.A., and Mantyh, P.W. (2010). Administration of a tropomyosin receptor kinase inhibitor attenuates sarcoma-induced nerve sprouting, neuroma formation and bone cancer pain. *Mol. Pain* *6*, 87.

Ghosh, A., Carnahan, J., and Greenberg, M.E. (1994). Requirement for BDNF in activity-dependent survival of cortical neurons. *Science* *263*, 1618–1623.

Ginés, S., Bosch, M., Marco, S., Gavalda, N., Díaz-Hernández, M., Lucas, J.J., Canals, J.M., and Alberch, J. (2006). Reduced expression of the TrkB receptor in Huntington's disease mouse models and in human brain. *Eur. J. Neurosci.* *23*, 649–658.

Ginsberg, S.D., Che, S., Wu, J., Counts, S.E., and Mufson, E.J. (2006). Down regulation of trk but not p75^{NTR} gene expression in single cholinergic basal forebrain neurons mark the progression of Alzheimer's disease. *J. Neurochem.* *97*, 475–487.

Glerup, S., Bolcho, U., Mølgaard, S., Bøggild, S., Vaegter, C.B., Smith, A.H., Nieto-Gonzalez, J.L., Ovesen, P.L., Pedersen, L.F., Fjorback, A.N., et al. (2016).

SorCS2 is required for BDNF-dependent plasticity in the hippocampus. *Mol. Psychiatry*.

Goedert, M., Spillantini, M.G., and Crowther, R.A. (1991). Tau Proteins and Neurofibrillary Degeneration. *Brain Pathol.* *1*, 279–286.

Gomes, J.R., Costa, J.T., Melo, C.V., Felizzi, F., Monteiro, P., Pinto, M.J., Inácio, A.R., Wieloch, T., Almeida, R.D., Grãos, M., et al. (2012). Excitotoxicity downregulates TrkB.FL signaling and upregulates the neuroprotective truncated TrkB receptors in cultured hippocampal and striatal neurons. *J. Neurosci. Off. J. Soc. Neurosci.* *32*, 4610–4622.

Gonul, D.A.S., Akdeniz, D.F., Taneli, D.F., Donat, D.O., Eker, D.Ç., and Vahip, D.S. (2005). Effect of treatment on serum brain-derived neurotrophic factor levels in depressed patients. *Eur. Arch. Psychiatry Clin. Neurosci.* *255*, 381–386.

Graham, D.L., Edwards, S., Bachtell, R.K., DiLeone, R.J., Rios, M., and Self, D.W. (2007). Dynamic BDNF activity in nucleus accumbens with cocaine use increases self-administration and relapse. *Nat. Neurosci.* *10*, 1029–1037.

Gray, E.G., Paula-Barbosa, M., and Roher, A. (1987). Alzheimer's Disease: Paired Helical Filaments and Cytomembranes. *Neuropathol. Appl. Neurobiol.* *13*, 91–110.

Gray, J., Yeo, G.S.H., Cox, J.J., Morton, J., Adlam, A.-L.R., Keogh, J.M., Yanovski, J.A., El Gharbawy, A., Han, J.C., Tung, Y.C.L., et al. (2006). Hyperphagia, severe obesity, impaired cognitive function, and hyperactivity associated with functional loss of one copy of the brain-derived neurotrophic factor (BDNF) gene. *Diabetes* *55*, 3366–3371.

Green, M.J., Matheson, S.L., Shepherd, A., Weickert, C.S., and Carr, V.J. (2011). Brain-derived neurotrophic factor levels in schizophrenia: a systematic review with meta-analysis. *Mol. Psychiatry* *16*, 960–972.

Grimm, J.W., Lu, L., Hayashi, T., Hope, B.T., Su, T.-P., and Shaham, Y. (2003). Time-Dependent Increases in Brain-Derived Neurotrophic Factor Protein Levels within the Mesolimbic Dopamine System after Withdrawal from Cocaine: Implications for Incubation of Cocaine Craving. *J. Neurosci.* *23*, 742–747.

Hackett, S.F., Friedman, Z., Freund, J., Schoenfeld, C., Curtis, R., DiStefano, P.S., and Campochiaro, P.A. (1998). A splice variant of trkB and brain-derived neurotrophic factor are co-expressed in retinal pigmented epithelial cells and promote differentiated characteristics. *Brain Res.* *789*, 201–212.

Hahn, C., Islamian, A.P., Renz, H., and Nockher, W.A. (2006). Airway epithelial cells produce neurotrophins and promote the survival of eosinophils during allergic airway inflammation. *J. Allergy Clin. Immunol.* *117*, 787–794.

Harrington, A.W., St Hillaire, C., Zweifel, L.S., Glebova, N.O., Philippidou, P., Halegoua, S., and Ginty, D.D. (2011). Recruitment of actin modifiers to TrkA endosomes governs retrograde NGF signaling and survival. *Cell* *146*, 421–434.

Hartikka, J., and Hefti, F. (1988). Comparison of nerve growth factor's effects on development of septum, striatum, and nucleus basalis cholinergic neurons in vitro. *J. Neurosci. Res.* *21*, 352–364.

Harward, S.C., Hedrick, N.G., Hall, C.E., Parra-Bueno, P., Milner, T.A., Pan, E., Laviv, T., Hempstead, B.L., Yasuda, R., and McNamara, J.O. (2016). Autocrine BDNF-TrkB signalling within a single dendritic spine. *Nature*.

Hashimoto, T., Bergen, S.E., Nguyen, Q.L., Xu, B., Monteggia, L.M., Pierri, J.N., Sun, Z., Sampson, A.R., and Lewis, D.A. (2005). Relationship of Brain-Derived Neurotrophic Factor and Its Receptor TrkB to Altered Inhibitory Prefrontal Circuitry in Schizophrenia. *J. Neurosci.* *25*, 372–383.

He, X.-P., Kotloski, R., Nef, S., Luikart, B.W., Parada, L.F., and McNamara, J.O. (2004). Conditional Deletion of TrkB but Not BDNF Prevents Epileptogenesis in the Kindling Model. *Neuron* *43*, 31–42.

Heerssen, H.M., Pazyra, M.F., and Segal, R.A. (2004). Dynein motors transport activated Trks to promote survival of target-dependent neurons. *Nat. Neurosci.* *7*, 596–604.

Heinrich, C., Lähtinen, S., Suzuki, F., Anne-Marie, L., Huber, S., Häussler, U., Haas, C., Larmet, Y., Castren, E., and Depaulis, A. (2011). Increase in BDNF-mediated TrkB signaling promotes epileptogenesis in a mouse model of mesial temporal lobe epilepsy. *Neurobiol. Dis.* *42*, 35–47.

Helgager, J., Huang, Y.Z., and Mcnamara, J.O. (2014). Brain-derived neurotrophic factor but not vesicular zinc promotes TrkB activation within mossy fibers of mouse hippocampus in vivo. *J. Comp. Neurol.* *522*, 3885–3899.

Hepburn, L., Prajsnar, T.K., Klapholz, C., Moreno, P., Loynes, C.A., Ogryzko, N.V., Brown, K., Schiebler, M., Hegyi, K., Antrobus, R., et al. (2014). A Spaetzle-like role for Nerve Growth Factor β in vertebrate immunity to *Staphylococcus aureus*. *Science* *346*, 641–646.

Hexner, E., Roboz, G., Hoffman, R., Luger, S., Mascarenhas, J., Carroll, M., Clementi, R., Bensen-Kennedy, D., and Moliterno, A. (2014). Open-label study

of oral CEP-701 (lestaurtinib) in patients with polycythaemia vera or essential thrombocythaemia with JAK2-V617F mutation. *Br. J. Haematol.* *164*, 83–93.

Heyman, E., Gamelin, F.-X., Goekint, M., Piscitelli, F., Roelands, B., Leclair, E., Di Marzo, V., and Meeusen, R. (2012). Intense exercise increases circulating endocannabinoid and BDNF levels in humans--possible implications for reward and depression. *Psychoneuroendocrinology* *37*, 844–851.

Holtzman, D.M., Li, Y., Parada, L.F., Kinsman, S., Chen, C.K., Valletta, J.S., Zhou, J., Long, J.B., and Mobley, W.C. (1992). p140trk mRNA marks NGF-responsive forebrain neurons: evidence that trk gene expression is induced by NGF. *Neuron* *9*, 465–478.

Howells, D.W., Porritt, M.J., Wong, J.Y., Batchelor, P.E., Kalnins, R., Hughes, A.J., and Donnan, G.A. (2000). Reduced BDNF mRNA expression in the Parkinson's disease substantia nigra. *Exp. Neurol.* *166*, 127–135.

Hu, Y., Wang, Y., Guo, T., Wei, W., Sun, C., Zhang, L., and Huang, J. (2007). Identification of brain-derived neurotrophic factor as a novel angiogenic protein in multiple myeloma. *Cancer Genet. Cytogenet.* *178*, 1–10.

Huang, Y.Z., Pan, E., Xiong, Z.-Q., and McNamara, J.O. (2008). Zinc-mediated transactivation of TrkB potentiates the hippocampal mossy fiber-CA3 pyramid synapse. *Neuron* *57*, 546–558.

Hutchison, M.R. (2013). Mice with a conditional deletion of the neurotrophin receptor TrkB are dwarfed, and are similar to mice with a MAPK14 deletion. *PLoS One* *8*, e66206.

Hyman, S.E. (2005). Addiction: A Disease of Learning and Memory. *Am. J. Psychiatry* *162*, 1414–1422.

Hyman, C., Hofer, M., Barde, Y.-A., Juhasz, M., Yancopoulos, G.D., Squinto, S.P., and Lindsay, R.M. (1991). BDNF is a neurotrophic factor for dopaminergic neurons of the substantia nigra. *Nature* *350*, 230–232.

Indo, Y. (2010). Nerve growth factor, pain, itch and inflammation: lessons from congenital insensitivity to pain with anhidrosis. *Expert Rev. Neurother.* *10*, 1707–1724.

Inoue, K., Tsuda, M., and Tozaki-Saitoh, H. (2007). Modification of neuropathic pain sensation through microglial ATP receptors. *Purinergic Signal.* *3*, 311–316.

Ip, N.Y., Ibáñez, C.F., Nye, S.H., McClain, J., Jones, P.F., Gies, D.R., Belluscio, L., Le Beau, M.M., Espinosa, R., and Squinto, S.P. (1992).

Mammalian neurotrophin-4: structure, chromosomal localization, tissue distribution, and receptor specificity. *Proc. Natl. Acad. Sci. U. S. A.* *89*, 3060–3064.

Jack Jr, C.R., Knopman, D.S., Jagust, W.J., Shaw, L.M., Aisen, P.S., Weiner, M.W., Petersen, R.C., and Trojanowski, J.Q. (2010). Hypothetical model of dynamic biomarkers of the Alzheimer's pathological cascade. *Lancet Neurol.* *9*, 119–128.

Jacobi, F., Rosi, S., Faravelli, C., Goodwin, R., Arbabzadeh-Bouchez, S., and Lépine, J.-P. (2005). The Epidemiology of Mood Disorders. In *Mood Disorders*, E.J.L. Griez, C. Faravelli, D.J. Nutt, and J. Zohar, eds. (John Wiley & Sons, Ltd), pp. 1–34.

Jadhav, T., Geetha, T., Jiang, J., and Wooten, M.W. (2008). Identification of a consensus site for TRAF6/p62 polyubiquitination. *Biochem. Biophys. Res. Commun.* *371*, 521–524.

Jang, S.-W., Liu, X., Chan, C.-B., Weinshenker, D., Hall, R.A., Xiao, G., and Ye, K. (2009). Amitriptyline is a TrkA and TrkB Receptor Agonist that Promotes TrkA/TrkB Heterodimerization and Has Potent Neurotrophic Activity. *Chem. Biol.* *16*, 644–656.

Jang, S.-W., Liu, X., Yepes, M., Shepherd, K.R., Miller, G.W., Liu, Y., Wilson, W.D., Xiao, G., Blanchi, B., Sun, Y.E., et al. (2010). A selective TrkB agonist with potent neurotrophic activities by 7,8-dihydroxyflavone. *Proc. Natl. Acad. Sci. U. S. A.* *107*, 2687–2692.

Jankovic, J. (2008). Parkinson's disease: clinical features and diagnosis. *J. Neurol. Neurosurg. Psychiatry* *79*, 368–376.

Jerónimo-Santos, A., Vaz, S.H., Parreira, S., Rapaz-Lérias, S., Caetano, A.P., Buée-Scherrer, V., Castrén, E., Valente, C.A., Blum, D., Sebastião, A.M., et al. (2014). Dysregulation of TrkB Receptors and BDNF Function by Amyloid- β Peptide is Mediated by Calpain. *Cereb. Cortex N. Y. N* *1991*.

Ji, R.-R., Samad, T.A., Jin, S.-X., Schmoll, R., and Woolf, C.J. (2002). p38 MAPK Activation by NGF in Primary Sensory Neurons after Inflammation Increases TRPV1 Levels and Maintains Heat Hyperalgesia. *Neuron* *36*, 57–68.

Jing, S., Tapley, P., and Barbacid, M. (1992). Nerve growth factor mediates signal transduction through trk homodimer receptors. *Neuron* *9*, 1067–1079.

Johnson, S.B., Blum, R.W., and Giedd, J.N. (2009). Adolescent Maturity and the Brain: The Promise and Pitfalls of Neuroscience Research in Adolescent Health Policy. *J. Adolesc. Health Off. Publ. Soc. Adolesc. Med.* *45*, 216–221.

Kaplan, D.R., Matsumoto, K., Lucarelli, E., and Thiele, C.J. (1993). Induction of TrkB by retinoic acid mediates biologic responsiveness to BDNF and differentiation of human neuroblastoma cells. *Eukaryotic Signal Transduction Group. Neuron* *11*, 321–331.

Kasemeier-Kulesa, J.C., Morrison, J.A., Lefcort, F., and Kulesa, P.M. (2015). TrkB/BDNF signalling patterns the sympathetic nervous system. *Nat. Commun.* *6*, 8281.

Katz, N., Borenstein, D.G., Birbara, C., Bramson, C., Nemeth, M.A., Smith, M.D., and Brown, M.T. (2011). Efficacy and safety of tanezumab in the treatment of chronic low back pain. *Pain* *152*, 2248–2258.

Kawamoto, K., Aoki, J., Tanaka, A., Itakura, A., Hosono, H., Arai, H., Kiso, Y., and Matsuda, H. (2002). Nerve Growth Factor Activates Mast Cells Through the Collaborative Interaction with Lysophosphatidylserine Expressed on the Membrane Surface of Activated Platelets. *J. Immunol.* *168*, 6412–6419.

Kemppainen, S., Rantamäki, T., Jerónimo-Santos, A., Lavasseur, G., Autio, H., Karpova, N., Kärkkäinen, E., Stavén, S., Miranda, H.V., Outeiro, T.F., et al. (2012). Impaired TrkB receptor signaling contributes to memory impairment in APP/PS1 mice. *Neurobiol. Aging* *33*, 1122.e23-1122.e39.

Kermani, P., Rafii, D., Jin, D.K., Whitlock, P., Schaffer, W., Chiang, A., Vincent, L., Friedrich, M., Shido, K., Hackett, N.R., et al. (2005). Neurotrophins promote revascularization by local recruitment of TrkB+ endothelial cells and systemic mobilization of hematopoietic progenitors. *J. Clin. Invest.* *115*, 653–663.

Kerr, B.J., Souslova, V., McMahon, S.B., and Wood, J.N. (2001). A role for the TTX-resistant sodium channel Nav 1.8 in NGF-induced hyperalgesia, but not neuropathic pain. *Neuroreport* *12*, 3077–3080.

Khan, N., and Smith, M.T. (2015). Neurotrophins and Neuropathic Pain: Role in Pathobiology. *Molecules* *20*, 10657–10688.

Kim, S.-E., Ko, I.-G., Shin, M.-S., Kim, C.-J., Jin, B.-K., Hong, H.-P., and Jee, Y.-S. (2013). Treadmill exercise and wheel exercise enhance expressions of neurotrophic factors in the hippocampus of lipopolysaccharide-injected rats. *Neurosci. Lett.* *538*, 54–59.

Kim, S.-H., Tokarski, J.S., Leavitt, K.J., Fink, B.E., Salvati, M.E., Moquin, R., Obermeier, M.T., Trainor, G.L., Vite, G.G., Stadnick, L.K., et al. (2008). Identification of 2-amino-5-(thioaryl)thiazoles as inhibitors of nerve growth factor receptor TrkA. *Bioorg. Med. Chem. Lett.* *18*, 634–639.

Klein, R., Parada, L.F., Coulier, F., and Barbacid, M. (1989). *trkB*, a novel tyrosine protein kinase receptor expressed during mouse neural development. *EMBO J.* *8*, 3701–3709.

Klein, R., Conway, D., Parada, L.F., and Barbacid, M. (1990a). The *trkB* tyrosine protein kinase gene codes for a second neurogenic receptor that lacks the catalytic kinase domain. *Cell* *61*, 647–656.

Klein, R., Martin-Zanca, D., Barbacid, M., and Parada, L.F. (1990b). Expression of the tyrosine kinase receptor gene *trkB* is confined to the murine embryonic and adult nervous system. *Dev. Camb. Engl.* *109*, 845–850.

Klein, R., Jing, S.Q., Nanduri, V., O'Rourke, E., and Barbacid, M. (1991a). The *trk* proto-oncogene encodes a receptor for nerve growth factor. *Cell* *65*, 189–197.

Klein, R., Nanduri, V., Jing, S., Lamballe, F., Tapley, P., Bryant, S., Cordon-Cardo, C., Jones, K.R., Reichardt, L.F., and Barbacid, M. (1991b). The *trkB* Tyrosine Protein Kinase Is a Receptor for Brain-Derived Neurotrophic Factor and Neurotrophin-3. *Cell* *66*, 395–403.

Klein, R., Lamballe, F., Bryant, S., and Barbacid, M. (1992). The *trkB* tyrosine protein kinase is a receptor for neurotrophin-4. *Neuron* *8*, 947–956.

Klein, R., Smeyne, R.J., Wurst, W., Long, L.K., Auerbach, B.A., Joyner, A.L., and Barbacid, M. (1993). Targeted disruption of the *trkB* neurotrophin receptor gene results in nervous system lesions and neonatal death. *Cell* *75*, 113–122.

Kogner, P., Barbany, G., Dominici, C., Castello, M.A., Raschellá, G., and Persson, H. (1993). Coexpression of messenger RNA for TRK protooncogene and low affinity nerve growth factor receptor in neuroblastoma with favorable prognosis. *Cancer Res.* *53*, 2044–2050.

Korte, M., Carroll, P., Wolf, E., Brem, G., Thoenen, H., and Bonhoeffer, T. (1995). Hippocampal long-term potentiation is impaired in mice lacking brain-derived neurotrophic factor. *Proc. Natl. Acad. Sci.* *92*, 8856–8860.

Kovalchuk, Y., Hanse, E., Kafitz, K.W., and Konnerth, A. (2002). Postsynaptic Induction of BDNF-Mediated Long-Term Potentiation. *Science* *295*, 1729–1734.

Kruk, J.S., Vasefi, M.S., Heikkila, J.J., and Beazely, M.A. (2013). Reactive oxygen species are required for 5-HT-induced transactivation of neuronal platelet-derived growth factor and TrkB receptors, but not for ERK1/2 activation. *PLoS One* *8*, e77027.

Kulakowski, S.A., Parker, S.D., and Personius, K.E. (2011). Reduced TrkB expression results in precocious age-like changes in neuromuscular structure, neurotransmission, and muscle function. *J. Appl. Physiol.* *111*, 844–852.

Kuramoto, S., Yasuhara, T., Agari, T., Kondo, A., Jing, M., Kikuchi, Y., Shinko, A., Wakamori, T., Kameda, M., Wang, F., et al. (2011). BDNF-secreting capsule exerts neuroprotective effects on epilepsy model of rats. *Brain Res.* *1368*, 281–289.

Lai, K.-O., Wong, A.S.L., Cheung, M.-C., Xu, P., Liang, Z., Lok, K.-C., Xie, H., Palko, M.E., Yung, W.-H., Tessarollo, L., et al. (2012). TrkB phosphorylation by Cdk5 is required for activity-dependent structural plasticity and spatial memory. *Nat. Neurosci.* *15*, 1506–1515.

Lamballe, F., Klein, R., and Barbacid, M. (1991). *trkC*, a new member of the *trk* family of tyrosine protein kinases, is a receptor for neurotrophin-3. *Cell* *66*, 967–979.

Lazaridis, I., Charalampopoulos, I., Alexaki, V.-I., Avlonitis, N., Padiaditakis, I., Efstathopoulos, P., Calogeropoulou, T., Castanas, E., and Gravanis, A. (2011). Neurosteroid dehydroepiandrosterone interacts with nerve growth factor (NGF) receptors, preventing neuronal apoptosis. *PLoS Biol.* *9*, e1001051.

Lee, F.S., and Chao, M.V. (2001). Activation of Trk neurotrophin receptors in the absence of neurotrophins. *Proc. Natl. Acad. Sci. U. S. A.* *98*, 3555–3560.

Lee, F.S., Rajagopal, R., Kim, A.H., Chang, P.C., and Chao, M.V. (2002). Activation of Trk neurotrophin receptor signaling by pituitary adenylate cyclase-activating polypeptides. *J. Biol. Chem.* *277*, 9096–9102.

Lee, R., Kermani, P., Teng, K.K., and Hempstead, B.L. (2001). Regulation of cell survival by secreted proneurotrophins. *Science* *294*, 1945–1948.

Leon, A., Buriani, A., Dal Toso, R., Fabris, M., Romanello, S., Aloe, L., and Levi-Montalcini, R. (1994). Mast cells synthesize, store, and release nerve growth factor. *Proc. Natl. Acad. Sci. U. S. A.* *91*, 3739–3743.

Levi-Montalcini, R. (1987). The nerve growth factor 35 years later. *Science* *237*, 1154–1162.

Li, S.-S., Liu, J.-J., Wang, S., Tang, Q.-L., Liu, B.-B., and Yang, X.-M. (2014). Clinical significance of TrkB expression in nasopharyngeal carcinoma. *Oncol. Rep.* *31*, 665–672.

Li, Y., Luikart, B.W., Birnbaum, S., Chen, J., Kwon, C.-H., Kernie, S.G., Bassel-Duby, R., and Parada, L.F. (2008). TrkB regulates hippocampal

neurogenesis and governs sensitivity to antidepressive treatment. *Neuron* 59, 399–412.

Li, Z., Chang, Z., Chiao, L.J., Kang, Y., 'an, Xia, Q., Zhu, C., Fleming, J.B., Evans, D.B., and Chiao, P.J. (2009). TrkB1 induces liver metastasis of pancreatic cancer cells by sequestering Rho GDP dissociation inhibitor and promoting RhoA activation. *Cancer Res.* 69, 7851–7859.

Li, Z., Zhang, Y., Tong, Y., Tong, J., and Thiele, C.J. (2015). Trk inhibitor attenuates the BDNF/TrkB-induced protection of neuroblastoma cells from etoposide in vitro and in vivo. *Cancer Biol. Ther.* 16, 477–483.

Lin, Y.-T., Ro, L.-S., Wang, H.-L., and Chen, J.-C. (2011). Up-regulation of dorsal root ganglia BDNF and trkB receptor in inflammatory pain: an in vivo and in vitro study. *J. Neuroinflammation* 8, 126.

Lindholm, D., Heumann, R., Meyer, M., and Thoenen, H. (1987). Interleukin-1 regulates synthesis of nerve growth factor in non-neuronal cells of rat sciatic nerve. *Nature* 330, 658–659.

Lindsay, R.M., and Harmor, A.J. (1989). Nerve growth factor regulates expression of neuropeptide genes in adult sensory neurons. *Nature* 337, 362–364.

Liot, G., Zala, D., Pla, P., Mottet, G., Piel, M., and Saudou, F. (2013). Mutant Huntingtin Alters Retrograde Transport of TrkB Receptors in Striatal Dendrites. *J. Neurosci.* 33, 6298–6309.

Liu, G., Gu, B., He, X.-P., Joshi, R.B., Wackerle, H.D., Rodriguiz, R.M., Wetsel, W.C., and McNamara, J.O. (2013). Transient Inhibition of TrkB Kinase Following Status Epilepticus Prevents Development of Temporal Lobe Epilepsy. *Neuron* 79, 31–38.

Liu, Y., Rutlin, M., Huang, S., Barrick, C.A., Wang, F., Jones, K.R., Tessarollo, L., and Ginty, D.D. (2012). Sexually Dimorphic BDNF Signaling Directs Sensory Innervation of the Mammary Gland. *Science* 338, 1357–1360.

Longo, F.M., and Massa, S.M. (2013). Small-molecule modulation of neurotrophin receptors: a strategy for the treatment of neurological disease. *Nat. Rev. Drug Discov.* 12, 507–525.

Lu, L., Dempsey, J., Liu, S.Y., Bossert, J.M., and Shaham, Y. (2004). A single infusion of brain-derived neurotrophic factor into the ventral tegmental area induces long-lasting potentiation of cocaine seeking after withdrawal. *J. Neurosci. Off. J. Soc. Neurosci.* 24, 1604–1611.

Mantyh, W.G., Jimenez-Andrade, J.M., Stake, J.I., Bloom, A.P., Kaczmarska, M.J., Taylor, R.N., Freeman, K.T., Ghilardi, J.R., Kuskowski, M.A., and Mantyh, P.W. (2010). Blockade of nerve sprouting and neuroma formation markedly attenuates the development of late stage cancer pain. *Neuroscience* *171*, 588–598.

Marshall, C.J. (1995). Specificity of receptor tyrosine kinase signaling: Transient versus sustained extracellular signal-regulated kinase activation. *Cell* *80*, 179–185.

Martin, K.J., Shpiro, N., Traynor, R., Elliott, M., and Arthur, J.S.C. (2011). Comparison of the specificity of Trk inhibitors in recombinant and neuronal assays. *Neuropharmacology* *61*, 148–155.

Martin-Zanca, D., Hughes, S.H., and Barbacid, M. (1986). A human oncogene formed by the fusion of truncated tropomyosin and protein tyrosine kinase sequences. *Nature* *319*, 743–748.

Martin-Zanca, D., Oskam, R., Mitra, G., Copeland, T., and Barbacid, M. (1989). Molecular and biochemical characterization of the human trk proto-oncogene. *Mol. Cell. Biol.* *9*, 24–33.

Martin-Zanca, D., Barbacid, M., and Parada, L.F. (1990). Expression of the trk proto-oncogene is restricted to the sensory cranial and spinal ganglia of neural crest origin in mouse development. *Genes Dev.* *4*, 683–694.

Martínez, A., Alcántara, S., Borrell, V., Río, J.A.D., Blasi, J., Otal, R., Campos, N., Boronat, A., Barbacid, M., Silos-Santiago, I., et al. (1998). TrkB and TrkC Signaling Are Required for Maturation and Synaptogenesis of Hippocampal Connections. *J. Neurosci.* *18*, 7336–7350.

Massa, S.M., Yang, T., Xie, Y., Shi, J., Bilgen, M., Joyce, J.N., Nehama, D., Rajadas, J., and Longo, F.M. (2010). Small molecule BDNF mimetics activate TrkB signaling and prevent neuronal degeneration in rodents. *J. Clin. Invest.* *120*, 1774–1785.

Mathi, S.K., Chan, J., and Watt, V.M. (1995). Insulin receptor-related receptor messenger ribonucleic acid: quantitative distribution and localization to subpopulations of epithelial cells in stomach and kidney. *Endocrinology* *136*, 4125–4132.

Matsumoto, K., Wada, R.K., Yamashiro, J.M., Kaplan, D.R., and Thiele, C.J. (1995). Expression of brain-derived neurotrophic factor and p145TrkB affects survival, differentiation, and invasiveness of human neuroblastoma cells. *Cancer Res.* *55*, 1798–1806.

Mazzaro, N., Barini, E., Spillantini, M.G., Goedert, M., Medini, P., and Gasparini, L. (2016). Tau-Driven Neuronal and Neurotrophic Dysfunction in a Mouse Model of Early Tauopathy. *J. Neurosci. Off. J. Soc. Neurosci.* *36*, 2086–2100.

McCarthy, C., and Walker, E. (2014). Tropomyosin receptor kinase inhibitors: a patent update 2009 - 2013. *Expert Opin. Ther. Pat.* *24*, 731–744.

McKelvey, L., Shorten, G.D., and O’Keeffe, G.W. (2013). Nerve growth factor-mediated regulation of pain signalling and proposed new intervention strategies in clinical pain management. *J. Neurochem.* *124*, 276–289.

McLean, C.A., Cherny, R.A., Fraser, F.W., Fuller, S.J., Smith, M.J., Konrad Vbeyreuther, Bush, A.I., and Masters, C.L. (1999). Soluble pool of A β amyloid as a determinant of severity of neurodegeneration in Alzheimer’s disease. *Ann. Neurol.* *46*, 860–866.

Mcmahon, S.B., Bennett, D.L.H., Priestley, J.V., and Shelton, D.L. (1995). The biological effects of endogenous nerve growth factor on adult sensory neurons revealed by a trkA-IgG fusion molecule. *Nat. Med.* *1*, 774–780.

Meakin, S.O., MacDonald, J.I.S., Gryz, E.A., Kubu, C.J., and Verdi, J.M. (1999). The Signaling Adapter FRS-2 Competes with Shc for Binding to the Nerve Growth Factor Receptor TrkA A MODEL FOR DISCRIMINATING PROLIFERATION AND DIFFERENTIATION. *J. Biol. Chem.* *274*, 9861–9870.

Melo, C.V., Mele, M., Curcio, M., Comprido, D., Silva, C.G., and Duarte, C.B. (2013). BDNF Regulates the Expression and Distribution of Vesicular Glutamate Transporters in Cultured Hippocampal Neurons. *PLOS ONE* *8*, e53793.

de Melo-Jorge, M., and PereiraPerrin, M. (2007). The Chagas’ disease parasite Trypanosoma cruzi exploits nerve growth factor receptor TrkA to infect mammalian hosts. *Cell Host Microbe* *1*, 251–261.

Middlemas, D.S., Lindberg, R.A., and Hunter, T. (1991). trkB, a neural receptor protein-tyrosine kinase: evidence for a full-length and two truncated receptors. *Mol. Cell. Biol.* *11*, 143–153.

Ming, G., Song, H., Berninger, B., Inagaki, N., Tessier-Lavigne, M., and Poo, M. (1999). Phospholipase C- γ and Phosphoinositide 3-Kinase Mediate Cytoplasmic Signaling in Nerve Growth Cone Guidance. *Neuron* *23*, 139–148.

Minichiello, L., Korte, M., Wolfner, D., Kühn, R., Unsicker, K., Cestari, V., Rossi-Arnaud, C., Lipp, H.-P., Bonhoeffer, T., and Klein, R. (1999). Essential

Role for TrkB Receptors in Hippocampus-Mediated Learning. *Neuron* 24, 401–414.

Minichiello, L., Calella, A.M., Medina, D.L., Bonhoeffer, T., Klein, R., and Korte, M. (2002). Mechanism of TrkB-mediated hippocampal long-term potentiation. *Neuron* 36, 121–137.

Minturn, J.E., Evans, A.E., Villablanca, J.G., Yanik, G.A., Park, J.R., Shusterman, S., Groshen, S., Hellriegel, E.T., Bensen-Kennedy, D., Matthay, K.K., et al. (2011). Phase I trial of lestaurtinib for children with refractory neuroblastoma: a new approaches to neuroblastoma therapy consortium study. *Cancer Chemother. Pharmacol.* 68, 1057–1065.

Miyamoto, Y., Yamauchi, J., Tanoue, A., Wu, C., and Mobley, W.C. (2006). TrkB binds and tyrosine-phosphorylates Tiam1, leading to activation of Rac1 and induction of changes in cellular morphology. *Proc. Natl. Acad. Sci. U. S. A.* 103, 10444–10449.

Mogi, M., Togari, A., Kondo, T., Mizuno, Y., Komure, O., Kuno, S., Ichinose, H., and Nagatsu, T. (1999). Brain-derived growth factor and nerve growth factor concentrations are decreased in the substantia nigra in Parkinson's disease. *Neurosci. Lett.* 270, 45–48.

Monteggia, L.M., Barrot, M., Powell, C.M., Berton, O., Galanis, V., Gemelli, T., Meuth, S., Nagy, A., Greene, R.W., and Nestler, E.J. (2004). Essential role of brain-derived neurotrophic factor in adult hippocampal function. *Proc. Natl. Acad. Sci. U. S. A.* 101, 10827–10832.

Moscatelli, I., Pierantozzi, E., Camaioni, A., Siracusa, G., and Campagnolo, L. (2009). p75 neurotrophin receptor is involved in proliferation of undifferentiated mouse embryonic stem cells. *Exp. Cell Res.* 315, 3220–3232.

Nakagawara, A., Arima-Nakagawara, M., Scavarda, N.J., Azar, C.G., Cantor, A.B., and Brodeur, G.M. (1993). Association between high levels of expression of the TRK gene and favorable outcome in human neuroblastoma. *N. Engl. J. Med.* 328, 847–854.

Nakagawara, A., Azar, C.G., Scavarda, N.J., and Brodeur, G.M. (1994). Expression and function of TRK-B and BDNF in human neuroblastomas. *Mol. Cell. Biol.* 14, 759–767.

Nakagawara, A., Liu, X.G., Ikegaki, N., White, P.S., Yamashiro, D.J., Nycum, L.M., Biegel, J.A., and Brodeur, G.M. (1995). Cloning and chromosomal localization of the human TRK-B tyrosine kinase receptor gene (NTRK2). *Genomics* 25, 538–546.

Nakamura, K., Martin, K.C., Jackson, J.K., Beppu, K., Woo, C.-W., and Thiele, C.J. (2006). Brain-derived neurotrophic factor activation of TrkB induces vascular endothelial growth factor expression via hypoxia-inducible factor-1alpha in neuroblastoma cells. *Cancer Res.* 66, 4249–4255.

Nakamura, T., Komiya, M., Sone, K., Hirose, E., Gotoh, N., Morii, H., Ohta, Y., and Mori, N. (2002). Grit, a GTPase-activating protein for the Rho family, regulates neurite extension through association with the TrkA receptor and N-Shc and CrkL/Crk adapter molecules. *Mol. Cell. Biol.* 22, 8721–8734.

Narisawa-Saito, M., Iwakura, Y., Kawamura, M., Araki, K., Kozaki, S., Takei, N., and Nawa, H. (2002). Brain-derived Neurotrophic Factor Regulates Surface Expression of α -Amino-3-hydroxy-5-methyl-4-isoxazolepropionic Acid Receptors by Enhancing the N-Ethylmaleimide-sensitive Factor/GluR2 Interaction in Developing Neocortical Neurons. *J. Biol. Chem.* 277, 40901–40910.

Näslund J, Haroutunian V, Mohs R, and et al (2000). Correlation between elevated levels of amyloid β -peptide in the brain and cognitive decline. *JAMA* 283, 1571–1577.

Nassenstein, C., Braun, A., Erpenbeck, V.J., Lommatzsch, M., Schmidt, S., Krug, N., Luttmann, W., Renz, H., and Virchow, J.C. (2003). The Neurotrophins Nerve Growth Factor, Brain-derived Neurotrophic Factor, Neurotrophin-3, and Neurotrophin-4 Are Survival and Activation Factors for Eosinophils in Patients with Allergic Bronchial Asthma. *J. Exp. Med.* 198, 455–467.

Nawa, H., Carnahan, J., and Gall, C. (1995). BDNF protein measured by a novel enzyme immunoassay in normal brain and after seizure: partial disagreement with mRNA levels. *Eur. J. Neurosci.* 7, 1527–1535.

Nguyen, K.Q., Rymar, V.V., and Sadikot, A.F. (2016). Impaired TrkB Signaling Underlies Reduced BDNF-Mediated Trophic Support of Striatal Neurons in the R6/2 Mouse Model of Huntington's Disease. *Front. Cell. Neurosci.* 10.

Nibuya, M., Morinobu, S., and Duman, R.S. (1995). Regulation of BDNF and trkB mRNA in rat brain by chronic electroconvulsive seizure and antidepressant drug treatments. *J. Neurosci. Off. J. Soc. Neurosci.* 15, 7539–7547.

Nikoletopoulou, V., Lickert, H., Frade, J.M., Rencurel, C., Giallonardo, P., Zhang, L., Bibel, M., and Barde, Y.-A. (2010). Neurotrophin receptors TrkA and TrkC cause neuronal death whereas TrkB does not. *Nature* 467, 59–63.

Ninkina, N., Grashchuck, M., Buchman, V.L., and Davies, A.M. (1997). TrkB variants with deletions in the leucine-rich motifs of the extracellular domain. *J. Biol. Chem.* *272*, 13019–13025.

Nwosu, L.N., Mapp, P.I., Chapman, V., and Walsh, D.A. (2016). Blocking the tropomyosin receptor kinase A (TrkA) receptor inhibits pain behaviour in two rat models of osteoarthritis. *Ann. Rheum. Dis.* *75*, 1246–1254.

Nykjaer, A., Lee, R., Teng, K.K., Jansen, P., Madsen, P., Nielsen, M.S., Jacobsen, C., Kliemannel, M., Schwarz, E., Willnow, T.E., et al. (2004). Sortilin is essential for proNGF-induced neuronal cell death. *Nature* *427*, 843–848.

Obermeier, A., Halfter, H., Wiesmüller, K.H., Jung, G., Schlessinger, J., and Ullrich, A. (1993). Tyrosine 785 is a major determinant of Trk--substrate interaction. *EMBO J.* *12*, 933–941.

Ohira, K., Shimizu, K., and Hayashi, M. (1999). Change of expression of full-length and truncated TrkB_s in the developing monkey central nervous system. *Dev. Brain Res.* *112*, 21–29.

Ohira, K., Kumanogoh, H., Sahara, Y., Homma, K.J., Hirai, H., Nakamura, S., and Hayashi, M. (2005). A Truncated Tropo-Myosine-Related Kinase B Receptor, T1, Regulates Glial Cell Morphology via Rho GDP Dissociation Inhibitor 1. *J. Neurosci.* *25*, 1343–1353.

Owolabi, J.B., Rizkalla, G., Tehim, A., Ross, G.M., Riopelle, R.J., Kamboj, R., Ossipov, M., Bian, D., Wegert, S., Porreca, F., et al. (1999). Characterization of antiallodynic actions of ALE-0540, a novel nerve growth factor receptor antagonist, in the rat. *J. Pharmacol. Exp. Ther.* *289*, 1271–1276.

Pandya, C.D., Kutiyawalla, A., and Pillai, A. (2013). BDNF-TrkB signaling and neuroprotection in schizophrenia. *Asian J. Psychiatry* *6*, 22–28.

Parain, K., Murer, M.G., Yan, Q., Faucheux, B., Agid, Y., Hirsch, E., and Raisman-Vozari, R. (1999). Reduced expression of brain-derived neurotrophic factor protein in Parkinson's disease substantia nigra. *Neuroreport* *10*, 557–561.

Parikh, V., Kozak, R., Martinez, V., and Sarter, M. (2007). Prefrontal acetylcholine release controls cue detection on multiple time scales. *Neuron* *56*, 141–154.

Parikh, V., Howe, W.M., Welchko, R.M., Naughton, S.X., D'Amore, D.E., Han, D.H., Deo, M., Turner, D.L., and Sarter, M. (2013). Diminished trkA receptor signaling reveals cholinergic-attentional vulnerability of aging. *Eur. J. Neurosci.* *37*, 278–293.

Passiglia, F., Caparica, R., Giovannetti, E., Giallombardo, M., Listi, A., Diana, P., Cirrincione, G., Caglevic, C., Ræz, L.E., Russo, A., et al. (2016). The potential of neurotrophic tyrosine kinase (NTRK) inhibitors for treating lung cancer. *Expert Opin. Investig. Drugs* 25, 385–392.

Patel, A., Yamashita, N., Ascaño, M., Bodmer, D., Boehm, E., Bodkin-Clarke, C., Ryu, Y.K., and Kuruvilla, R. (2015). RCAN1 links impaired neurotrophin trafficking to aberrant development of the sympathetic nervous system in Down syndrome. *Nat. Commun.* 6.

Patterson, S.L., Abel, T., Deuel, T.A.S., Martin, K.C., Rose, J.C., and Kandel, E.R. (1996). Recombinant BDNF Rescues Deficits in Basal Synaptic Transmission and Hippocampal LTP in BDNF Knockout Mice. *Neuron* 16, 1137–1145.

Paves, H., and Saarma, M. (1997). Neurotrophins as in vitro growth cone guidance molecules for embryonic sensory neurons. *Cell Tissue Res.* 290, 285–297.

Peng, S., Wu, J., Mufson, E.J., and Fahnstock, M. (2005). Precursor form of brain-derived neurotrophic factor and mature brain-derived neurotrophic factor are decreased in the pre-clinical stages of Alzheimer's disease. *J. Neurochem.* 93, 1412–1421.

Petrenko, A.G., Zozulya, S.A., Deyev, I.E., and Eladari, D. (2013). Insulin receptor-related receptor as an extracellular pH sensor involved in the regulation of acid-base balance. *Biochim. Biophys. Acta* 1834, 2170–2175.

Pierotti, M.A., Bongarzone, I., Borrello, M.G., Greco, A., Pilotti, S., and Sozzi, G. (1996). Cytogenetics and molecular genetics of carcinomas arising from thyroid epithelial follicular cells. *Genes. Chromosomes Cancer* 16, 1–14.

Pinkstaff, J.K., Chappell, S.A., Mauro, V.P., Edelman, G.M., and Krushel, L.A. (2001). Internal initiation of translation of five dendritically localized neuronal mRNAs. *Proc. Natl. Acad. Sci. U. S. A.* 98, 2770–2775.

Plotkin, J.L., Day, M., Peterson, J.D., Xie, Z., Kress, G.J., Rafalovich, I., Kondapalli, J., Gertler, T.S., Flajolet, M., Greengard, P., et al. (2014). Impaired TrkB receptor signaling underlies corticostriatal dysfunction in Huntington's disease. *Neuron* 83, 178–188.

Poduslo, J.F., and Curran, G.L. (1996). Permeability at the blood-brain and blood-nerve barriers of the neurotrophic factors: NGF, CNTF, NT-3, BDNF. *Brain Res. Mol. Brain Res.* 36, 280–286.

Poon, W.W., Blurton-Jones, M., Tu, C.H., Feinberg, L.M., Chabrier, M.A., Harris, J.W., Jeon, N.L., and Cotman, C.W. (2011). β -Amyloid impairs axonal BDNF retrograde trafficking. *Neurobiol. Aging* 32, 821–833.

Poon, W.W., Carlos, A.J., Aguilar, B.L., Berchtold, N.C., Kawano, C.K., Zograbyan, V., Yaoprake, T., Shelanski, M., and Cotman, C.W. (2013). β -Amyloid (A β) Oligomers Impair Brain-derived Neurotrophic Factor Retrograde Trafficking by Down-regulating Ubiquitin C-terminal Hydrolase, UCH-L1. *J. Biol. Chem.* 288, 16937–16948.

Prencipe, G., Minnone, G., Strippoli, R., Pasquale, L.D., Petrini, S., Caiello, I., Manni, L., Benedetti, F.D., and Bracci-Laudiero, L. (2014). Nerve Growth Factor Downregulates Inflammatory Response in Human Monocytes through TrkA. *J. Immunol.* 192, 3345–3354.

Primiani, C.T., Ryan, V.H., Rao, J.S., Cam, M.C., Ahn, K., Modi, H.R., and Rapoport, S.I. (2014). Coordinated Gene Expression of Neuroinflammatory and Cell Signaling Markers in Dorsolateral Prefrontal Cortex during Human Brain Development and Aging. *PLoS ONE* 9.

Proenca, C.C., Song, M., and Lee, F.S. (2016). Differential effects of BDNF and neurotrophin 4 (NT4) on endocytic sorting of TrkB receptors. *J. Neurochem.* 138, 397–406.

Puehringer, D., Orel, N., Lüningschrör, P., Subramanian, N., Herrmann, T., Chao, M.V., and Sendtner, M. (2013). EGF transactivation of Trk receptors regulates the migration of newborn cortical neurons. *Nat. Neurosci.* 16, 407–415.

Pyle, A.D., Lock, L.F., and Donovan, P.J. (2006). Neurotrophins mediate human embryonic stem cell survival. *Nat. Biotechnol.* 24, 344–350.

Rafii, M.S., Baumann, T.L., Bakay, R.A.E., Ostrove, J.M., Siffert, J., Fleisher, A.S., Herzog, C.D., Barba, D., Pay, M., Salmon, D.P., et al. (2014). A phase I study of stereotactic gene delivery of AAV2-NGF for Alzheimer's disease. *Alzheimers Dement. J. Alzheimers Assoc.* 10, 571–581.

Rantamäki, T., and Yalcin, I. (2016). Antidepressant drug action--From rapid changes on network function to network rewiring. *Prog. Neuropsychopharmacol. Biol. Psychiatry* 64, 285–292.

Rantamäki, T., Hendolin, P., Kankaanpää, A., Mijatovic, J., Piepponen, P., Domenici, E., Chao, M.V., Männistö, P.T., and Castrén, E. (2007). Pharmacologically diverse antidepressants rapidly activate brain-derived neurotrophic factor receptor TrkB and induce phospholipase-Cgamma signaling pathways in mouse brain. *Neuropsychopharmacol. Off. Publ. Am. Coll. Neuropsychopharmacol.* 32, 2152–2162.

Rantamäki, T., Vesa, L., Antila, H., Di Lieto, A., Tammela, P., Schmitt, A., Lesch, K.-P., Rios, M., and Castrén, E. (2011). Antidepressant drugs transactivate TrkB neurotrophin receptors in the adult rodent brain independently of BDNF and monoamine transporter blockade. *PloS One* 6, e20567.

Rantamäki, T., Kemppainen, S., Autio, H., Stavén, S., Koivisto, H., Kojima, M., Antila, H., Miettinen, P.O., Kärkkäinen, E., Karpova, N., et al. (2013). The impact of Bdnf gene deficiency to the memory impairment and brain pathology of APP^{swe}/PS1^{dE9} mouse model of Alzheimer's disease. *PloS One* 8, e68722.

Reibel, S., Larmet, Y., Lê, B.-T., Carnahan, J., Marescaux, C., and Depaulis, A. (2000). Brain-derived neurotrophic factor delays hippocampal kindling in the rat. *Neuroscience* 100, 777–788.

Reinhardt, R.R., Chin, E., Zhang, B., Roth, R.A., and Bondy, C.A. (1994). Selective coexpression of insulin receptor-related receptor (IRR) and TRK in NGF-sensitive neurons. *J. Neurosci. Off. J. Soc. Neurosci.* 14, 4674–4683.

Ren, Q., Ma, M., Yang, C., Zhang, J.-C., Yao, W., and Hashimoto, K. (2015). BDNF–TrkB signaling in the nucleus accumbens shell of mice has key role in methamphetamine withdrawal symptoms. *Transl. Psychiatry* 5, e666.

Ren, Q., Ma, M., Ishima, T., Morisseau, C., Yang, J., Wagner, K.M., Zhang, J.-C., Yang, C., Yao, W., Dong, C., et al. (2016). Gene deficiency and pharmacological inhibition of soluble epoxide hydrolase confers resilience to repeated social defeat stress. *Proc. Natl. Acad. Sci. U. S. A.* 113, E1944–1952.

Riccio, A., Pierchala, B.A., Ciarallo, C.L., and Ginty, D.D. (1997). An NGF-TrkA-Mediated Retrograde Signal to Transcription Factor CREB in Sympathetic Neurons. *Science* 277, 1097–1100.

Rivera, C., Li, H., Thomas-Crusells, J., Lahtinen, H., Viitanen, T., Nanobashvili, A., Kokaia, Z., Airaksinen, M.S., Voipio, J., Kaila, K., et al. (2002). BDNF-induced TrkB activation down-regulates the K⁺–Cl[–] cotransporter KCC2 and impairs neuronal Cl[–] extrusion. *J. Cell Biol.* 159, 747–752.

Rivera, C., Voipio, J., Thomas-Crusells, J., Li, H., Emri, Z., Sipilä, S., Payne, J.A., Minichiello, L., Saarma, M., and Kaila, K. (2004). Mechanism of activity-dependent downregulation of the neuron-specific K–Cl cotransporter KCC2. *J. Neurosci. Off. J. Soc. Neurosci.* 24, 4683–4691.

Roblin, D., Yosipovitch, G., Boyce, B., Robinson, J., Sandy, J., Mainero, V., Wickramasinghe, R., Anand, U., and Anand, P. (2015). Topical TrkA Kinase Inhibitor CT327 is an Effective, Novel Therapy for the Treatment of Pruritus due to Psoriasis: Results from Experimental Studies, and Efficacy and Safety of

CT327 in a Phase 2b Clinical Trial in Patients with Psoriasis. *Acta Derm. Venereol.* *95*, 542–548.

Rolfo, C., Ruiz, R., Giovannetti, E., Gil-Bazo, I., Russo, A., Passiglia, F., Giallombardo, M., Peeters, M., and Raez, L. (2015). Entrectinib: a potent new TRK, ROS1, and ALK inhibitor. *Expert Opin. Investig. Drugs* *24*, 1493–1500.

Romanczyk, T.B., Weickert, C.S., Webster, M.J., Herman, M.M., Akil, M., and Kleinman, J.E. (2002). Alterations in *trkB* mRNA in the human prefrontal cortex throughout the lifespan. *Eur. J. Neurosci.* *15*, 269–280.

Roos, R.A. (2010). Huntington's disease: a clinical review. *Orphanet J. Rare Dis.* *5*, 40.

Rose, C.R., Blum, R., Pichler, B., Lepier, A., Kafitz, K.W., and Konnerth, A. (2003). Truncated TrkB-T1 mediates neurotrophin-evoked calcium signalling in glia cells. *Nature* *426*, 74–78.

Ruggeri, P., Farina, A.R., Di Ianni, N., Cappabianca, L., Ragone, M., Ianni, G., Gulino, A., and Mackay, A.R. (2014). The TrkAIII Oncoprotein Inhibits Mitochondrial Free Radical ROS-Induced Death of SH-SY5Y Neuroblastoma Cells by Augmenting SOD2 Expression and Activity at the Mitochondria, within the Context of a Tumour Stem Cell-like Phenotype. *PLoS ONE* *9*.

Rukwied, R., Mayer, A., Kluschina, O., Obreja, O., Schley, M., and Schmelz, M. (2010). NGF induces non-inflammatory localized and lasting mechanical and thermal hypersensitivity in human skin. *Pain* *148*, 407–413.

Russo, M., Misale, S., Wei, G., Siravegna, G., Crisafulli, G., Lazzari, L., Corti, G., Rospo, G., Novara, L., Mussolin, B., et al. (2016). Acquired Resistance to the TRK Inhibitor Entrectinib in Colorectal Cancer. *Cancer Discov.* *6*, 36–44.

Saarelainen, T., Hendolin, P., Lucas, G., Koponen, E., Sairanen, M., MacDonald, E., Agerman, K., Haapasalo, A., Nawa, H., Aloyz, R., et al. (2003). Activation of the TrkB neurotrophin receptor is induced by antidepressant drugs and is required for antidepressant-induced behavioral effects. *J. Neurosci. Off. J. Soc. Neurosci.* *23*, 349–357.

Sadri-Vakili, G., Kumaresan, V., Schmidt, H.D., Famous, K.R., Chawla, P., Vassoler, F.M., Overland, R.P., Xia, E., Bass, C.E., Terwilliger, E.F., et al. (2010). Cocaine-Induced Chromatin Remodeling Increases Brain-Derived Neurotrophic Factor Transcription in the Rat Medial Prefrontal Cortex, Which Alters the Reinforcing Efficacy of Cocaine. *J. Neurosci.* *30*, 11735–11744.

Sahbaie, P., Liang, D.-Y., Shi, X.-Y., Sun, Y., and Clark, J.D. (2016). Epigenetic regulation of spinal cord gene expression contributes to enhanced

postoperative pain and analgesic tolerance subsequent to continuous opioid exposure. *Mol. Pain* 12.

Sandhya, V.K., Raju, R., Verma, R., Advani, J., Sharma, R., Radhakrishnan, A., Nanjappa, V., Narayana, J., Somani, B.L., Mukherjee, K.K., et al. (2013). A network map of BDNF/TRKB and BDNF/p75NTR signaling system. *J. Cell Commun. Signal.* 7, 301–307.

Sariola, H., Saarma, M., Sainio, K., Arumae, U., Palgi, J., Vaahtokari, A., Thesleff, I., and Karavanov, A. (1991). Dependence of kidney morphogenesis on the expression of nerve growth factor receptor. *Science* 254, 571–573.

Scharfman, H.E., Goodman, J.H., Sollas, A.L., and Croll, S.D. (2002). Spontaneous Limbic Seizures after Intrahippocampal Infusion of Brain-Derived Neurotrophic Factor. *Exp. Neurol.* 174, 201–214.

Schecterson, L.C., and Bothwell, M. (1992). Novel roles for neurotrophins are suggested by BDNF and NT-3 mRNA expression in developing neurons. *Neuron* 9, 449–463.

Schlessinger, J., and Ullrich, A. (1992). Growth factor signaling by receptor tyrosine kinases. *Neuron* 9, 383–391.

Schnack, H.G., van Haren, N.E.M., Nieuwenhuis, M., Hulshoff Pol, H.E., Cahn, W., and Kahn, R.S. (2016). Accelerated Brain Aging in Schizophrenia: A Longitudinal Pattern Recognition Study. *Am. J. Psychiatry* 173, 607–616.

Schneider, R., and Schweiger, M. (1991). A novel modular mosaic of cell adhesion motifs in the extracellular domains of the neurogenic trk and trkB tyrosine kinase receptors. *Oncogene* 6, 1807–1811.

Schnitzer, T.J., Lane, N.E., Birbara, C., Smith, M.D., Simpson, S.L., and Brown, M.T. (2011). Long-term open-label study of tanezumab for moderate to severe osteoarthritic knee pain. *Osteoarthr. Cartil. OARS Osteoarthr. Res. Soc.* 19, 639–646.

Sclabas, G.M., Fujioka, S., Schmidt, C., Li, Z., Frederick, W.A.I., Yang, W., Yokoi, K., Evans, D.B., Abbruzzese, J.L., Hess, K.R., et al. (2005). Overexpression of tropomyosin-related kinase B in metastatic human pancreatic cancer cells. *Clin. Cancer Res. Off. J. Am. Assoc. Cancer Res.* 11, 440–449.

Shaikh, S.S., Chen, Y.-C., Halsall, S.-A., Nahorski, M.S., Omoto, K., Young, G.T., Phelan, A., and Woods, C.G. (2016). A Comprehensive Functional Analysis of NTRK1 Missense Mutations Causing Hereditary Sensory and Autonomic Neuropathy Type IV (HSAN IV). *Hum. Mutat.* n/a-n/a.

Sharma, N., Deppmann, C.D., Harrington, A.W., Hillaire, C.S., Chen, Z.-Y., Lee, F., and Ginty, D.D. (2010). Long distance control of synapse assembly by target-derived NGF. *Neuron* 67, 422–434.

Shi, Y., Mantuano, E., Inoue, G., Campana, W.M., and Gonias, S.L. (2009). Ligand binding to LRP1 transactivates Trk receptors by a Src family kinase-dependent pathway. *Sci. Signal.* 2, ra18.

Shirayama, Y., Chen, A.C.-H., Nakagawa, S., Russell, D.S., and Duman, R.S. (2002). Brain-derived neurotrophic factor produces antidepressant effects in behavioral models of depression. *J. Neurosci. Off. J. Soc. Neurosci.* 22, 3251–3261.

Shutov, L.P., Warwick, C.A., Shi, X., Gnanasekaran, A., Shepherd, A.J., Mohapatra, D.P., Woodruff, T.M., Clark, J.D., and Usachev, Y.M. (2016). The Complement System Component C5a Produces Thermal Hyperalgesia via Macrophage-to-Nociceptor Signaling That Requires NGF and TRPV1. *J. Neurosci.* 36, 5055–5070.

Silhol, M., Bonnichon, V., Rage, F., and Tapia-Arancibia, L. (2005). Age-related changes in brain-derived neurotrophic factor and tyrosine kinase receptor isoforms in the hippocampus and hypothalamus in male rats. *Neuroscience* 132, 613–624.

Silos-Santiago, I., Fagan, A.M., Garber, M., Fritsch, B., and Barbacid, M. (1997). Severe Sensory Deficits but Normal CNS Development in Newborn Mice Lacking TrkB and TrkC Tyrosine Protein Kinase Receptors. *Eur. J. Neurosci.* 9, 2045–2056.

Singh, K.K., Park, K.J., Hong, E.J., Kramer, B.M., Greenberg, M.E., Kaplan, D.R., and Miller, F.D. (2008). Developmental axon pruning mediated by BDNF-p75NTR-dependent axon degeneration. *Nat. Neurosci.* 11, 649–658.

Siuciak, J.A., Lewis, D.R., Wiegand, S.J., and Lindsay, R.M. (1997). Antidepressant-like effect of brain-derived neurotrophic factor (BDNF). *Pharmacol. Biochem. Behav.* 56, 131–137.

Smeyne, R.J., Klein, R., Schnapp, A., Long, L.K., Bryant, S., Lewin, A., Lira, S.A., and Barbacid, M. (1994). Severe sensory and sympathetic neuropathies in mice carrying a disrupted Trk/NGF receptor gene. *Nature* 368, 246–249.

Sompol, P., Liu, X., Baba, K., Paul, K.N., Tosini, G., Iuvone, P.M., and Ye, K. (2011). N-acetylserotonin promotes hippocampal neuroprogenitor cell proliferation in sleep-deprived mice. *Proc. Natl. Acad. Sci. U. S. A.* 108, 8844–8849.

Soppet, D., Escandon, E., Maragos, J., Middlemas, D.S., Reid, S.W., Blair, J., Burton, L.E., Stanton, B.R., Kaplan, D.R., Hunter, T., et al. (1991). The neurotrophic factors brain-derived neurotrophic factor and neurotrophin-3 are ligands for the trkB tyrosine kinase receptor. *Cell* 65, 895–903.

Stachel, S.J., Sanders, J.M., Henze, D.A., Rudd, M.T., Su, H.-P., Li, Y., Nanda, K.K., Egbertson, M.S., Manley, P.J., Jones, K.L.G., et al. (2014). Maximizing Diversity from a Kinase Screen: Identification of Novel and Selective pan-Trk Inhibitors for Chronic Pain. *J. Med. Chem.* 57, 5800–5816.

Stein, A.T., Ufret-Vincenty, C.A., Hua, L., Santana, L.F., and Gordon, S.E. (2006). Phosphoinositide 3-kinase binds to TRPV1 and mediates NGF-stimulated TRPV1 trafficking to the plasma membrane. *J. Gen. Physiol.* 128, 509–522.

Stoilov, P., Castren, E., and Stamm, S. (2002). Analysis of the Human TrkB Gene Genomic Organization Reveals Novel TrkB Isoforms, Unusual Gene Length, and Splicing Mechanism. *Biochem. Biophys. Res. Commun.* 290, 1054–1065.

Strohmaier, C., Carter, B.D., Urfer, R., Barde, Y.A., and Dechant, G. (1996). A splice variant of the neurotrophin receptor trkB with increased specificity for brain-derived neurotrophic factor. *EMBO J.* 15, 3332–3337.

Suo, D., Park, J., Harrington, A.W., Zweifel, L.S., Mihalas, S., and Deppmann, C.D. (2014). Coronin-1 is a neurotrophin endosomal effector that is required for developmental competition for survival. *Nat. Neurosci.* 17, 36–45.

Tacconelli, A., Farina, A.R., Cappabianca, L., Desantis, G., Tessitore, A., Vetuschi, A., Sferra, R., Rucci, N., Argenti, B., Screpanti, I., et al. (2004). TrkA alternative splicing: a regulated tumor-promoting switch in human neuroblastoma. *Cancer Cell* 6, 347–360.

Tacconelli, A., Farina, A.R., Cappabianca, L., Cea, G., Panella, S., Chioda, A., Gallo, R., Cinque, B., Sferra, R., Vetuschi, A., et al. (2007). TrkAIII expression in the thymus. *J. Neuroimmunol.* 183, 151–161.

The BDNF Study Group (1999). A controlled trial of recombinant methionyl human BDNF in ALS. *Neurology* 52, 1427–1427.

Thiele, C.J., Li, Z., and McKee, A.E. (2009). On Trk--the TrkB signal transduction pathway is an increasingly important target in cancer biology. *Clin. Cancer Res. Off. J. Am. Assoc. Cancer Res.* 15, 5962–5967.

Thoenen, H., and Barde, Y.A. (1980). Physiology of nerve growth factor. *Physiol. Rev.* 60, 1284–1335.

Thress, K., Macintyre, T., Wang, H., Whitston, D., Liu, Z.-Y., Hoffmann, E., Wang, T., Brown, J.L., Webster, K., Omer, C., et al. (2009). Identification and preclinical characterization of AZ-23, a novel, selective, and orally bioavailable inhibitor of the Trk kinase pathway. *Mol. Cancer Ther.* 8, 1818–1827.

Todd, D., Gowers, I., Dowler, S.J., Wall, M.D., McAllister, G., Fischer, D.F., Dijkstra, S., Fratantoni, S.A., Bospoort, R. van de, Veenman-Koepke, J., et al. (2014). A Monoclonal Antibody TrkB Receptor Agonist as a Potential Therapeutic for Huntington's Disease. *PLOS ONE* 9, e87923.

Tong, L., Balazs, R., Thornton, P.L., and Cotman, C.W. (2004). β -Amyloid Peptide at Sublethal Concentrations Downregulates Brain-Derived Neurotrophic Factor Functions in Cultured Cortical Neurons. *J. Neurosci.* 24, 6799–6809.

Traversa, S., Bagnod, R., Barone, D., Rossa, L.B.R., Fumero, S., Mainero, V., Marconi, A., Oderda, C., Pincelli, C., Lorenzetto, C., et al. (2014). Polymer conjugates of K-252A and derivatives thereof.

Triaca, V., Sposato, V., Bolasco, G., Ciotti, M.T., Pelicci, P., Bruni, A.C., Cupidi, C., Maletta, R., Feligioni, M., Nisticò, R., et al. (2016). NGF controls APP cleavage by downregulating APP phosphorylation at Thr668: relevance for Alzheimer's disease. *Aging Cell* 15, 661–672.

Trivedi, M.H., Rush, A.J., Wisniewski, S.R., Nierenberg, A.A., Warden, D., Ritz, L., Norquist, G., Howland, R.H., Lebowitz, B., McGrath, P.J., et al. (2006). Evaluation of Outcomes With Citalopram for Depression Using Measurement-Based Care in STAR*D: Implications for Clinical Practice. *Am. J. Psychiatry* 163, 28–40.

Tsoufias, P., Soppet, D., Escandon, E., Tessarollo, L., Mendoza-Ramirez, J.L., Rosenthal, A., Nikolic, K., and Parada, L.F. (1993). The rat *trkC* locus encodes multiple neurogenic receptors that exhibit differential response to neurotrophin-3 in PC12 cells. *Neuron* 10, 975–990.

Unsain, N., Nuñez, N., Anastasia, A., and Mascó, D.H. (2008). Status epilepticus induces a TrkB to p75 neurotrophin receptor switch and increases brain-derived neurotrophic factor interaction with p75 neurotrophin receptor: An initial event in neuronal injury induction. *Neuroscience* 154, 978–993.

Vaegter, C.B., Jansen, P., Fjorback, A.W., Glerup, S., Skeldal, S., Kjolby, M., Richner, M., Erdmann, B., Nyengaard, J.R., Tessarollo, L., et al. (2011). Sortilin associates with Trk receptors to enhance anterograde transport and neurotrophin signaling. *Nat. Neurosci.* 14, 54–61.

Vaishnavi, A., Capelletti, M., Le, A.T., Kako, S., Butaney, M., Ercan, D., Mahale, S., Davies, K.D., Aisner, D.L., Pilling, A.B., et al. (2013). Oncogenic

and drug-sensitive NTRK1 rearrangements in lung cancer. *Nat. Med.* *19*, 1469–1472.

Valent, A., Danglot, G., and Bernheim, A. (1997). Mapping of the tyrosine kinase receptors trkA (NTRK1), trkB (NTRK2) and trkC (NTRK3) to human chromosomes 1q22, 9q22 and 15q25 by fluorescence in situ hybridization. *Eur. J. Hum. Genet.* *5*, 102–104.

Valenzuela, D.M., Maisonpierre, P.C., Glass, D.J., Rojas, E., Nuñez, L., Kong, Y., Gies, D.R., Stitt, T.N., Ip, N.Y., and Yancopoulos, G.D. (1993). Alternative forms of rat TrkC with different functional capabilities. *Neuron* *10*, 963–974.

Vassoler, F.M., White, S.L., Schmidt, H.D., Sadri-Vakili, G., and Pierce, R.C. (2013). Epigenetic inheritance of a cocaine-resistance phenotype. *Nat. Neurosci.* *16*, 42–47.

Verheij, M.M.M., Vendruscolo, L.F., Caffino, L., Giannotti, G., Cazorla, M., Fumagalli, F., Riva, M.A., Homberg, J.R., Koob, G.F., and Contet, C. (2016). Systemic Delivery of a Brain-Penetrant TrkB Antagonist Reduces Cocaine Self-Administration and Normalizes TrkB Signaling in the Nucleus Accumbens and Prefrontal Cortex. *J. Neurosci. Off. J. Soc. Neurosci.* *36*, 8149–8159.

Vidaurre, O.G., Gascón, S., Deogracias, R., Sobrado, M., Cuadrado, E., Montaner, J., Rodríguez-Peña, A., and Díaz-Guerra, M. (2012). Imbalance of neurotrophin receptor isoforms TrkB-FL/TrkB-T1 induces neuronal death in excitotoxicity. *Cell Death Dis.* *3*, e256.

Walsh, D.M., Klyubin, I., Fadeeva, J.V., Cullen, W.K., Anwyl, R., Wolfe, M.S., Rowan, M.J., and Selkoe, D.J. (2002). Naturally secreted oligomers of amyloid β protein potently inhibit hippocampal long-term potentiation in vivo. *Nature* *416*, 535–539.

Wang, T., Yu, D., and Lamb, M.L. (2009). Trk kinase inhibitors as new treatments for cancer and pain. *Expert Opin. Ther. Pat.* *19*, 305–319.

Watson, F.L., Heerssen, H.M., Moheban, D.B., Lin, M.Z., Sauvageot, C.M., Bhattacharyya, A., Pomeroy, S.L., and Segal, R.A. (1999). Rapid Nuclear Responses to Target-Derived Neurotrophins Require Retrograde Transport of Ligand–Receptor Complex. *J. Neurosci.* *19*, 7889–7900.

Webster, M.J., Herman, M.M., Kleinman, J.E., and Shannon Weickert, C. (2006). BDNF and trkB mRNA expression in the hippocampus and temporal cortex during the human lifespan. *Gene Expr. Patterns* *6*, 941–951.

Wehner, A.B., Milen, A.M., Albin, R.L., and Pierchala, B.A. (2016). The p75 neurotrophin receptor augments survival signaling in the striatum of pre-symptomatic Q175(WT/HD) mice. *Neuroscience* 324, 297–306.

Wehrman, T., He, X., Raab, B., Dukipatti, A., Blau, H., and Garcia, K.C. (2007). Structural and Mechanistic Insights into Nerve Growth Factor Interactions with the TrkA and p75 Receptors. *Neuron* 53, 25–38.

Weickert, C.S., Hyde, T.M., Lipska, B.K., Herman, M.M., Weinberger, D.R., and Kleinman, J.E. (2003). Reduced brain-derived neurotrophic factor in prefrontal cortex of patients with schizophrenia. *Mol. Psychiatry* 8, 592–610.

Weickert, C.S., Ligons, D.L., Romanczyk, T., Ungaro, G., Hyde, T.M., Herman, M.M., Weinberger, D.R., and Kleinman, J.E. (2005). Reductions in neurotrophin receptor mRNAs in the prefrontal cortex of patients with schizophrenia. *Mol. Psychiatry* 10, 637–650.

Weishaupt, N., Blesch, A., and Fouad, K. (2012). BDNF: the career of a multifaceted neurotrophin in spinal cord injury. *Exp. Neurol.* 238, 254–264.

Weiss, G.J., Hidalgo, M., Borad, M.J., Laheru, D., Tibes, R., Ramanathan, R.K., Blaydorn, L., Jameson, G., Jimeno, A., Isaacs, J.D., et al. (2012). Phase I study of the safety, tolerability and pharmacokinetics of PHA-848125AC, a dual tropomyosin receptor kinase A and cyclin-dependent kinase inhibitor, in patients with advanced solid malignancies. *Invest. New Drugs* 30, 2334–2343.

White, A.O., Kramár, E.A., López, A.J., Kwapis, J.L., Doan, J., Saldana, D., Davatolhagh, M.F., Alagband, Y., Blurton-Jones, M., Matheos, D.P., et al. (2016). BDNF rescues BAF53b-dependent synaptic plasticity and cocaine-associated memory in the nucleus accumbens. *Nat. Commun.* 7, 11725.

Wiesmann, C., Ultsch, M.H., Bass, S.H., and de Vos, A.M. (1999). Crystal structure of nerve growth factor in complex with the ligand-binding domain of the TrkA receptor. *Nature* 401, 184–188.

Wong, A.W., Xiao, J., Kemper, D., Kilpatrick, T.J., and Murray, S.S. (2013a). Oligodendroglial expression of TrkB independently regulates myelination and progenitor cell proliferation. *J. Neurosci. Off. J. Soc. Neurosci.* 33, 4947–4957.

Wong, J., Webster, M.J., Cassano, H., and Weickert, C.S. (2009). Changes in alternative brain-derived neurotrophic factor transcript expression in the developing human prefrontal cortex. *Eur. J. Neurosci.* 29, 1311–1322.

Wong, J., Rothmond, D.A., Webster, M.J., and Shannon Weickert, C. (2013b). Increases in Two Truncated TrkB Isoforms in the Prefrontal Cortex of People With Schizophrenia. *Schizophr. Bull.* 39, 130–140.

Woolf, C.J., Safieh-Garabedian, B., Ma, Q.-P., Crilly, P., and Winter, J. (1994). Nerve growth factor contributes to the generation of inflammatory sensory hypersensitivity. *Neuroscience* *62*, 327–331.

Wu, J., Renn, C.L., Faden, A.I., and Dorsey, S.G. (2013). TrkB.T1 Contributes to Neuropathic Pain after Spinal Cord Injury through Regulation of Cell Cycle Pathways. *J. Neurosci.* *33*, 12447–12463.

Xie, W., Song, Y.-J., Li, D., Pan, L.-P., Wu, Q.-J., and Tian, X. (2014). The suppression of epileptiform discharges in cultured hippocampal neurons is regulated via alterations in full-length tropomyosin-related kinase type B receptors signalling activity. *Eur. J. Neurosci.* *40*, 2564–2575.

Xu, B., Zang, K., Ruff, N.L., Zhang, Y.A., McConnell, S.K., Stryker, M.P., and Reichardt, L.F. (2000). Cortical Degeneration in the Absence of Neurotrophin Signaling: Dendritic Retraction and Neuronal Loss after Removal of the Receptor TrkB. *Neuron* *26*, 233–245.

Yacoubian, T.A., and Lo, D.C. (2000). Truncated and full-length TrkB receptors regulate distinct modes of dendritic growth. *Nat. Neurosci.* *3*, 342–349.

Yeo, G.S.H., Connie Hung, C.-C., Rochford, J., Keogh, J., Gray, J., Sivaramakrishnan, S., O’Rahilly, S., and Farooqi, I.S. (2004). A de novo mutation affecting human TrkB associated with severe obesity and developmental delay. *Nat. Neurosci.* *7*, 1187–1189.

Ying, Z., Roy, R.R., Edgerton, V.R., and Gómez-Pinilla, F. (2005). Exercise restores levels of neurotrophins and synaptic plasticity following spinal cord injury. *Exp. Neurol.* *193*, 411–419.

Ylikoski, J., Pirvola, U., Moshnyakov, M., Palgi, J., Arumäe, U., and Saarma, M. (1993). Expression patterns of neurotrophin and their receptor mRNAs in the rat inner ear. *Hear. Res.* *65*, 69–78.

Yozu, A., Haga, N., Funato, T., Owaki, D., Chiba, R., and Ota, J. (2016). Hereditary sensory and autonomic neuropathy types 4 and 5: Review and proposal of a new rehabilitation method. *Neurosci. Res.* *104*, 105–111.

Yu, T., Calvo, L., Anta, B., López-Benito, S., López-Bellido, R., Vicente-García, C., Tessarollo, L., Rodriguez, R.E., and Arévalo, J.C. (2014). In Vivo Regulation of NGF-Mediated Functions by Nedd4-2 Ubiquitination of TrkA. *J. Neurosci.* *34*, 6098–6106.

Yu, X., Liu, L., Cai, B., He, Y., and Wan, X. (2008). Suppression of anoikis by the neurotrophic receptor TrkB in human ovarian cancer. *Cancer Sci.* *99*, 543–552.

Zafra, F., Hengerer, B., Leibrock, J., Thoenen, H., and Lindholm, D. (1990). Activity dependent regulation of BDNF and NGF mRNAs in the rat hippocampus is mediated by non-NMDA glutamate receptors. *EMBO J.* *9*, 3545–3550.

Zarate, C.A., Singh, J.B., Carlson, P.J., Brutsche, N.E., Ameli, R., Luckenbaugh, D.A., Charney, D.S., and Manji, H.K. (2006). A randomized trial of an N-methyl-D-aspartate antagonist in treatment-resistant major depression. *Arch. Gen. Psychiatry* *63*, 856–864.

Zhang, Q., Descamps, O., Hart, M.J., Poksay, K.S., Spilman, P., Kane, D.J., Gorostiza, O., John, V., and Bredesen, D.E. (2014). Paradoxical Effect of TrkA Inhibition in Alzheimer's Disease Models. *J. Alzheimers Dis. JAD* *40*, 605–617.

Zhang, W., Liu, L.-Y., and Xu, T.-L. (2008). Reduced potassium-chloride co-transporter expression in spinal cord dorsal horn neurons contributes to inflammatory pain hypersensitivity in rats. *Neuroscience* *152*, 502–510.

Zheng, C., Geetha, T., Gearing, M., and Babu, J.R. (2015). Amyloid β -abrogated TrkA ubiquitination in PC12 cells analogous to Alzheimer's disease. *J. Neurochem.* *133*, 919–925.

Zhong, P., Liu, Y., Hu, Y., Wang, T., Zhao, Y., and Liu, Q. (2015). BDNF interacts with endocannabinoids to regulate cocaine-induced synaptic plasticity in mouse midbrain dopamine neurons. *J. Neurosci. Off. J. Soc. Neurosci.* *35*, 4469–4481.

Zuccato, C., Marullo, M., Conforti, P., MacDonald, M.E., Tartari, M., and Cattaneo, E. (2008). Systematic assessment of BDNF and its receptor levels in human cortices affected by Huntington's disease. *Brain Pathol. Zurich Switz.* *18*, 225–238.

ACKNOWLEDGEMENTS

My sincere gratitude goes to Tõnis Timmusk for accepting me in his lab even though it was rather unplanned. Thank you for the support, patience and guidance throughout all those years. I was also lucky to have a second supervisor, Mati Karelson, who provided my education in basic computer chemistry and was important for the third publication of this thesis.

I was very fortunate to have the most wonderful students Rahel and Elina, whose contribution in the progression of this thesis was substantial and helped me learn a lot about team-work. I also thank all the current and former members of the Timmusk lab, especially Kaur, Ave, Mari, Jürgen, Mari, Hanna, Mari, Indrek, Kaja, Kati, Priit, Laura, Rix and Marko, for advice, help and positive atmosphere. I also thank Urmas Arumäe for reviewing this thesis and all my co-authors.

I am deeply grateful to my previous supervisor Andres Merits for providing me the opportunity to learn basic molecular biology techniques and showing what a great human mind can be capable of. You keep on inspiring me. My former colleagues from the Merits lab – Anna, Pirjo, Ingrid, Kaja and Inga, thank you all for being so much more than just colleagues.

My awesome course mates and friends Helen, Ave Kris, Tuuli, Agne and Eneli – thank you for all the uplifting conversations about science, politics, maternity and life in general. I owe my thanks to my sister Lea and brother-in-law Peeter for the content and essence of all those summers and Christmas holidays we have spent together.

My choice to study the life sciences has been greatly influenced by my amazing parents, especially by my father Juhan, who has managed to infect me with his overwhelming passion for science and the quest to uncover the secrets of the natural world. My deepest gratitude goes to my mother Anna not only for letting me play with “color-changing” liquids in her lab when I was little, but also for her endless high-quality and loving baby-sitting for my children.

I am utterly and forever proud of the three lives who sparked within me. Helin, Tuule-Mai and Loits – when I look at you, I see infinite possibilities. I see the future.

Lastly, my deepest appreciation and thank you goes to my husband Ago. For love, support, understanding, inspiration, jokes. For everything.

You are the best.

ABSTRACT

The complex structure and physiology of the nervous system develops using intricate mechanisms where cell survival and migration, neurite growth or pruning, and adjusting the synaptic strength are precisely regulated. For many neural cell types, tropomyosin-related kinases (Trks) are involved in the modulation of all these regulatory levels, because these proteins are the transmembrane receptors of neurotrophins (NTs). The intracellular signal cascades starting from Trks are plentiful and lead to various outcomes that range from fast local effects to long-lasting changes resulting from influencing the transcription level of many genes. The outcome of NT signal is determined by the isoform of the Trk receptor it activates. Previously, many isoforms of Trks have been known. Some of those, such as TrkAIII, TrkB-T1 and TrkB-T-Shc, have very different signalling capabilities compared to the full-length receptors. Also, a distinct expression pattern has been described for different Trk protein isoforms and mRNAs encoding them.

This thesis focuses on TrkA, a receptor of nerve growth factor (NGF), and TrkB, a receptor for both brain-derived neurotrophic factor (BDNF) and NT-4. A characterization of the variability of *TrkA* and *TrkB* transcripts is given. This leads to a more precise overview of *TrkA* and *TrkB* gene structures and also of putative protein isoforms. Many novel transcription start-sites and splice forms are described for *TrkA*. For *TrkB*, one novel 5' exon and one novel 3' exon were identified. A thorough examination of the expression level of both *TrkA* and *TrkB* alternative transcripts in different human tissues was also performed, including the analysis of the expression of *TrkB* in the prefrontal cortex (PFC) throughout the human lifespan. In addition, the characteristics of some of the previously unknown putative protein isoforms is presented. However, the in vivo existence of these proteins still needs verification.

Both TrkA and TrkB have also been known to be actively contributing to the development and progression of many disease states. For example, both of these kinases are overactive in chronic pain and some types of cancers. For this reason, one of the aims of this work was to find new inhibitors for Trk kinases. Novel potent and selective pan-Trk kinase inhibitors were identified from the group of 2-oxindoles that could potentially be used for further development of therapeutics against pain and/or cancer.

KOKKUVÕTE

Närvisüsteemi keeruline struktuur ja füsioloogia tekivad täpselt reguleeritud mehhanismide tulemusel, mis mõjutavad rakkude ellujäämist ja migratsiooni, neuriitide kasvu või kärpimist ning sünapsi tugevust. Paljude närvirakkude alamtüüpide puhul on kõikidel nendel regulaatorsetel tasanditel olulisel kohal tropomüosiini-seoseliste kinaaside (Trk) perekond, sest selle liikmed on neurotrofiinide (NT) plasmamembraani läbivad retseptorid. Trk retseptoritelt lähtuvaid rakusiseseid signaaliradu on palju ning nende tulemid on väga mitmekesised, ulatudes kiiretest kohalikest efektidest pikaajaliste muutusteni, mis on tingitud mitmete geenide transkriptsioonitaseme mõjutamisest. NT signaali mõju rakule määrab NT-ga seondunud Trk valgu isovorm. Varasemalt on teada mitmeid erinevaid Trk retseptorite isovorme. Neist mõne, näiteks TrkAIII, TrkB-T1 ja TrkB-T-Shc, signaliseerimine erineb oluliselt täispika retseptorkinaasi omast. Ühtlasi on erinevate valguisovormide ning ka neid kodeerivate mRNA-de avaldumismustrites leitud olulisi erinevusi.

Käesolev töö keskendub TrkA-le, mis on närvikasvufaktori (NGF) retseptor, ning TrkB-le, ajast pärineva neurotroofse teguri (BDNF) ja NT-4 retseptorile. *TrkA* ja *TrkB* transkriptide mitmekesisus on põhjalikult iseloomustatud. Selle analüüsi tulemusel tekib täpsem ülevaade nende geenide struktuurist ning ühtlasi ka TrkA ja TrkB võimalikest valguisovormidest. *TrkA* puhul leiti palju senitundmatuid transkriptsiooni alguskohti ning splaissvorme, samas kui *TrkB* geenil tuvastati üks uudne 5' ekson ja üks uudne 3' ekson. Töö raames teostati ka põhjalik ekspressioonitasemete analüüs inimese erinevates kudedes nii *TrkA* kui ka *TrkB* transkriptidele, mis hõlmas *TrkB* ekspressiooni analüüsimist inimese prefrontaalses ajukoos erinevate vanuserühmade lõikes. Lisaks sellele kirjeldati mõningaid võimalikke TrkA ja TrkB valguisovorme, kuigi nende *in vivo* avaldumine ning füsioloogiline roll vajab veel kinnitamist.

Nii TrkA kui ka TrkB on olulised mitmete haiguste kujunemisel, näiteks on mõlemad kinaasid üleaktiveeritud kroonilise valu ning mõningate vähitüüpide puhul. Sellel põhjusel oli üheks käesoleva töö eesmärgiks leida uusi Trk kinaaside inhibiitoreid. Uudsed inhibiitorid, mis toimivad Trk kinaasidele madalas nanomolaarses kontsentratsioonis ja on selektiivsed, identifitseeriti 2-oksindoolide grupist. Edasised katsed näitavad, kas neid ühendeid on võimalik arendada valuvaigistava ning vähivastase toimega ravimiteks.

PUBLICATION I

I. **Luberg, K.**, Wong, J., Weickert, C.S., and Timmusk, T. (2010). Human TrkB gene: novel alternative transcripts, protein isoforms and expression pattern in the prefrontal cerebral cortex during postnatal development. *J. Neurochem.* 113, 952–964.

Human TrkB gene: novel alternative transcripts, protein isoforms and expression pattern in the prefrontal cerebral cortex during postnatal development

Kristi Luberg,^{*†} Jenny Wong,^{‡§¶} Cynthia Shannon Weickert^{‡§**} and Tõnis Timmusk^{*†}

^{*}Department of Gene Technology, Tallinn University of Technology, Tallinn, Estonia

[†]Competence Center for Cancer Research, Tallinn, Estonia

[‡]Schizophrenia Research Institute, Sydney, Australia

[§]Schizophrenia Research Laboratory, Prince of Wales Medical Research Institute, Randwick, New South Wales, Australia

[¶]School of Medical Sciences, Faculty of Medicine, University of New South Wales, Sydney, New South Wales, Australia

^{**}School of Psychiatry, Faculty of Medicine, University of New South Wales, Sydney, New South Wales, Australia

Abstract

Brain-derived neurotrophic factor and neurotrophin-4 high-affinity receptor tropomyosin related kinase (Trk) B is required for the differentiation and maintenance of specific neuron populations. Misregulation of TrkB has been reported in many human diseases, including cancer, obesity and neurological and psychiatric disorders. Alternative splicing that generates receptor isoforms with different functional properties also regulates TrkB function. Here, we describe numerous novel isoforms of TrkB proteins, including isoforms generated by alternative splicing of cassette exons in the regions encoding both the extracellular and intracellular domain and also N-terminally truncated isoforms encoded by novel 5' exon-containing transcripts. We also characterize the intracellular localization and phosphorylation potential of novel

TrkB isoforms and find that these proteins have unique properties. In addition, we describe the expression profiles of all the known human TrkB transcripts in adult tissues and also during postnatal development in the human prefrontal cortex. We show that transcripts encoding the full-length TrkB receptor and the C-terminally truncated TrkB-T1 have different expression profiles as compared to the proteins they encode. Identification of 36 potential TrkB protein isoforms suggests high complexity in the synthesis, regulation and function of this important neurotrophin receptor emphasizing the need for further study of these novel TrkB variants.

Keywords: alternative splicing, brain-derived neurotrophic factor, expression analysis, phosphorylation, transcription, TrkB.

J. Neurochem. (2010) **113**, 952–964.

Tropomyosin related kinase B (TrkB; official name – NTRK2) is a receptor for neurotrophins brain-derived neurotrophic factor, neurotrophin (NT) 4 and, in a lower affinity, NT-3 (Squinto *et al.* 1991; Klein *et al.* 1992). TrkB is closely related to TrkA and TrkC, which are receptors for neurotrophins nerve-growth factor and NT-3, respectively (Lewin and Barde 1996). TrkB is an essential modulator of neural differentiation and cell survival. Dysregulation of TrkB has been associated with various neurological diseases, diverse type of cancers, obesity and eating disorders (Desmet and Peeper 2006; Farooqi and O'Rahilly 2006; Altar *et al.* 2009).

Interaction with two TrkB receptor molecules by one neurotrophin homodimer triggers the intrinsic tyrosine kinase activity of the TrkB intracellular portion leading to auto-

phosphorylation at multiple tyrosine residues in the cytoplasmic domain of the receptor. These phosphotyrosines serve as docking sites for proteins such as Shc and phospholipase C- γ (PLC- γ), which are activated by tyrosine phosphorylation and link TrkB to downstream signaling

Received December 1, 2009; revised manuscript received February 17, 2010; accepted February 19, 2010.

Address correspondence and reprint requests to Tõnis Timmusk, Department of Gene Technology, Tallinn University of Technology, Akadeemia tee 15, 12618 Tallinn, Estonia.

E-mail: tonis.timmusk@ttu.ee

Abbreviations used: DLPFC, dorsolateral prefrontal cortex; EST, expressed sequence tag; IG-like, immunoglobulin-like; IRES, internal ribosome entry site; NT, neurotrophin; PLC- γ , phospholipase C- γ ; Trk, tropomyosin related kinase; UTR, untranslated region.

pathways (Reichardt 2006). The signals transmitted by activated TrkB promote survival, neurogenesis and synaptogenesis in neurons (Binder and Scharfman 2004), and cellular proliferation, invasivity and resistance to anoikis and chemotherapy in cancer cells accompanied by poor prognosis for cancer patients (Nakagawara *et al.* 1994; Eggert *et al.* 2001; Douma *et al.* 2004; Yu *et al.* 2008; Au *et al.* 2009; Li *et al.* 2009b). Brain-derived neurotrophic factor-activated TrkB is a mediator of many other functions, including activity-dependent synaptic plasticity (Kang *et al.* 1997; Yamada and Nabeshima 2003) and angiogenesis (Kermani *et al.* 2005; Kermani and Hempstead 2007). In addition, changes in TrkB signaling accompany and can lead to various nervous system disorders, including mood and anxiety disorders and neurodegenerative diseases, which make TrkB an important target for drug development (Allen *et al.* 1999; Pillai 2008; Rantamaki and Castren 2008; Altar *et al.* 2009).

The TrkB gene is relatively large (Fig. 1), spanning more than 350 kbp, and is located on chromosome 9 (Nakagawara *et al.* 1995). A thorough examination of the TrkB gene and its transcripts conducted by Stoilov and coworkers revealed the existence of 24 exons in the TrkB gene with the first five exons serving as alternative transcription start-sites and displaying intricate patterns of splicing (Stoilov *et al.* 2002). It has been shown that these five exons form an internal ribosome entry site (IRES) guiding the ribosome to the translational start site which is located in exon 5 (Dobson *et al.* 2005). Exons 5–14 encode the extracellular portion of the TrkB receptor which contains a signal sequence for membrane localization, post-translationally glycosylated cysteine and leucine rich regions, and two immunoglobulin-like (IG-like) domains (Schneider and Schweiger 1991; Shelton *et al.* 1995). Exon 12 encodes the second IG-like domain that has been postulated to be the region responsible for binding neurotrophins (Urfer *et al.* 1995). The transmembrane domain of TrkB is encoded by exon 15 and the intracellular tyrosine kinase domain is encoded by exons 20–24 (Middlemas *et al.* 1991).

Additional to the full-length TrkB receptor, the human TrkB gene is known to encode C-terminal truncated receptors TrkB-T1 and TrkB-T-Shc, which are generated by the usage of exon 16 or exon 19, respectively. Exons 16 and 19 contain alternative polyadenylation signals and translational stop-codons (Klein *et al.* 1990; Stoilov *et al.* 2002). Both TrkB-T1 and TrkB-T-Shc may act as dominant negative inhibitors of the full-length receptor by preventing ligand-induced phosphorylation (Brodeur *et al.* 2009). In addition, it has been suggested that TrkB-T1 may have signaling properties that are different from the signal pathways activated by the full-length TrkB, such as evoking calcium signaling and mediating Rho GDP dissociation inhibitor 1 functions (Rose *et al.* 2003; Ohira *et al.* 2005). It has been found that TrkB-T1 can induce liver metastasis of pancreatic cancer cells by

promoting RhoA activation (Li *et al.* 2009a). Interestingly, a recent study showed a decrease in the expression level of TrkB-T1 in the frontal region of the brain in 10 of 28 suicide completers (Ernst *et al.* 2009).

The intracellular juxtamembrane region-encoding exon 17 of TrkB has been shown to be a cassette exon (Stoilov *et al.* 2002). An isoform of TrkB which lacks the extracellular juxtamembrane region encoded by exon 13 has been shown to exist in the human retinal pigmented epithelial cells (Hackett *et al.* 1998). Additional splice variants have been described in mouse (C-terminal truncated isoforms and isoforms lacking leucine-rich regions), rat (C-terminal truncated isoforms) and chicken (isoforms with deletions in the extracellular and intracellular juxtamembrane regions; Middlemas *et al.* 1991; Garner *et al.* 1996; Strohmaier *et al.* 1996; Ninkina *et al.* 1997; Kumanogoh *et al.* 2008).

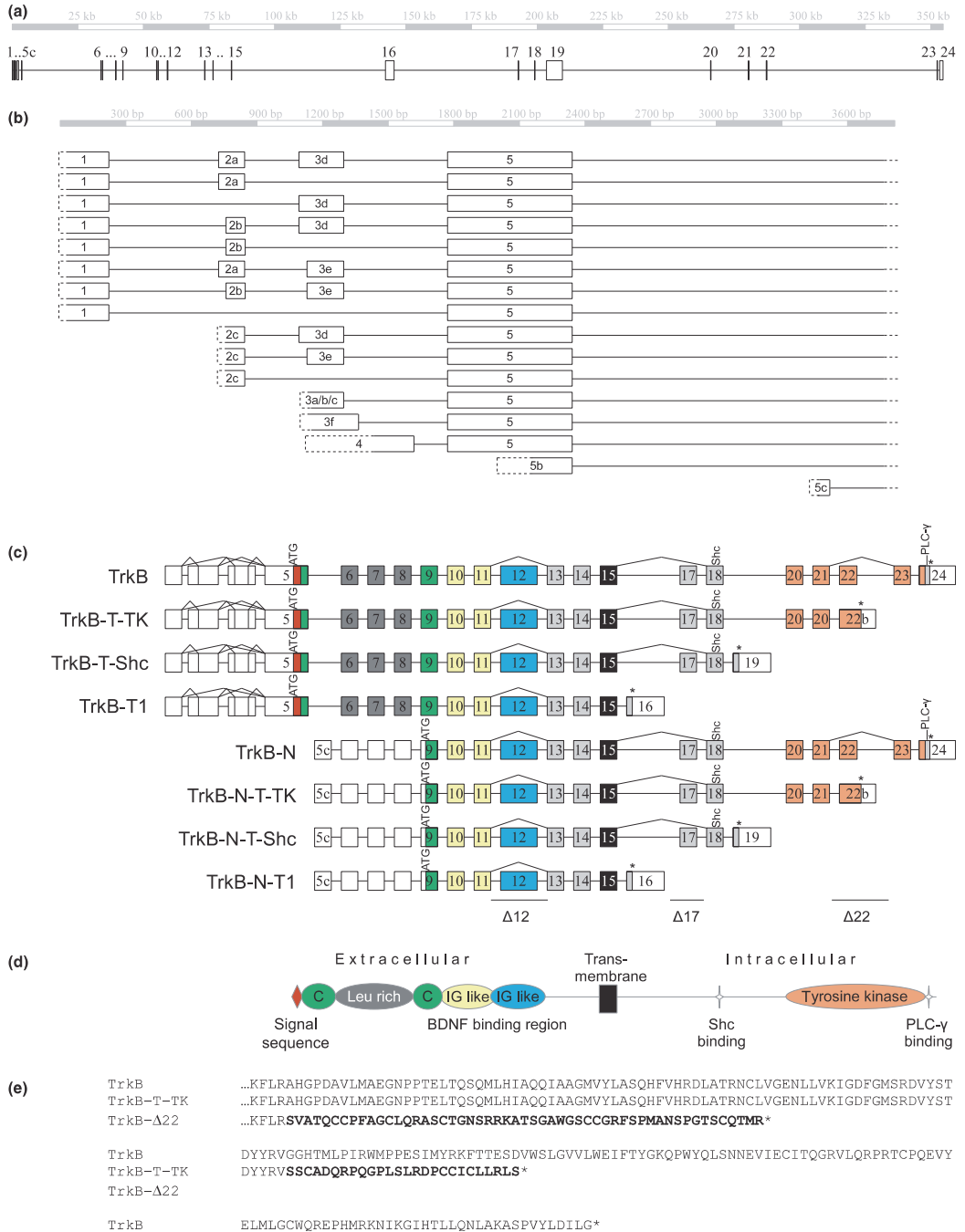
Temporal fluctuations in the expression level of mRNAs encoding the full-length TrkB and truncated TrkB-T1 receptors have been described in the dorsolateral prefrontal cortex (DLPFC), temporal cortex and hippocampus using *in situ* hybridization (Romanczyk *et al.* 2002; Webster *et al.* 2006). The DLPFC is important for higher level cognitive processing and working memory in humans. The maturation process of the DLPFC is protracted extending up to the first two decades of life making the DLPFC a good system for characterizing developmentally-regulated events (Bourgeois 1997). In the DLPFC, the expression levels of the full-length TrkB receptor-encoding mRNAs were highest in the young adult age group and lowest in the aged, whereas the level of the mRNAs encoding the TrkB-T1 isoform showed only minor increases over the postnatal life span.

As the TrkB gene has many functions in different tissues during development and in adulthood, both in health and disease, detailed knowledge of its structure, alternatively spliced mRNAs and protein isoforms is very important. In this study we have re-examined the human TrkB gene structure, identified novel isoforms of human TrkB transcripts that encode novel proteins and characterized tissue-specific expression patterns of alternative TrkB mRNAs. In addition, we have characterized age-related expression patterns of alternative TrkB mRNAs in the human DLPFC.

Materials and methods

Computer analysis and RT-PCR were performed as described previously (Koppel *et al.* 2009). Primers used for the analysis of TrkB mRNA expression and for cloning of TrkB riboprobes and full-length TrkB transcripts for protein expression are shown in Table S1. Quantitative PCR and western blotting were performed as described in Wong *et al.* (2009); and RNAse protection assay as detailed in Timmusk *et al.* (1993).

HEK293 cells were grown in Dulbecco's Modified Eagle's Medium (Invitrogen, Carlsbad, CA, USA) containing 10% fetal bovine serum and transfected with PEI reagent (InBio, Tallinn,



Estonia). For immunofluorescence, the cells were grown on cover slips, fixed with 4% paraformaldehyde (Scharlau, Barcelona, Spain), blocked with 2% bovine serum albumine (Sigma, St Louis, MO, USA) and stained with Alexa Fluor 488-conjugated concanavalin A (Invitrogen), primary anti-V5 antibody (Sigma, V8137) and secondary Alexa Fluor 568-conjugated goat anti-rabbit antibody (Invitrogen). Cover slips were mounted using ProLong Gold antifade reagent with 4',6-diamidino-2-phenylindole (DAPI; Invitrogen). Labeled cells were analyzed using the LSM 510 (Zeiss, Oberkochen, Germany) confocal microscopy system.

For immunoprecipitation, cells were lysed with radioimmunoprecipitation buffer. 0.5 mg of a 1 mg/mL total protein extract was immunoprecipitated with 1.8 µg mouse anti-V5 antibody (Invitrogen) or anti-TrkB antibody (Santa Cruz Biotechnology, Santa Cruz, CA, USA, SC-8316). Precipitated proteins were analysed with western blotting using mouse anti-phosphotyrosine (Millipore Corporation, Bedford, MA, USA, 4G10) or mouse anti-V5 antibody.

Detailed information of materials and methods can be found in Appendix S1.

Results

Structure and alternative transcripts of the human TrkB gene

The human TrkB gene structure and expression profiles of its alternative transcripts were analyzed by bioinformatics and RT-PCR. For this purpose, we first used the Blat application to align human TrkB mRNAs and expressed sequence tags (ESTs) from GenBank to the genome in order to determine the exon/intron sites of transcripts that have been entered into the public databases. Expression of alternative splice variants in different tissues was verified by RT-PCR and sequencing of PCR products. The gene structure arising from this analysis is depicted on Fig. 1. In most part, this study uses the nomenclature described by Stoilov *et al.* (2002). In addition, we identified the existence of a novel exon, exon 5c, which is located approximately 1200 bp downstream of exon 5. Exon 5c comprises a new transcription start site. Finally, we identified novel splice variants of the human TrkB transcripts that are described in detail below.

Exons 1, 2, 3, 4 and the majority of exon 5 constitute the conventional 5' untranslated region (UTR) of the human TrkB gene. All of these exons can serve as transcription start sites (Stoilov *et al.* 2002). In GenBank, there are more than 200 ESTs covering the region corresponding to the TrkB

gene. A majority of these were identified in a study characterizing alternative promoters of human genes (Kimura *et al.* 2006). According to Stoilov and coworkers and the alignment of the TrkB ESTs, the alternative splicing pattern of TrkB exons 1–5 is rather complex, arising from exon skipping (exons 2 and 3) and the usage of alternative 5' and 3' exon splice sites for exons 2, 3 and 4 (Fig. 1b). It has been shown that the G/C rich exons 1–5 exhibit internal initiation entry site (IRES) activity that functions to guide and enhance the translation initiation from exon 5 (Dobson *et al.* 2005). The IRES was localized to the exon 5 and at least six sub-regions were shown to either promote or inhibit the IRES activity. Therefore, we hypothesized that the intricate splicing pattern of the TrkB 5' UTR might be tissue-specific with variable translation initiation regulation capabilities in different tissues. However, RT-PCR experiments did not support this hypothesis, as all the tissues studied showed highly similar patterns of expression and splicing of exons 1–5 (Fig. S1a). Thus, the functional meaning of this intricate splicing still remains to be determined.

To date, all TrkB isoforms have been considered to include exon 5 which also contains the start codon for protein translation. Here, we describe a novel exon that we named 5c, which is located approximately 1200 bp downstream of exon 5 (Fig. 1a–c). None of the ESTs or the mRNA in GenBank containing exon 5c includes exons 1–5. Therefore, we hypothesized that exon 5c serves as an alternative transcription start-site for TrkB mRNAs. This assumption was supported by RT-PCR which did not render any products with primers specific for TrkB exons 1 and 5c, 2 and 5c, 3 and 5c, 4 and 5c or 5 and 5c (data not shown). RT-PCR analysis of TrkB transcripts containing exon 5c showed that these mRNAs were expressed mainly in the nervous system with the highest expression in the cerebellum (Fig. 2). The novel exon 5c is not specific to humans as we detected TrkB transcripts containing exon 5c in the mouse brain (Fig. S1b and c). *In silico* analysis showed that protein translation of human TrkB transcripts containing exon 5c are likely to start from exon 9 (Fig. 1c). This creates N-terminally truncated TrkB proteins that lack 156 N-terminal amino acid residues encoding the signal sequence, leucine-rich repeats and most of the cysteine-rich repeats compared to the full-length protein. We have named the novel protein isoforms TrkB-N, TrkB-N-T-TK, TrkB-N-T-Shc and TrkB-N-T1 according to

Fig. 1 Structure of the human TrkB gene and predicted TrkB protein isoforms. Exons are shown as boxes and introns are shown as lines. Exons and introns are drawn to scale (in a and b). (a) Schematic representation of all TrkB exons (numbers are shown above exons) and introns. (b) Alternative 5' exons of TrkB transcripts; (c) TrkB transcripts grouped by the type of protein isoforms they encode. Names of alternative protein isoforms are shown on the left. 5' and 3' UTR regions are shown as empty boxes, sequences encoding protein

are shown as filled boxes and numbered. Shown are locations of tyrosine residues important for Shc-binding (Shc) and PLC-γ binding (PLC-γ). ATG, translation initiation codon; *Translation stop codon. (d) Schematic representation of TrkB protein domains. C, cysteine rich region; Leu rich, leucine rich region; IG like, immunoglobulin like-domain. (e) Amino acid sequences of the C-termini of TrkB, TrkB-T-TK and TrkB-Δ22 protein isoforms. Isoform-specific unique amino acids are shown in bold.

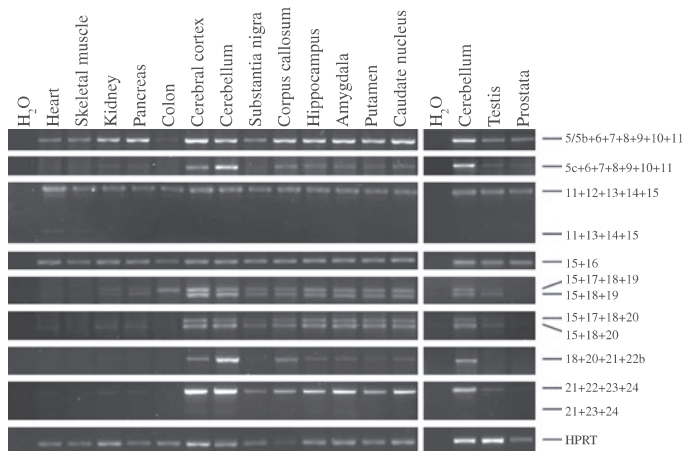


Fig. 2 Semi-quantitative analysis of expression levels of alternative TrkB transcripts in different human tissues. Numbers of amplified TrkB exons are shown on the right. Hypoxanthine guanine phosphoribosyltransferase (HPRT) was used as the housekeeping control.

the C-termini of these proteins that are encoded by exons 24, 22b, 19 and 16, respectively. Because of the lack of N-terminal signal sequence, it is highly unlikely that these protein isoforms could be transported to the cell membrane, although they contain the region that functions as a transmembrane domain in the full-length TrkB receptor.

We observed exon skipping in the case of three exons outside the 5' UTR: for exons 12, 17 and 22 (Figs 1c and 2). Skipping of exon 17 has been described before (Stoilov *et al.* 2002), however, the possible tissue-specificity and the function of the proteins (named as TrkB- Δ 17, TrkB-T-TK- Δ 17, TrkB-T-Shc- Δ 17, TrkB-N- Δ 17, TrkB-N-T-TK- Δ 17 and TrkB-N-T-Shc- Δ 17) encoded by these transcripts has not been studied so far. Interestingly, the splice donor site of exon 17 is present in the genome sequence of all mammals analyzed by us but is lost in mouse (Fig. S1d). Alternative splicing of human TrkB exon 12 and 22 is first described in this study. Skipping of exons 12 or 17 does not lead to a frame-shift in the encoded protein. Exon 12 encodes for 101 amino acids in the extracellular domain and exon 17 for 16 amino acids in the intracellular juxtamembrane domain of the TrkB protein. Skipping of exon 12 leads to production of protein isoforms without the neurotrophin-binding domain (TrkB- Δ 12, TrkB-T-TK- Δ 12, TrkB-T-Shc- Δ 12, TrkB-T1- Δ 12, TrkB-N- Δ 12, TrkB-N-T-TK- Δ 12, TrkB-N-T-Shc- Δ 12 and TrkB-N-T1- Δ 12; Fig. 1c), suggesting that these protein isoforms may be phosphorylated ligand-independently. Although skipping of exon 22 causes a frame-shift, the first translational stop-codon remains in exon 24, the most 3' exon, and thus, these mRNAs will most probably not be subject to non-sense-mediated decay. The resulting protein (named TrkB- Δ 22) is 139 amino acids shorter than the full length TrkB protein, lacks the PLC- γ binding site and part of the tyrosine kinase domain, and has 53 different amino acids

in its C-terminus as compared to the full length TrkB protein (Fig. 1c–e). Sequence analysis showed that the unique C-terminus of mouse putative TrkB isoform TrkB- Δ 22 has the same length as human TrkB- Δ 22 and that the regions covering the 53 C-terminal amino acids of mouse and human TrkB- Δ 22 are 76% homologous (data not shown). According to our RT-PCR studies, skipping of exon 17 was a relatively frequent event in all tissues studied, with approximately 50% of transcripts lacking exon 17. In contrast, skipping of exons 12 and 22 was a rare event. Skipping of exon 12 was observed in the heart and skeletal muscle, and at lower levels also in the brain, and skipping of exon 22 was noticed at extremely low levels in the frontal cerebral cortex and left cerebellum.

Additional diversity among TrkB protein isoforms is achieved by the use of alternative 3' exons in the TrkB mRNAs. Our results showed that TrkB transcripts containing exon 16 were expressed in all tissues studied, and transcripts with exon 19 or 24 were expressed mainly in neural tissues (Fig. 2), as described earlier (Shelton *et al.* 1995; Stoilov *et al.* 2002). In addition, we identified a new transcript of the human TrkB gene that encodes a novel truncated isoform of the TrkB protein. This transcript includes an extended version of exon 22 as the 3' exon, that we named 22b, which contains a translational stop-codon. Proteins encoded by these mRNAs (named TrkB-T-TK) lack the 114 C-terminal amino acids of the full-length TrkB encoding part of the tyrosine kinase and the PLC- γ binding site and have unique 27 amino acids in their C-termini (Fig. 1c and e). We found that TrkB mRNAs containing exon 22b were predominantly expressed in the nervous system (Fig. 2). The region covering the 27 C-terminal amino acids of the human TrkB-T-TK is not conserved among other mammals, as the mouse putative TrkB-T-TK

isoform has only six unique C-terminal amino acids, with the first four amino acids being identical with the human homologue (data not shown).

Next, the relative quantities of alternative TrkB transcripts were studied. RT-PCR analysis showed that the frequency of exon 17 skipping was approximately 50%, whereas the skipping of exons 12 or 22 was a very rare event (less than 1%). For the determination of relative quantities of alternative 5' and 3' exons we used the RNase protection assay.

Quantification of mRNAs containing exon 5c compared to mRNAs with the conventional TrkB 5' UTR (containing exon 5; Fig. 3) showed that the levels of transcripts with exon 5c were much lower than transcripts with exon 5. In the cerebellum, 5.7% of all TrkB mRNAs started with exon 5c and 94.3% lacked exon 5c and thus started with the conventional 5' UTR. In the frontal cerebral cortex, 0.2% TrkB transcripts included exon 5c and 99.8% used exon 5.

Comparison of transcripts with alternative 3' exons revealed that TrkB mRNAs containing exons 24 and 16 were the most abundant. Approximately 60% of all the TrkB transcripts in both cerebellum and frontal cerebral cortex incorporated exon 24. In the frontal cerebral cortex, 32% of TrkB transcripts contained exon 16, and 8.2% contained exon 19. Extremely low levels of transcripts with the

extended form of the exon 22 (22b) were detected using this method in the cerebral cortex. However, in the cerebellum, 11.7% of TrkB transcripts contained exon 22b. Of all the TrkB mRNAs in the cerebellum only 16.4% contained exon 16 and only 6.6% contained exon 19.

Taken together, *in silico* translation of novel TrkB mRNA alternative transcripts revealed the potential existence of many TrkB protein isoforms (Fig. 1c) that have not been described to date: protein isoforms with truncated N-terminal domain lacking sequences encoded by exons 5–8; protein isoforms lacking sequences encoded by exon 12, protein isoforms lacking sequences encoded by exon 22 and having unique C-termini encoded by exons 23 and 24 in an unconventional reading frame; protein isoforms with truncated C-terminal domain encoded by exon 22b. We were able to confirm the existence of all the alternative full-length transcripts of TrkB in the human brain, including the novel transcripts described in this study, by using RT-PCR analysis with primers targeting alternative translation initiation and stop codons (Fig. S1e). However, we did not detect previously described TrkB mRNA isoforms without exon 13 (Hackett *et al.* 1998), possibly because they are in low abundance or because tissues where these isoforms are expressed were not included in our study. Together, our

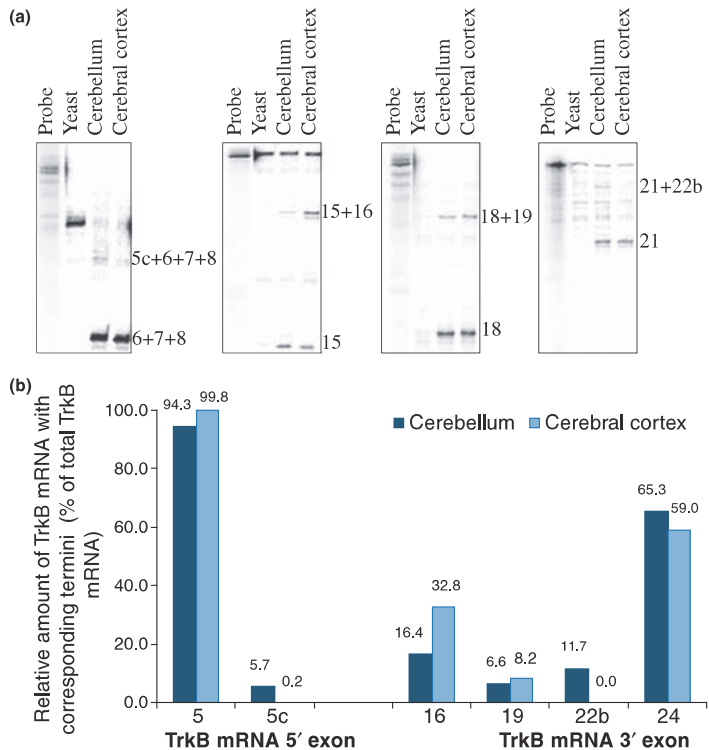


Fig. 3 Relative quantification of the alternative 5' and 3' termini of human TrkB transcripts. RNA extracted from the human left cerebellum and frontal cerebral cortex was used for RNase protection assay. (a) Exons contained in protected RNA fragments are shown on the right. (b) Relative quantities of TrkB transcripts with alternative 5' and 3' termini.

present findings in accordance with reports previously published suggest that at least 36 different protein isoforms are encoded by the human TrkB gene (Fig. 1c).

Regulation of TrkB mRNA and protein expression in the human prefrontal cerebral cortex during postnatal development

Next, we determined the expression profiles of the major known and novel TrkB transcripts identified in this study during postnatal development of the human prefrontal cortex. We investigated the expression profiles of TrkB transcripts containing alternative 5' exons 5 and 5c, alternative 3' exons 16, 19, 22b and 24, as well as transcripts with and without exon 17. For this purpose, we isolated RNA from a set of 52 postmortem prefrontal cerebral cortices and performed RT-qPCR studies using primers specific for alternative TrkB transcripts. The subjects were divided into seven pre-defined groups based on their age. The data were normalized to the geometric mean of the expression levels of four control (housekeeping) genes including cyclophilin A, glucuronidase beta, ubiquitin C and porphobilinogen deaminase.

To determine the most significant changes occurring in postnatal brain development, we statistically analyzed age groups with the highest and lowest change in mRNA expression for all the alternative TrkB transcripts. Expression levels of TrkB mRNAs with exon 24, encoding the full length TrkB receptor containing the tyrosine kinase domain, did not change from neonates to infants (Fig. 4a). Interestingly, expression levels peaked in the toddler stage, decreased slightly during school age, remained relatively unchanged up to the young adult stage and decreased significantly in adulthood as compared to neonates ($t = 2.60$, $df = 12$, $p = 0.02$). In contrast, expression levels of TrkB mRNAs containing exon 16, encoding the TrkB-T1 receptor lacking the tyrosine kinase domain, were relatively similar between neonates and infants, but decreased in toddlers and in the school age group where it reached significance compared to neonates ($t = 3.76$, $df = 9$, $p = 0.004$; Fig. 4b). Expression levels of TrkB-T1 mRNA then increased to the level of neonates in the young adult and adult age groups. While TrkB mRNAs containing exon 19 encoding the TrkB-T-Shc protein isoform were low in the neonatal cortex, transcript levels increased by 5-fold during infancy but this did not reach statistical significance ($t = -1.47$, $df = 14$, $p = 0.16$). This is likely because of the variability in the infant group. Expression then decreased gradually during later postnatal development with a 40% reduction in adults (compared to infants; Fig. 4c).

Next, we examined the expression levels of TrkB transcripts with and without exon 17. Interestingly, alternative splicing of exon 17 was developmentally regulated: expression of transcripts with and without exon 17 was lowest in neonates but differed thereafter (Fig. 4d). Expres-

sion of transcripts containing exon 17 increased gradually from neonates up to school age where the levels were significantly higher than in neonates ($t = -2.27$, $df = 9$, $p = 0.049$). Expression then decreased gradually during later postnatal development. In contrast, the levels of transcripts lacking exon 17 were not significantly changed across postnatal development. Although expression levels during infancy was increased 2-fold from neonates, this remained relatively stable into adulthood (Fig. 4d).

We next examined the changes in mRNA expression of TrkB transcripts containing exons 5 and 5c. Expression levels of TrkB mRNAs containing exon 5 were not significantly changed across postnatal development (Fig. 4e). Expression of TrkB mRNAs with exon 5c increased during postnatal development reaching their highest level in young adults as compared to neonates, although this did not reach statistical significance ($t = -1.52$, $df = 10$, $p = 0.17$). No further change was observed in adulthood (Fig. 4e).

We next determined the changes in TrkB transcripts containing exon 22b across postnatal development. The expression levels of transcripts containing exon 22b were variable. Transcript expression was lower in infants as compared to neonates, increased in toddlers and decreased again in school age (Fig. 4f). Thereafter, expression levels remained unchanged and decreased again in adulthood (neonate to adults: $t = 1.89$, $df = 10$, $p = 0.09$). However, changes in expression were not statistically significant.

To determine whether TrkB mRNA levels coincide with the levels of corresponding TrkB protein isoforms, lysates from the human prefrontal cerebral cortex were analysed using western blotting. Considering that the number of potential TrkB protein isoforms is as high as 36 (Fig. 1c) and that many TrkB protein isoforms have similar sizes, we chose the anti-TrkB antibody that does not recognize the minor N-terminally truncated TrkB-N isoforms to make the interpretation of results easier. The results (Fig. 5a) indicated that there are many different isoforms of TrkB proteins expressed, most of which cannot be identified using this method. The two most highly expressed protein isoforms are probably TrkB-T1 (molecular weight ~ 90 kDa) and the full-length TrkB protein (molecular weight ~ 140 kDa). We detected significant differences in the expression level of these isoforms in the human prefrontal cortex throughout the human lifespan (Fig. 5b and c). Namely, the expression level of full-length TrkB was significantly higher in infants as compared to neonates ($t = -2.25$, $df = 18$, $p = 0.04$) and decreasing in older age groups. The expression level of the truncated TrkB-T1 isoform, however, rose steadily from neonates to teenagers ($t = -3.94$, $df = 13$, $p = 0.002$) and decreased slightly in older age groups. We also quantified signals from an isoform of approximately 100 kDa corresponding most probably to TrkB-T-Shc. The expression level of this isoform did not show significant changes (Fig. S1f). Thus, our data suggest that the expression patterns of the full-

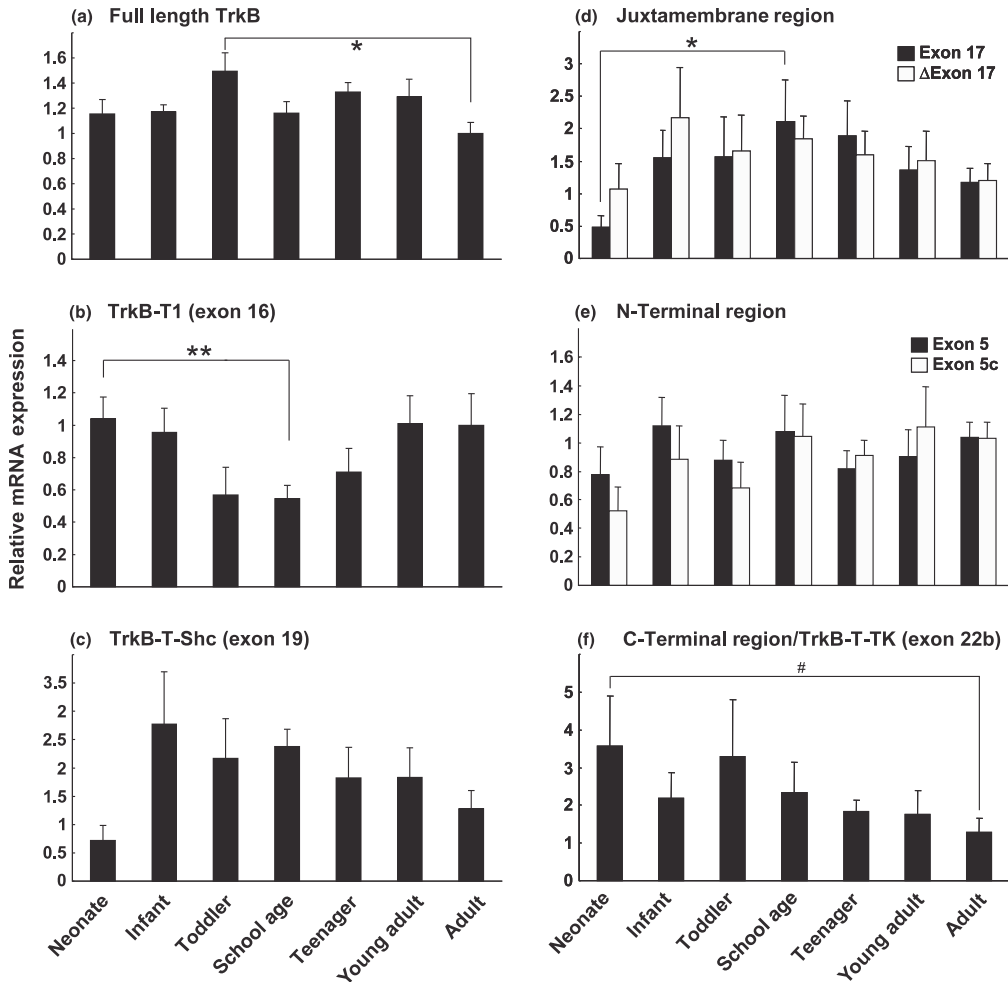


Fig. 4 Regulation of TrkB mRNA expression in the human prefrontal cerebral cortex during postnatal development. Expression of TrkB transcripts encoding: (a) full length TrkB (exon 24), (b) truncated TrkB-T1 (exon 16), (c) TrkB-T-Shc (exon 19), (d) juxtamembrane region [with and without exon 17 (Δ 17)], (e) N-terminal region (exon 5 and exon 5c)

and (f) C-terminal region or TrkB-T-TK (exon 22b). Data are expressed relative to the adult age group as $\Delta\Delta$ CT and presented as mean + SEM. *Significance $p < 0.05$; ** $p < 0.005$; #Trends toward significance.

length TrkB and TrkB-T1 protein isoforms differ from the expression patterns of the transcripts encoding these proteins during the postnatal development of human cerebral cortex.

Intracellular localization and phosphorylation of novel protein isoforms of TrkB

Bioinformatic analysis did not predict a signal sequence for membrane localization in the novel N-terminal truncated isoforms of the TrkB receptor encoded by transcripts with exon 5c. Because of this, we were interested in the

intracellular localization of these proteins. Considering that approximately 50% of TrkB transcripts in humans do not contain exon 17 (Fig. 2), and because exon 17 is not used in mouse TrkB transcripts because of the loss of the splice donor site of exon 17 (Fig. S1d), TrkB-N- Δ 17 was chosen for the analysis as a representative of N-terminal truncated isoforms. In addition, the novel C-terminal truncated TrkB-T-TK- Δ 17 isoform (encoded by the exon 22b) and the full-length TrkB and TrkB- Δ 17 receptor isoforms with intact tyrosine kinase domains, were studied for their intracellular

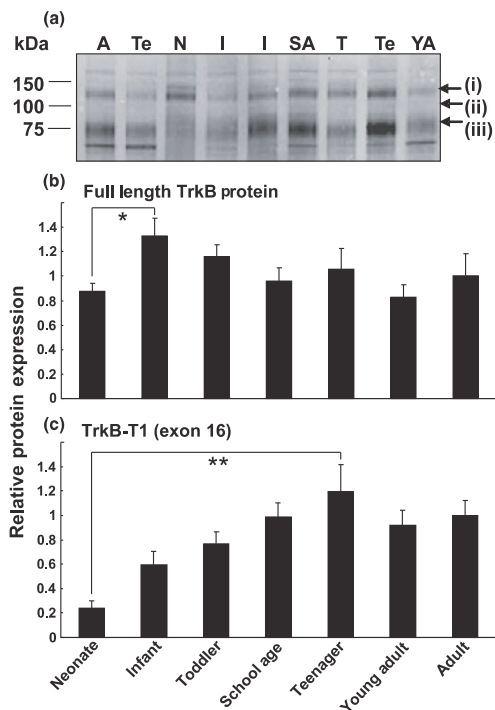


Fig. 5 Expression of TrkB protein isoforms in the human prefrontal cerebral cortex during postnatal development. (a) Representative western blot analysis of TrkB expression in the human prefrontal cerebral cortex during postnatal development. N, neonate; I, infant; T, toddler; SA, school age; YA, young adult; A, adult; (i) full-length TrkB; (ii) TrkB-T-Shc; (iii) TrkB-T1. (b and c) Quantification of the expression levels of the full-length TrkB (b) and TrkB-T1 (c) isoforms. Data are expressed relative to the adult age group as $\Delta\Delta$ CT and presented as mean + SEM. *Significance $p < 0.05$; ** $p < 0.005$.

localization pattern. DNA sequences encoding these protein isoforms were cloned into expression vector encoding C-terminal V5-His tagged TrkB fusion proteins, transfected into HEK293 cells and intracellular localization of tagged proteins was studied. Our results (Fig. 6) showed that all tested TrkB isoforms localized to the cell membrane and to the cytoplasm, with the exception of TrkB-N- Δ 17 which lacks a membrane-localization signal sequence and was found only in the cytoplasm.

The TrkB-T-TK protein isoforms encoded by TrkB mRNAs with exon 22b lack a part of the intracellular tyrosine kinase (Fig. 1c). To study if these protein isoforms contain intrinsic tyrosine kinase activity, we expressed a representative of this type of human TrkB protein isoforms, TrkB-T-TK- Δ 17, in HEK293 cells and compared the autophosphorylation levels of this isoform with the levels

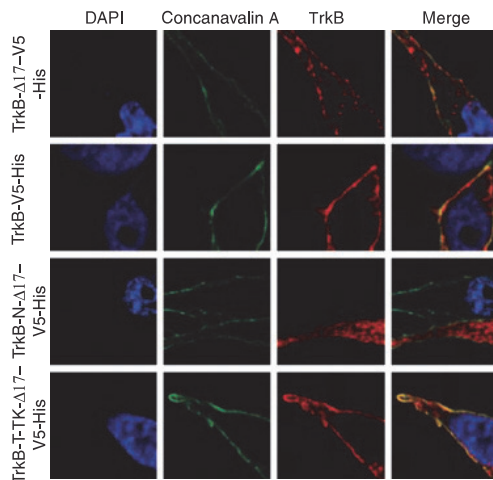


Fig. 6 Intracellular localization of different TrkB protein isoforms. Over-expression of TrkB isoforms in HEK293 cells. Red – TrkB; green – concanavalin A; blue – DAPI.

of autophosphorylation of TrkB, TrkB- Δ 17 and TrkB-N- Δ 17. Our results (Fig. 7a) showed that in contrast to all other TrkB protein isoforms tested, the TrkB-T-TK- Δ 17 protein was not autophosphorylated.

We next studied whether the TrkB-T-TK- Δ 17 isoform could be phosphorylated *in trans* by other TrkB isoforms that are enzymatically active. This aspect is especially interesting, as the TrkB-T-TK- Δ 17 isoform contains the tyrosine residue used by the full-length receptor for Shc protein binding. Therefore, we co-expressed E2 tagged TrkB and V5-His tagged TrkB fusion proteins in HEK293 cells to determine if the E2-tagged full-length TrkB receptor is capable of phosphorylating the V5-His tagged TrkB-T-TK- Δ 17 protein. We detected two different sub-populations of TrkB isoforms, probably because of different levels of post-translational modifications of the over-expressed proteins. TrkB-T-TK- Δ 17-V5-His proteins had molecular weights of approximately 120 kDa and 100 kDa, whereas TrkB-E2 proteins had molecular weights of approximately 140 and 120 kDa. Although the TrkB-E2 protein co-immunoprecipitated with the V5-His-tagged TrkB isoforms and despite the fact that signals from TrkB-E2 partially overlapped with signals from TrkB-T-TK- Δ 17-V5-His, we could detect a TrkB-T-TK- Δ 17-V5-His-specific signal corresponding to the 100 kDa isoform of TrkB-T-TK- Δ 17-V5-His proteins using the anti-phosphotyrosine antibody (Fig. 7b). This result indicates that similarly to other tested isoforms of TrkB, TrkB-T-TK- Δ 17 can be phosphorylated *in trans* by the full-length kinase domain-containing TrkB-E2 isoform. This would suggest that the novel C-terminal truncated isoforms encoded by TrkB transcripts with exon 22b could act as functional

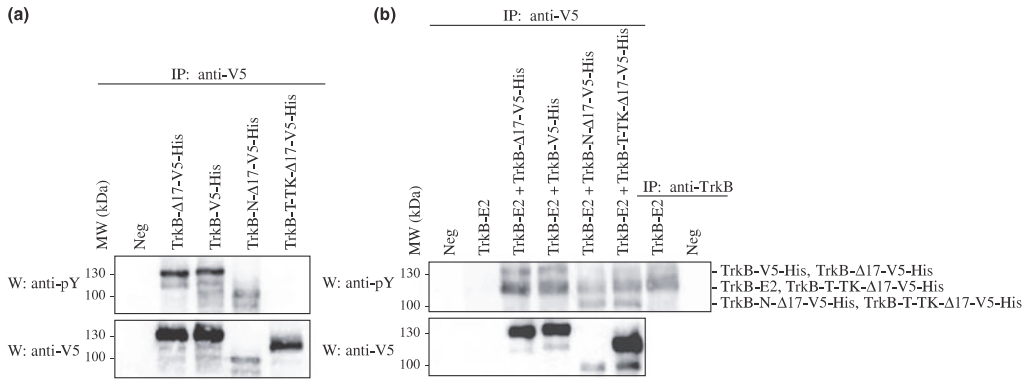


Fig. 7 Auto-phosphorylation and *in trans* phosphorylation potential of different TrkB protein isoforms. (a) HEK293 cells were transfected with expression constructs encoding V5-His tagged TrkB, TrkB-Δ17, TrkB-N-Δ17 and TrkB-T-TK-Δ17 proteins. The cells were lysed and subjected to immunoprecipitation with anti-V5 antibody 48 h post-transfection. Precipitated proteins were analysed with anti-phosphotyrosine (anti-pY) and anti-V5 antibodies using SDS-PAGE and

western blotting techniques. (b) HEK293 cells were co-transfected with V5-His tagged expression plasmids encoding TrkB, TrkB-Δ17, TrkB-N-Δ17 and E2 tagged TrkB. The cells were lysed and subjected to immunoprecipitation with anti-V5 or anti-TrkB antibodies 48 h post-transfection. Precipitated proteins were analysed with anti-phosphotyrosine (anti-pY) and anti-V5 antibodies using SDS-PAGE and western blotting techniques.

signaling receptors that can be activated by the full-length TrkB which can then transfer the signal to Shc.

Discussion

In this study, we have re-examined the structure, alternative splicing pattern and spatio-temporal expression profile of the human TrkB gene. The 5' UTR of the gene is known to be complex, however, we have shown an even more diversified structure of the region formed by the use of alternative promoters and alternative splicing generating at least 16 different 5' UTRs. The 5' UTR of the TrkB gene has previously been shown to possess an IRES that contains sub-regions of translation activation or inhibition (Dobson *et al.* 2005). Thus, the 5' UTR is likely to regulate the expression of TrkB proteins at the level of translation. This would explain the rationale behind the existence of so many alternative 5' UTRs. Because of this, we were interested to know whether there was a tissue-specific regulation of transcription initiation and splicing of the TrkB 5' UTR. As our results indicated, all the tissues studied showed highly similar patterns of expression of TrkB exons 1–5, suggesting that the tissue-specific expression of TrkB receptors is not affected by the use of alternative 5' UTRs. It is still possible, however, that tissue-specific factors such as 5' UTR binding proteins could differentially affect the spatial regulation of translation efficiency in different tissues.

Interestingly, we have described a novel 5' exon named 5c, which gives rise to novel N-terminal truncated TrkB proteins. All other TrkB 5' UTRs are linked to transcripts encoding

proteins with identical N-termini. The new exon 5c was expressed mainly in the nervous system with the highest levels observed in the cerebellum, where approximately 6% of all TrkB transcripts start with exon 5c. There are many different protein isoforms that are encoded by transcripts starting with exon 5c, depending on the 3' exons and alternative splicing, but all of them lack the signal sequence for intra-membrane localization, the whole leucine-rich domain and one cysteine-rich domain. We studied in detail the isoform TrkB-N-Δ17 that encodes a tyrosine kinase domain, and showed that, as predicted, this isoform is not localized to the cell plasma membrane, but is instead cytosolic. In addition, TrkB-N-Δ17 becomes phosphorylated if over-expressed in HEK293 cells, which suggests a unique function for these proteins – activated TrkB-N-Δ17 isoforms can potentially phosphorylate other, yet unidentified proteins in the cytosol and hence, take part in signaling cascades. Because of spatial restrictions, TrkB-N-Δ17 isoforms are unlikely to be activated by neurotrophins – from translation to secretion, neurotrophins are kept stored in membranous compartments, such as the endoplasmic reticulum (ER), Golgi complex and extracellular space, and thus, cannot come into contact with the cytosolic TrkB-N-Δ17 isoform. It is possible that the novel TrkB isoforms can be activated independently of neurotrophins by other cytosolic proteins. For example, it has been shown that TrkB receptor can be transactivated in the cytosol independently of neurotrophins by G-protein-coupled receptors, including adenosine 2A receptor, pituitary adenylate cyclase-activating polypeptide receptors and dopamine D₁ receptor (Lee and Chao 2001;

Lee *et al.* 2002; Rajagopal *et al.* 2004; Iwakura *et al.* 2008), or Src family kinases activated by zinc ions (Huang *et al.* 2008). The same proteins could be responsible for activating the novel N-terminally truncated TrkB isoforms. In addition, under certain conditions, the expression level of TrkB-N isoforms can rise and at higher intracellular concentrations the proteins can be autophosphorylated, as we have demonstrated by TrkB-N- Δ 17 over-expression studies.

In this study, we have also characterized a novel 3' exon of TrkB transcripts – an extended form of exon 22, named 22b. Similar to transcripts with exon 5c, exon 19 or exon 24, TrkB mRNAs with exon 22b present a highly specific spatial expression pattern – they are mainly expressed in neural tissues. Remarkably, transcripts with exon 22b account for approximately 10% of all TrkB-encoding transcripts in the cerebellum – an expression level that is higher than that of previously described TrkB-T-Shc isoform-encoding transcripts. No statistically significant age-related differences in the expression level of TrkB mRNAs with exon 22b could be detected in the DLPFC, however it is possible that these transcripts are temporally regulated in some other brain region, for example, in the cerebellum, where these mRNAs are expressed at a higher level, and thus, seem to have a more important function. A representative of the proteins encoded by transcripts with exon 22b, named TrkB-T-TK- Δ 17, was localized to the cell plasma membrane when over-expressed and although it cannot get autophosphorylated because of a disruption in the tyrosine kinase domain, it can be phosphorylated by the full-length TrkB receptor. Phosphorylated TrkB-T-TK- Δ 17 protein could function as an important signaling molecule – for example, it contains a docking site for Shc protein binding and can, thus, activate signaling cascades leading to survival and differentiation of the cell. On the other hand, the TrkB-T-TK- Δ 17 protein does not contain a docking site for PLC- γ and therefore, cannot activate the signaling cascades involving this signaling molecule. Hence, it can be concluded that TrkB-T-TK- Δ 17 exerts different effects compared to the full length TrkB receptor. It is also possible, that the unique C-terminal sequence of 27 amino acids of TrkB-T-TK- Δ 17 contains additional binding sites for yet unidentified proteins.

It is of interest to note that unlike the TrkB-T-TK- Δ 17 isoform, another C-terminal truncated isoform of TrkB, named TrkB-T-Shc, which also contains a binding site for Shc protein and is expressed mainly in the nervous system, cannot be phosphorylated by the full-length receptor (Stoilov *et al.* 2002). Therefore, it can be concluded that these structurally similar truncated isoforms of TrkB receptor most probably have very distinct functions.

Exon 17 of the TrkB gene has been described to be a cassette exon (Stoilov *et al.* 2002), but thus far, no functional relevance has been connected to the alternative splicing of this exon. We have shown here that proteins with or without sequences encoded by exon 17 showed identical localization

patterns and phosphorylation capabilities. However, the mRNAs encoding them displayed different expression patterns in the DLPFC – no statistically significant fluctuation was seen in the expression level of transcripts without exon 17. This is in contrast to transcripts with exon 17, which showed a relatively low expression level in neonates, peaking in school age, and after which the expression level started to descend gradually. This finding indicates that the presence of exon 17 is likely to have functional significance. It is possible, for example, that the presence or absence of protein sequences encoded by exon 17 is influencing the receptor's ability to transfer signals to downstream signaling molecules.

In this study, we confirmed the spatial expression patterns of full-length TrkB and C-terminal truncated TrkB-T1-encoding transcripts described previously (Shelton *et al.* 1995; Stoilov *et al.* 2002) – nervous system specific versus ubiquitous expression pattern, respectively. In contrast, the temporal regulation of expression of these isoforms did not compare with previous data (Romanczyk *et al.* 2002). As was described previously using *in situ* hybridization in the DLPFC, the expression level of mRNAs encoding the full-length TrkB peaked in young adults while the levels of TrkB-T1 isoform-encoding transcripts did not show remarkable change throughout the lifespan (Romanczyk *et al.* 2002). On the other hand, using qPCR, we showed in this study that full-length TrkB-encoding transcripts are expressed at their highest level in the toddler age group but fall remarkably in adults. For TrkB-T1-encoding mRNAs, we found a relatively high expression level in the neonate, infant, young adult and adult age groups, and a lower expression level in toddlers and school aged children. This difference could be the result of either different quantification methods used or the result of analysing different cohorts. Interestingly, the expression patterns of the full-length TrkB and TrkB-T1 proteins differed from the expression patterns of the transcripts encoding these proteins during the postnatal development of human cerebral cortex. We have observed a similar phenomenon for TrkC transcripts and protein isoforms (Beltaifa *et al.* 2005). These results suggest that in addition to transcriptional control, post-transcriptional mechanisms are involved in the regulation of the expression of neurotrophin receptors.

We also detected minor quantities of TrkB mRNAs with the exclusion of exon 12 in heart and skeletal muscle. Proteins encoded by these mRNAs (TrkB- Δ 12) lack the second IG-like domain, which is important for binding neurotrophins, and are similar to a variant of TrkA receptor (Δ TrkA) that has been found in acute myeloid leukemia cells (Reuther *et al.* 2000). Δ TrkA lacks part of the second IG-like domain and was shown to be constitutively active in promoting cell growth and resistance to apoptosis (Reuther *et al.* 2000). It would be of interest to determine whether the functional properties of TrkB- Δ 12 and Δ TrkA are similar or

whether the TrkB-Δ12 protein is activated by some ligand molecules.

Taken together, we have performed a detailed analysis of the human TrkB gene structure, expression profile of alternatively spliced transcripts, and protein isoforms encoded by alternatively spliced transcripts. Our findings emphasize the structural and functional variability of alternative TrkB receptor isoforms and suggest a diversified role of the receptor in the functioning of the human nervous system.

Acknowledgements

We thank Epp Väli for technical assistance, Heiti Paves for help in confocal microscopy and Enn Jõeeste from North Estonian Regional Hospital, Tallinn, for collaboration. KL and TT are supported by Estonian Ministry of Education and Research (Grant 0140143), Estonian Enterprise and Baltic Technology Development Ltd. CSW is supported by the Schizophrenia Research Institute utilising infrastructure funding from NSW Health, the University of New South Wales School of Psychiatry, and the Prince of Wales Medical Research Institute. JW is supported by the National Health and Medical Research Council Postdoctoral Training Fellowship (568884).

Supporting information

Additional Supporting Information may be found in the online version of this article:

Appendix S1. Supplementary Materials and Methods.

Figure S1. Semiquantitative analysis of expression levels of the conventional 5' UTR region of alternative TrkB transcripts in different human tissues.

Table S1. Primers and cycling conditions used for PCR analyses of the expression of TrkB gene in different human tissues.

As a service to our authors and readers, this journal provides supporting information supplied by the authors. Such materials are peer-reviewed and may be re-organized for online delivery, but are not copy-edited or typeset. Technical support issues arising from supporting information (other than missing files) should be addressed to the authors.

References

Allen S. J., Wilcock G. K. and Dawbarn D. (1999) Profound and selective loss of catalytic TrkB immunoreactivity in Alzheimer's disease. *Biochem. Biophys. Res. Commun.* **264**, 648–651.

Altar C. A., Vawter M. P. and Ginsberg S. D. (2009) Target identification for CNS diseases by transcriptional profiling. *Neuropsychopharmacology* **34**, 18–54.

Au C. W., Siu M. K., Liao X., Wong E. S., Ngan H. Y., Tam K. F., Chan D. C., Chan Q. K. and Cheung A. N. (2009) Tyrosine kinase B receptor and BDNF expression in ovarian cancers – effect on cell migration, angiogenesis and clinical outcome. *Cancer Lett.* **281**, 151–161.

Beltaifa S., Webster M. J., Ligons D. L., Fatula R. J., Herman M. M., Kleinman J. E. and Weickert C. S. (2005) Discordant changes in cortical TrkC mRNA and protein during the human lifespan. *Eur. J. Neurosci.* **21**, 2433–2444.

Binder D. K. and Scharfman H. E. (2004) Brain-derived neurotrophic factor. *Growth Factors* **22**, 123–131.

Bourgeois J. P. (1997) Synaptogenesis, heterochrony and epigenesis in the mammalian neocortex. *Acta Paediatr. Suppl.* **422**, 27–33.

Brodeur G. M., Mintum J. E., Ho R., Simpson A. M., Iyer R., Varela C. R., Light J. E., Kolla V. and Evans A. E. (2009) Trk receptor expression and inhibition in neuroblastomas. *Clin. Cancer Res.* **15**, 3244–3250.

Desmet C. J. and Peeper D. S. (2006) The neurotrophic receptor TrkB: a drug target in anti-cancer therapy? *Cell. Mol. Life Sci.* **63**, 755–759.

Dobson T., Minic A., Nielsen K., Amiott E. and Krushel L. (2005) Internal initiation of translation of the TrkB mRNA is mediated by multiple regions within the 5' leader. *Nucleic Acids Res.* **33**, 2929–2941.

Douma S., Van Laar T., Zevenhoven J., Meuwissen R., Van Garderen E. and Peeper D. S. (2004) Suppression of anoikis and induction of metastasis by the neurotrophic receptor TrkB. *Nature* **430**, 1034–1039.

Eggert A., Grotzer M. A., Ikegaki N., Zhao H., Cnaan A., Brodeur G. M. and Evans A. E. (2001) Expression of the neurotrophin receptor TrkB is associated with unfavorable outcome in Wilms' tumor. *J. Clin. Oncol.* **19**, 689–696.

Ernst C., Deleva V., Deng X. *et al.* (2009) Alternative splicing, methylation state, and expression profile of tropomyosin-related kinase B in the frontal cortex of suicide completers. *Arch. Gen. Psychiatry* **66**, 22–32.

Farooqi S. and O'Rahilly S. (2006) Genetics of obesity in humans. *Endocr. Rev.* **27**, 710–718.

Gamer A. S., Menegay H. J., Boeshore K. L., Xie X. Y., Voci J. M., Johnson J. E. and Large T. H. (1996) Expression of TrkB receptor isoforms in the developing avian visual system. *J. Neurosci.* **16**, 1740–1752.

Hackett S. F., Friedman Z., Freund J., Schoenfeld C., Curtis R., DiStefano P. S. and Campochiaro P. A. (1998) A splice variant of trkB and brain-derived neurotrophic factor are co-expressed in retinal pigmented epithelial cells and promote differentiated characteristics. *Brain Res.* **789**, 201–212.

Huang Y. Z., Pan E., Xiong Z. Q. and McNamara J. O. (2008) Zinc-mediated transactivation of TrkB potentiates the hippocampal mossy fiber-CA3 pyramid synapse. *Neuron* **4**, 546–558.

Iwakura Y., Nawa H., Sora I. and Chao M. V. (2008) Dopamine D1 receptor-induced signaling through TrkB receptors in striatal neurons. *J. Biol. Chem.* **23**, 15799–15806.

Kang H., Welcher A. A., Shelton D. and Schuman E. M. (1997) Neurotrophins and time: different roles for TrkB signaling in hippocampal long-term potentiation. *Neuron* **19**, 653–664.

Kermani P. and Hempstead B. (2007) Brain-derived neurotrophic factor: a newly described mediator of angiogenesis. *Trends Cardiovasc. Med.* **17**, 140–143.

Kermani P., Rafii D., Jin D. K. *et al.* (2005) Neurotrophins promote revascularization by local recruitment of TrkB+ endothelial cells and systemic mobilization of hematopoietic progenitors. *J. Clin. Invest.* **115**, 653–663.

Kimura K., Wakamatsu A., Suzuki Y. *et al.* (2006) Diversification of transcriptional modulation: large-scale identification and characterization of putative alternative promoters of human genes. *Genome Res.* **16**, 55–65.

Klein R., Conway D., Parada L. F. and Barbacid M. (1990) The trkB tyrosine protein kinase gene codes for a second neurogenic receptor that lacks the catalytic kinase domain. *Cell* **61**, 647–656.

Klein R., Lamballe F., Bryant S. and Barbacid M. (1992) The trkB tyrosine protein kinase is a receptor for neurotrophin-4. *Neuron* **8**, 947–956.

Koppel I., Aid-Pavlidis T., Jaanson K., Sepp M., Pruunsild P., Palm K. and Timmusk T. (2009) Tissue-specific and neural activity-regu-

- lated expression of human BDNF gene in BAC transgenic mice. *BMC Neurosci.* **10**, 68.
- Kumanogoh H., Asami J., Nakamura S. and Inoue T. (2008) Balanced expression of various TrkB receptor isoforms from the Ntrk2 gene locus in the mouse nervous system. *Mol. Cell. Neurosci.* **39**, 465–477.
- Lee F. S. and Chao M. V. (2001) Activation of Trk neurotrophin receptors in the absence of neurotrophins. *Proc. Natl Acad. Sci. USA* **6**, 3555–3560.
- Lee F. S., Rajagopal R., Kim A. H., Chang P. C. and Chao M. V. (2002) Activation of Trk neurotrophin receptor signaling by pituitary adenylate cyclase-activating polypeptides. *J. Biol. Chem.* **11**, 9096–9102.
- Lewin G. R. and Barde Y. A. (1996) Physiology of the neurotrophins. *Annu. Rev. Neurosci.* **19**, 289–317.
- Li Z., Chang Z., Chiao L. J., Kang Y., Xia Q., Zhu C., Fleming J. B., Evans D. B. and Chiao P. J. (2009a) TrkB-T1 induces liver metastasis of pancreatic cancer cells by sequestering Rho GDP dissociation inhibitor and promoting RhoA activation. *Cancer Res.* **69**, 7851–7859.
- Li Z., Beutel G., Rhein M. *et al.* (2009b) High-affinity neurotrophin receptors and ligands promote leukemogenesis. *Blood* **113**, 2028–2037.
- Middlemas D. S., Lindberg R. A. and Hunter T. (1991) TrkB, a neural receptor protein-tyrosine kinase: evidence for a full-length and two truncated receptors. *Mol. Cell. Biol.* **11**, 143–153.
- Nakagawara A., Azar C. G., Scavarda N. J. and Brodeur G. M. (1994) Expression and function of TRK-B and BDNF in human neuroblastomas. *Mol. Cell. Biol.* **14**, 759–767.
- Nakagawara A., Liu X. G., Ikegaki N., White P. S., Yamashiro D. J., Nycum L. M., Biegel J. A. and Brodeur G. M. (1995) Cloning and chromosomal localization of the human TRK-B tyrosine kinase receptor gene (NTR2). *Genomics* **25**, 538–546.
- Ninkina N., Grashchuck M., Buchman V. L. and Davies A. M. (1997) TrkB variants with deletions in the leucine-rich motifs of the extracellular domain. *J. Biol. Chem.* **272**, 13019–13025.
- Ohira K., Kumanogoh H., Sahara Y., Homma K. J., Hirai H., Nakamura S. and Hayashi M. (2005) A truncated tropomyosin-related kinase B receptor, T1, regulates glial cell morphology via Rho GDP dissociation inhibitor 1. *J. Neurosci.* **25**, 1343–1353.
- Pillai A. (2008) Brain-derived neurotrophic factor/TrkB signaling in the pathogenesis and novel pharmacotherapy of schizophrenia. *Neurosignals* **16**, 183–193.
- Rajagopal R., Chen Z. Y., Lee F. S. and Chao M. V. (2004) Transactivation of Trk neurotrophin receptors by G-protein-coupled receptor ligands occurs on intracellular membranes. *J. Neurosci.* **30**, 6650–6658.
- Rantamaki T. and Castren E. (2008) Targeting TrkB neurotrophin receptor to treat depression. *Expert Opin. Ther. Targets* **12**, 705–715.
- Reichardt L. F. (2006) Neurotrophin-regulated signalling pathways. *Philos. Trans. R. Soc. Lond. B Biol. Sci.* **361**, 1545–1564.
- Reuther G. W., Lambert Q. T., Caligiuri M. A. and Der C. J. (2000) Identification and characterization of an activating TrkA deletion mutation in acute myeloid leukemia. *Mol. Cell. Biol.* **20**, 8655–8666.
- Romanczyk T. B., Weickert C. S., Webster M. J., Herman M. M., Akil M. and Kleinman J. E. (2002) Alterations in trkB mRNA in the human prefrontal cortex throughout the lifespan. *Eur. J. Neurosci.* **15**, 269–280.
- Rose C. R., Blum R., Pichler B., Lepier A., Kafitz K. W. and Konnerth A. (2003) Truncated TrkB-T1 mediates neurotrophin-evoked calcium signalling in glia cells. *Nature* **426**, 74–78.
- Schneider R. and Schweiger M. (1991) A novel modular mosaic of cell adhesion motifs in the extracellular domains of the neurogenic trk and trkB tyrosine kinase receptors. *Oncogene* **6**, 1807–1811.
- Shelton D. L., Sutherland J., Gripp J., Camerato T., Armanini M. P., Phillips H. S., Carroll K., Spencer S. D. and Levinson A. D. (1995) Human trks: molecular cloning, tissue distribution, and expression of extracellular domain immunoadhesins. *J. Neurosci.* **15**, 477–491.
- Squinto S. P., Stitt T. N., Aldrich T. H. *et al.* (1991) TrkB encodes a functional receptor for brain-derived neurotrophic factor and neurotrophin-3 but not nerve growth factor. *Cell* **65**, 885–893.
- Stoilov P., Castren E. and Stamm S. (2002) Analysis of the human TrkB gene genomic organization reveals novel TrkB isoforms, unusual gene length, and splicing mechanism. *Biochem. Biophys. Res. Commun.* **290**, 1054–1065.
- Strohmaier C., Carter B. D., Urfer R., Barde Y. A. and Dechant G. (1996) A splice variant of the neurotrophin receptor trkB with increased specificity for brain-derived neurotrophic factor. *EMBO J.* **15**, 3332–3337.
- Timmusk T., Palm K., Metsis M., Reintam T., Paalme V., Saarma M. and Persson H. (1993) Multiple promoters direct tissue-specific expression of the rat BDNF gene. *Neuron* **10**, 475–489.
- Urfer R., Tsoulfas P., O'Connell L., Shelton D. L., Parada L. F. and Presta L. G. (1995) An immunoglobulin-like domain determines the specificity of neurotrophin receptors. *EMBO J.* **14**, 2795–2805.
- Webster M. J., Herman M. M., Kleinman J. E. and Shannon Weickert C. (2006) BDNF and trkB mRNA expression in the hippocampus and temporal cortex during the human lifespan. *Gene Expr. Patterns* **6**, 941–951.
- Wong J., Webster M. J., Cassano H. and Weickert C. S. (2009) Changes in alternative brain-derived neurotrophic factor transcript expression in the developing human prefrontal cortex. *Eur. J. Neurosci.* **29**, 1311–1322.
- Yamada K. and Nabeshima T. (2003) Brain-derived neurotrophic factor/TrkB signaling in memory processes. *J. Pharmacol. Sci.* **91**, 267–270.
- Yu X., Liu L., Cai B., He Y. and Wan X. (2008) Suppression of anoikis by the neurotrophic receptor TrkB in human ovarian cancer. *Cancer Sci.* **99**, 543–552.

Supplementary Materials and Methods

Computer analysis and RT-PCR

The human TrkB gene structure and transcripts in the public databases were identified by analyzing genomic, mRNA, and expressed sequence tag (EST) databases using the Blat algorithm (<http://genome.ucsc.edu>). Based on this analysis, primers were designed to analyze the expression of TrkB mRNAs and to construct plasmids for TrkB riboprobe design and cloning of TrkB isoforms (Supplementary Table 1). Reverse transcription and PCR for spatially regulated TrkB expression analyses was performed as described previously (Koppel et al. 2009). PCR with primers specific for the ubiquitously expressed hypoxanthine guanine phosphoribosyltransferase (HPRT) was performed as a control to determine the amount of human template cDNA in different PCRs.

Quantitative PCR

Analysis of cohort demographics, RNA extraction, reverse transcription and normalization of qPCR results for the study of temporally regulated expression of alternative TrkB transcripts in the human DLPFC were performed as described by Wong et al 2009. Levels of transcripts encoding the full-length TrkB and C-terminal truncated TrkB-T1 receptors were measured by qPCR using an ABI Prism 7900 sequence detection system with a 384-well format. Control probes or housekeeping genes used to calculate the geometric mean were chosen from Applied Biosystems (Assays-on-Demand, Applied Biosystems, Foster City, CA) and included cyclophilin A (Cat # hs99999904-m1), GUSB (glucuronidase, beta Cat #

hs99999908-m1), UBC (ubiquitin C Cat # hs00824723-m1), and PBGD (porphobilinogen deaminase Cat # hs00609297-m1). ABI probes used for amplification of the two major TrkB transcripts were: full length TrkB (Cat # hs01093098-m1) and TrkB-T1 (Cat # hs01093110-m1). Each 10 μ l PCR reaction contained 3 μ l of cDNA, 0.5 μ l of 20X primer/probe mixture, 5 μ l of RT-PCR Mastermix Plus (Eurogentec, Seraing, Belgium) containing Hot Goldstar DNA Polymerase, dNTPs with dUTP, uracil-N-glycosylase, passive reference, and optimized buffer components; and 1.5 μ l DEPC deionized water. For TrkB transcripts, 3 ng/ μ l of cDNA was used for the amplification. Samples were run with an 8 point standard curve using serial dilutions of pooled cDNA derived from RNA obtained from brain tissue (pooled from all cases). Several no template controls were also included which produced no signal. PCR cycling conditions were: 50°C for 2 minutes, 95°C for 10 minutes, 40 cycles of 95°C for 15 seconds and 59°C or 60°C for 1 minute. PCR data were obtained with the Sequence Detector Software (SDS version 2.0, Applied Biosystems). SDS software plotted real-time fluorescence intensity. The threshold was set within the linear phase of the amplicon profiles. Measurements for all samples were performed in triplicates. The geometric mean of the four housekeeping genes used was calculated as previously described (Vandesompele et al. 2002). None of the housekeeping genes varied across development (ANOVA $p > 0.05$ for all housekeeping genes and geometric mean). The $2^{-\Delta\Delta CT}$ method was used for the analysis of gene expression (Livak & Schmittgen, 2001) where the adult group was set as the control group to which other developmental groups were normalized. To identify other TrkB transcript isoforms, reactions were conducted in 10 μ l reactions with 40 ng of cDNA as template and using the qPCR Kit for SYBR® Green I, No ROX (Eurogentec), primers and reaction conditions are detailed in Supplementary Table 1, and LightCycler 2.0 (Roche).

Western blotting

To measure the protein expression levels of full length TrkB and TrkB-T1, ~40 mg of frozen tissue from the DLPFC was homogenized as previously described (Wong et al. 2009). Protein concentrations were determined using the Bradford protein assay (Sigma-Aldrich). Samples of equal protein (10 μ g) were assayed by western blotting in blinded and randomized order and the entire cohort was run in duplicate as previously described (Wong et al. 2009). Samples of equal protein (20 μ g) were assayed by western blotting by SDS-PAGE on 12% Bis-Tris gels (BioRad). Proteins were transferred onto nitrocellulose membranes and incubated with blocking solution (5 % w/v non-fat milk, 0.1 % v/v Tween-20 in PBS (PBST); RT; 1 h). Membranes were incubated with a primary antibody for human TrkB (TrkB antibody diluted 1:3000 in 5% BSA-PBST; 4 °C; overnight; TrkB: Cell Signaling Technology Cat # 4603) or β -actin (diluted 1:10,000 in blocking solution; 4 °C; overnight; Millipore Cat # MAB1501). Membranes were washed 3 x 10 minutes with PBST and incubated with peroxidase-conjugated affinity purified secondary antibodies, anti-rabbit (diluted 1:1000 in 5% BSA-PBST for TrkB) or anti-mouse (diluted 1:5000 in blocking solution for β -actin) (Millipore) at RT for 1 h. After further washing, bound antibodies were incubated with enhanced chemiluminescence reagent (Millipore) and visualized by chemiluminescence on a Chemidoc Imaging System (BioRad). Bands were quantitated by densitometry using the Quantity One 1-D Analysis Software v4.6.5 (BioRad). The geometric mean of the duplicate western runs were calculated and used as the average for statistical analysis. Population outliers were removed when calculated data points for each sample were greater than two

standard deviations from the mean for that age group. No population outliers were detected for full length TrkB and TrkB-T1. Statistical analyses were conducted using Statistica 7 (StatSoft Inc., 2000, STATISTICA for Windows). Two-tail unpaired t-tests were conducted to assess significance of changes in full length TrkB and TrkB-T1 protein between the highest and lowest expressing age groups. A $p < 0.05$ was considered statistically significant.

Ribonuclease protection assay (RPA)

For construction of plasmids for riboprobe synthesis, DNA fragments specific for the alternative TrkB transcripts were amplified from cDNA template from the human left cerebellum using a mix of FirePol (Solis Biodyne) and Pfu (Fermentas) enzymes, and primers (detailed in Supplemental material Table 1). PCR products were cloned into EcoRV-linearized pBluescript II KS+ vector (Fermentas) and verified by sequencing. For riboprobe production, the plasmids were linearized and antisense RNA was synthesized using Ambion MAXI Script T7/T3 kit according to the manufacturer's instructions using ^{32}P -UTP. RPA was performed as described previously using the RPA kit from Ambion (Timmusk et al. 1993).

Cloning of TrkB isoforms

To clone the TrkB isoforms, PCR was conducted using Expand Long Template PCR System (Roche) according to manufacturer's instructions using cDNA from the left cerebellum as template and primers: TrkB_5F_Kozak and TrkB_24R_nonstop (Supplementary Table 1). PCR products were cloned into pcDNA3.1/V5-His-TOPO vector

(Invitrogen) to obtain the pcDNA3.1/TrkB- Δ 17-V5-His construct encoding C-terminal V5-His tagged TrkB- Δ 17. Subsequent PCRs were conducted using a mix of FirePol (Solis Biodyne) and Pfu (Fermentas) enzymes to obtain constructs pcDNA3.1/TrkB-V5-His, pcDNA3.1/TrkB-N- Δ 17-V5-His and pcDNA3.1/TrkB-T-TK- Δ 17-V5-His encoding C-terminal V5-His tagged TrkB, TrkB-N- Δ 17 and TrkB-T-TK- Δ 17, respectively (for primers used see Supplementary Table 1). These PCR products were first cloned into pTZ57R vector (Fermentas) and subcloned into the pcDNA3.1/TrkB- Δ 17-V5-His vector using the following restriction enzymes: Eco47III and ScaI (to obtain pcDNA3.1/TrkB-V5-His), BamHI and Eco47III (for pcDNA3.1/TrkB-N- Δ 17-V5-His), XbaI and ScaI (for pcDNA3.1/TrkB-T-TK- Δ 17-V5-His). The pQM/TrkB-E2 construct was obtained by excising and ligating the TrkB coding region of the pcDNA3.1/TrkB-V5-His vector (cut with BamHI and EcoRV) into the pQM-CMV-E2Tag-C-A vector (Abcam; cut with SmaI and BamHI; all restriction enzymes were purchased from Fermentas). Constructs were verified by sequencing.

Immunofluorescence and confocal microscopy

50 % confluent HEK293 cells grown in Dulbecco's Modified Eagle's Medium (DMEM; Gibco Invitrogen) containing 10% fetal bovine serum on cover slips were transfected with PEI reagent (InBio) according to the manufacturer's instructions. 48 h post transfection, the cells were fixed with 4 % paraformaldehyde (PFA; Scharlau) in PBS for 15 minutes and blocked with 2 % bovine serum albumine (BSA; Sigma) in PBS for 20 minutes. Alexa Fluor 488-conjugated concanavalin A (Invitrogen) was used in 30 μ g/ml concentration in 0.2 % BSA in PBS for 10 minutes to stain the cell membrane. Stained cells were fixed again with 4

% PFA in PBS for 15 minutes, permeabilized with 0.1 % Triton X-100 (Amresco) in PBS for 1 minute and blocked overnight with 2 % BSA in PBS. Between treatments with different agents, the cover slips were washed with PBS. Staining of TrkB isoforms were conducted using a primary anti-V5 antibody (Sigma, V8137) in 1:1500 dilution in 0.2 % BSA in PBS for 1 h, followed by washes with PBS, and secondary Alexa Fluor 568-conjugated goat anti-rabbit antibody (Invitrogen) in 1:2000 dilution in 0.2 % BSA in PBS. Cover slips were rinsed and mounted using ProLong Gold antifade reagent with DAPI (Invitrogen). Labeled cells were analyzed using the LSM 510 (Zeiss) confocal microscopy system.

Immunoprecipitation

70 % confluent HEK293 cells grown in DMEM containing 10 % fetal bovine serum on 60 mm plates were transfected with PEI reagent according to the manufacturer's instructions and lysed with 200 μ l radioimmunoprecipitation buffer [RIPA: 50 mM TrisHCl, pH 8; 150 mM NaCl; 1% NP-40; 0.5 % sodium deoxycholate; 0.5 % SDS, 1 mM DTT; Complete Protease Inhibitor Cocktail (Roche) and PhosSTOP Phosphatase Inhibitor Cocktail (Roche)]. 0.5 mg of a 1 mg/ml total protein extract was immunoprecipitated with 1.8 μ g mouse anti-V5 antibody (Invitrogen) or anti-TrkB antibody (Santa Cruz, SC-8316) overnight in the presence of 25 μ l of GammaBind Plus Sepharose beads (GE Healthcare). The beads were then washed 2 x with PBS and heated for 2 min at 85 °C with 30 μ l of 1 x Laemmli buffer. 10 μ l of precipitated proteins were separated on 6 % SDS-PAGE and transferred onto PVDF membranes using a conventional semi-dry method. Membranes were blocked with 5 % BSA in PBS-Tween (PBS and 0.05 % Tween 20) overnight and incubated with primary antibodies

(1:2000 mouse anti-phosphotyrosine (Millipore, 4G10) or 1:6000 mouse anti-V5) in 2 % BSA in PBS-Tween for 1 h. Subsequently, the membranes were washed with PBS-Tween and incubated with secondary goat HRP-conjugated anti-mouse antibody (Pierce) in 1:6000 dilution in 2 % BSA in PBS-Tween for 1 h. The signal was detected using SuperSignal West Femto Maximum Sensitivity Substrate (Pierce) and with the ImageQuant 400 Imager system (GE Healthcare) according to manufacturers' instructions.

Supplementary References

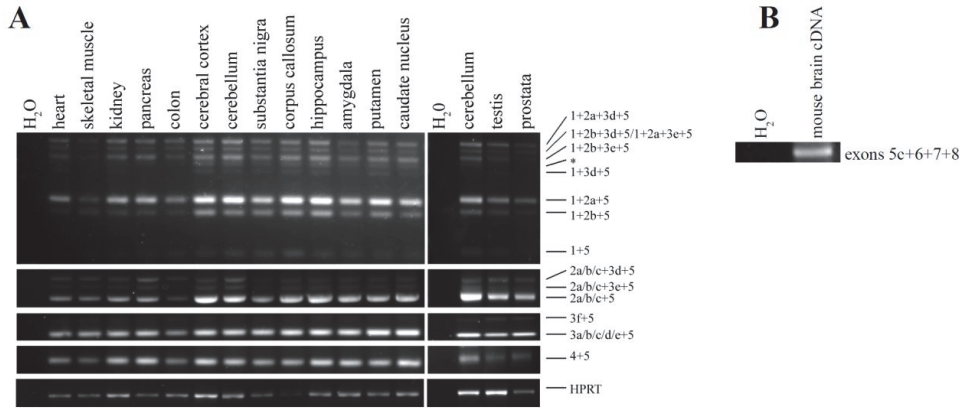
Koppel I., Aid-Pavlidis T., Jaanson K., Sepp M., Pruunsild P., Palm K. and Timmusk T. (2009) Tissue-specific and neural activity-regulated expression of human BDNF gene in BAC transgenic mice. *BMC Neurosci* 10, 68.

Livak K. J. and Schmittgen T. D. (2001) Analysis of relative gene expression data using real-time quantitative PCR and the 2(-Delta Delta C(T)) Method. *Methods* 4, 402-408.

Timmusk T., Palm K., Metsis M., Reintam T., Paalme V., Saarma M. and Persson H. (1993) Multiple promoters direct tissue-specific expression of the rat BDNF gene. *Neuron* 10, 475-489.

Vandesompele J., De Paepe A. and Speleman F. (2002) Elimination of primer-dimer artifacts and genomic coamplification using a two-step SYBR green I real-time RT-PCR. *Anal Biochem* 1, 95-98.

Wong J., Webster M. J., Cassano H. and Weickert C. S. (2009) Changes in alternative brain-derived neurotrophic factor transcript expression in the developing human prefrontal cortex. *Eur J Neurosci* 29, 1311-1322.



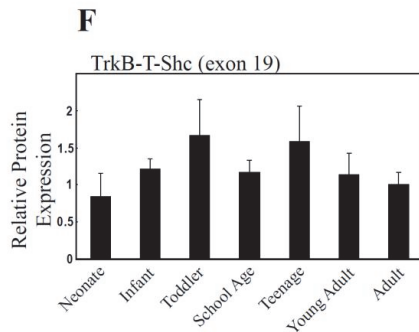
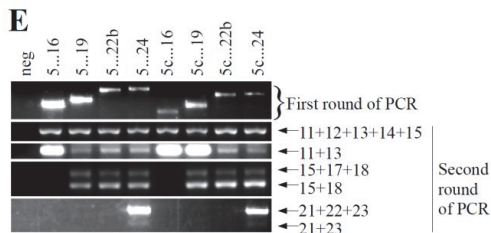
C

Human ...GTGTTTGATACTGAGATAGGCAGCCCT-AAAGTGGGGCTTGGGCTGTGGCCCTCCGGTTGTCGAGTGGCGCATGCAATTTTTC-CCTCCAC
 Orangutan ...GTATTTGATACTGAGATAGGCAGCCCT-AAAGTGGGGCTTGGGCTGTGGCCCTCCGGTTGTCGAGTGGCGCATGCAATTTTTC-CCTCCAC
 Dog ...GTGTTTGATACTGAGATAGGCAGCCCTGAAAATAGGGCTTGGGCTGTGGCCCTCCGGTTGCGAGTGGCGCATGCTTTTTT-CCTCC-T
 Horse ...GTGTTTGACACAGAGTAGGCAGCCCGAAAAGCAGAGTGGGCTGTGGCCCTCCGGTTGGGAGTGGCGCATGCTTTTTCTGCCTCCAC
 Rat ...GTGATTGGACTGAGAAAGGCAGCCCTGAAAATATGGCTTGGGCTGTGGCCCTCCGGTTGGGAGTGGCGCATGCACTCCCT-CCCCAA
 Mouse ...GTGATTGAGACTGAGAAAGGCAGCCCTGTAAGTAGGGCTTGGGCTGTGGCCCTCCGGTTGGGAGTGGCGCATGCACTCCCT-CCCCAA

Human -AGAAAACATACAACCATGT-TTCTGCCAACGTAGTTGAC-----CAAGATAACCTG-----TTTTTAAATgtaagtaaga..
 Orangutan -AGAAAACATACAACCATGT-TTCTGCCAACGTAGTTGAC-----CAAGATAACCTG-----TTTTTAAATgtaagtaaga..
 Dog GAGAAAACGCACGCC-TGT-TTCTGCCAACGTAGTTGAC-----TGAGATAACCTG-----TTTTTAAATgtaagtaaga..
 Horse -AGAAAACGCACCTCC-TGT-TTCTGCCAACATAGTTGAC-----CGAGATAACCTG-----TTTTTGAATgtaagtaaga..
 Rat TGTACAAGGG-----TGTTTTCTGCCAGTGCAGCTGCCAGTGCCAAAGGCATCAAGATAACCTGTTTTGGTTTTTAAATgtaagtagga..
 Mouse TGTACAAGGG-----TGTTTTCTGCCAATGCAGCTGCCAGTGCCAAAGGAGTCAAGATAACCTGTTTTGGTTTTTAAATgtaagtagga..

D

Human ...ttgtgtggttttcagATTCTCATGGTTGGATTGGGAAAGTAAATCAAGACAAGGTGTTGgtaagtagtact...
 Orangutan ...ttgtgtggttttcagATTCTCATGGTTGGATTGGGAAAGTAAATCAAGACAAGGTGTTGgtaagtagtact...
 Dog ...ttgtgtggttttcagATTCTCATGGTTGGATTGGGAAAGTAAATCAAGACAAGGTGTTGgtaagtagtact...
 Horse ...ttgtgtggttttcagATTCTCATGGTTGGATTGGGAAAGTAAATCAAGACAAGGTGTTGgtaagtagtact...
 Rat ...ttgtgtggttttcagATTCTCATGGTTGGATTGGGAAAGTAAATCAAGACAAGGTGTTGgtaagtagtact...
 Mouse ...ttgtgtggttttcagATTCTCATGGTTGGCAATGGGAAAGTAAAGTCAAGACAAGGTGTTGggaagtggtact...



Supplementary Figure 1

Supplementary Figure 1. A – Semiquantitative analysis of expression levels of the conventional 5' UTR region of alternative TrkB transcripts in different human tissues. Numbers of amplified TrkB exons are shown on the right. Asterisk indicates a PCR artefact. Hypoxanthine guanine phosphoribosyltransferase (HPRT) was used as the housekeeping control. **B** – RT-PCR analysis of mouse TrkB transcripts encoding exons 5c, 6, 7 and 8. **C** and **D** – sequence alignment of human, orangutan, dog, horse, rat and mouse genomic sequences encoding the (putative) TrkB exon 5c (**C**) and exon 17 (**D**), and the flanking areas. Capital letters indicate exons and lower case introns. Differences from the human sequence are in bold. **E** – nested RT-PCR of the full-length transcripts of TrkB in human cerebellum. Exons amplified during the first round of PCR are shown above. No product was detected in the negative control PCR reactions without cDNA for each primer combination (data not shown). Exons amplified during the second round of PCR are shown on the right. PCR products from the first round of PCR were used as templates for the second round of PCR. Neg – negative control: for the first round of PCR, the reaction was performed with cDNA and without primers; for the second round of PCR, the reaction was performed with cDNA and primers. All amplicons were verified by sequencing. **F** – Quantification of the expression level of TrkB-T-Shc protein isoform in the human prefrontal cerebral cortex during postnatal development. Data is expressed relative to the adult age group as $\Delta\Delta\text{CT}$ and presented as mean + SEM.

Supplementary Table 1.

Primers and cycling conditions used for PCR analyses of the expression of TrkB gene in different human tissues:

Aplified TrkB exons	Primers (5' -> 3')	Amplicon length (bp)	PCR cycles	Primer annealing temperature (°C)	PCR product extension time (s)
1 ... 5	trkB_1F CACCCTAGCACACATGAACAC trkB_5R2 GCGCAGATTCCCTTGTTAGATG	409; 374; 339; 287; 200; 165; 78	38	52	35
2a/b/c ... 5	trkB_2F CGGAGGAACGGTTCATCTTAG trkB_5R2 GCGCAGATTCCCTTGTTAGATG	282; 244; 73	38	52	35
3a/b/c/d/e/f ... 5	trkB_3F GGTAGCAGGAGCCTGGAC trkB_5R2 GCGCAGATTCCCTTGTTAGATG	237; 160	38	52	35
4 ... 5	trkB_4F CGAAGAGAGAGTGGGCAC trkB_5R2 GCGCAGATTCCCTTGTTAGATG	103	38	52	35
5/5b ... 11	trkB_5F ACTGGCTGCTAGGGATGTC trkB_11R GCACAGTGAGGTTGACAGAATC	863	38	52	60
5c ... 11	trkB_5cF AACGTAGTTGACCAAGATAACCTG trkB_11R GCACAGTGAGGTTGACAGAATC	670	38	52	60
11 ... 15	trkB_11F CACAGGGCTCCTTAAGGATAAC trkB_15R TCATGCCAAACTGGAGTGTCT	657; 350	38	61	60
15 ... 16	trkB_15F TCTATGCTGTGGTGGTGATTG trkB_16R GAGTCCAGCTTACATGGCAG	209	38	52	45
15 ... 19	trkB_15F TCTATGCTGTGGTGGTGATTG trkB-shc antisense AGAACTCTTCTCCTCCATCAG	449; 401	38	52	45
15 ... 20	trkB_15F TCTATGCTGTGGTGGTGATTG trkB_20R GCCACCAAGATCTGTCCCTG	459; 409	38	52	60
18 ... 22b	trkB_18F CCCAGCCTCCGTTATCAG trkB_22bR CTCCAGAGCCATGAGAAACAC	868	38	52	60
21 ... 24	trkB_21F TTCTATGGCGTCTGCGTG trkB_24R CATCAGCTCATACACCTCTG	551; 316	38	60	45
HPRT	hmrHPRTIs GATGATGAACCAGGTTATGAC hmrHPRTas GTCCTTTTACCAGCAAGCTTG	470	29	57	30

Primers and cycling conditions used for qPCR analyses of the temporally regulated expression of trkB gene in human prefrontal cerebral cortex :

Aplified TrkB exons	Primers (5' -> 3')	Amplicon length (bp)	Primer annealing temperature (°C)	PCR product extension time (s)
5/5b ... 6	trkB_5F ACTGGCTGCTAGGGATGTC trkB_6R2 CAGATTTCTCAGTCCCACATAAG	302	60	15
5c ... 6	trkB_5cF AACGTAGTTGACCAAGATAACCTG trkB_6R2 CAGATTTCTCAGTCCCACATAAG	106	58	10
18 ... 19	trkB_18F CCCAGCCTCCGTTATCAG trkB-shc antisense AGAACTCTTCTCCTCCATCAG	301	62	15
21 ... 22b	trkB_21F TTCTATGGCGTCTGCGTG trkB_22bR2 CTGATCTGCACAGTACTCA	339	61	15
17 ... 18	trkB_17F CTCATGGTTGGATTGGGAAAG trkB_18R CTGGCTTGAGCTGACTGTTG	227	61	10
15 + 18 (Δ17)	trkB_15_18F CAAGTTTGGCATGAAAGGCCCA trkB_18R CTGGCTTGAGCTGACTGTTG	200	61	10

Primers and cycling conditions used for the design of RPA riboprobes:

Aplified TrkB exons	Primers (5' -> 3')	Amplicon length (bp)	PCR cycles	Primer annealing temperature (°C)	PCR product extension time (s)
5c ... 8	trkB_5cF AACGTAGTTGACCAAGATAACCTG mrTrkB_8R CAAGTCAAGGTGGCGGAAATG	326	43	55	30
15 ... 16	trkB_15F TCTATGCTGTGGTGGTGATTG trkB_16R GAGTCCAGCTTACATGGCAG	209	43	55	30
18 ... 19	trkB_18F CCCAGCCTCCGTTATCAG trkB-shc antisense AGAACTCTTCTCCTCCATCAG	301	43	55	30
21 ... 22b	trkB_21F TTCTATGGCGTCTGCGTG trkB_22bR CTCCAGAGCCATGAGAAACAC	460	43	55	30

Primers and cycling conditions used for amplifying TrkB coding region for cloning:

Aplified TrkB exons	Primers (5' -> 3')	Amplicon length (bp)	PCR cycles	Primer annealing temperature (°C)	PCR product extension time (s)
5 ... 24	trkB_5F_Kozak CACCATGTCGTCCTGGATAAGGT trkB_24R_nonstop GCCTAGAATGTCCAGGTAGAC	2518	41	55	150
9 ... 12	trkB_9F_Kozak CACCATGTGGATCAAGACTCTCCAAG trkB_12R GAGGCAGCCGTGGTACTC	567	44	55	70
11 ... 22b	trkB_11F CACAGGGCTCCTAAGGATAAC trkB_22bR2 CTGATCTGCACAGCTACTCA	1457	46	55	80
18 ... 22b	trkB_18F CCCAGCCTCCGTTATCAG trkB22bR_nstop TGACAGCCTCAGCAAACAAATAC	811	46	55	80

PUBLICATION II

II. **Luberg, K.***, Park, R. *, Aleksejeva, E. *, and Timmusk, T. (2015). Novel transcripts reveal a complex structure of the human TRKA gene and imply the presence of multiple protein isoforms. *BMC Neurosci.* 16, 78.

RESEARCH ARTICLE

Open Access



Novel transcripts reveal a complex structure of the human *TRKA* gene and imply the presence of multiple protein isoforms

Kristi Luberg^{1,2†}, Rahel Park^{1,2,3†}, Elina Aleksejeva^{1,2,4†} and Tõnis Timmusk^{1,2*}

Abstract

Background: Tropomyosin-related kinase A (TRKA) is a nerve growth factor (NGF) receptor that belongs to the tyrosine kinase receptor family. It is critical for the correct development of many types of neurons including pain-mediating sensory neurons and also controls proliferation, differentiation and survival of many neuronal and non-neuronal cells. *TRKA* (also known as *NTRK1*) gene is a target of alternative splicing which can result in several different protein isoforms. Presently, three human isoforms (TRKAI, TRKAIII and TRKAIII) and two rat isoforms (TRKA L0 and TRKA L1) have been described.

Results: We show here that human *TRKA* gene is overlapped by two genes and spans 67 kb—almost three times the size that has been previously described. Numerous transcription initiation sites from eight different 5' exons and a sophisticated splicing pattern among exons encoding the extracellular part of TRKA receptor indicate that there might be a large variety of alternative protein isoforms. *TrkA* genes in rat and mouse appear to be considerably shorter, are not overlapped by other genes and display more straightforward splicing patterns. We describe the expression profile of alternatively spliced *TRKA* transcripts in different tissues of human, rat and mouse, as well as analyze putative endogenous TRKA protein isoforms in human SH-SY5Y and rat PC12 cells. We also characterize a selection of novel putative protein isoforms by portraying their phosphorylation, glycosylation and intracellular localization patterns. Our findings show that an isoform comprising mainly of TRKA kinase domain is capable of entering the nucleus.

Conclusions: Results obtained in this study refer to the existence of a multitude of *TRKA* mRNA and protein isoforms, with some putative proteins possessing very distinct properties.

Keywords: TRKA, NTRK1, 5' RACE, Glycosylation, Nuclear localization, Isoforms, Alternative splicing

Background

Tropomyosin-related kinase A (*TRKA*, official name neurotrophic tyrosine kinase, receptor, type 1, or *NTRK1*) gene encodes the high affinity receptor for a neurotrophin nerve growth factor (NGF). TRKA with the highly similar receptors TRKB and TRKC belongs to the group of tyrosine kinase receptors. TRKB binds neurotrophins brain-derived

neurotrophic factor (BDNF) and neurotrophin-4 (NT-4) while TRKC is the predominant receptor for neurotrophin NT-3, although TRKA and TRKB can also be activated by NT-3 [1]. Signaling initiated by the NGF-TRKA complex is crucial for the development of pain-mediating sensory neurons [2], postganglionic sympathetic neurons [3] and basal forebrain cholinergic neurons [4]. NGF also affects cells of non-neuronal tissues, such as epithelial and smooth muscle cells, and is very important in thymic tissues [5].

Neurotrophin binding to the TRK extracellular domain leads to receptor's dimerization, activation of its intrinsic kinase activity and autophosphorylation. Subsequently, the signaling pathways similar for all the TRK receptors

*Correspondence: tonis.timmusk@ttu.ee

[†]Kristi Luberg, Rahel Park and Elina Aleksejeva contributed equally to this work

¹Department of Gene Technology, Tallinn University of Technology, Akadeemia tee 15, 12618 Tallinn, Estonia

Full list of author information is available at the end of the article

are activated. These include the rat sarcoma/mitogen-activated protein kinase (Ras-MAPK), phosphatidylinositol 3 kinase (PI3K) and phospholipase C- γ 1 (PLC- γ 1) pathways to promote survival and differentiation, and adjust synaptic plasticity [6–8].

In addition, several neurotrophin independent signaling events have been described, including transactivation of receptor tyrosine kinases by adenosine 2A receptors [9, 10], pituitary adenylate cyclase-activating polypeptide receptor [11], low-density lipoprotein receptor-related protein 1 [12], epidermal growth factor receptor [13] and antidepressants [14].

Human *TRKA* gene is located on chromosome 1 and has been described to span 23 kb. Seventeen exons (named 1...17; Fig. 1), that are relatively well conserved in rat and mouse as compared to human *TRKA* gene, [the basic local alignment search tool (BLAST) algorithm gives 85 % of similarity in both cases] have been characterized [15–17].

The extracellular portion of TRKA receptor, coded by exons 1–10, is responsible for ligand binding and is subjected to post-translational glycosylation. A sequence coded by exon 1 directs the receptor to the cell membrane. The predominant part of the extracellular region constitutes of the first and second immunoglobulin-like (Ig-like) domains coded by exons 6...8, of which the second is directly in contact with NGF [18]. The transmembrane domain of TRKA is encoded by exon 11 and the intracellular tyrosine kinase domain by exons 13...17 [19, 20].

The glycosylation of the receptor's extracellular segment plays an important role in signaling and localization of the protein. There are four N-glycosylation sites that are highly conserved within the TRK family and at least five more variable sites that are used in TRKA. The lack of glycosylation results in autophosphorylation and constitutive kinase activity of the core protein as well as incapability to be directed to the cell membrane [21, 22].

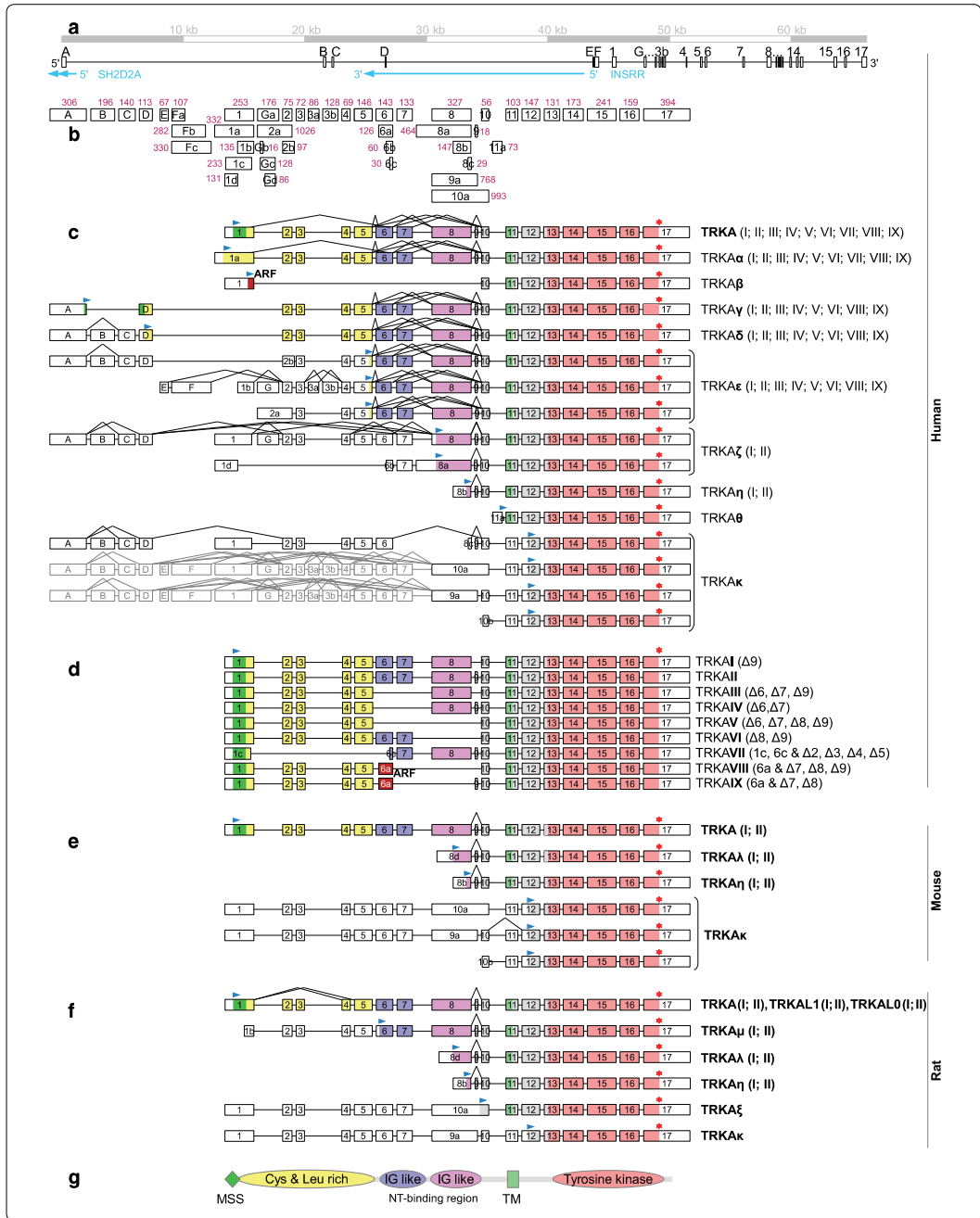
TRKA gene is a target of alternative splicing which can result in several different protein isoforms. At the moment, only three human isoforms (TRKAI, TRKAII

and TRKAIII) and two additional rat isoforms (TRKA L0 and TRKA L1) have been described. TRKAII is the full-length isoform. In mRNA encoding TRKAI an 18 bp exon 9 has been spliced out resulting in a protein lacking 6 aa in the juxtamembrane region of the TRKA receptor. The full-length TRKAII is mainly expressed in neuronal tissues and TRKAI in non-neuronal tissues. They appear to have no relevant difference in binding to NGF [23]. In contrast, binding to NT-3 is significantly stronger in the case of TRKAII compared to TRKAI [24]. The third alternatively spliced transcript *TRKAIII* is lacking exons 6, 7 and 9. This results in the absence of the first immunoglobulin-like domain and several N-glycosylation sites. As a consequence, TRKAIII is not able to bind NGF and is instead constantly autophosphorylated and activated. Alternative splicing of *TRKA* mRNA to generate the isoform TRKAIII is upregulated by hypoxia. TRKAIII is expressed in undifferentiated early neural progenitors, in a subset of neural crest-derived tumors (notably in neuroblastomas) and in thymus, a physiologically hypoxic organ [25, 26]. Unlike TRKAI/II, this isoform is not inserted in the plasma membrane, but is retained in endoplasmic reticulum (ER) and Golgi complex and promotes genetic instability [27]. In rats, similarly to humans, exon nine can be spliced out [23]. In addition, rat splice variants termed TRKAL1 and TRKAL0 lack respectively either two of the leucine-rich motifs or all three [28]. Isoforms of TRKA in mouse have not yet been described.

A genetic disorder congenital insensitivity to pain with anhidrosis (CIPA), also called hereditary sensory and autonomic neuropathy type IV, has various symptoms such as absence of reaction to noxious stimuli (insensitivity to pain), anhidrosis (inability to sweat), self-mutilating behavior and mental retardation. CIPA is caused by non-functional or absent TRKA receptor due to mutations in *TRKA* gene [29]. On the other hand, excessive NGF-TRKA signaling hypersensitizes pain-mediating neurons resulting in chronic pain [30] or causes allergic skin inflammation [29], hyper-responsiveness of airway epithelial cells and/or aberrant activation of sensory

(See figure on next page.)

Fig. 1 Human *TRKA* gene locus and predicted protein isoforms of human, rat and mouse TRKA. Exons are illustrated as boxes and introns as lines. Exons are drawn to scale in **a–f** and introns in **a**. **a** Chromosomal organization of the human *TRKA* gene. Also shown are two genes encoded from the opposite strand and partially (*SH2D2A*) or entirely (*INSRR*) overlapping the *TRKA* gene. **b** All human *TRKA* exons with size in bp-s shown in dark pink. Representational scheme of *TRKA* alternative transcripts and putative protein isoforms of human (**c** and **d**), mouse (**e**) and rat (**f**) origin, based on the results of 5' RACE, RT-PCR study and in silico analysis. The names of encoded proteins are noted on the right. Alternative N-termini as compared to the conventional TRKAII isoform are labeled as α , β , γ , δ , ϵ , ζ , η , θ , κ , λ , μ and ξ . Only one ORF per transcript has been marked with start site (blue arrowhead) and stop codon (red asterisk). Roman numerals designate protein isoforms missing various parts of the extracellular region as illustrated for TRKAI...TRKAIX **d**. Exons 10a and 9a can either serve as 5' exons or be the products of intron retention (due to this, the block of exons upstream of exons 10a and 9a is illustrated in gray). ARF alternative reading-frame. The L0 isoform of rat TRKA is produced from transcripts that do not include exons 2–4 and L1 from mRNAs missing exons 2 and 3. **g** the protein domains of TRKAII (MSS membrane signal sequence, Cys and Leu rich region cysteine and leucine rich region, IG like immunoglobulin-like domain, TM transmembrane)



neurons, implicated in acute conditions such as asthma [31].

Alterations in *TRKA* expression or mutations in the gene have been detected in several tumors. *TRKA* was discovered as an oncogene in colon carcinoma fused with tropomyosin gene [32]. Genomic DNA rearrangements of *TRK* genes can influence carcinogenic progression in non-neuronal tissues such as breast cancer [33], papillary thyroid carcinoma [34] and medullary thyroid carcinoma [35]. In neuroblastomas, *TRKA* upregulation is seen in tumors with good prognosis, while *TRKB* is up-regulated in unfavorable and aggressive tumors [36]. However, *TRKA* can also be involved in the late stages of cancer progression by promoting stress-resistance and neovascularization—for example in neuroblastomas by *TRKAII* isoform [37]. During the progression of Alzheimer's disease, all *TRK* receptors are down-regulated in cholinergic neurons of nucleus basalis, a brain region which dysfunction is associated with cognitive decline in Alzheimer's disease [38]. The cholinergic neurons depend on NGF which is synthesized by the target cells within the hippocampus and cortex. *TRKA* expression is also decreased in the parietal cortex of patients with Alzheimer's disease [39, 40]. Moreover, the withdrawal of NGF in differentiated rat pheochromocytoma PC12 cells initiates the accumulation of beta-amyloid protein and is followed by apoptotic death [41].

In this study, we show that the *TRKA* gene in rat, mouse and especially human is more complex than previously thought. We also show that the human *TRKA* has multiple 5' terminal exons and an intricate splicing pattern involving exons that encode the extracellular part of *TRKA* protein. It can be theorized that these novel *TRKA* transcripts encode numerous *TRKA* protein isoforms which have not yet been characterized.

Results

An elaborate arrangement of the human *TRKA* gene revealed by novel transcription initiation sites

In silico analysis of the human *TRKA* gene structure using UCSC genome browser [42] to align the *TRKA* mRNAs and expressed sequence tags (ESTs) from GenBank to the genomic sequence indicated a higher level of

variability among *TRKA* transcripts and a longer span of the gene than previously described in the literature. For this reason, we performed reverse transcription polymerase chain reaction (RT-PCR) and rapid amplification of 5' complementary DNA ends (5' RACE) analyses to better describe *TRKA* gene and its transcripts. In the RT-PCR study, we used a selection of adult and fetal tissues and different regions of the nervous system. Also included were neuroblastoma cell-lines SH-SY-5Y and SK-NMC which are known to express *TRKA*. Total RNA from SH-SY-5Y neuroblastoma cells and thalamus were used in 5' RACE experiments as these tissues showed relatively high levels of *TRKA* expression in our preliminary experiments. From the information obtained of mRNAs, we predicted potential *TRKA* protein isoforms and named them in this study as follows: isoforms with different N-termini from the conventional *TRKAII* are named as α , β , γ , δ , ϵ , ζ , η , θ and κ (Fig. 1c), isoforms which lack different parts in their extracellular portion are distinguished with roman numerals I...IX (Fig. 1d; protein sequences are listed in Additional file 1).

We detected multiple transcription start-sites in exon 1, most of which are located upstream of the conventional translation start-site in the position 156860935 nt of the GRCh38 human genome assembly (Fig. 2). However, there is an additional in-frame ATG in the position 156860857 nt that was included in some forms of exon 1 (named in this study as 1a). If this AUG is sterically accessible for the ribosome, an N-terminally elongated protein (named here as *TRKA α*) compared to the conventional *TRKAII* would be produced. On the other hand, some transcripts had a shorter exon 1 (exon 1b) with no in-frame AUG codons. Translation from mRNAs with exon 1b probably starts from the next in-frame AUG which is in exon 5 (in genomic position 156868231 nt) creating *TRKA ϵ* . The online transmembrane topology and signal peptide predictor Phobius [43] predicts no membrane signal sequences for *TRKA α* or *TRKA ϵ* .

Analysis of GenBank sequences [GenBank:DA013446, GenBank:DB265639, GenBank:AK126428] revealed the presence of a novel 5' terminus of *TRKA* mRNAs formed by alternative transcription initiation and usage of four novel exons that are in this study termed as A, B, C and D

(See figure on next page.)

Fig. 2 The human *TRKA* gene has numerous transcription start sites producing more alternative 5' exons than mouse and rat *TrkA* genes. Results of the 5' RACE analysis of *TRKA* mRNA of human (combined results of extracts from thalamus and SH-SY-5Y cell line), mouse (brain at embryonic day 13) and rat (PC12 cell line). Novel transcription start-sites are indicated in *blue bold letters* and marked with a *blue arrow head*. Transcription initiation sites deduced from GenBank sequences of previously described mRNAs and ESTs that are obtained with 5' RACE analysis are displayed in *bold underlined letters* and designated with *black asterisks* with the corresponding GenBank accession numbers shown. *Red and bold letters* indicate alternative putative translation start sites with the conventional translation initiation site (producing *TRKAII* protein isoform) *underlined*. The translational start site from alternative reading frame that is used if exons 2...9 are spliced out in human tissues between exons 1 and 10 is indicated in *pink bold letters*. Exons are marked with *grey background*. The numbering is based on the human genome assembly GRCh38 (hg38), the mouse genome assembly GRCh38 (mm10) or the rat genome assembly RGSC6.0 (rn6)

HUMAN

Exon A

156815483 GCTCTAGGAG GGGCGGGAAA GGCACACAG CCTTCCAGAT GGACAGAGTC ATTCCTGGC CTGGAGGATG AAGAACAATG ATGCAGBAAG TCACCCTAGA GCCCAGAATG

Exon E

156859168 CCTAAACAGA TTGGTTCGCA GGGACCTTTC CGTCTCTCC ACCCTCCCGG CCAAGTCAAA ATATTTAGCC TGACAACTGA GGGGAGGACA GGTCTGTTGG 156859267

Exon 1

156860798 CGGGGGCCGC TGGCTCCGCC CTCTTCTGCC GGTGGGCTT TTAACACCGC CCACGGCACA TGTCTGGGGA GGCTGGCAG CTGCAGCTGG GAGCGCACAG ACGGCTGCCG

Exon G (Ca: 156863406-156863581, Gb: 156863422-156863437, Gc: 156863422-156863549, Gd: 156863464-156863549)

156863328 CTTTTCAGT GTCTGTGTTT CACTCTCTCT TTGTTTTCTP GCCCGCTGC CCCACCCCTC CTCTGTGAGC CTTTTCATCT TCTGTCTCTP CTCTCTCTCT CTCTGTGCTP

Exons 8 (156873633-156873959), 9 (156874383-156874400), 9a (156873633-156874400), 10 (156874571-156874626) and 10a (156873633-156874626)

156873583 TCCTTCCAGC TGGGCGCTGA CPTCTGCTG TTGCTCTTTC TGGCCACAG TCCCGGCCAG TGTGAGCTG CACACGGCGG TGGAGATCA CCACCTGTGC ATCCCTCTCT

Exon 11a

156874711 CAGGGAGATC ACTACCATCT GGCTGAGCT CTGACGCCA CCGGCACAG CACTGCAGGG GTCCCGAGG GAGGATGAGG CAGTCTGGA TGCAGATGA 156874810

MOUSE

Exon 1

87795257 TCCTGGTGGC TAGCTTTTAA CACGCCCCG CGCACGTGTC GCGCGAGCC GGGCGGGCC AGCTAGGAG GCACGGACGG CTGGCGGCC CGAGCAGGC GGGCGCCGC

Exon 8

87784057 TTCCCTGGAT TCCGTCACG CAGTTCGCCA CTTCTGTCA CATGCTTCT TCCCAGTGC CCAGCCAGTG TGCACCTGG CCTAGCGGTG GAGCAGCATC ATTGGTGCAT

Exon 10

87783149 TGTGCCCGT GTCCCCACAG ACGGTAAACG CACATCAAGA GACCCAGTGG AAGAARAAGA TGAARACCCCT TTTGGGGTGA GTGTGGGTA TGAARACTGA 87783050

RAT

Exon 1

187160464 CGGCAGCGG GCGCGGGCG GGCCCTGGGT GCCGCCCTCT CTTGGTGGCT AGTCTTTTAA ACCGCCCCGC GCACGTGTC GCGCGAGCCG GCGCGCGCA GCCAGGAGCG

Exon 8

187149370 TCCTTCCCCT CCCAGTTCG CCACTTCTCG TCACCTGCTT TCTCCCATG TCCAGCCAG TGTGACTGTG GGCAAAGCCG TGGAAACAGA TCACCTGTGC ATTCCCTCTC

(Fig. 1). We confirmed with 5' RACE using mRNAs from adult human thalamus that exon A serves as a transcriptional start-site (Fig. 2). Exon A is located approximately 45 kb upstream of exon 1 and therefore the size of *TRKA* gene is 67 kb—almost three times bigger than previously thought. It is of interest to note that exon A is in the intron between the second and the third exon of sarcoma protein homology 2 domain protein 2A (*SH2D2A*) gene that is encoded on the complementary strand from *TRKA*. The transcription start sites of these genes are in a head-to-head orientation and lie less than 1 kb apart. On the same strand and upstream from *SH2D2A* gene, there is insulin receptor-related protein (*INSRR*) gene which is completely embedded into *TRKA* gene (Fig. 1a). Thus, *TRKA* is overlapped by two genes and that is rather unusual according to Veeramachaneni and associates, who identified only 18 overlapping gene trios in the human genome [44]. Transcription start sites of *TRKA* exon 1 and *INSRR* gene are in a nearby head-to-head orientation and are less than 2 kb apart. *TRKA* exon D and a coding exon in *INSRR* gene overlap by more than 80 bp.

Translation of transcripts with exons A and D followed by exons 2, 3, etc., starts most probably from an AUG near the end of exon A (from the genomic position 156815830 nt) producing *TRKA* γ . Besides this major ORF, these transcripts also have many small upstream ORFs (uORFs) in different reading-frames that are no bigger than 111 nt. For mRNAs with exons A-C-D or A-B-C-D, the primary ORF starts in exon D (from genomic position 156842144 nt) generating *TRKA* δ . uORFs of these transcripts are longer, reaching 336 nt. Phobius predicts membrane signal sequence for *TRKA* γ but not for *TRKA* δ .

Using 5' RACE analysis, we also identified novel exons E, G and 11a as alternative *TRKA* 5' exons (Fig. 2). Exon E is located 1.5 kb upstream of exon 1 and may be followed by novel exon F which has three alternative 3' termini (generating Fa, Fb and Fc exon variants). Exon E is even closer to the *INSRR* gene than exon 1, but does not overlap with it. RT-PCR also revealed two novel exons located downstream of exon 3 that are named in this study as 3a and 3b that can be spliced into mRNAs with 5' exons E and Fa (Figs. 1b, 3). Exon G is located between exons 1 and 2, specifically 2.3 kb downstream of exon 1, and has alternative versions Ga, Gb, Gc and Gd that differ from each other in both 5' and 3' splice sites (Fig. 2). Using RT-PCR we also detected intron retention between exons G and 2 generating an extended exon that is here named as 2a. The major ORF of mRNAs with exons E, F, G and 2a is located to exons 5...17 and encodes *TRKA* ϵ . All of these mRNAs have 1...3 uORFs in alternative reading frames that are less than 168 nt, with the exception of

transcripts that start with exon 2a in which case there are 18 uORFs with a maximum length of 321 nt.

The 5' exon 11a is located 95 bp downstream of exon 10 and transcripts with this exon encode for *TRKA* θ which has no predicted membrane signal sequence. The first ATG is located near the 3' end of exon 11a at genomic position 156874785 nt. There are no uORFs on these mRNAs.

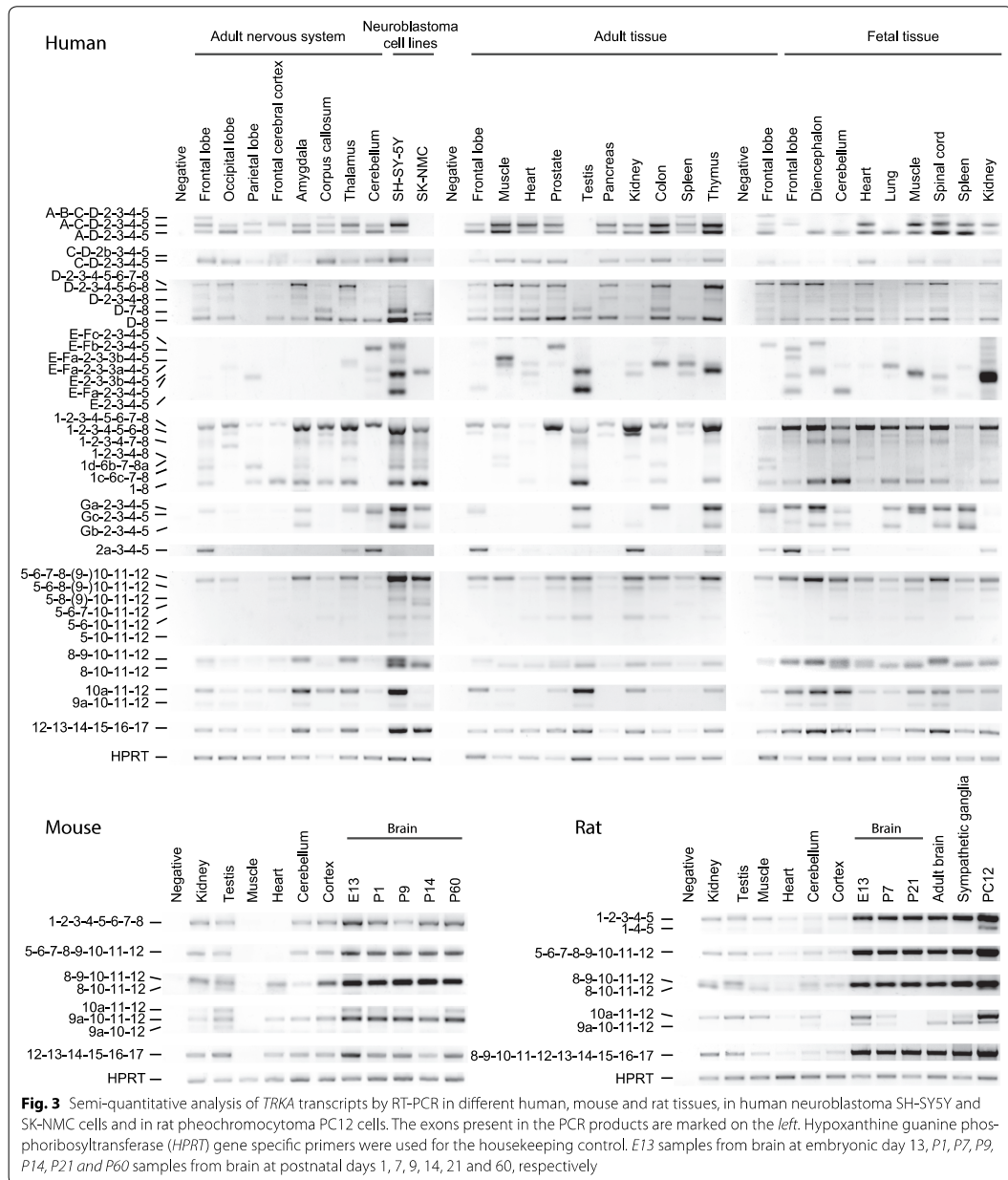
The exon complexes A...D and E-F and exons 1, G, 2a and 11a are all mutually exclusive as we didn't observe any transcripts with different combinations of these 5' exons or exon complexes.

Surprisingly, we also detected transcription initiation from exon 10 and from many different nucleotides within exon 8 (Fig. 2). Most of the mRNAs that have exon 8 as the 5' exon contain in-frame AUG codons present near the 3' end of exon 8 (this variant of the exon is named in here as 8b). Assuming that the first of these codons (at genomic position 156873905 nt) serves as a translational start-site, the protein produced is *TRKA* η . These transcripts have no uORFs. *TRKA* transcripts that start with exon 8c that is shorter than 8b, which contains no in-frame AUG codons, or with 10b have a major ORF situated in exons 12...17 with the first ATG in genomic position 156875555 nt and encoding *TRKA* κ protein isoform. 2 uORFs with a maximum length of 171 nt are also present.

According to one EST and our 5' RACE results, transcription can also start in the intron between exons 8 and 9, from exon 10a which contains exons 9 and 10 and the intron between them (Fig. 2). With RT-PCR we also detected the presence of exon 9a that is similar to exon 10a, but its 3' end coincides with the one in exon 9 (the intron between exons 9 and 10 is spliced out in this case). With RT-PCR (data not shown) we detected the presence of exons 9a and 10a in transcripts that have additional exons in 5' direction and in that case exons 9a and 10a are the products of intron retention as they span from the 5' end of exon 8 to the 3' end of exon 9 or 10, respectively. In either case, there are multiple ORFs in these transcripts, but the ORF that extends into the 3' exons and which translation would salvage these mRNAs from nonsense mediated decay (NMD), encodes for *TRKA* κ protein isoform. However, the true functionality of these transcripts is presently unknown.

Human *TRKA* exons 2...9 encoding the extracellular domain are all cassette exons with an intricate splicing pattern

Several exons of the human *TRKA* gene can be spliced out. All of these encode parts of the extracellular domain of *TRKA* protein. The splicing of cassette exon 9 has been



described and the protein isoform encoded by exons 1...17 is known as TRKAI and the exclusion of amino acids encoded by exon 9 leads to the production TRKAI protein isoform [23]. Formerly, exclusion of exons 6, 7

and 9 from *TRKA* mRNA has also been reported, giving rise to a protein isoform TRKAIII [25]. We detected alternative splicing of all exons encoding the extracellular domain, with the only exception of exon 10 (Figs. 1c, d,

3). Additionally to the mRNA isoforms described previously, alternative splicing that does not disturb the reading frame of transcripts was detected as the exclusion of exon complexes 6-7 (producing TRKAIV), 6-7-8-9 (TRKAV), 8-9 (TRKAVI) and 2-3-4-5. In the latter case, alternative splice sites are used for exons 1 and 6 resulting in exons 1c (20 nt shorter from the conventional exon 1 from the 3' end) and 6c (113 nt shorter from exon 6 from the 5' end). The protein encoded by transcripts with exons 1c-6c-7...17 is TRKAVII. Theoretically, the same splicing patterns can also be present in transcripts with other 5' termini and thus, the putative protein isoforms of human TRKA also include TRKA α I, TRKA α II, TRKA γ I, etc.

Moreover, there are many splice forms that produce a frame-shift. This includes transcripts with exons 6a-10 and 6a-9-10 and lacking exons 7 and 8 (and 9 in the former case; Fig. 1c) as identified with 5' RACE analysis. Exon 6a is a shorter version of exon 6 with 17 nt missing from the 5' end as compared to exon 6. The sequence of exon 6a is read in an alternative reading frame, producing isoforms TRKAVIII and TRKAIX, respectively. Alternative reading-frame of exon 1 is most probably used with transcripts which are missing the complex of exons 2...9, generating TRKA β which lacks membrane signal sequence according to Phobius program. Translational start-site most probably used in this case is located 100 nt from the 3' end of exon 1 (at genomic position 156861047 nt). One uORF of 294 nt is present in that mRNA.

One of the many types of human TRKA transcripts identified with RT-PCR contained exons 1d-6b-7-8a with exons 2...5 spliced out. Exon 1d is 122 nt shorter from exon 1 from the 3' terminus, exon 6b is 83 nt shorter from exon 6 from the 5' end, and 8a is an extended form of exon 8 with additional 137 nt in its 5' terminus. This mRNA most probably encodes for TRKA ζ II with the translational initiation site in exon 8 (at genomic position 156873668 nt) although it has 4 uORFs with the maximum length of 297 nt. TRKA ζ II possesses no predicted membrane signal sequences.

With RT-PCR we identified the exclusion of exon 7 or exon complexes 2...6, 2...7, 5-6, 5...7, and 7...9 that also produce frame-shifts. To escape the NMD pathway, the ORF expressed from these transcripts should encode TRKA κ (in case exons 7-8-9 are spliced out) or TRKA ξ I/ TRKA ξ II (in case of other splice-combinations). However, all these mRNAs contain uORFs that are in some cases rather large. Therefore, the exact function (if any) of these transcripts is uncertain.

With primers located in TRKA exons C and 5 two PCR products with similar lengths (cDNA from frontal cerebral cortex, Fig. 3) were identified with sequencing. It appeared that the longer product contained an extended

form of exon 2 with additional 22 bp in its 3' end (that we named 2b) compared to the normal exon 2. This induces a frameshift and results in a premature stop codon. To escape the NMD pathway, the protein translated from that transcript should be TRKA ϵ , regardless of multiple uORFs with maximum length of 189 nt.

Trka alternative transcripts lacking exons 2...3 (TrkALI) or exons 2...4 (TrkALO) have been found in Wistar rats [28]. However, we did not detect such transcripts of human TRKA gene, suggesting that these transcripts might be rodent-specific.

Expression pattern of TRKA transcripts in human tissues and cell-lines

Next, we wanted to elucidate the expression pattern of TRKA transcripts in different tissues. To this purpose, we examined TRKA transcript expression with RT-PCR analysis in a selection of human tissues, brain regions and two neuroblastoma cell-lines. The results (Fig. 3) indicated that transcripts with 5' exons A-D were expressed in most examined tissues, except in adult testis and frontal cerebral cortex as well as fetal frontal lobe. Expression of this transcript was also seen in neuroblastoma SH-SY5Y cells, but not in neuroblastoma SK-NMC cells. Transcripts with exons A-C-D were widely expressed in different tissues apart from adult testis, fetal diencephalon, cerebellum and lung, and SK-NMC cells. The rare splice variant with exons A-B-C-D was expressed at very low levels in several tissues, more significantly in adult frontal lobe, corpus callosum, and spleen as well as in fetal spinal cord. The expression of exon 2b was even rarer, as we detected it only in frontal cerebral cortex.

The transcript including exons D and 8, and excluding exons 2...7 had a wide expression pattern with the exception of adult parietal lobe and with relatively higher expression in SH-SY5Y cells and adult prostate and thymus. The expression of mRNAs with exons D-7-8 with an absence of exons 2...6 was not unanimous and displayed higher levels in adult corpus callosum, muscle, heart, testis and colon, fetal cerebellum, heart and spinal cord, and SH-SY5Y cell line. Human TRKA transcripts with exons D-2-3-4-5-6-8 (missing exon 7) and D-2-3-4-8 (missing exons 5-6-7) were expressed in low levels in all studied tissues except adult parietal lobe and the SK-NMC cell line. We did not observe mRNAs with exons D-2-3-4-5-6-7-8 in adult cerebellum, testis and spleen, fetal lung and SK-NMC cells. The highest expression of these mRNAs was found in adult amygdala, thalamus, muscle and thymus.

Exon complex 1...8 was detected in mRNAs from all tissues studied, with especially high levels in adult amygdala, thalamus, prostate, kidney and thymus, fetal diencephalon, heart and spinal cord and SH-SY5Y cells. mRNAs with

exons 1c-6c-7-8 were detected in low levels in adult frontal and parietal lobe, amygdala, muscle, testis and colon and neuroblastomas. Relatively low levels of transcripts with exons 1-2-3-4-5-6-8 (with exon 7 spliced out), 1-2-3-4-7-8, 1-2-3-4-8 and/or 1d-6b-7-8a that are all encoding the TRKA ζ isoform, were observed in all tissues analyzed with the exception of adult parietal lobe, frontal cerebral cortex and cerebellum. The expression of transcripts with exon 1 and 8 (missing the cassette of exons 2...7) was highest in SK-NMC cells, testis and fetal cerebellum, and below detection limit in adult occipital lobe, cerebellum, muscle, prostate, pancreas, kidney and spleen.

Novel 5' exons E, F and G were expressed in many tissues with the highest levels in cerebellum, neuroblastomas, testis, colon, thymus and fetal frontal lobe, diencephalon, lung, muscle and spinal cord. Adult frontal cerebral cortex, corpus callosum, pancreas and fetal heart were the tissues where expression of these exons was below the detection limit. Exon 2a was expressed in only a small selection of tissues, most notably in frontal lobe, cerebellum and kidney.

Splicing in the region of exons 6...8 was a rare event with the highest prevalence of transcripts lacking exon 7 or exons 7...9. Splice forms where exons 8-9, 6-7-8-9 or 6-7 are spliced out appeared to be neuroblastoma specific, as they were detected only in the samples from SH-SY5Y and SK-NMC cells. These mRNAs encode TRKA proteins without one or two Ig-like domains.

The transcript containing exon 9 is predominately expressed in neural tissues while the exclusion of exon 9 has been observed in peripheral tissues [23, 24]. In that respect, the results of this study are in accordance with previous findings. In some tissues, such as adult prostate, fetal diencephalon and heart as well as in neuroblastoma SH-SY5Y, both of the transcripts were detected.

Transcripts with exon 10a were detected in many tissues with the exceptions of SK-NMC cells, adult heart, pancreas and spleen. The novel exon 9a was expressed at minute levels in frontal lobe, occipital lobe, amygdala, thalamus, muscle, testis, fetal diencephalon and spinal cord and neuroblastoma cells.

We failed to design PCR primers with which it would be possible to amplify *TRKA* sequences with exon 11a. Most probably the expression level of these transcripts is very low.

All analyzed *TRKA* transcript variants shared common 3' exons as we did not detect any alternative splicing after exon 11. Therefore, the expression pattern of exons 12...17 corresponded to *TRKA* mRNA overall levels and was the highest in adult amygdala, thalamus, testis, neuroblastomas and in fetal diencephalon and spinal cord according to PCR results with primers targeting exon 12 and 17 (Fig. 3).

Mouse and rat *TrkA* mRNAs display smaller variability than human *TRKA* transcripts

To examine whether the complex splicing pattern seen in human tissues is conserved in other mammals, mouse and rat samples were also analyzed. Rat and mouse tissues to be examined were chosen according to previous results in human and taking into consideration the tissue and/or mRNA availability. Rat PC12 cell line was included in the rat expression panel as it has been shown to express high levels of *TrkA* and has been the major tool to perform research on TRKA receptor, including this study [45].

Total RNA isolated from mouse brain E13 tissue and rat PC12 cells was used in 5' RACE experiments as these tissues showed relatively high levels of *TrkA* expression. Our 5' RACE results and a few mouse sequences in public databases indicated that most often transcription is initiated from exon 1 upstream of the conventional translation-start site at position 87795144 of the GRCh38 mouse genome assembly and at 187160312 of the RGSC6.0 rat genome assembly (Fig. 2). However, we detected rat *TrkA* mRNAs that have 5' end in exon 1, but downstream of this AUG. This variant of exon 1 is named here as 1b and the major ORF of rat *TrkA* transcripts containing exon 1b starts from exon 6 at genomic position 187153794 and encodes TRKA μ protein (Fig. 1f). Three small uORFs with length up to 63 nt are also present.

A sequence in GenBank [GenBank:AK148691], that has been obtained by 5' RACE, and also sequences from our 5' RACE results additionally characterize both mouse and rat *TrkAs* with 5' termini inside exon 8 (named in this case as 8d or 8b, for longer and shorter versions, respectively). These transcripts encode TRKA λ and TRKA η proteins, both of which have translation-initiation sites in exon 8: TRKA λ at genomic position 87783826 (mouse) or 187149147 (rat), and TRKA η at position 87783724 (mouse) or 187149045 (rat). Mouse and rat transcripts with 5' exons 8d and 8b have uORFs up to 282 nt, with the exception of mouse mRNAs with exon 8b, which have no uORFs.

Similarly to human mRNA, we also identified transcription initiation from within *TrkA* exon 10 (named in that case as 10b) in mouse mRNA, but not in rat mRNA. Translation from mouse *TrkA* mRNAs with 10b as 5' terminus most probably starts from exon 12 (at genomic position 87782262) producing TRKA κ protein, similarly to the human orthologue. 3 uORFs up to 114 nt are also present.

We did not observe 5' exons of rat or mouse *TrkA* alternative to exon 1, 8 or 10 and PCR with primers designed based on sequence similarities with human exons A and D did not give any results in samples from either mouse or rat tissues. *TrkA* genes of mouse and rat therefore

do not overlap with either *SH2D2A* or *INSRR* genes, although the latter one is very close to *TrkA* exon 1 in case of both species.

Analysis of *TrkA* transcripts in mouse and rat revealed that both express exons 9a and 10a and therefore, potentially also TRKA κ (Fig. 1e, f). As we did not detect exons 9a or 10a in 5' RACE experiments using mouse or rat samples, it can be concluded that these exons are produced in these animals only by intron retention and not by alternative transcription initiation mechanism seen in human. In case of rat transcripts with exon 10a, the potential translational start-site is most probably located in the intron between exons 9 and 10 and TRKA ξ protein is generated (Fig. 1f). However, mouse and rat mRNAs with exons 9a or 10a have many uORFs, some of which are very large.

Furthermore, exon 9 is a cassette exon in both mouse and rat and exon 11 can be spliced out in mouse. While the splice variants lacking exons 2 and 3 or exons 2...4 have been described in literature, we identified only the latter one [28].

A membrane signal sequence was not detected by Phobius prediction tool for any novel putative TRKA isoforms in rat or mouse with N-termini other than the conventional Met of TRKAI/TRKAII.

Expression of *TrkA* mRNAs in mouse tissues

The expression of *TrkA* mRNA was studied in a selection of adult neuronal and non-neuronal tissues as well as in developmental samples from mouse brain at gestation day 13 (E13) and at postnatal days 1, 9, 14 and 60 (P1, P9, P14 and P60, respectively; Fig. 3). According to the expression level of exons 12...17, common to all possible splice forms, the samples examined showed relatively similar overall *TrkA* expression levels with the exception of muscle tissue, where *TrkA* mRNA was almost undetectable. The 5' region of transcripts from heart sample was identified only when the number of PCR cycles was increased (data not shown). The developmental tissues analyzed had a fairly higher expression level of *TrkA*.

In human and rat *TRKA* transcripts, exon 9 was spliced out in non-neuronal tissues and included in neuronal tissues. In mouse, this rule seems not to apply, as *TrkA* mRNAs without exon 9 were observed only in testes as a minor product in addition to the major form with exon 9.

Interestingly, PCR with primers amplifying exons 10a and 9a predominately gave rise to products with exon 9a not with 10a, which is in contrast to our results in human and rat tissues. It can be concluded that the regulation of splicing in the region around exon 9 of the *TrkA* mRNA in mouse is different from that in rat and human.

Furthermore, a splice form lacking exon 11 was detected in mouse testis sample only when exon 9a was included in the transcript.

Analysis of mouse samples provided evidence that alternative transcription initiation and splicing of *TrkA* gene is less complex in mouse than in human. However, a novel splice form, lacking exon 11 and not seen in human, was identified. *TrkA* expression in muscle was almost undetectable in mouse while the overall level of *TRKA* in human muscle tissue was not significantly lower than in other tissues.

Expression of *TrkA* mRNAs in rat tissues

TrkA expression was detected in all rat tissues analyzed (Fig. 3). The overall mRNA levels were higher in developmental brain samples [embryonic day (E) 13, postnatal day (P) 7 and P21], in adult whole brain and sympathetic ganglia and in PC12 cell line, and lowest in heart.

Splice variant lacking exons 2 and 3 was detected in minor quantities in PC12 cells. *TrkA* transcript, where exon 9 has been spliced out, was observed in kidney, testis, muscle, heart—the analyzed non-neuronal tissues, and also in the PC12 cells. In the rest of the samples and also in testis and PC12 cells, the major transcript contained exon 9. The splicing pattern of *TrkA* exon 9 in different rat tissues was similar to human, but different from mouse.

Similarly to human, transcripts with exon 10a were more frequent than transcripts with exon 9a, with the exception of adult whole brain and sympathetic ganglia. In cortex and in P21 brain, neither was detected. Yet in most of the other neuronal tissues and in PC12 cells, both transcript variants were observed. Interestingly, the expression levels of transcripts with exons 10a and 9a were fluctuating during the development: in embryonic brain from gestation day 13, a relatively high level of transcripts with 10a exon was observed as well as relatively low levels of 9a variant. Thereafter, the level of these mRNAs started to decrease, as P7 brain had lower levels of these splice variants and at P21 the signal of *TrkA* mRNAs with exons 10a or 9a was not detected. However, the transcript with exon 9a was observed again in the adult whole brain.

Interestingly, the expression of *TRKA* in human and rat muscle tissues followed a similar pattern while in mouse it was undetectable. Heart displayed contrary expression profiles by having relatively low *TRKA* transcription levels in human and rat and higher levels in mouse.

Endogenous TRKA protein isoforms in PC12 and SH-SY5Y cells

To examine the expression of *TrkA* on protein level, PC12 cell line from rat was chosen for the experiments as it has

been used widely for research on TRKA. Of TRK receptors, it is known to express predominantly TRKA and to be NGF responsive [45]. The SH-SY5Y cell line was added to analyses as it showed the highest levels of *TRKA* mRNA expression among human samples in the RT-PCR studies.

We tested many antibodies and according to results obtained with siRNA treated PC12 cell lysates, the most effective antibody to detect the low levels of endogenous TRKA was an anti-TRKA rabbit polyclonal antibody by Millipore (#06-574, see also “Methods”). The epitope of this antibody localizes to the extracellular region of TRKA protein, consequently it would not be able to recognize several putative isoforms excluding this region. Another promising antibody was an anti-TRK rabbit monoclonal antibody by Cell Signaling (#4609, see also Methods), which recognizes all three TRK receptors and has its epitope around Y785 of TRKA C-terminus. Lastly, we also used an anti-pTRKA antibody from Cell Signaling (#9141, see also “Methods”) that only recognizes phosphorylated TRK proteins. 5 min NGF treatment before the lysis of the cells was used to activate the intrinsic phosphorylation ability of TRKA proteins. Both anti-TRK and anti-pTRKA antibodies are therefore presumably capable of distinguishing all putative TRKA isoforms that contain the kinase domain.

In PC12 cells the full-length TRKAI/TRKAI protein of ≈ 100 kDa and its glycosylated forms ≈ 120 and 140 kDa were detected by both anti-TRK (#4609) and anti-TRKA (#06-574) antibodies (Fig. 4a). Using anti-TRK (#4609) antibody the signal from smaller proteins than 100 kDa

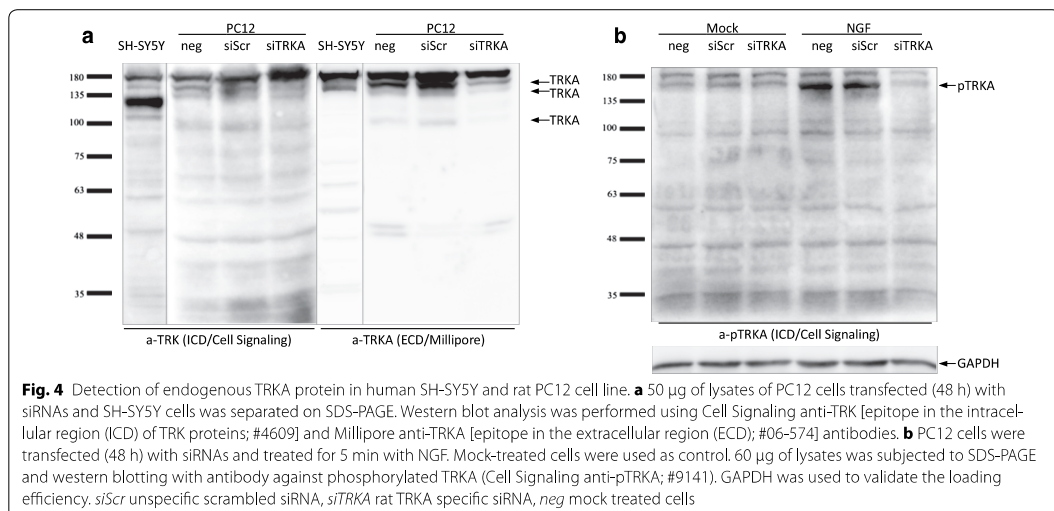
was not observed. Similarly, the anti-pTRKA (#9141) antibody detected only the full-length pTRKAI/pTRKAI in its glycosylated form (≈ 140 kDa; Fig. 4b) which is the type of TRKA expressed on the cell surface and is therefore accessible to extracellular NGF. In our current study we were not able to distinguish with the given antibodies in PC12 cells the predicted novel TRKA isoforms. This could be caused by the poor ability of antibodies to recognize low levels of endogenous TRKA.

In SH-SY5Y cells the signals corresponding to 120 and 140 kDa probably represent the differently glycosylated TRKA proteins. The anti-pTRKA antibody did not detect signals from SH-SY5Y cell lysates even if the cells had been previously treated with NGF (data not shown) suggesting that TRKA receptors are not functional in proliferating SH-SY5Y cells used for analysis.

Interestingly, by all three antibodies used a ~ 180 kDa signal was detected, which identity remains to be elucidated. If this is indeed TRKA, e.g., a very stable hyperglycosylated form, it appears to be a type that does not respond to NGF treatment (Fig. 4b).

TRKAI putative isoforms differ in autocatalysis rate

We were next interested in describing novel putative TRKA isoforms in more detail. Most of the detected human *TRKA* transcripts have out of frame uORFs relative to the ORF that is depicted in Fig. 1c. None of these uORFs reach the 3' exons of *TRKA*. Due to this, if the longest ORF is not translated, the mRNA would be subjected to NMD, a process which promotes the degradation of mRNAs undergoing premature translation



termination. We hypothesized that these transcripts might undergo leaky scanning or reinitiation that would exclude them from NMD as the uORF sequences start with AUG surrounded with weak Kozak sequences [46].

TRKA isoforms with different N-termini can each have several splice forms (except TRKA β , TRKA θ and TRKA κ); however, the functional implications of the exclusion of six amino acids encoded by exon 9 (resulting in TRKA λ , TRKA α , TRKA γ , etc.) have been described before [23, 24]. Also, transcripts encoding TRKA isoforms other than type I and II showed relatively low level of expression. Accordingly, TRKA isoforms of type I, III, IV, V, VI, VII, VIII and IX were omitted from further analysis for simplicity.

To determine whether N-terminal differences of putative TRKA isoforms influence autophosphorylation capacity, a selection of potential TRKA isoforms was cloned and the expression constructs of TRKAII-V5-His, TRKA γ II-V5-His, TRKA δ II-V5-His, TRKA ϵ II-V5-His, TRKA ζ II-V5-His and TRKA κ -V5-His were transfected into human embryonic kidney 293 cells (HEK293), followed by lysis and V5-tag-aimed immunoprecipitation to eliminate endogenous phospho-tyrosine (pY)-proteins from Western blot analysis. Total precipitated protein was visualized with an antibody against V5-tag and phosphorylated subportion with anti-pY antibody. All isoforms were expressed efficiently (Fig. 5a, left panel) and displayed catalytic activity (Fig. 5a, right panel). It was repeatedly observed that TRKA κ -V5-His immunoprecipitate contained pY-proteins besides TRKA κ -V5-His. These proteins were of higher molecular weight than the expected ~40 kD TRKA κ -V5-His protein and were not present in precipitates containing other TRKA isoforms. If this was a result of co-precipitation, it can be assumed that these protein interactions are so strong as to withstand the harsh detergent conditions of radioimmunoprecipitation assay (RIPA) lysis buffer. Phosphorylated proteins of unknown origin were not seen with other overexpressed TRKA proteins.

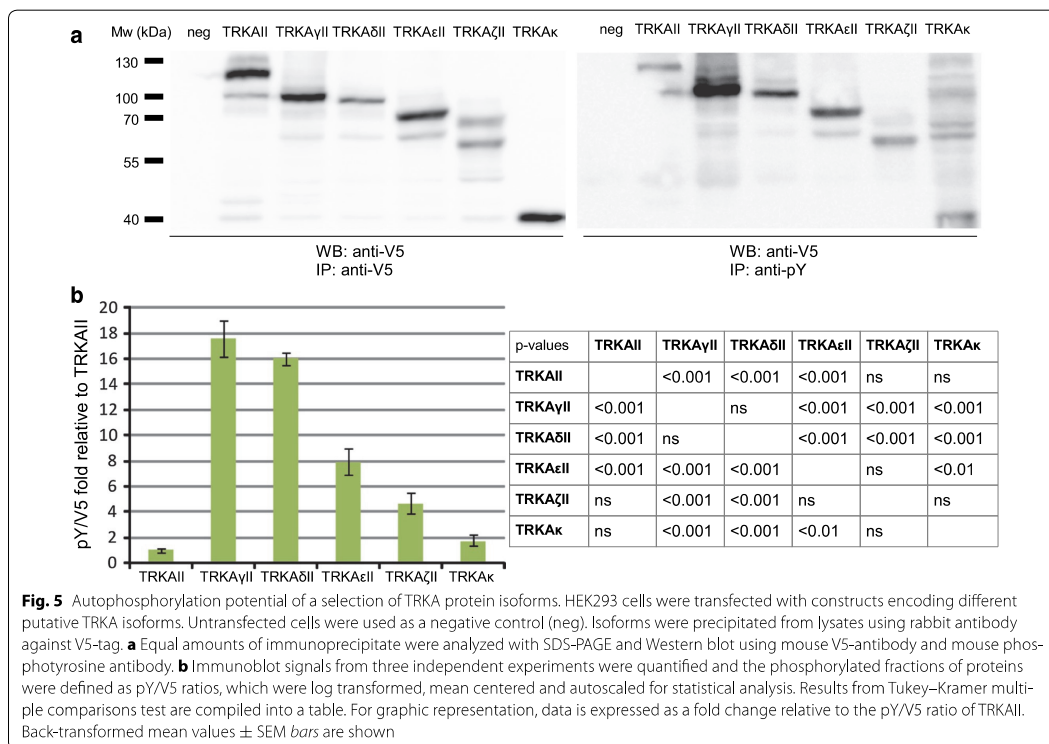
Isoforms seemed to vary in the extent of autophosphorylation. To better characterize this variation, Western blot signals were quantified with densitometric analysis. Data was converted into an anti-pY to anti-V5 signal ratio (pY/V5) for each isoform and presented as a fold change relative to the pY/V5 ratio of TRKAII. Significance of differences of these ratios over three independent experiments was determined with Repeated Measures ANOVA and with a post hoc multiple comparisons test (Tukey–Kramer). The results are shown in Fig. 5b.

When protein expression level is very high, such as in cancer, even those kinase receptors exhibit autocatalysis that under normal physiological conditions are repressed. In the current experiment, the amount of protein

monomer was not the sole determinant of autophosphorylation, since for every isoform the strength of V5 signal does not correlate with the strength of pY signal. Most notably, TRKA γ II-V5-His and TRKA δ II-V5-His were sixteen times more phosphorylated relative to TRKAII-V5-His. pY/V5 ratio difference between TRKA γ II-V5-His and TRKA δ II-V5-His was not statistically significant, as likely there are no biologically significant differences concerning autophosphorylation rate of these isoforms, since these proteins vary only by the presence or absence of a predicted signal peptide. TRKA ϵ II-V5-His displayed two-fold smaller rate of simultaneous kinase activation as compared to TRKA γ II and TRKA δ II. This difference might have biological relevance, since TRKA ϵ II protein almost entirely lacks cysteine-flanked leucine-rich motifs that could stimulate dimerisation in TRKA γ II and TRKA δ II. TRKA κ -V5-His, a protein corresponding to the intracellular domain of TRKAII had an autoactivation capacity comparable to TRKAII, possibly because TRKA κ lacks extracellular domains which could facilitate dimerisation and subsequent autophosphorylation as seen for other putative TRKAII isoforms.

TRKA ζ II is a glycoprotein residing in intracellular compartments

We noticed that TRKAII-V5-His and TRKA ζ II-V5-His lysates showed signals from larger proteins than can be estimated (Fig. 5a). Based on an analogy to immunoblot pattern observed for TRKAII-V5-His it was assumed that TRKA ζ II-V5-His could also be glycosylated similarly to TRKAII. To clarify this issue, HEK293 cells were transfected with expression constructs of TRKAII-V5-His, TRKA γ II-V5-His and TRKA ζ II-V5-His, followed by treatment with tunicamycin, an inhibitor of N-linked glycosylation. Lysates were analyzed with an anti-V5 antibody. Tunicamycin inhibition was effective as tunicamycin-treated cells transiently expressing TRKAII-V5-His contained only the unmodified form of the receptor (Fig. 6a). TRKA γ II-V5-His was included because it was the only novel putative TRKA isoform for which the Phobius prediction tool estimated a membrane signal sequence and thus it could be directed to the ER-Golgi route where it can be glycosylated. However, since the predicted size of the protein without glycosylation coincided with the Mw of the protein seen on SDS-gel (Fig. 5a), it seemed that the signal sequence of TRKA γ II is nonfunctional. In accordance with this finding, tunicamycin did not change the electrophoretic mobility of TRKA γ II and the intracellular localization of TRKA γ II-V5-His appeared to be cytosolic (Fig. 6b). On the other hand, the disappearance of signal from the protein with bigger Mw in case of TRKA ζ II-V5-His-transfected and tunicamycin-treated cells is a clear indication that this isoform is modified at least on



one of the five consensus N-glycosylation sites (N-X-S/T sequons) it has. This finding seems to place TRKA ζ -V5-His to the ER-Golgi route, where N-glycosyltransferases reside. However, as opposed to the full-length TRKAII, TRKA ζ II did not reach plasma membrane in HEK293 cells transiently transfected with TRKA ζ II-V5-His expression plasmid (Fig. 6b).

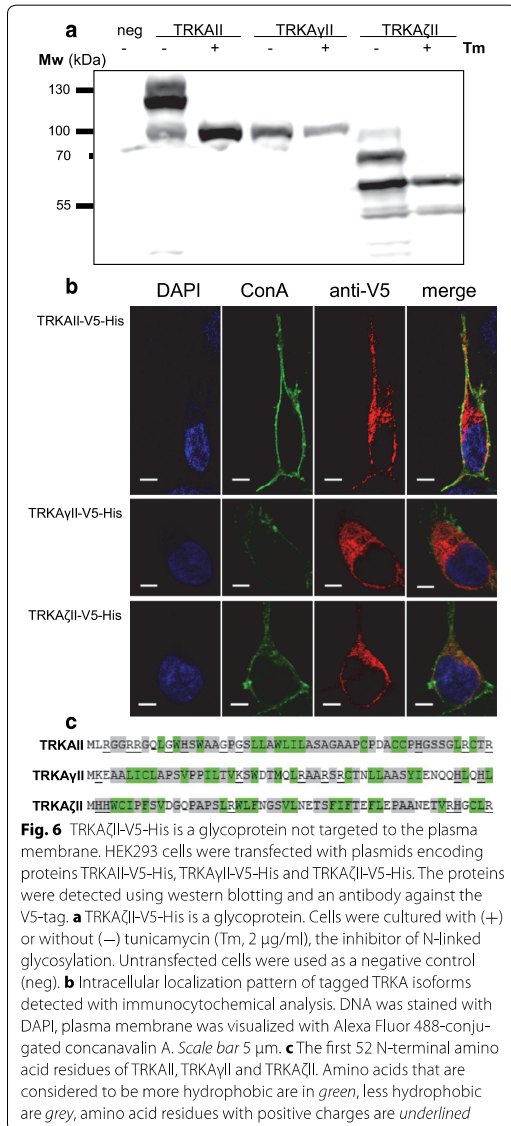
Usually, proteins are targeted to the ER when nascent signal peptide is revealed during the first translational round [47]. Signal peptides are not conserved among secretory and integral proteins, but generally consist of 20–30 residues with positively charged aa residues in the N-terminus followed by a hydrophobic core of at least six residues. However, yet undefined structural features seem to be also important [48]. Phobius prediction tool for signal peptides estimated that TRKAYII could be directed to plasma membrane while TRKA ζ II cannot. Although TRKAYII has a longer stretch of hydrophobic amino acids in the N-terminus compared to TRKA ζ II, this hydrophobic core is preceded by a lysine and glutamate, whereas TRKA ζ II has two histidines in the N-terminus (Fig. 6c). Only about 10 % of histidine residues are in a positively charged state at physiological pH, however,

apparently this serves to be a recognizable signal peptide, whereas TRKAYII's N-terminus does not.

TRKA κ localizes to the cytoplasm and the nucleus

Initial experiments with putative TRKA protein isoforms in HEK293 cells revealed that additionally to cytosolic distribution, TRKA κ -V5-His is also present in the nucleus. To confirm this finding, immunocytochemical analysis was carried out in HEK293 cells and primary rat cortical neurons transfected with the expression construct encoding TRKA κ -V5-His or TRKAII-V5-His as a control. Although TRKAII-V5-His was restrained to the cytoplasm and the plasma membrane, the ability of TRKA κ -V5-His to localize to the nucleus of neuronal cells was confirmed, however, various types of localization were observed (Fig. 7a). Therefore, this effect is not cell-type specific.

Since fixation and permeabilization procedures preceding immunocytochemistry can alter protein localization pattern, the nuclear translocation of TRKA κ was verified in HEK293 cells with live imaging of EGFP-tagged protein by directly observing the fluorescence of EGFP. Moreover, TRKA κ -EGFP has a significantly bigger molecular weight (70 kDa) than TRKA κ -V5-His (42 kDa)



(See figure on next page.)

Fig. 7 TRKAκ isoform's localization into the nucleus. **a** immunocytochemical analysis revealing TRKAκ-V5-His and TRKAI-V5-His localization in primary rat neurons and HEK293 cells. DNA was stained with DAPI. To mark glycoproteins embedded in the plasma membrane, Alexa Fluor 488-conjugated concanavalin A (con A) was used, and TRKA-V5-His proteins were visualized with anti-V5-tag antibodies and secondary Alexa Fluor 568-conjugated antibodies. Scale bar 5 µm. **b** Nuclear accumulation of EGFP-fused TRKAκ in HEK293 cells. Cells were transfected with constructs encoding TRKAκ-EGFP or EGFP, and mCherry-NLS (the marker for nucleus). Live cells were imaged with a confocal microscope. Scale bar 5 µm. **c** HEK293 were fixed and subjected to immunocytochemistry 24 h p.t. of expression constructs encoding TRKAI-V5-His, TRKAκ-V5-His, TRKAκ-EGFP or EGFP. The cells were visualized with confocal microscopy and counted by determining the localization of given protein of interest in n number of cells. The graph shows pooled results of two independent experiments. C = N, the signal was observed uniformly in cytosol and nucleus; C > N, the signal was greater in cytosol than in nucleus; C < N, the signal was greater in nucleus than in cytosol

and cannot diffuse to the nucleus passively. The control EGFP displayed a uniform localization pattern, while in some cells the signal of TRKAκ-EGFP was clearly accumulated in the cell nucleus (Fig. 7b).

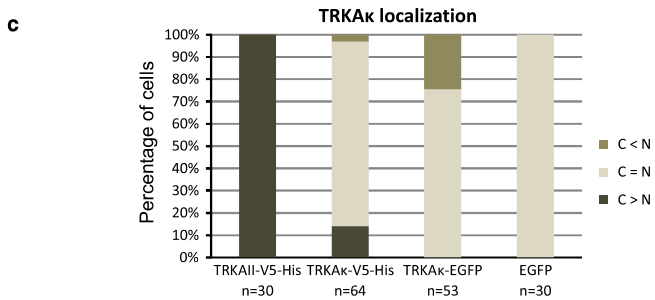
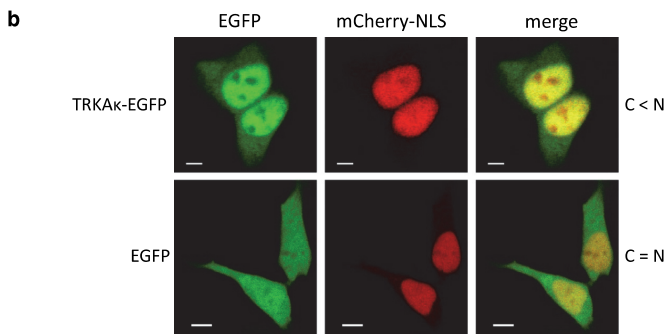
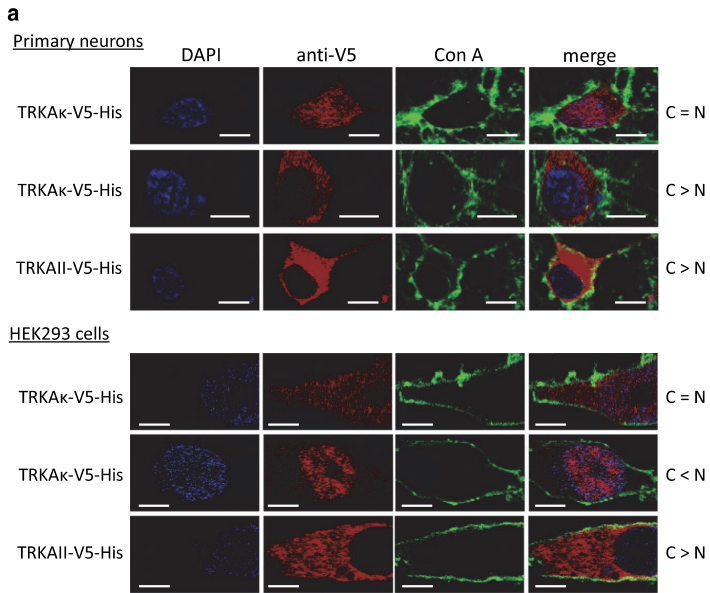
To better describe this phenomenon, we used immunocytochemistry to quantify the intracellular localization of overexpressed TRKAκ-V5-His and TRKAκ-EGFP in HEK293 cells. While the control TRKAI-V5-His was restricted to cytosol and plasma membrane, as expected, TRKAκ with the same tag entered nucleus in more than 80 % of cells and 3 % of cells expressing TRKAκ-V5-His displayed signal that was predominantly in the nucleus (Fig. 7c). On the other hand, EGFP protein was uniformly distributed between cytosol and nucleus in all cells examined. When TRKAκ was linked to EGFP, then the level of signal from cell nucleus exceeded that from the cytosol in 25 % of cells (Fig. 7c). Therefore, our experiments clearly indicate that TRKAκ is able to enter cell nucleus.

There is no conventional nuclear localization signal (NLS) present in TRKA. Nevertheless, in the proximity of N-terminus of TRKAκ a signal sequence SPT that has been shown to mediate the recognition by Importin-7 (Imp7) was identified. There is numerous evidence of Imp7 translocating a variety of proteins such as Smads, extracellular signal-regulated kinase 2 (Erk2) and early growth response protein 1 and glucocorticoid receptor (Egr-1) to the nucleus [49–52]. A hypothesis of the translocation of TRKAκ to the nucleus by Imp7 via the SPT sequence was proposed. Cellular localization of TRKAκ-SPT-EGFP (lacking the putative signal sequence) bared no significant difference with TRKAκ-EGFP (data not shown). Therefore, it can be concluded that the sequence eliminated was not responsible for the accumulation of the TRKA intracellular fragment to the nucleus and Imp7 was most probably not involved in the transportation of TRKAκ to the nucleus.

Discussion

TRKA gene organization and expression in human, mouse and rat

As more and more mRNA sequence information becomes available, it is becoming evident that overlapping genes are more common than previously thought [53, 54]. Even so, gene trios seem to be relatively rare [44].



In this study we describe *TRKA* gene, which in human is overlapped by two genes of the opposite strand—*INSRR* and *SH2D2A*. More specifically, these genes are overlapped by novel *TRKA* 5' exons A...D with the transcription-initiation site in exon A. Despite our efforts, we were unable to identify these exons in mouse or rat. As the transcription-initiation sites of human *TRKA* exon A and *SH2D2A* are less than 1 kb apart, it can be speculated that the unidirectional promoter of *SH2D2A* has become bidirectional at one point in the evolutionary history of human, therefore giving rise to this novel 5' terminus of *TRKA*. There is probably a complex interaction between the expression of these three genes, as they might influence each other in synergistic or competitive way during and after transcription. For example, the close proximity of *INSRR* and *TRKA* promoters might render the genomic region accessible to transcriptional machinery simultaneously for both genes. In accordance with this, it has been shown that *TRKA* and *INSRR* expression patterns are highly similar [55]. On the other hand, *TRKA* exon D overlaps an exon of *INSRR* gene by more than 80 bp and this might result in partly double-stranded mRNAs and gene silencing as the respective regions in mRNA transcripts are complementary.

It should be noted that while we did not identify novel 5' exons of rodent *TrkA*, no previous 5' RACE analyses of rat *TrkA* were recorded in literature to our knowledge. We identified numerous additional transcription-initiation sites and alternative splicing patterns of human *TRKA* which indicate the possible existence of many protein isoforms. Overall—all of the tissues under study expressed many types of 5' *TRKA* exons. The translatability of many of these proteins could be debated as most of these mRNAs contain uORFs. However, according to bioinformatics studies, approximately half of mammalian protein-coding transcripts contain uORFs [56]. It has been shown that even when a strong Kozak sequence surrounds the AUG in uORF or when up to four uORFs precede the main ORF, nearly 10 % of ribosomes are capable of leaky scanning or reinitiation up to five times [46]. The alternative transcripts carrying several uORFs could also use these sequences as a regulatory element for adjusting the specific protein levels to match the necessities of the cell. Also, some of the uORFs may be inaccessible for ribosomes due to RNA secondary structure. It remains to be determined which of these novel transcripts represent functional *TRKA* mRNAs and which can be considered as transcriptional noise.

Characteristics of putative novel *TRKA* protein isoforms

In TRK proteins, a kinase monomer is kept in an inactive conformation through autoinhibition mechanism (the projection of one tyrosine residue into the active

site). However, since kinase domain structure allows the movement of its parts to some degree, every monomer is occasionally freed from inhibited state and is able to phosphorylate in trans [57]. This spontaneous activity is deterred by the properties of the extracellular domain, such as the presence of glycan side chains [21, 22]. In accordance to this, the autocatalysis rates of potential *TRKA* isoforms tested in this study were very different with the highest levels seen for *TRKA γ II*, *TRKA δ II* and *TRKA ϵ II*. All these isoforms contain part of the extracellular domain of the prototypic *TRKAII* and are not glycosylated, as indicated by protein mobility pattern on SDS-PAGE and the lack of functional membrane signal sequences which renders them inaccessible to N-glycosyltransferases that are located in the Golgi apparatus. Phosphorylation of *TRKA γ II* and *TRKA δ II* could also be enhanced by the presence of unique amino acid residue stretch encoded by exons A and D.

We identified a putative *TRKA* isoform *TRKA ζ II* which was glycosylated in the ER-Golgi route and must therefore possess a functional membrane-signal sequence. However, when overexpressed, this protein was not transported to the plasma membrane, but got stalled intracellularly. Similarly, *TRKAIII* is also known to be retained intracellularly with a highly autoactivated *TRKAIII*-pool residing in the ER/Golgi intermediate compartment [27]. It has been suggested that *TRKAIII* is not directed to the plasma membrane, because it lacks a site for the addition of a glycan moiety acting as a signal for further translocation. On the basis of current study, *TRKA ζ II*-V5-His seems to be confined to intracellular compartments similarly to *TRKAIII*. *TRKA ζ II* protein contains the juxtamembrane region that is omitted in *TRKAIII* but just as *TRKAIII* it does not have the first Ig-like domain. Thus, the first Ig-like domain could serve an important regulatory function in the trafficking of *TRKA* protein.

Among several alternative *TRKA* variants, an interesting putative isoform, termed *TRKA κ* , emerged from our study. The protein constitutes primarily of the receptor's tyrosine kinase domain. There are several reasons why this variant drew our attention. First, it is noteworthy that while the alternative splicing pattern observed in rat and mouse bares little similarities to the complexity seen in humans, the expression of transcripts with exons 9a and 10a that contribute to *TRKA κ* -encoding mRNAs was detected in all species examined. Second, these mRNAs have a distinct expression pattern in different tissues, leaving room for further speculation about the possible importance of this isoform in diverse cellular frameworks. The rationale for further investigations of this protein includes also the possibility that proteolysis may generate a *TRKA κ* -like fragment, as under excitotoxic

conditions or in response to amyloid- β peptide the highly similar TRKB receptor has been recently shown to be subjected to proteolytic cleavage, resulting in a kinase-domain containing soluble protein fragment [58–60]. This type of process has also been detected for another receptor tyrosine kinase called erythroblastic leukemia viral oncogene homolog-4 (ErbB-4). The ectodomain of ErbB-4 is cut by metalloprotease and the intracellular domain that is cleaved by γ -secretase is thereafter translocated to nucleus [61]. Cleavage of the TRKA extracellular domain producing an ectodomain fragment and membrane-bound truncated TRKA fragments with intracellular kinase domain has been demonstrated, but no soluble fraction of TRKA kinase domain has yet been discovered [62].

The most intriguing property of TRKA κ is undoubtedly its intracellular localization which varies from cytosolic to nuclear. Under physiological conditions passive flux through nuclear pore complex is very restricted for molecules bigger than 30 kDa [63]. Thus, a TRKA κ -like protein (35 kDa) especially when it's EGFP-tagged ($\Sigma \approx 70$ kDa) would only gain access to the nucleus with the aid of active transport or facilitated diffusion. Appearance of distribution patterns where TRKA κ -V5-His or TRKA κ -EGFP signal was more strongly detected in the cytosol or the nucleus could suggest that the movement of TRKA κ to the nucleus is regulated, since active transport of TRKA κ might be dependent on the availability of adapter proteins that are only expressed in a certain time frame during cell-cycle or under certain cellular physiological states. Alternatively, TRKA κ could shift towards passive nuclear accumulation when high-affinity nuclear anchoring proteins in the nucleus do not allow its export and/or impede its free diffusion.

Previously, by using the method of immunocytochemistry, TRKA has been detected in the nuclei of various cells, such as melanocytic tumors [64], ovarian carcinoma [65], human glioma cell line U251 [66], rat pheochromocytoma cell line PC12 and cultured hepatic stellate cells [67]. In liver cells TRKA nuclear immunoreactivity was observed when antibody against C-terminus was used, whereas antibody against N-terminus did not reveal TRKA. Overall, it is not clear whether nuclear TRKA seen in those studies represents the whole receptor, its proteolytic fragment, an alternative isoform or non-specific staining. Our current study implies that neither HEK293 cells nor rat primary neurons contain transporting machinery necessary for whole receptor translocation into the nucleus, although this could possibly be otherwise in different cell types. However, our results established that TRKA κ tagged to V5-His or EGFP is definitely present in the nucleus whether it is encoded by specific

mRNAs or proteolytically generated from the full-length receptor.

As compared to many other TRKA isoforms, TRKA κ displayed relatively low autocatalysis rate which is particularly interesting in the light of the finding that TRKA κ was bound to other pY-proteins, while for more highly phosphorylated isoforms of TRKA it was not possible to detect interactions of this intensity. Presumably only the small p-TRKA κ fraction was capable of interacting with these proteins, since they were tyrosine-phosphorylated and it can be assumed that this modification was mediated by the kinase activity of p-TRKA κ . Alternatively, the situation may be reversed as some of these proteins may be tyrosine kinases phosphorylating TRKA κ . However, given that this was the only TRKA isoform displaying nuclear localization, it can be suggested that there are high-affinity substrates for TRKA that may reside inside the nucleus.

Identical protein to TRKA κ was characterized by Coullier and coworkers when different deletion-mutants of TRKA were assessed on the ability to transform NIH 3T3 cells [68]. They found that this protein is a functional kinase, but has no transforming ability just as the full-length receptor. Interestingly, in melanomas, nuclear expression of phosphorylated TRKA was more pronounced in primary tumors relative to metastases [64]; however, in ovarian carcinoma nuclear expression was not more characteristic to any stage of cancer progression [65]. Thus, it is unclear whether TRKA nuclear activity contributes to malignant phenotype or aids to maintain a stable state.

The novel cytoplasmic and nuclear isoforms of TRKA cannot be activated by NGF or NT-3 because neurotrophins are directed to membrane-bound ER-lumen and to the vesicles of the Golgi complex already during their synthesis. Therefore, their interaction with those TRKA isoforms is sterically impossible. However, these TRKA proteins can undergo spontaneous autoactivation or, alternatively, there might be some other activating factors within the cell which are yet unidentified.

Conclusions

TRK receptors have crucial roles in processes with various outcomes such as proliferation, survival and differentiation. Thus, the activity of these receptors has to be regulated for the correct cellular fate. Control at mRNA level through alternative splicing and several alternative transcription initiation sites provides mechanisms to diversify the pool of TRK proteins with different properties.

In this study, *TRKA* transcripts were studied in silico, by 5' RACE and by semiquantitative analyses. The

expression patterns of alternative *TRKA* transcripts were analyzed in different human brain regions and peripheral human, mouse and rat tissues. Many novel alternative transcript variants were detected in human tissues and the presence of a large number of *TRKA* protein isoforms was predicted that differ in N-termini and protein sequences of the extracellular domain encoded by alternatively spliced exons. In rat and mouse tissues the splicing observed was less intricate. Our experiments showed that soluble *TRKA* isoforms, which contain parts of unglycosylated extracellular domain, are highly autocatalytic in comparison to plasma membrane-embedded glycosylated *TRKAII* receptor. One of the putative isoforms, *TRKAÇII*, is a glycoprotein residing in intracellular compartments similarly to isoform *TRKAIII*. Therefore, it can be inferred that the first Ig-like domain in *TRKAI/II* that is missing in both *TRKAIII* and *TRKAÇII*, is necessary for the translocation of receptor to the plasma membrane. One of the putative isoforms that is composed mainly of the kinase domain, named *TRKAκ*, displayed a relatively low level of autocatalysis rate. Interestingly, *TRKAκ* was detected in the nucleus and cytoplasm of transiently transfected fixed as well as live cells.

These findings lay ground to future studies in the field of alternative *TRKA* isoforms, as there seems to be an immensely larger variability among *TRKA* proteins with different properties than is presently known.

Methods

All experiments with human postmortem tissues were approved by the ethics committee of medical studies at National Institute for Health Development of Estonia (Permit Number: 402). The protocols involving animals were approved by the ethics committee of animal experiments at Ministry of Agriculture of Estonia (Permit Number: 45). Human RNAs used in this study were acquired from BD Biosciences (thymus, muscle, heart, prostate, testis, pancreas, kidney and colon samples), from BioChain Inc. (human spleen and fetal tissues), or were extracted from frozen adult human postmortem brain regions obtained from North Estonian Regional Hospital, Tallinn. Rat tissues were obtained from Sprague–Dawley rats and mouse tissues from NMRI mice housed under a 12 h light/dark cycle in local animal facility with *ad libitum* access to water and food.

RT-PCR and 5' RACE

In silico analysis of the *TRKA* gene structure and transcripts, reverse transcription and PCR methodology have been described before [69]. 5' RACE experiments were conveyed with GeneRacer Kit (Invitrogen) according to the manufacturer's protocol (Invitrogen). For PCR,

HotFire polymerase from Solis Biodyne was used. All primers used in this study are listed in Additional file 2, *TRKA* ESTs identified with sequencing have been submitted and the corresponding GenBank accession numbers can be found in Additional file 3.

Generation of expression constructs

To generate the V5-His-tagged *TRKAII* isoform, PCR was conducted to amplify the coding region from human frontal cerebral cortex cDNA and cloned into pcDNA3.1 (Invitrogen). Sequences encoding N-terminal parts of different *TRKA* isoforms were amplified from human frontal lobe or muscle cDNA and ligated with plasmid pTZ57R/T of InsTAclone™ PCR Cloning Kit (Fermentas). Verified sequences were subcloned into the pcDNA3.1/*TRKAII*-V5-His vector using the following restriction enzymes: *HindIII* and *NarI* (for pcDNA3.1/*TRKAγII*-V5-His), *XbaI* and *Eco47III* (for pcDNA3.1/*TRKAδII*-V5-His), *HindIII* and *BalI* (for pcDNA3.1/*TRKAεII*-V5-His), *HindIII* and *PagI* (for pcDNA3.1/*TRKAÇII*-V5-His), *XbaI* and *NcoI* (for pcDNA3.1/*TRKAκ*-V5-His).

EGFP-tagged *TRKAκ* was generated by excising the V5-His tag-coding sequence from the pcDNA3.1/*TRKAκ*-V5-His plasmid and substituting it with EGFP-coding sequence from pEGFP-N2 (Clontech). For this, *Cfr42I* (in case of pcDNA3.1/*TRKAκ*-V5-His) and *NotI* (for pEGFP-N2) restriction enzymes were used, followed by DNA-blunting with T4 DNA polymerase in the presence of dNTPs and a final restriction with *BamHI* enzyme. Restriction products of interest were ligated. All restriction enzymes were purchased from Fermentas and all DNA constructs were verified by sequencing.

Cell culture and transfection

HEK293 cells were grown in Minimum Essential Medium (MEM) with Earle's salts and L-Glutamine containing 10 % fetal bovine serum (FBS) and 1 % penicillin/streptomycin. LipoD293™ DNA In Vitro Transfection Reagent (SignaGen) was used in HEK293 cell transfections. PC12 cells were maintained in Dulbecco's Modified Eagle's Medium (DMEM) containing 6 % FBS, 6 % horse serum (HS) and 1 % penicillin/streptomycin. SH-SY5Y cells were grown in DMEM/Ham's F12 in 1:1 ratio, containing 10 % FBS and 1 % penicillin/streptomycin. For NGF treatments, growth medium with 50 ng/ml of NGF (PeproTech) was added 5 min prior to harvesting the cell culture. All growth media components were purchased from PAA Laboratories GmbH.

Cerebral cortex was dissected from Sprague–Dawley rat embryos at embryonic day 21. Cells were dissociated with 0.25 % trypsin (Invitrogen), followed by treatment with 0.05 % DNase I (Roche). Cells were grown

on poly-L-lysine-coated cover slips in Neurobasal A medium (Invitrogen) with B27 supplement (Invitrogen), 1 % penicillin/streptomycin, and 1 mM L-glutamine (PAA Laboratories GmbH). Mitotic inhibitor 5-fluoro-2'-deoxyuridine (Sigma) was added to the medium (10 μ M) at 2 days in vitro (DIV). Primary neurons were transfected at 7 DIV using Lipofectamine 2000 transfection reagent (Invitrogen) as advised by the manufacturer.

The Silencer Select small interfering RNA (siRNA), with nucleotide sequence GUACUUCAGUGAUAC-CUGUtt, targeting rat *TrkA* and negative unspecific siRNA (#1) were from Ambion (Life Technologies). SiRNAs were transfected to PC12 cells with Lipofectamine RNAiMax Transfection Reagent (Invitrogen) with final 10 nM siRNA concentration, according to the manufacturer's instructions. Cells were harvested 24–48 h after transfection.

Western blotting

Western blotting has been described previously [70]. Antibodies used included: rabbit anti-TRKA (#06-574; 1:1000) and mouse anti-pY (#05-1050; 1:2000) from Millipore; rabbit anti-TRK (#4609; 1:500) and rabbit anti-phospho-TRKA (#9141; 1:1000) from Cell Signaling; mouse anti-V5 (#R960-25; 1:5000) from Invitrogen; mouse anti-GAPDH (#G8795; 1:5000) from Sigma-Aldrich.

N-linked glycosylation was inhibited from 6 h after transfection by adding tunicamycin (2 μ g/ml; AppliChem) and cells were lysed 9 h later in RIPA buffer.

Immunoprecipitation, immunofluorescence and confocal microscopy were done as described previously [70].

Live imaging

All live imaging experiments were done at 37 °C, in a chamber supplied with 5 % CO₂. Zeiss LSM 5 DUO confocal laser scanning microscope with Zeiss confocal scan software was used for imaging. Coverslips containing cultured HEK293 cells were transferred into a metal chamber. For all experiments a 63 \times glycine immersion fluorescence objective (LSI Plan-Neofluar 63 \times /1.3 ImmKorr DIC M27) was used.

Additional files

Additional file 1: Sequences of putative TRKA protein isoforms. Red indicates sequences that are not found in TRKAlI isoform. (A) Isoforms with different N-termini compared to TRKAlI. (B) Exclusion of parts of the extracellular domain as exemplified in the case of isoforms with the conventional N-terminus.

Additional file 2: Primers and cycling conditions used in this study.

Additional file 3: GenBank accession numbers of ESTs identified in this study.

Abbreviations

BLAST: basic local alignment search tool; BDNF: brain-derived neurotrophic factor; CIPA: congenital insensitivity to pain with anhidrosis; DIV: days in vitro; DMEM: Dulbecco's Modified Eagle's Medium; Egr-1: early growth response protein 1 and glucocorticoid receptor; ER: endoplasmic reticulum; ErbB-4: erythroblastic leukemia viral oncogene homolog-4; EST: expressed sequence tag; Erk2: extracellular signal-regulated kinase 2; FBS: fetal bovine serum; GPCRs: G protein-coupled receptors; HS: horse serum; HEK293: human embryonic kidney cells; Ig-like: immunoglobulin-like; Imp7: Importin-7; INSRR: insulin receptor-related protein; MEM: minimum essential medium; NGF: nerve growth factor; NTRK1: neurotrophic tyrosine kinase, receptor, type 1; NT-4: neurotrophin-4; NMD: nonsense mediated decay; NLS: nuclear localization signal; PI3 K: phosphatidylinositol 3 kinase; pY: phospho-tyrosine; PLC- γ 1: phospholipase C- γ 1; RIPA: radioimmunoprecipitation assay; 5' RACE: rapid amplification of 5' complementary DNA ends; Ras-MAPK: rat sarcoma/mitogen-activated protein kinase; RT-PCR: reverse transcription polymerase chain reaction; SH2D2A: sarcoma protein homology 2 domain protein 2A; TRKA: tropomyosin-related kinase A; uORF: upstream ORF.

Authors' contributions

KL and RP carried out 5' RACE and RT-PCR analyses and drafted the manuscript. RP also performed live cell imaging, cell counting and detection of endogenous TRKA proteins. EA carried out cloning, phosphorylation, glycosylation and immunocytochemistry of TRKA protein isoforms. TT conceived the study and participated in its design and coordination and helped to draft the manuscript. All authors read and approved the final manuscript.

Author details

¹ Department of Gene Technology, Tallinn University of Technology, Akadeemia tee 15, 12618 Tallinn, Estonia. ² Competence Center for Cancer Research, Tallinn, Estonia. ³ Present Address: VIB lab for Systems Biology & CMPG Lab for Genetics and Genomics, Leuven, Belgium. ⁴ Present Address: French National Institute for Agricultural Research, Paris, France.

Acknowledgements

We thank Epp Väli and Maila Rähn for technical assistance and are grateful to Heiti Paves for instructions and help concerning the confocal microscope, Mari Sepp for enlightening advice and Kaur Jaanson and Indrek Koppel for good counsel. We thank as well Enn Jöeste from North Estonian Regional Hospital, Tallinn, for collaboration. This study was supported by Estonian Research Council (institutional research funding IUT19-18), National R&D program "Biotechnology" (Grant AR12171), Estonian Enterprise grant to Competence Center for Cancer Research, Estonian Academy of Sciences and Genecode Ltd.

Competing interests

The authors declare that they have no competing interests.

Received: 20 February 2015 Accepted: 9 November 2015

Published online: 18 November 2015

References

- Chao MV. Neurotrophins and their receptors: a convergence point for many signalling pathways. *Nat Rev Neurosci*. 2003;4:299–309.
- Marmigère F, Ernfors P. Specification and connectivity of neuronal subtypes in the sensory lineage. *Nat Rev Neurosci*. 2007;8:114–27.
- Davies AM. Extracellular signals regulating sympathetic neuron survival and target innervation during development. *Auton Neurosci Basic Clin*. 2009;151:39–45.
- Fagan AM, Garber M, Barbacid M, Silos-Santiago I, Holtzman DM. A role for TrkA during maturation of striatal and basal forebrain cholinergic neurons in vivo. *J Neurosci Off J Soc Neurosci*. 1997;17:7644–54.
- Freund-Michel V, Frossard N. The nerve growth factor and its receptors in airway inflammatory diseases. *Pharmacol Ther*. 2008;117:52–76.
- Minichiello L, Calella AM, Medina DL, Bonhoeffer T, Klein R, Korte M. Mechanism of TrkB-mediated hippocampal long-term potentiation. *Neuron*. 2002;36:121–37.
- Ohmichi M, Decker SJ, Saltiel AR. Activation of phosphatidylinositol-3 kinase by nerve growth factor involves indirect coupling of the trk proto-oncogene with src homology 2 domains. *Neuron*. 1992;9:769–77.

8. Skaper SD. The neurotrophin family of neurotrophic factors: an overview. *Methods Mol Biol Clifton NJ*. 2012;846:1–12.
9. Lee FS, Chao MV. Activation of Trk neurotrophin receptors in the absence of neurotrophins. *Proc Natl Acad Sci USA*. 2001;98:3555–60.
10. Rajagopal R, Chao MV. A role for Fyn in Trk receptor transactivation by G-protein-coupled receptor signaling. *Mol Cell Neurosci*. 2006;33:36–46.
11. Lee FS, Rajagopal R, Kim AH, Chang PC, Chao MV. Activation of Trk neurotrophin receptor signaling by pituitary adenylate cyclase-activating polypeptides. *J Biol Chem*. 2002;277:9096–102.
12. Shi Y, Mantuano E, Inoue G, Campana WM, Gonias SL. Ligand binding to LRP1 transactivates Trk receptors by a Src family kinase-dependent pathway. *Sci Signal*. 2009; 2:ra18.
13. Puehringer D, Orel N, Lüningschrör P, Subramanian N, Herrmann T, Chao MV, Sendtner M. EGF transactivation of Trk receptors regulates the migration of newborn cortical neurons. *Nat Neurosci*. 2013;16:407–15.
14. Rantamäki T, Vesa L, Anttila H, Di Lieto A, Tammela P, Schmitt A, Lesch K-P, Rios M, Castrén E. Antidepressant drugs transactivate TrkB neurotrophin receptors in the adult rodent brain independently of BDNF and monoamine transporter blockade. *PLoS One*. 2011;6:e20567.
15. Indo Y, Mardy S, Tsuruta M, Karim MA, Matsuda I. Structure and organization of the human TRKA gene encoding a high affinity receptor for nerve growth factor. *Jpn J Hum Genet*. 1997;42:343–51.
16. Meakin SO, Suter U, Drinkwater CC, Welcher AA, Shooter EM. The rat trk protooncogene product exhibits properties characteristic of the slow nerve growth factor receptor. *Proc Natl Acad Sci USA*. 1992;89:2374–8.
17. Okazaki Y, Furuno M, Kasukawa T, Adachi J, Bono H, Kondo S, Nikaïdo I, Osato N, Saito R, Suzuki H, Yamanaoka I, Kiyosawa H, Yagi K, Tomaru Y, Hasegawa Y, Nogami A, Schönbach C, Gobjori T, Baldarelli R, Hill DP, Bult C, Hume DA, Quackenbush J, Schriml LM, Kanapin A, Matsuda H, Batalov S, Beisel KW, Blake JA, Bradt D, et al. Analysis of the mouse transcriptome based on functional annotation of 60,770 full-length cDNAs. *Nature*. 2002;420:563–73.
18. Urfer R, Tsoulfas P, O'Connell L, Shelton DL, Parada LF, Presta LG. An immunoglobulin-like domain determines the specificity of neurotrophin receptors. *EMBO J*. 1995;14:2795–805.
19. Schneider R, Schweiger M. A novel modular mosaic of cell adhesion motifs in the extracellular domains of the neurogenic trk and trkB tyrosine kinase receptors. *Oncogene*. 1991;6:1807–11.
20. Huang EJ, Reichardt LF. Trk receptors: roles in neuronal signal transduction. *Annu Rev Biochem*. 2003;72:609–42.
21. Jullien J, Guili V, Reichardt LF, Rudkin BB. Molecular kinetics of nerve growth factor receptor trafficking and activation. *J Biol Chem*. 2002;277:38700–8.
22. Watson FL, Porcionatto MA, Bhattacharyya A, Stiles CD, Segal RA. TrkA glycosylation regulates receptor localization and activity. *J Neurobiol*. 1999;39:323–36.
23. Barker PA, Lomen-Hoerth C, Gensch EM, Meakin SO, Glass DJ, Shooter EM. Tissue-specific alternative splicing generates two isoforms of the trkA receptor. *J Biol Chem*. 1993;268:15150–7.
24. Clary DO, Reichardt LF. An alternatively spliced form of the nerve growth factor receptor TrkA confers an enhanced response to neurotrophin 3. *Proc Natl Acad Sci USA*. 1994;91:11133–7.
25. Tacconelli A, Farina AR, Cappabianca L, Desantis G, Tessitore A, Vetuschi A, Sferra R, Rucci N, Argenti B, Screpanti I, Gulino A, Mackay AR. TrkA alternative splicing: a regulated tumor-promoting switch in human neuroblastoma. *Cancer Cell*. 2004;6:347–60.
26. Tacconelli A, Farina AR, Cappabianca L, Cea G, Panella S, Chioda A, Gallo R, Cinque B, Sferra R, Vetuschi A, Campese AF, Screpanti I, Gulino A, Mackay AR. TrkAIII expression in the thymus. *J Neuroimmunol*. 2007;183:151–61.
27. Farina AR, Tacconelli A, Cappabianca L, Cea G, Panella S, Chioda A, Romanelli A, Pedone C, Gulino A, Mackay AR. The alternative TrkAIII splice variant targets the centrosome and promotes genetic instability. *Mol Cell Biol*. 2009;29:4812–30.
28. Dubus P, Parrens M, El-Mokhtari Y, Ferrer J, Groppi A, Merlio JP. Identification of novel trkA variants with deletions in leucine-rich motifs of the extracellular domain. *J Neuroimmunol*. 2000;107:42–9.
29. Miura Y, Mardy S, Awaya Y, Nihei K, Endo F, Matsuda I, Indo Y. Mutation and polymorphism analysis of the TRKA (NTRK1) gene encoding a high-affinity receptor for nerve growth factor in congenital insensitivity to pain with anhidrosis (CIPA) families. *Hum Genet*. 2000;106:116–24.
30. Hefli FF, Rosenthal A, Walicke PA, Wyatt S, Vergara G, Shelton DL, Davies AM. Novel class of pain drugs based on antagonism of NGF. *Trends Pharmacol Sci*. 2006;27:85–91.
31. Nassenstein C, Schulte-Herbrüggen O, Renz H, Braun A. Nerve growth factor: the central hub in the development of allergic asthma? *Eur J Pharmacol*. 2006;533:195–206.
32. Martin-Zanca D, Oskam R, Mitra G, Copeland T, Barbacid M. Molecular and biochemical characterization of the human trk proto-oncogene. *Mol Cell Biol*. 1989;9:24–33.
33. Lagadec C, Meignan S, Adriaenssens E, Foveau B, Vanhecke E, Romon R, Toillon R-A, Oxombre B, Hondermarck H, Le Bourhis X. TrkA overexpression enhances growth and metastasis of breast cancer cells. *Oncogene*. 2009;28:1960–70.
34. Bongarzone I, Vigneri P, Mariani L, Collini P, Pilotti S, Pierotti MA. RET/NTRK1 rearrangements in thyroid gland tumors of the papillary carcinoma family: correlation with clinicopathological features. *Clin Cancer Res Off J Am Assoc Cancer Res*. 1998;4:223–8.
35. Gimm O, Dziema H, Brown J, de la Puente A, Hoang-Vu C, Dralle H, Plass C, Eng C. Mutation analysis of NTRK2 and NTRK3, encoding 2 tyrosine kinase receptors, in sporadic human medullary thyroid carcinoma reveals novel sequence variants. *Int J Cancer J Int Cancer*. 2001;92:70–4.
36. Eggert A, Ikegaki N, Liu XG, Brodeur GM. Prognostic and biological role of neurotrophin-receptor TrkA and TrkB in neuroblastoma. *Klin Pädiatr*. 2000;212:200–5.
37. Tacconelli A, Farina AR, Cappabianca L, Gulino A, Mackay AR. Alternative TrkAIII splicing: a potential regulated tumor-promoting switch and therapeutic target in neuroblastoma. *Future Oncol Lond Engl*. 2005;1:689–98.
38. Ginsberg SD, Che S, Wu J, Counts SE, Mufson EJ. Down regulation of trk but not p75NTR gene expression in single cholinergic basal forebrain neurons mark the progression of Alzheimer's disease. *J Neurochem*. 2006;97:475–87.
39. Hock C, Heese K, Müller-Spahn F, Hulette C, Rosenberg C, Otten U. Decreased trkA neurotrophin receptor expression in the parietal cortex of patients with Alzheimer's disease. *Neurosci Lett*. 1998;241:151–4.
40. Salehi A, Verhaagen J, Dijkhuizen PA, Swaab DF. Co-localization of high-affinity neurotrophin receptors in nucleus basalis of Meynert neurons and their differential reduction in Alzheimer's disease. *Neuroscience*. 1996;75:373–87.
41. Matrone C, Di Luzio A, Meli G, D'Aguzzo S, Severini C, Ciotti MT, Cattaneo A, Calissano P. Activation of the amyloidogenic route by NGF deprivation induces apoptotic death in PC12 cells. *J Alzheimers Dis JAD*. 2008;13:81–96.
42. UCSC Genome Browser Home. <https://genome.ucsc.edu/>.
43. Phobius. <http://phobius.sbc.su.se/>.
44. Veeramachaneni V, Makalowski W, Galdzicki M, Sood R, Makalowska I. Mammalian overlapping genes: the comparative perspective. *Genome Res*. 2004;14:280–6.
45. Kaplan DR, Martin-Zanca D, Parada LF. Tyrosine phosphorylation and tyrosine kinase activity of the trk proto-oncogene product induced by NGF. *Nature*. 1991;350:158–60.
46. Wang X-Q, Rothnagel JA. 5'-untranslated regions with multiple upstream AUG codons can support low-level translation via leaky scanning and reinitiation. *Nucleic Acids Res*. 2004;32:1382–91.
47. Blobel G. Protein targeting (Nobel lecture). *Chembiochem Eur J Chem Biol*. 2000;1:86–102.
48. Stroud RM, Walter P. Signal sequence recognition and protein targeting. *Curr Opin Struct Biol*. 1999;9:754–9.
49. Chuderland D, Konson A, Seger R. Identification and characterization of a general nuclear translocation signal in signaling proteins. *Mol Cell*. 2008;31:850–61.
50. Chen J, Liu MY, Parish CR, Chong BH, Khachigian L. Nuclear import of early growth response-1 involves importin-7 and the novel nuclear localization signal serine-proline-serine. *Int J Biochem Cell Biol*. 2011;43:905–12.
51. Freedman ND, Yamamoto KR. Importin 7 and importin alpha/importin beta are nuclear import receptors for the glucocorticoid receptor. *Mol Biol Cell*. 2004;15:2276–86.
52. Yao X, Chen X, Cottonham C, Xu L. Preferential utilization of Imp7/8 in nuclear import of Smads. *J Biol Chem*. 2008;283:22867–74.
53. Ho M-R, Tsai K-W, Lin W. A unified framework of overlapping genes: towards the origination and endogenous regulation. *Genomics*. 2012;100:231–9.

54. Sanna CR, Li W-H, Zhang L. Overlapping genes in the human and mouse genomes. *BMC Genom*. 2008;9:169.
55. Reinhardt RR, Chin E, Zhang B, Roth RA, Bondy CA. Selective coexpression of insulin receptor-related receptor (IRR) and TRK in NGF-sensitive neurons. *J Neurosci Off J Soc Neurosci*. 1994;14:4674–83.
56. Calvo SE, Pagliarini DJ, Mootha VK. Upstream open reading frames cause widespread reduction of protein expression and are polymorphic among humans. *Proc Natl Acad Sci USA*. 2009;106:7507–12.
57. Lemmon MA, Schlessinger J. Cell signaling by receptor tyrosine kinases. *Cell*. 2010;141:1117–34.
58. Gomes JR, Costa JT, Melo CV, Felizzi F, Monteiro P, Pinto MJ, Inácio AR, Wieloch T, Almeida RD, Grãos M, Duarte CB. Excitotoxicity downregulates TrkB.FL signaling and upregulates the neuroprotective truncated TrkB receptors in cultured hippocampal and striatal neurons. *J Neurosci Off J Soc Neurosci*. 2012;32:4610–22.
59. Vidaurre OG, Gascón S, Deogracias R, Sobrado M, Cuadrado E, Montaner J, Rodríguez-Peña A, Díaz-Guerra M. Imbalance of neurotrophin receptor isoforms TrkB-FL/TrkB-T1 induces neuronal death in excitotoxicity. *Cell Death Dis*. 2012;3:e256.
60. Jerónimo-Santos A, Vaz SH, Parreira S, Rapaz-Lérias S, Caetano AP, Buée-Scherer V, Castrén E, Valente CA, Blum D, Sebastião AM, Diógenes MJ. Dysregulation of TrkB receptors and BDNF Function by amyloid- β peptide is mediated by calpain. *Cereb Cortex*. 2015;25:3107–21.
61. Ni CY, Murphy MP, Golde TE, Carpenter G. gamma -Secretase cleavage and nuclear localization of ErbB-4 receptor tyrosine kinase. *Science*. 2001;294:2179–81.
62. Díaz-Rodríguez E, Cabrera N, Esparis-Ogando A, Montero JC, Pandiella A. Cleavage of the TrkA neurotrophin receptor by multiple metalloproteases generates signalling-competent truncated forms. *Eur J Neurosci*. 1999;11:1421–30.
63. Talcott B, Moore MS. Getting across the nuclear pore complex. *Trends Cell Biol*. 1999;9:312–8.
64. Flørenes VA, Maelandsmo GM, Holm R, Reich R, Lazarovici P, Davidson B. Expression of activated TrkA protein in melanocytic tumors: relationship to cell proliferation and clinical outcome. *Am J Clin Pathol*. 2004;122:412–20.
65. Davidson B, Reich R, Lazarovici P, Nesland JM, Skrede M, Risberg B, Tropé CG, Flørenes VA. Expression and activation of the nerve growth factor receptor TrkA in serous ovarian carcinoma. *Clin Cancer Res Off J Am Assoc Cancer Res*. 2003;9:2248–59.
66. Gong A, Zhang Z, Xiao D, Yang Y, Wang Y, Chen Y. Localization of phosphorylated TrkA in carrier vesicles involved in its nuclear translocation in U251 cell line. *Sci China Ser C Life Sci Chin Acad Sci*. 2007;50:141–6.
67. Bonacchi A, Taddei ML, Petrai I, Efsen E, Defranco R, Nosi D, Torcia M, Rosini P, Formigli L, Rombouts K, Zecchi S, Milani S, Pinzani M, Laffi G, Marra F. Nuclear localization of TRK-A in liver cells. *Histol Histopathol*. 2008;23:327–40.
68. Coulier F, Martin-Zanca D, Ernst M, Barbacid M. Mechanism of activation of the human trk oncogene. *Mol Cell Biol*. 1989;9:15–23.
69. Luberg K, Wong J, Weickert CS, Timmusk T. Human TrkB gene: novel alternative transcripts, protein isoforms and expression pattern in the prefrontal cerebral cortex during postnatal development. *J Neurochem*. 2010;113:952–64.
70. Sepp M, Kannike K, Eesmaa A, Urb M, Timmusk T. Functional diversity of human basic helix-loop-helix transcription factor TCF4 isoforms generated by alternative 5' exon usage and splicing. *PLoS One*. 2011;6:e22138.

**Submit your next manuscript to BioMed Central
and take full advantage of:**

- Convenient online submission
- Thorough peer review
- No space constraints or color figure charges
- Immediate publication on acceptance
- Inclusion in PubMed, CAS, Scopus and Google Scholar
- Research which is freely available for redistribution

Submit your manuscript at
www.biomedcentral.com/submit



Additional file 1

A

TrkAII	1	-----MLRGGRRGQLGWHWSWAAGPGSLLAWLILASAGAAPCPDACCPHGSSGLRCTR	54
TrkAαII	1	M SGEAWQLQLGAHRRLLPRLSEAGAAAMLRGGRRGQLGWHWSWAAGPGSLLAWLILASAGAAPCPDACCPHGSSGLRCTR	80
TrkAβ		-----	
TrkAγII	1	-----MKEAALICLAPSVPPILTVKSWDT	24
TrkAδII		-----	
TrkAεII		-----	
TrkAζII		-----	
TrkAηII		-----	
TrkAθ		-----	
TrkAκ		-----	
TrkAII	55	ALDSLHLHPGAENLTLEYIENQQHLQHLELRDLRGLGELRNLTIVKSGLRFVADPAFHFTPRLSRLNLSFNALESLSWKT	134
TrkAαII	81	ALDSLHLHPGAENLTLEYIENQQHLQHLELRDLRGLGELRNLTIVKSGLRFVADPAFHFTPRLSRLNLSFNALESLSWKT	160
TrkAβ		-----	
TrkAγII	25	MQLRAARSRCTNLLAAS YIENQQHLQHLELRDLRGLGELRNLTIVKSGLRFVADPAFHFTPRLSRLNLSFNALESLSWKT	104
TrkAδII	1	MQLRAARSRCTNLLAAS YIENQQHLQHLELRDLRGLGELRNLTIVKSGLRFVADPAFHFTPRLSRLNLSFNALESLSWKT	80
TrkAεII		-----	
TrkAζII		-----	
TrkAηII		-----	
TrkAθ		-----	
TrkAκ		-----	
TrkAII	135	VQGLSLQELVLSGNPLHCSALRWLQRWEEELGGVPEQKLQCHGQGPLAHMPNASC	214
TrkAαII	161	VQGLSLQELVLSGNPLHCSALRWLQRWEEELGGVPEQKLQCHGQGPLAHMPNASC	240
TrkAβ		-----	
TrkAγII	105	VQGLSLQELVLSGNPLHCSALRWLQRWEEELGGVPEQKLQCHGQGPLAHMPNASC	184
TrkAδII	81	VQGLSLQELVLSGNPLHCSALRWLQRWEEELGGVPEQKLQCHGQGPLAHMPNASC	160
TrkAεII	1	-----MPNASC	29
TrkAζII		-----	
TrkAηII		-----	
TrkAθ		-----	
TrkAκ		-----	
TrkAII	215	CQVEGRGLEQAGWILTELEQSATVMKSGGLPSLGLTLANVTSDLNRKNVTCWAENDVGRAEVSQVNVSPFASVQLHTAV	294
TrkAαII	241	CQVEGRGLEQAGWILTELEQSATVMKSGGLPSLGLTLANVTSDLNRKNVTCWAENDVGRAEVSQVNVSPFASVQLHTAV	320
TrkAβ		-----	
TrkAγII	185	CQVEGRGLEQAGWILTELEQSATVMKSGGLPSLGLTLANVTSDLNRKNVTCWAENDVGRAEVSQVNVSPFASVQLHTAV	264
TrkAδII	161	CQVEGRGLEQAGWILTELEQSATVMKSGGLPSLGLTLANVTSDLNRKNVTCWAENDVGRAEVSQVNVSPFASVQLHTAV	240
TrkAεII	30	CQVEGRGLEQAGWILTELEQSATVMKSGGLPSLGLTLANVTSDLNRKNVTCWAENDVGRAEVSQVNVSPFASVQLHTAV	109
TrkAζII		-----	
TrkAηII		-----	
TrkAθ		-----	
TrkAκ		-----	
TrkAII	295	EMHHWCIPFSDVGGPAPSLRWLFNGSVLNETSFIIFTEFLEPAANETVRHGCLRLNQPTHVNNNGNYTLAANPFQASASI	374
TrkAαII	321	EMHHWCIPFSDVGGPAPSLRWLFNGSVLNETSFIIFTEFLEPAANETVRHGCLRLNQPTHVNNNGNYTLAANPFQASASI	400
TrkAβ		-----MPAAPAPR	1
TrkAγII	265	EMHHWCIPFSDVGGPAPSLRWLFNGSVLNETSFIIFTEFLEPAANETVRHGCLRLNQPTHVNNNGNYTLAANPFQASASI	344
TrkAδII	241	EMHHWCIPFSDVGGPAPSLRWLFNGSVLNETSFIIFTEFLEPAANETVRHGCLRLNQPTHVNNNGNYTLAANPFQASASI	320
TrkAεII	110	EMHHWCIPFSDVGGPAPSLRWLFNGSVLNETSFIIFTEFLEPAANETVRHGCLRLNQPTHVNNNGNYTLAANPFQASASI	189
TrkAζII	1	-MHHWCIPFSDVGGPAPSLRWLFNGSVLNETSFIIFTEFLEPAANETVRHGCLRLNQPTHVNNNGNYTLAANPFQASASI	79
TrkAηII		-----	
TrkAθ		-----	
TrkAκ		-----	
TrkAII	375	MAAFMDNPFEPNEDPIPVSFSPVDTNSTSGDPVEKKDETFFGVSVAVGLAVFACFLFSTLLLVLNKCGRRNKFGINRPA	454
TrkAαII	401	MAAFMDNPFEPNEDPIPVSFSPVDTNSTSGDPVEKKDETFFGVSVAVGLAVFACFLFSTLLLVLNKCGRRNKFGINRPA	480
TrkAβ	10	DCDAPGMGPWIASTTCPAQRTRLSY TNSTSGDPVEKKDETFFGVSVAVGLAVFACFLFSTLLLVLNKCGRRNKFGINRPA	89
TrkAγII	345	MAAFMDNPFEPNEDPIPVSFSPVDTNSTSGDPVEKKDETFFGVSVAVGLAVFACFLFSTLLLVLNKCGRRNKFGINRPA	424
TrkAδII	321	MAAFMDNPFEPNEDPIPVSFSPVDTNSTSGDPVEKKDETFFGVSVAVGLAVFACFLFSTLLLVLNKCGRRNKFGINRPA	400
TrkAεII	190	MAAFMDNPFEPNEDPIPVSFSPVDTNSTSGDPVEKKDETFFGVSVAVGLAVFACFLFSTLLLVLNKCGRRNKFGINRPA	269
TrkAζII	80	MAAFMDNPFEPNEDPIPVSFSPVDTNSTSGDPVEKKDETFFGVSVAVGLAVFACFLFSTLLLVLNKCGRRNKFGINRPA	159
TrkAηII	1	MAAFMDNPFEPNEDPIPVSFSPVDTNSTSGDPVEKKDETFFGVSVAVGLAVFACFLFSTLLLVLNKCGRRNKFGINRPA	74
TrkAθ	1	-----MRQVSVAVGLAVFACFLFSTLLLVLNKCGRRNKFGINRPA	40
TrkAκ		-----	
TrkAII	455	VLAPEDGLAMSLHFMTLGGSSLSPTTEGKSGLQGHIIENPQYFSDACVHHIKRRDIVLKWELGEGAFGKVF	534
TrkAαII	481	VLAPEDGLAMSLHFMTLGGSSLSPTTEGKSGLQGHIIENPQYFSDACVHHIKRRDIVLKWELGEGAFGKVF	560
TrkAβ	90	VLAPEDGLAMSLHFMTLGGSSLSPTTEGKSGLQGHIIENPQYFSDACVHHIKRRDIVLKWELGEGAFGKVF	169
TrkAγII	425	VLAPEDGLAMSLHFMTLGGSSLSPTTEGKSGLQGHIIENPQYFSDACVHHIKRRDIVLKWELGEGAFGKVF	504
TrkAδII	401	VLAPEDGLAMSLHFMTLGGSSLSPTTEGKSGLQGHIIENPQYFSDACVHHIKRRDIVLKWELGEGAFGKVF	480
TrkAεII	270	VLAPEDGLAMSLHFMTLGGSSLSPTTEGKSGLQGHIIENPQYFSDACVHHIKRRDIVLKWELGEGAFGKVF	349
TrkAζII	160	VLAPEDGLAMSLHFMTLGGSSLSPTTEGKSGLQGHIIENPQYFSDACVHHIKRRDIVLKWELGEGAFGKVF	239
TrkAηII	75	VLAPEDGLAMSLHFMTLGGSSLSPTTEGKSGLQGHIIENPQYFSDACVHHIKRRDIVLKWELGEGAFGKVF	154
TrkAθ	41	VLAPEDGLAMSLHFMTLGGSSLSPTTEGKSGLQGHIIENPQYFSDACVHHIKRRDIVLKWELGEGAFGKVF	120
TrkAκ	1	-----MSLHFMTLGGSSLSPTTEGKSGLQGHIIENPQYFSDACVHHIKRRDIVLKWELGEGAFGKVF	71

TrkAII 535 EQDKMLVAVKALKEASESARQDFQREAEALLTMLQHQHIVRFFGVCTEGRPLLMVFEYMRHGDLNRFRLRSHGPDAKLLAGG 614
 TrkAαII 561 EQDKMLVAVKALKEASESARQDFQREAEALLTMLQHQHIVRFFGVCTEGRPLLMVFEYMRHGDLNRFRLRSHGPDAKLLAGG 640
 TrkAβ 170 EQDKMLVAVKALKEASESARQDFQREAEALLTMLQHQHIVRFFGVCTEGRPLLMVFEYMRHGDLNRFRLRSHGPDAKLLAGG 249
 TrkAγII 505 EQDKMLVAVKALKEASESARQDFQREAEALLTMLQHQHIVRFFGVCTEGRPLLMVFEYMRHGDLNRFRLRSHGPDAKLLAGG 584
 TrkAδII 481 EQDKMLVAVKALKEASESARQDFQREAEALLTMLQHQHIVRFFGVCTEGRPLLMVFEYMRHGDLNRFRLRSHGPDAKLLAGG 560
 TrkAεII 350 EQDKMLVAVKALKEASESARQDFQREAEALLTMLQHQHIVRFFGVCTEGRPLLMVFEYMRHGDLNRFRLRSHGPDAKLLAGG 429
 TrkAζII 240 EQDKMLVAVKALKEASESARQDFQREAEALLTMLQHQHIVRFFGVCTEGRPLLMVFEYMRHGDLNRFRLRSHGPDAKLLAGG 319
 TrkAηII 155 EQDKMLVAVKALKEASESARQDFQREAEALLTMLQHQHIVRFFGVCTEGRPLLMVFEYMRHGDLNRFRLRSHGPDAKLLAGG 234
 TrkAθ 121 EQDKMLVAVKALKEASESARQDFQREAEALLTMLQHQHIVRFFGVCTEGRPLLMVFEYMRHGDLNRFRLRSHGPDAKLLAGG 200
 TrkAκ 72 EQDKMLVAVKALKEASESARQDFQREAEALLTMLQHQHIVRFFGVCTEGRPLLMVFEYMRHGDLNRFRLRSHGPDAKLLAGG 151

TrkAII 615 EDVAPGPLGLGQLLAVASQVAAGMVYLAGLHFVHRDLATRNCVLVGGQLVVKIGDFGMSRDIYSTDYRVGGRTMLPIRWM 694
 TrkAαII 641 EDVAPGPLGLGQLLAVASQVAAGMVYLAGLHFVHRDLATRNCVLVGGQLVVKIGDFGMSRDIYSTDYRVGGRTMLPIRWM 720
 TrkAβ 250 EDVAPGPLGLGQLLAVASQVAAGMVYLAGLHFVHRDLATRNCVLVGGQLVVKIGDFGMSRDIYSTDYRVGGRTMLPIRWM 329
 TrkAγII 585 EDVAPGPLGLGQLLAVASQVAAGMVYLAGLHFVHRDLATRNCVLVGGQLVVKIGDFGMSRDIYSTDYRVGGRTMLPIRWM 664
 TrkAδII 561 EDVAPGPLGLGQLLAVASQVAAGMVYLAGLHFVHRDLATRNCVLVGGQLVVKIGDFGMSRDIYSTDYRVGGRTMLPIRWM 640
 TrkAεII 430 EDVAPGPLGLGQLLAVASQVAAGMVYLAGLHFVHRDLATRNCVLVGGQLVVKIGDFGMSRDIYSTDYRVGGRTMLPIRWM 509
 TrkAζII 420 EDVAPGPLGLGQLLAVASQVAAGMVYLAGLHFVHRDLATRNCVLVGGQLVVKIGDFGMSRDIYSTDYRVGGRTMLPIRWM 399
 TrkAηII 235 EDVAPGPLGLGQLLAVASQVAAGMVYLAGLHFVHRDLATRNCVLVGGQLVVKIGDFGMSRDIYSTDYRVGGRTMLPIRWM 314
 TrkAθ 201 EDVAPGPLGLGQLLAVASQVAAGMVYLAGLHFVHRDLATRNCVLVGGQLVVKIGDFGMSRDIYSTDYRVGGRTMLPIRWM 280
 TrkAκ 152 EDVAPGPLGLGQLLAVASQVAAGMVYLAGLHFVHRDLATRNCVLVGGQLVVKIGDFGMSRDIYSTDYRVGGRTMLPIRWM 231

TrkAII 695 PPESILYRKFTTESDVSFVGVVWEIFTYGGKQPWYQLSNTAIDCITQGRELERPRACPPPEVYAIMRGCWQREPQQRHSI 774
 TrkAαII 721 PPESILYRKFTTESDVSFVGVVWEIFTYGGKQPWYQLSNTAIDCITQGRELERPRACPPPEVYAIMRGCWQREPQQRHSI 800
 TrkAβ 330 PPESILYRKFTTESDVSFVGVVWEIFTYGGKQPWYQLSNTAIDCITQGRELERPRACPPPEVYAIMRGCWQREPQQRHSI 409
 TrkAγII 665 PPESILYRKFTTESDVSFVGVVWEIFTYGGKQPWYQLSNTAIDCITQGRELERPRACPPPEVYAIMRGCWQREPQQRHSI 744
 TrkAδII 641 PPESILYRKFTTESDVSFVGVVWEIFTYGGKQPWYQLSNTAIDCITQGRELERPRACPPPEVYAIMRGCWQREPQQRHSI 720
 TrkAεII 510 PPESILYRKFTTESDVSFVGVVWEIFTYGGKQPWYQLSNTAIDCITQGRELERPRACPPPEVYAIMRGCWQREPQQRHSI 589
 TrkAζII 400 PPESILYRKFTTESDVSFVGVVWEIFTYGGKQPWYQLSNTAIDCITQGRELERPRACPPPEVYAIMRGCWQREPQQRHSI 479
 TrkAηII 315 PPESILYRKFTTESDVSFVGVVWEIFTYGGKQPWYQLSNTAIDCITQGRELERPRACPPPEVYAIMRGCWQREPQQRHSI 394
 TrkAθ 281 PPESILYRKFTTESDVSFVGVVWEIFTYGGKQPWYQLSNTAIDCITQGRELERPRACPPPEVYAIMRGCWQREPQQRHSI 360
 TrkAκ 232 PPESILYRKFTTESDVSFVGVVWEIFTYGGKQPWYQLSNTAIDCITQGRELERPRACPPPEVYAIMRGCWQREPQQRHSI 311

TrkAII 775 KDVHARLQALQAAPPVYLDVLG 796
 TrkAαII 801 KDVHARLQALQAAPPVYLDVLG 822
 TrkAβ 410 KDVHARLQALQAAPPVYLDVLG 431
 TrkAγII 745 KDVHARLQALQAAPPVYLDVLG 766
 TrkAδII 721 KDVHARLQALQAAPPVYLDVLG 742
 TrkAεII 590 KDVHARLQALQAAPPVYLDVLG 611
 TrkAζII 480 KDVHARLQALQAAPPVYLDVLG 501
 TrkAηII 395 KDVHARLQALQAAPPVYLDVLG 416
 TrkAθ 361 KDVHARLQALQAAPPVYLDVLG 382
 TrkAκ 312 KDVHARLQALQAAPPVYLDVLG 333

B

TrkAI 1 MLRGGRRGQLGWHSWAAGPGSLAWLILASAGAAPCPDACCPHGSSGLRCTR DGALDSLHLLPGAENLTELYIENQQHLQ 80
 TrkAII 1 MLRGGRRGQLGWHSWAAGPGSLAWLILASAGAAPCPDACCPHGSSGLRCTR DGALDSLHLLPGAENLTELYIENQQHLQ 80
 TrkAIII 1 MLRGGRRGQLGWHSWAAGPGSLAWLILASAGAAPCPDACCPHGSSGLRCTR DGALDSLHLLPGAENLTELYIENQQHLQ 80
 TrkAIV 1 MLRGGRRGQLGWHSWAAGPGSLAWLILASAGAAPCPDACCPHGSSGLRCTR DGALDSLHLLPGAENLTELYIENQQHLQ 80
 TrkAV 1 MLRGGRRGQLGWHSWAAGPGSLAWLILASAGAAPCPDACCPHGSSGLRCTR DGALDSLHLLPGAENLTELYIENQQHLQ 80
 TrkAVI 1 MLRGGRRGQLGWHSWAAGPGSLAWLILASAGAAPCPDACCPHGSSGLRCTR DGALDSLHLLPGAENLTELYIENQQHLQ 80
 TrkAVII 1 MLRGGRRGQLGWHSWAAGPGSLAWLILASAGAAPCPDACCPHGSSGLRCTR DGALDSLHLLPGAENLTELYIENQQHLQ 80
 TrkAVIII 1 MLRGGRRGQLGWHSWAAGPGSLAWLILASAGAAPCPDACCPHGSSGLRCTR DGALDSLHLLPGAENLTELYIENQQHLQ 80
 TrkAIX 1 MLRGGRRGQLGWHSWAAGPGSLAWLILASAGAAPCPDACCPHGSSGLRCTR DGALDSLHLLPGAENLTELYIENQQHLQ 80

TrkAI 81 HLELRDLRGLGELRNLTIVKSLGRFVADAFHFTPRLSRLNLSFNALESLSWKT VQGLSLQELVLSGNPLHCSCALRWLQ 160
 TrkAII 81 HLELRDLRGLGELRNLTIVKSLGRFVADAFHFTPRLSRLNLSFNALESLSWKT VQGLSLQELVLSGNPLHCSCALRWLQ 160
 TrkAIII 81 HLELRDLRGLGELRNLTIVKSLGRFVADAFHFTPRLSRLNLSFNALESLSWKT VQGLSLQELVLSGNPLHCSCALRWLQ 160
 TrkAIV 81 HLELRDLRGLGELRNLTIVKSLGRFVADAFHFTPRLSRLNLSFNALESLSWKT VQGLSLQELVLSGNPLHCSCALRWLQ 160
 TrkAV 81 HLELRDLRGLGELRNLTIVKSLGRFVADAFHFTPRLSRLNLSFNALESLSWKT VQGLSLQELVLSGNPLHCSCALRWLQ 160
 TrkAVI 81 HLELRDLRGLGELRNLTIVKSLGRFVADAFHFTPRLSRLNLSFNALESLSWKT VQGLSLQELVLSGNPLHCSCALRWLQ 160
 TrkAVII 81 -----
 TrkAVIII 81 HLELRDLRGLGELRNLTIVKSLGRFVADAFHFTPRLSRLNLSFNALESLSWKT VQGLSLQELVLSGNPLHCSCALRWLQ 160
 TrkAIX 81 HLELRDLRGLGELRNLTIVKSLGRFVADAFHFTPRLSRLNLSFNALESLSWKT VQGLSLQELVLSGNPLHCSCALRWLQ 160

TrkAI 161 RWEEEGGGVPEQKQLQCHGQGLAHMPNASC GVPPTLKVQVPNASVDVGDVLLRCQVEGRGLEQAGWILTELEQSATVMK 240
 TrkAII 161 RWEEEGGGVPEQKQLQCHGQGLAHMPNASC GVPPTLKVQVPNASVDVGDVLLRCQVEGRGLEQAGWILTELEQSATVMK 240
 TrkAIII 161 RWEEEGGGVPEQKQLQCHGQGLAHMPNASC ----- 191
 TrkAIV 161 RWEEEGGGVPEQKQLQCHGQGLAHMPNASC ----- 191
 TrkAV 161 RWEEEGGGVPEQKQLQCHGQGLAHMPNASC ----- 191
 TrkAVI 161 RWEEEGGGVPEQKQLQCHGQGLAHMPNASC GVPPTLKVQVPNASVDVGDVLLRCQVEGRGLEQAGWILTELEQSATVMK 240
 TrkAVII 65 -----TELEQSATVMK 76
 TrkAVIII 161 RWEEEGGGVPEQKQLQCHGQGLAHMPNASC **PGAQCLGGCGRRAAAVPGGGAGPGAGRLDPRHRAVSHGD**----- 233
 TrkAIX 161 RWEEEGGGVPEQKQLQCHGQGLAHMPNASC **PGAQCLGGCGRRAAAVPGGGAGPGAGRLDPRHRAVSHGD**----- 233

TrkAI	241	SGGLPSLGLTLANVTSDLNRKNVTCWAENDVGRAEVSQVNVVSPASVQLHTAVEMHHWCIPFSVDGQPAPSLRWLFNGS	320
TrkAII	241	SGGLPSLGLTLANVTSDLNRKNVTCWAENDVGRAEVSQVNVVSPASVQLHTAVEMHHWCIPFSVDGQPAPSLRWLFNGS	320
TrkAIII	192	-----VPASVQLHTAVEMHHWCIPFSVDGQPAPSLRWLFNGS	228
TrkAIV	192	-----VPASVQLHTAVEMHHWCIPFSVDGQPAPSLRWLFNGS	228
TrkAV		-----	
TrkAVI	241	SGGLPSLGLTLANVTSDLNRKNVTCWAENDVGRAEVSQVNVVSY-----	284
TrkAVII	77	SGGLPSLGLTLANVTSDLNRKNVTCWAENDVGRAEVSQVNVVSPASVQLHTAVEMHHWCIPFSVDGQPAPSLRWLFNGS	155
TrkAVIII		-----	
TrkAIX		-----	
TrkAI	321	VLNETSFI FTEFLEPAANETVRHGCLRLNQPTHVNNNGNYTLAANFFGQASASIMAAAFMDNPFEPNPEDEPI-----DT	394
TrkAII	321	VLNETSFI FTEFLEPAANETVRHGCLRLNQPTHVNNNGNYTLAANFFGQASASIMAAAFMDNPFEPNPEDEPIVVSFSPVDT	400
TrkAIII	229	VLNETSFI FTEFLEPAANETVRHGCLRLNQPTHVNNNGNYTLAANFFGQASASIMAAAFMDNPFEPNPEDEPI-----DT	302
TrkAIV	229	VLNETSFI FTEFLEPAANETVRHGCLRLNQPTHVNNNGNYTLAANFFGQASASIMAAAFMDNPFEPNPEDEPIVVSFSPVDT	308
TrkAV	192	-----DT	193
TrkAVI		-----T	285
TrkAVII	156	VLNETSFI FTEFLEPAANETVRHGCLRLNQPTHVNNNGNYTLAANFFGQASASIMAAAFMDNPFEPNPEDEPIVVSFSPVDT	235
TrkAVIII	234	-----DT	235
TrkAIX	234	-----VSFSPVDT	241
TrkAI	395	NSTSGDPEVKKDETPFGVSVAVGLAVFACFLSTLLLVLNKCGRNFKGINRPAVLAPEDGLAMSLHFMTLGGSSLSPT	474
TrkAII	401	NSTSGDPEVKKDETPFGVSVAVGLAVFACFLSTLLLVLNKCGRNFKGINRPAVLAPEDGLAMSLHFMTLGGSSLSPT	480
TrkAIII	303	NSTSGDPEVKKDETPFGVSVAVGLAVFACFLSTLLLVLNKCGRNFKGINRPAVLAPEDGLAMSLHFMTLGGSSLSPT	382
TrkAIV	309	NSTSGDPEVKKDETPFGVSVAVGLAVFACFLSTLLLVLNKCGRNFKGINRPAVLAPEDGLAMSLHFMTLGGSSLSPT	388
TrkAV	194	NSTSGDPEVKKDETPFGVSVAVGLAVFACFLSTLLLVLNKCGRNFKGINRPAVLAPEDGLAMSLHFMTLGGSSLSPT	273
TrkAVI	286	NSTSGDPEVKKDETPFGVSVAVGLAVFACFLSTLLLVLNKCGRNFKGINRPAVLAPEDGLAMSLHFMTLGGSSLSPT	365
TrkAVII	236	NSTSGDPEVKKDETPFGVSVAVGLAVFACFLSTLLLVLNKCGRNFKGINRPAVLAPEDGLAMSLHFMTLGGSSLSPT	315
TrkAVIII	236	NSTSGDPEVKKDETPFGVSVAVGLAVFACFLSTLLLVLNKCGRNFKGINRPAVLAPEDGLAMSLHFMTLGGSSLSPT	315
TrkAIX	242	NSTSGDPEVKKDETPFGVSVAVGLAVFACFLSTLLLVLNKCGRNFKGINRPAVLAPEDGLAMSLHFMTLGGSSLSPT	321
TrkAI	475	GKSGLQGHI IENPQYFSDACVHHIKRRDIVLKWELGEGAFGKVF LAECHNLLPEQDKMLVAVKALKEASESARQDFQRE	554
TrkAII	481	GKSGLQGHI IENPQYFSDACVHHIKRRDIVLKWELGEGAFGKVF LAECHNLLPEQDKMLVAVKALKEASESARQDFQRE	560
TrkAIII	383	GKSGLQGHI IENPQYFSDACVHHIKRRDIVLKWELGEGAFGKVF LAECHNLLPEQDKMLVAVKALKEASESARQDFQRE	462
TrkAIV	389	GKSGLQGHI IENPQYFSDACVHHIKRRDIVLKWELGEGAFGKVF LAECHNLLPEQDKMLVAVKALKEASESARQDFQRE	468
TrkAV	274	GKSGLQGHI IENPQYFSDACVHHIKRRDIVLKWELGEGAFGKVF LAECHNLLPEQDKMLVAVKALKEASESARQDFQRE	353
TrkAVI	366	GKSGLQGHI IENPQYFSDACVHHIKRRDIVLKWELGEGAFGKVF LAECHNLLPEQDKMLVAVKALKEASESARQDFQRE	445
TrkAVII	316	GKSGLQGHI IENPQYFSDACVHHIKRRDIVLKWELGEGAFGKVF LAECHNLLPEQDKMLVAVKALKEASESARQDFQRE	395
TrkAVIII	316	GKSGLQGHI IENPQYFSDACVHHIKRRDIVLKWELGEGAFGKVF LAECHNLLPEQDKMLVAVKALKEASESARQDFQRE	395
TrkAIX	322	GKSGLQGHI IENPQYFSDACVHHIKRRDIVLKWELGEGAFGKVF LAECHNLLPEQDKMLVAVKALKEASESARQDFQRE	401
TrkAI	555	AELLTMLQHQHIVRFFGVCTEGRPLLMVFEYMRHGDLLNRFLRSHGPDAKLLAGGEDVAPGFLGLGQLLAVASQVAAGMVY	634
TrkAII	561	AELLTMLQHQHIVRFFGVCTEGRPLLMVFEYMRHGDLLNRFLRSHGPDAKLLAGGEDVAPGFLGLGQLLAVASQVAAGMVY	640
TrkAIII	463	AELLTMLQHQHIVRFFGVCTEGRPLLMVFEYMRHGDLLNRFLRSHGPDAKLLAGGEDVAPGFLGLGQLLAVASQVAAGMVY	542
TrkAIV	469	AELLTMLQHQHIVRFFGVCTEGRPLLMVFEYMRHGDLLNRFLRSHGPDAKLLAGGEDVAPGFLGLGQLLAVASQVAAGMVY	548
TrkAV	354	AELLTMLQHQHIVRFFGVCTEGRPLLMVFEYMRHGDLLNRFLRSHGPDAKLLAGGEDVAPGFLGLGQLLAVASQVAAGMVY	433
TrkAVI	446	AELLTMLQHQHIVRFFGVCTEGRPLLMVFEYMRHGDLLNRFLRSHGPDAKLLAGGEDVAPGFLGLGQLLAVASQVAAGMVY	525
TrkAVII	396	AELLTMLQHQHIVRFFGVCTEGRPLLMVFEYMRHGDLLNRFLRSHGPDAKLLAGGEDVAPGFLGLGQLLAVASQVAAGMVY	475
TrkAVIII	396	AELLTMLQHQHIVRFFGVCTEGRPLLMVFEYMRHGDLLNRFLRSHGPDAKLLAGGEDVAPGFLGLGQLLAVASQVAAGMVY	475
TrkAIX	402	AELLTMLQHQHIVRFFGVCTEGRPLLMVFEYMRHGDLLNRFLRSHGPDAKLLAGGEDVAPGFLGLGQLLAVASQVAAGMVY	481
TrkAI	635	LAGLHFVHRDLATRNLVGGQLVVKIGDFGMSRDIYSTDYRVGGRTMLPIRWMPPEIILYRKFTTESDVWSFGVVLWEI	714
TrkAII	641	LAGLHFVHRDLATRNLVGGQLVVKIGDFGMSRDIYSTDYRVGGRTMLPIRWMPPEIILYRKFTTESDVWSFGVVLWEI	720
TrkAIII	543	LAGLHFVHRDLATRNLVGGQLVVKIGDFGMSRDIYSTDYRVGGRTMLPIRWMPPEIILYRKFTTESDVWSFGVVLWEI	622
TrkAIV	549	LAGLHFVHRDLATRNLVGGQLVVKIGDFGMSRDIYSTDYRVGGRTMLPIRWMPPEIILYRKFTTESDVWSFGVVLWEI	628
TrkAV	434	LAGLHFVHRDLATRNLVGGQLVVKIGDFGMSRDIYSTDYRVGGRTMLPIRWMPPEIILYRKFTTESDVWSFGVVLWEI	513
TrkAVI	526	LAGLHFVHRDLATRNLVGGQLVVKIGDFGMSRDIYSTDYRVGGRTMLPIRWMPPEIILYRKFTTESDVWSFGVVLWEI	605
TrkAVII	476	LAGLHFVHRDLATRNLVGGQLVVKIGDFGMSRDIYSTDYRVGGRTMLPIRWMPPEIILYRKFTTESDVWSFGVVLWEI	555
TrkAVIII	476	LAGLHFVHRDLATRNLVGGQLVVKIGDFGMSRDIYSTDYRVGGRTMLPIRWMPPEIILYRKFTTESDVWSFGVVLWEI	555
TrkAIX	482	LAGLHFVHRDLATRNLVGGQLVVKIGDFGMSRDIYSTDYRVGGRTMLPIRWMPPEIILYRKFTTESDVWSFGVVLWEI	561
TrkAI	715	FTYGKQPWYQLSNTAIDCITQGRELERPRACPEVYAIMRGCWQREPQQRHSIKDVHARLQALAQAPPVYLDVLG	790
TrkAII	721	FTYGKQPWYQLSNTAIDCITQGRELERPRACPEVYAIMRGCWQREPQQRHSIKDVHARLQALAQAPPVYLDVLG	796
TrkAIII	623	FTYGKQPWYQLSNTAIDCITQGRELERPRACPEVYAIMRGCWQREPQQRHSIKDVHARLQALAQAPPVYLDVLG	698
TrkAIV	629	FTYGKQPWYQLSNTAIDCITQGRELERPRACPEVYAIMRGCWQREPQQRHSIKDVHARLQALAQAPPVYLDVLG	704
TrkAV	514	FTYGKQPWYQLSNTAIDCITQGRELERPRACPEVYAIMRGCWQREPQQRHSIKDVHARLQALAQAPPVYLDVLG	589
TrkAVI	606	FTYGKQPWYQLSNTAIDCITQGRELERPRACPEVYAIMRGCWQREPQQRHSIKDVHARLQALAQAPPVYLDVLG	681
TrkAVII	556	FTYGKQPWYQLSNTAIDCITQGRELERPRACPEVYAIMRGCWQREPQQRHSIKDVHARLQALAQAPPVYLDVLG	631
TrkAVIII	556	FTYGKQPWYQLSNTAIDCITQGRELERPRACPEVYAIMRGCWQREPQQRHSIKDVHARLQALAQAPPVYLDVLG	631
TrkAIX	562	FTYGKQPWYQLSNTAIDCITQGRELERPRACPEVYAIMRGCWQREPQQRHSIKDVHARLQALAQAPPVYLDVLG	637

Additional file 2

Primers and cycling conditions

RT-PCR analysis

Human tissues

Primer	Primer sequence (5'→3')	Location (exon)	Annealing temperature (°C)	Synthesis time (s)	Nr of cycles	Amplicon size
Forward	CAACTCGGCGCATGAAGGAG	A	59	35	42	727 (A-B-C-D-2-3-4-5); 531 (A-C-D-2-3-4-5); 391 (A-D-2-3-4-5)
Reverse	CGCAGGGCACAAGAACAGTG	5				
Forward	CTTGGTTGGACATCTAAGACCTG	C	61	30	46	416 (C-D-2b-3-4-5); 394 (C-D-2-3-4-5)
Reverse	CGCAGGGCACAAGAACAGTG	5				
Forward	CTAGATCTCGGTGCACAAACTTG	D	62	20	46	896 (D-2-3-4-5-6-7-8); 763 (D-2-3-4-5-6-8); 474 (D-2-3-4-8); 391 (D-7-8); 258 (D-8)
Reverse	GTTGCCGTTGTTGACGTGGGTG	8				
Forward	CTGACAACTGAGGGGAGGAC	E	61	30	40	610 (E-Fc-2-3-4-5); 562 (E-Fb-2-3-4-5); 515 (E-Fa-2-3-3b-4-5); 473 (E-Fa-2-3-3a-4-5); 408 (E-2-3-3b-4-5); 387 (E-Fa-2-3-4-5); 280 (E-2-3-4-5)
Reverse	CGCAGGGCACAAGAACAGTG	5				
Forward	GCTTGGCTGATACTGGCATCTG	1	62	60	42	1005 (1-2-3-4-5-6-7-8); 872 (1-2-3-4-5-6-8); 716 (1-2-3-4-7-8); 583 (1-2-3-4-8); 575 (1d-6b-7-8a); 510 (1c-6c-7-8); 367 (1-8)
Reverse	GTTGCCGTTGTTGACGTGGGTG	8				
Forward	CTCTCTCTCTCTCTTGGCTG	G	61	30	40	424 (Ga-2-3-4-5); 392 (Gc-2-3-4-5); 274 (Gb-2-3-4-5)
Reverse	GTTCAGGCACTCCGCCAGTC	5				
Forward	CTCATTGCTCTCTCTCTTTC	2a	61	30	39	1119 (2a-3-4-5)
Reverse	GTTCAGGCACTCCGCCAGTC	5				
Forward	GGCGGAGTGCCTGAACAGAAG	5	60	70	35	924 (5-6-7-8-9-10-11-12); 791 (5-6-8-9-10-11-12); 648 (5-8-9-10-11-12); 579 (5-6-7-10-11-12); 446 (5-6-10-11-12); 303 (5-10-11-12)
Reverse	GGAGCTGCCACCCAATGTCATG	12				
Forward	AGTTCACCCCGAGGACCCCATC	8	59	30	33	275 (8-9-10-11-12); 257 (8-10-11-12)
Reverse	GGAGCTGCCACCCAATGTCATG	12				
Forward	GCTTCTCTCTCCCTCTGCTG	10a	61	30	35	444 (10a-11-12); 274 (9a-10-11-12)
Reverse	GGAGCTGCCACCCAATGTCATG	12				
Forward	GCAAAGGCTCTGGGCTCCAAG	12	61	80	34	884 (12-13-14-15-16-17)
Reverse	CTTGATGCTGTGGCGTTGCTG	17				

Mouse tissues

Primer	Primer sequence (5'→3')	Location (exon)	Annealing temperature (°C)	Synthesis time (s)	Nr of cycles	Amplicon size
Forward	ACTTCGTTGATGCTGGCCTGTG	1	61	65	36	1015 (1-2-3-4-5-6-7-8)
Reverse	AGTCCCGTTGTTGACATGCGTG	8				
Forward	GCAATTTCCTGTGCCCTGTC	5	57	65	35	989 (5-6-7-8-9-10-11-12)
Reverse	AAAGAGAACTGCCACCCAGTGTG	12				
Forward	AGTTCGTTGTTGACATGCGTG	8	55	45	33	279 (8-9-10-11-12); 261 (8-10-11-12)
Reverse	AAAGAGAACTGCCACCCAGTGTG	12				
Forward	CTATCCCATAAAGGATCATCTG	10a	57	35	38	496 (10a-11-12); 339 (9a-10-11-12); 236 (9a-10-12)
Reverse	AAAGAGAACTGCCACCCAGTGTG	12				
Forward	CTGGGTGGCAGTTCTCTTTC	12	57	65	32	925 (12-13-14-15-16-17)
Reverse	CGTGCACATCCTTCATGCTGAG	17				

Rat tissues

Primer	Primer sequence (5'→3')	Location (exon)	Annealing temperature (°C)	Synthesis time (s)	Nr of cycles	Amplicon size
Forward	GACTTCGTTGATGCTGGCCTGTG	1	57	30	36	405 (1-2-3-4-5); 258 (1-4-5)
Reverse	CACAATAGGGCAGGACAGCAAGTG	5				
Forward	AGCAGGAGGATTTGTGTGGTGTG	5	57	60	33	951 (5-6-7-8-9-10-11-12)
Reverse	AAAGAGAACTGCCACCCAGTGTG	12				
Forward	AGTTCGTTGTTGACATGCGTG	8	55	45	33	279 (8-9-10-11-12); 261 (8-10-11-12)
Reverse	AAAGAGAACTGCCACCCAGTGTG	12				
Forward	GTCTGGCCTCTGCTTGTATGAC	10a	59	45	40	707 (10a-11-12); 550 (9a-10-11-12)
Reverse	AAAGAGAACTGCCACCCAGTGTG	12				
Forward	AGTTCACCCCTGAGGACCCCATC	8	57	70	33	1185 (8-9-10-11-12-13-14-15-16-17)
Reverse	CGTGCACATCCTTCATGCTGAG	17				

HPRT (human, mouse, rat)

Primer	Primer sequence (5'→3')	Location (exon)	Annealing temperature (°C)	Synthesis time (s)	Nr of cycles
Forward	GATGATGAACCAGGTTATGAC		57	30	30
Reverse	GTCCITTTTACCAGCAAGCTTG				

5' RACE analysis

Human tissues

1. round of PCR

Primer	Primer sequence (5'→3')	Location (exon)	Annealing temperature (°C)	Synthesis time (s)	Nr of cycles
Forward	CGACTGGAGCAGGAGGACACTGA		1) 72; 2) 70; 3) 66	30	1) 5; 2) 5; 3) 25
Reverse	CCACGAAACGGAGACCACTCTTC	3			
Forward	CGACTGGAGCAGGAGGACACTGA		1) 72; 2) 70; 3) 64	75	1) 4; 2) 4; 3) 30
Reverse	GGAGCTGCCACCCAATGTCATG	12			

2. round of PCR

Primer	Primer sequence (5'→3')	Location (exon)	Annealing temperature (°C)	Synthesis time (s)	Nr of cycles
Forward	GGACTGACATGGACTGAAGGAGTA		67	30	34
Reverse	CCCCTCAGATCACGGAGCTCCAGA	2			
Forward	GGACTGACATGGACTGAAGGAGTA		67	30	34
Reverse	CGGGTCTCCAGATGTGCTGTAGT	10			
Forward	GGACTGACATGGACTGAAGGAGTA		65	30	45
Reverse	GCACCGAGATCTAGCAGCCGCACG	D			

2. round of PCR (with Phusion polymerase from New England Biolabs)

Primer	Primer sequence (5'→3')	Location (exon)	Annealing temperature (°C)	Synthesis time (s)	Nr of cycles
Forward	GGACTGACATGGACTGAAGGAGTA		72	20	33
Reverse	AGAAAGGAAGAGGACGCAAGAC	11			

Mouse and rat tissues

1. round of PCR

Primer	Primer sequence (5'→3')	Location (exon)	Annealing temperature (°C)	Synthesis time (s)	Nr of cycles
Forward	CGACTGGAGCACGAGGACACTGA		1) 72; 2) 70; 3) 64	60	1) 4; 2) 4; 3) 30
Reverse	GTGACTGAGCCGAGGGGTGA	3			
Forward	CGACTGGAGCACGAGGACACTGA		1) 72; 2) 70; 3) 64	60	1) 4; 2) 4; 3) 30
Reverse	GAAGTGTAGGGACATGCCAGC	12			

2. round of PCR

Primer	Primer sequence (5'→3')	Location (exon)	Annealing temperature (°C)	Synthesis time (s)	Nr of cycles
Forward	GGACACTGACATGGACTGAAGGAGTA		65	60	25
Reverse	CACAAAGCGGAGGCCACTCTTCACG	3			
Forward	GGACACTGACATGGACTGAAGGAGTA		65	60	25
Reverse	CCCAGGCCCTGCAGGTCTCAAAC	2			
Forward	GGACACTGACATGGACTGAAGGAGTA		65	60	25
Reverse	GCAGGGCGGTTGATCCCAAATTG	12			
Forward	GGACACTGACATGGACTGAAGGAGTA		65	60	25
Reverse	CTCCACTGGTCTCTTGATGTGCTG	10			

Cloning of TrkA protein isoform-encoding sequences

Primer	Primer sequence (5'→3')	Location (exon)	Annealing temperature (°C)	Synthesis time (s)	Nr of cycles
Forward	CACCATGCTGCGAGGCGGAC	1	1) 54; 2) 57	150	1) 9; 2) 33
Reverse	CTGCTGGGAGCTATGGGGGATG	17			
Forward	CACCATGAAGGAGGCCGCCCTC	A	1) 56; 2) 59	70	1) 4; 2) 40
Reverse	CGCAGGGCACAAAGAACAGTG	5			
Forward	CACCATGCAGTTGCGGGCTGCTAG	D	1) 56; 2) 59	70	1) 4; 2) 40
Reverse	GTTCAGGCACTCCGCCAGTC	5			
Forward	CACCATGCCAATGCCAGCTGTG	5	1) 56; 2) 59	70	1) 4; 2) 40
Reverse	GTTGCCGTTGTTGACGTGGGTG	8			
Forward	CACCATGCACCACTGGTGCATC	8	1) 56; 2) 59	70	1) 4; 2) 24
Reverse	GCCCAGGACATCCAGGTAGACAG	17			
Forward	CACCATGTCCCTGCATTTTCATGAC	12	1) 56; 2) 59	70	1) 4; 2) 40
Reverse	CAGTCCCTGGCCCACTAGACAG	15			

Additional file 3

ESTs identified with 5' RACE of human samples	
Exons	Accession nr
E-2	JZ719179
1b-2	JZ719180
E-2	JZ719181
Gd-2	JZ719182
E-Fa-2	JZ719183
Gb-2	JZ719184
8b-9-10-11	JZ719185
Ga-2	JZ719186
10b-11	JZ719187
8b-10-11	JZ719188
8b-10-11	JZ719189
8b-9-10-11	JZ719191
8b-10-11	JZ719192
10b-11	JZ719193
8c-10-11	JZ719194
Gb-2-3-4-8-10	JZ719195
1a-2-3-4-5-6a-10	JZ719196
1a-2-3-4-5-6a-9-10	JZ719197
1-2	JZ719198
1-2	JZ719199
1a-2	JZ719200
1a	JZ719201
A-D	JZ719202
11a-11	JZ719203
1-10-11	JZ719204
1-8-10-11	JZ719205

ESTs identified with RT-PCR of human samples	
Exons	Accession nr
A-B-C-D-2-3-4	JZ719206
A-C-D-2-3-4	JZ719207
A-D-2-3-4	JZ719208
C-D-2b-3-4-5	JZ719209
C-D-2-3-4-5	JZ719210
D-2-3-4-5-6-7-8	JZ719211
D-2-3-4-5-6-8	JZ719212
D-2-3-4-8	JZ719213
D-7-8	JZ719214
D-8	JZ719215
E-Fc-2-3-4	JZ719216
E-Fb-2-3-4	JZ719217
E-Fa-2-3-3b-4-5	JZ719218
E-Fa-2-3-3a-4	JZ719219
E-Fa-2-3-4	JZ719220
E-2-3-3b-4-5	JZ719221
E-2-3-4	JZ719222
1-2-3-4-5-6-7-8	JZ719223
1-2-3-4-5-6-8	JZ719224
1-2-3-4-7-8	JZ719225
1-2-3-4-8	JZ719226
1d-6b-7-8a	JZ719227
1c-6c-7-8	JZ719228
1-8	JZ719229
Ga-2-3-4-5	JZ719230
Gc-2-3-4-5	JZ719231
Gb-2-3-4-5	JZ719232
2a-3-4-5	JZ719233
5-6-7-8-9-10-11-12	JZ719234
5-6-7-8-10-11-12	JZ719235
5-6-8-9-10-11-12	JZ719236
5-6-8-10-11-12	JZ719237
5-8-9-10-11-12	JZ719238
5-8-10-11-12	JZ719239
5-6-7-10-11-12	JZ719240
5-6-10-11-12	JZ719241
5-10-11-12	JZ719242
8-9-10-11-12	JZ719243
8-10-11-12	JZ719244
10a-11-12	JZ719245
9a-10-11-12	JZ719246
12-13-14-15-16-17	JZ719247

ESTs identified with 5' RACE of mouse samples	
Exons	Accession nr
1-2	JZ880805
1-2-3	JZ880806
8d-9-10	JZ880807
10b	JZ880808

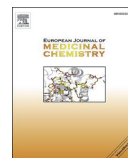
ESTs identified with RT-PCR of mouse samples	
Exons	Accession nr
1-2-3-4-5-6-7-8	JZ719248
5-6-7-8-9-10-11-12	JZ719249
8-9-10-11-12	JZ719250
8-10-11-12	JZ719251
10a-11-12	JZ719252
9a-10-11-12	JZ719253
9a-10-12	JZ719254
12-13-14-15-16-17	JZ719255

ESTs identified with 5' RACE of rat samples	
Exons	Accession nr
1-2	JZ880809
1-2	JZ880810
1-2	JZ880811
1-2	JZ880812
1-2	JZ880813
1b-2	JZ880814
8d-10	JZ880815
8b-9-10	JZ880816
8b-9-10	JZ880817

ESTs identified with RT-PCR of rat samples	
Exons	Accession nr
1-2-3-4-5	JZ719256
1-4-5	JZ719257
5-6-7-8-9-10-11-12	JZ719258
8-9-10-11-12	JZ719259
8-10-11-12	JZ719260
10a-11-12	JZ719261
9a-10-11-12	JZ719262
8-9-10-11-12-13-14-15-16-17	JZ719263

PUBLICATION III

III. Tammiku-Taul, J.*, Park, R.*, Jaanson, K., **Luberg, K.**, Dobchev, D.A., Kananovich, D., Noole, A., Mandel, M., Kaasik, A., Lopp, M., Timmusk, T., and Karelson, M. (2016). Indole-like Trk receptor antagonists. *Eur. J. Med. Chem.* 121, 541–552.



Research paper

Indole-like Trk receptor antagonists



Jaana Tammiku-Taul^{a, b, 1}, Rahel Park^{c, 1, 2}, Kaur Jaanson^c, Kristi Luberg^c,
Dimitar A. Dobchev^b, Dzmitry Kananovich^b, Artur Noole^b, Merle Mandel^d,
Allen Kaasik^d, Margus Lopp^b, Tõnis Timmusk^{c, *}, Mati Karelson^{a, b, **}

^a University of Tartu, Institute of Chemistry, Ravila 14A, Tartu, 50411, Estonia

^b Tallinn University of Technology, Department of Chemistry, Akadeemia 15, Tallinn, 12618, Estonia

^c Tallinn University of Technology, Department of Gene Technology, Akadeemia 15, Tallinn, 12618, Estonia

^d University of Tartu, Institute of Biomedicine and Translational Medicine, Department of Pharmacology, Ravila 19, Tartu, 50411, Estonia

ARTICLE INFO

Article history:

Received 9 November 2015

Received in revised form

1 June 2016

Accepted 2 June 2016

Available online 4 June 2016

Keywords:

TrkA

TrkB

Antagonist

Fragment-based QSAR

2-Oxindole

ABSTRACT

The virtual screening for new scaffolds for TrkA receptor antagonists resulted in potential low molecular weight drug candidates for the treatment of neuropathic pain and cancer. In particular, the compound (Z)-3-((5-methoxy-1H-indol-3-yl)methylene)-2-oxindole and its derivatives were assessed for their inhibitory activity against Trk receptors. The IC₅₀ values were computationally predicted in combination of molecular and fragment-based QSAR. Thereafter, based on the structure-activity relationships (SAR), a series of new compounds were designed and synthesized. Among the final selection of 13 compounds, (Z)-3-((5-methoxy-1-methyl-1H-indol-3-yl)methylene)-N-methyl-2-oxindole-5-sulfonamide showed the best TrkA inhibitory activity using both biochemical and cellular assays and (Z)-3-((5-methoxy-1-methyl-1H-indol-3-yl)methylene)-2-oxindole-5-sulfonamide was the most potent inhibitor of TrkB and TrkC.

© 2016 Published by Elsevier Masson SAS.

1. Introduction

The tropomyosin receptor kinase (Trk) family includes three homologous receptor tyrosine kinases: TrkA, TrkB, and TrkC, that specifically bind the neurotrophins nerve growth factor (NGF), brain-derived neurotrophic factor (BDNF), and neurotrophin 4 (NT4) and neurotrophin 3 (NT3), respectively. Activation of Trk receptors by the neurotrophins plays an important role in diverse biological responses, including differentiation, proliferation, survival, and other functional regulation of cells [1].

Neurotrophins are proteins that modulate the growth, maintenance, and survival of neurons [2]. In addition, NGF and BDNF

function as key contributors in chronic neuropathic pain as well as hyperalgesia related to diverse pain states [3,4]. Hereditary sensory and autonomic neuropathy type V (HSANV) is caused by mutations in NGF gene, leading to the loss of ability to perceive deep pain [5]. Mutations in its receptor TrkA result in HSNIV, which is characterized by congenital insensitivity to pain, anhidrosis, and mental retardation [6].

Neurotrophin receptors have also been found to play an important role in the development and progression of tumor cells [7,8]. Alterations in Trk receptor expression, genomic rearrangements or mutations in the gene have been reported in different human cancers, e.g. pancreatic [9–12], prostate [13–15], breast [16–18], ovarian carcinoma [19,20], malignant melanomas [21], thyroid [22], and neuroblastoma [23,24]. Interestingly, TrkB receptor has been described to act as a suppressor of anoikis, a type of apoptosis important in prevention of metastasis [25], highlighting the importance of Trk receptor activity in tumor progression and formulating Trk receptors as potent targets of cancer therapy.

Changes in BDNF and its receptor expression are important in several central nervous system disorders, most notably the enhanced signaling in epilepsy and decreased or increased (depending on the brain region) levels in depression [26–28]. For this reason, inhibition of TrkB has been proposed as a candidate

* Corresponding author. Tallinn University of Technology, Department of Gene Technology, Akadeemia 15, Tallinn, 12618, Estonia.

** Corresponding author. University of Tartu, Institute of Chemistry, Ravila 14A, Tartu, 50411, Estonia.

E-mail addresses: tonis.timmusk@ttu.ee (T. Timmusk), mati.karelson@ut.ee (M. Karelson).

¹ These authors contributed equally to this work.

² Present address: Laboratory for Genetics and Genomics, Centre of Microbial and Plant Genetics (CMPG), Department of Microbial and Molecular Systems, KU Leuven, Gaston Geenslaan 1, 3001 Leuven (Heverlee), Belgium.

therapy for epilepsy. In a mouse model, inhibition of TrkB prevented recurrent seizures and alleviated anxiety-like behavior accompanied with a lower level of destructed hippocampal neurons [29].

Neurotrophins and their receptors have also been implicated to be important in age-related changes in cognition and Alzheimer's disease (AD). Although reports in this field are conflicting with some describing elevated levels of NGF in AD, the prevalent opinion seems to be that increasing the level of NGF or the activity of TrkA is therapeutic for AD [30,31]. Therefore, all inhibitors of Trk receptors might inflict unwanted side-effects if they are able to cross the blood-brain barrier.

In recent studies, several small molecule TrkA inhibitors have been shown to be effective in neuropathic and inflammatory pain models, able to attenuate cancer-induced pain as well as to block the development of some tumor cells [6,8,32]. Still, more potent and more Trk-selective inhibitors are searched for a therapeutic treatment of pain, cancer, and/or epilepsy.

The aim of the current study was to identify and characterize new low molecular weight antagonists of Trk receptors as drug candidates for the treatment of pain and cancer, using methods of computational modeling (molecular QSAR [33] and fragment-based QSAR [34]), chemical synthesis, and testing the compounds biochemically as well as in cellular assays. Several potent and highly Trk-selective inhibitors were identified. Future studies will determine if the compounds are able to penetrate the blood-brain barrier and if so, further drug development will be undertaken to render the inhibitors more specific for peripheral organs and less capable of inducing any unwanted side-effects due to Trk inhibition in the central nervous system.

This study was concentrated on indole-like Trk inhibitors. Some oxindoles and aza-oxindoles have been reported as selective TrkA inhibitors [35], a series of new 7-azaindole derivatives have demonstrated anticancer and antiangiogenic effects in human breast cancer cells [36], and oxindole amides and ureas have been investigated to elucidate the role of Trk receptors in cancer biology and other disease areas [37]. The indoles described in this study are targeting the ATP-binding pocket of the kinase domain, which is highly similar in the Trk family. Therefore, while TrkA was chosen as a representative for computational predictions and for the majority of the assays, the compounds are prevalently pan-Trk inhibitors.

2. Results and discussion

2.1. Model development

The data set obtained consisted of 47 indoles (Fig. 1 and Table S1 in Supplementary material). Using the QSARModel program [33], several multiple linear regression (MLR) models [38] were developed:

$$P = P_0 + \sum_{i=1}^n a_i D_i \quad (1)$$

Equation (1) correlates the studied property/activity P (P_0 - intercept) (in our case $\log IC_{50}$) with a certain number n of molecular descriptors D_i weighted by the regression coefficients a_i . Up to seven-parameters models were composed. As the compounds belong to three different structural classes and the corresponding biochemical assays differ from each other [35–37], the data set was investigated for outliers. Models based on four, five, and six descriptors with the best correlation were tested. The outliers mentioned below are rather related to the eventually selected model. At first 4 outliers (compounds 38, 40, 43, and 46 in Table S1),

thereafter 3 outliers (compounds 7, 31, and 47 in Table S1) were identified by modified leverage analyses, i.e. compounds with large deviations from the model s^2 were removed:

$$\left(\log IC_{50}(\text{predicted}) - \log IC_{50}(\text{observed}) \right)^2 > s^2 \quad (2)$$

The final best MLR model of four descriptors possessed statistical characteristics is shown in Table 1. The coefficient of determination (Pearson's squared correlation coefficient) is $R^2 = 0.770$ for the data set of 40 compounds.

An ABC validation test [39] was applied to estimate the predictivity of Equation (1), taking into account the property data distribution. The ABC method consists of sorting the data in an ascending order according to the observed (experimental) values and three subsets (A, B, C) are formed: the 1st, 4th, 7th, etc. data points comprised the first subset (A), the 2nd, 5th, 8th, etc. comprised the second subset (B), and the 3rd, 6th, 9th, etc. comprised the third subset (C). Then three training sets were prepared as the combinations of any two subsets. Subsequently, the tested MLR model was rebuilt for each of the training sets, (AB, AC, and BC), with the same descriptors but with optimized regression coefficients. Further, these three models AB, AC, and BC were used to predict the property values for the C, B, and A subsets, respectively. The prediction was assessed based on the coefficient of determination R^2 between the predicted and observed property values. The final result was estimated by the averaged squared correlation coefficient by the three "external" sets C, B, and A. As regarding this ABC validation, the averaged R^2 is close to the R^2 of model, which is good for prediction purposes. In addition to the ABC validation, the standard leave-one-out cross-validation (R^2_{cv}) for the QSAR model resulted in $R^2_{cv} = 0.708$.

The descriptors appearing in the QSAR model (Table 1) are related to the stability, energy partition, and shape of the molecules [38]. The quantum-chemical descriptors, the lowest atomic state energy (AM1) for C atoms and the lowest atomic state energy (AM1) for H atoms are related to the ground states of these atoms in the molecule. The lower is the energy, the more stable is the atomic system and, thus, the more stable is the molecule with large C and H content. Besides, atomic state energies in QSAR models can be related to the change in the ligand electronic structure, steric hindrance, and the corresponding energetic effects in binding to the receptor. The quantum-chemical descriptor, the maximum electrophilic reactivity index (AM1) for C atoms comes from the LUMO coefficients and estimates the relative reactivity of the atoms within the molecule for a given series of compounds and is related to the activation energy of the corresponding chemical reaction. Since most atoms are the C atoms in the present investigation, this descriptor can be responsible for the reactivity of compounds. The quantum-chemical descriptors related to the frontier molecular orbitals such as various reactivity indices indirectly account also for the short-range intermolecular interactions, due to partial overlap of these orbitals. The molecular volume/XYZ box (AM1) is the geometrical descriptor that describes the bulk related properties and, by normalizing the descriptor with a unit box, shows how compact the molecule is.

2.2. Generation of a stable cell-line to monitor TrkA activity

A stably transfected cell line was generated in order to assess the capability of the compounds to inhibit the activation of TrkA receptor in the cellular context. Once the endogenous TrkA of the PC-12/luc/Elk1 cell line becomes activated, the downstream events will result in phosphorylation of Elk1, the GAL4-dbd fused to Elk1 binds then to GAL4 UAS and activates the transcription of luciferase

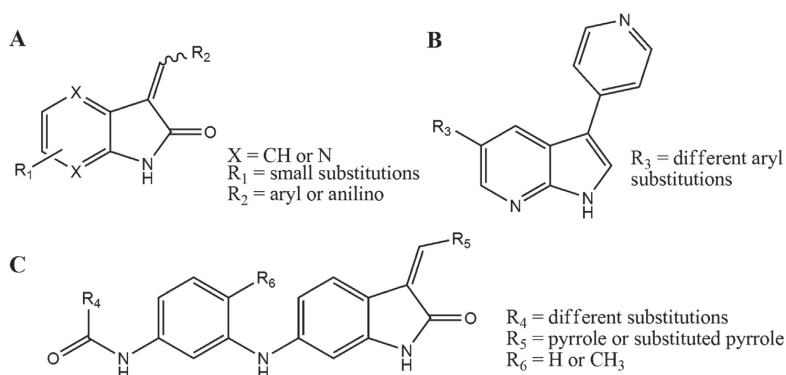


Fig. 1. Structures of compounds in the data set. (A) oxindoles and aza-oxindoles, (B) 3,5-disubstituted 7-azaindoles, (C) oxindole amides and ureas.

Table 1

Best MLR QSAR model, its statistics and validation.^a

Statistics	
N = 40 n = 4 ^b R ² = 0.770 R ² _{cv} = 0.708 F = 29.316 s ² = 0.225	
Equation and descriptors	
$\log IC_{50} = 71.968 + 0.618 \times D1 + 0.648 \times D2 - 54.116 \times D3 - 2.291 \times D4$	
D1 – Lowest atomic state energy (AM1) for C atoms D2 – Lowest atomic state energy (AM1) for H atoms D3 – Max electrophilic reactivity index (AM1) for C atoms D4 – Molecular volume/XYZ box (AM1)	
Validation	
ABC Cross-validation results	
AB: R ² = 0.780; R ² _{cv} = 0.696	
BC: R ² = 0.720; R ² _{cv} = 0.436	
AC: R ² = 0.822; R ² _{cv} = 0.735	
R ² _{avg} = 0.744; R ² _{cv,avg} = 0.622	

^a N – number of compounds in the training set; n – number of descriptors; R² – Pearson's squared correlation coefficient, R²_{cv} – squared correlation coefficient for leave-one-out validation, F – Fisher statistics, s² – squared standard deviation of the model.

^b The four-parameter model was selected due to the breaking point in the graph n vs. R², R²_{cv}.

(Fig. 2). To address the suitability of the generated system for screening application, the Z'-factor was determined [40] (see also Experimental section). The Z'-factor for this assay based on the negative control NGF and the known TrkA inhibitor AZ-23 [41] as the positive control was measured to be 0.647 after 6 h, 0.765 after 18 h, and 0.652 after 24 h of treatment (Fig. 3). Z'-factor value above 0.5 is considered an indication of a high quality assay [40]. The timeframe of 18 h with the highest Z'-factor value was chosen for subsequent experiments.

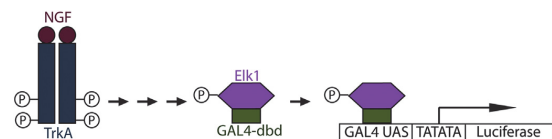


Fig. 2. Mechanism of luciferase induction in PC-12/luc/Elk1 cell line. Upon binding of NGF to TrkA the Elk1 portion of expressed Elk1/GAL4-dbd protein will become phosphorylated. Thereafter, the fusion protein will bind on GAL4 UAS and the transcription of Luciferase gene is activated.

2.3. Characterization of new potent TrkA inhibitors

TrkA was selected as a representative of Trk receptors for virtual screening of compounds targeting the ATP-binding pocket. At first, virtual screening for new scaffolds using Tanimoto similarity was made by search in ZINC [42], MolPort [43], and ChEMBL [44] databases. According to the obtained results, measurements by cellular assays were carried out for four compounds. In the next step, (Z)-3-((5-methoxy-1H-indol-3-yl)methylene)-2-oxindole (**2**; code numbers used are based on our virtual screening) and its 47 derivatives were found as potential TrkA inhibitors (see Scheme 1). The respective descriptors obtained by the FQSARModel program [34] (see Experimental section) were used in the full-molecular QSAR model (Fig. 4A, red points) to predict their IC₅₀ values according to Equation (3) (see Table 1).

Commercially available compounds were purchased (Table S2) and measured for the inhibitory activity using cellular and biochemical assays (Table 2; detailed data of cellular assays is presented in Table S3). The best experimental result from the first series (**2-2a42**) was obtained for compound **2a22**. According to the structure-activity relationships (SAR), the sulfonamide has the strongest influence on the inhibitory activity among the pharmacophores. Compounds without this functionality show somewhat

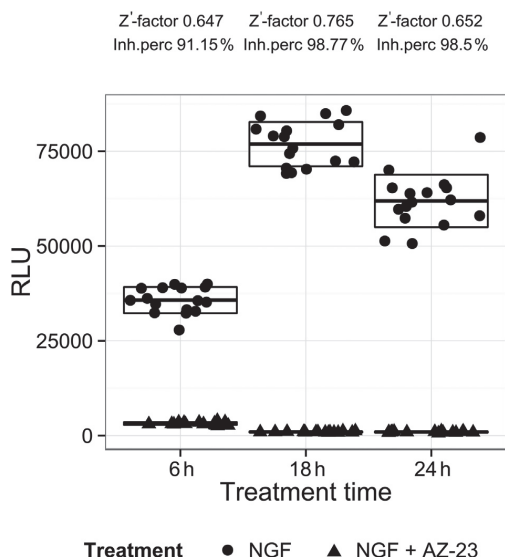


Fig. 3. Z-factor of assay system using PC-12/luc/Elk1 cell line at different treatment times. PC-12/luc/Elk1 cells on 96-well plate were treated for 6 h, 18 h or 24 h with either 50 ng/mL of NGF or 50 ng/mL of NGF together with 5 nM of AZ-23. Each graph point represents luciferase induction of one test well.

less activity (**2**, **2a31**, **2a42**) or are mostly inactive (**2a33**, **2a41**).

Since the discovery of Prontosil prodrug against bacterial infection, sulfonamides have been widely exploited in pharmacy. Apart from the bacterial infections, sulfonamides are used for numerous other clinical indications. Typically, they have been applied as thiazide and loop diuretics [45]. The sulfonamide COX-1/COX-2 and COX-2 inhibitors such as Celecoxib, SC-558, Rofecoxib, and DuP-697 have been prescribed against inflammation [46,47], pain [48,49], and cancers [50,51]. Another area of sulfonamide drugs includes HIV protease [52] and reverse transcriptase inhibitors [53].

Therefore, sulfonamides are a well-studied class of compounds in medicinal chemistry, with ample data available on their pharmacokinetic, pharmacodynamics, and ADME/Tox properties [54]. Some sulfonamides are characterized by rapid oral absorption and their metabolic pathways are well understood [55]. The available large data enables robust optimization of the compound's structure to find the best drug-like properties.

Hence, our interest was turned to possible sulfonamide derivatives of indoles. Based on compound **2a22**, five compounds were synthesized (**2a23**, **2a25**, **3a23**, **3a25**, **4a22**), combining the substitutions at the indole and/or oxindole rings. The cellular and biochemical assays showed contradictory results (see Table 2), thus, the following discussion is based on the biochemical assays as more directly related to TrkA kinase activity. Besides, due to the modeling data set [35–37], the predicted IC_{50} values correspond to the biochemical assays. The substitution of methoxy group by hydroxyl group in indole (R_2) increased the activity (**2a23** and **2a25** vs. **3a23** and **3a25**, respectively) but *N*-methylation in indole (R_1) and *N,N*-dimethylation in sulfonamide of oxindole (R_3) reduced the TrkA inhibiting effect (**2a25** and **3a25** vs. **2a23** and **3a23**). Nevertheless, the biochemically measured IC_{50} values were similar for these four compounds. The *N*-methylation in compounds has insignificant effect on their inhibitory activity. Among the studied compounds,

the best TrkA inhibitor according to both the cellular (10.0 nM) and biochemical (3.7 nM) assays was **4a22** that has *N*-methylated indole and *N*-methylated sulfonamide functionalities. Still, its activity was comparable to compound **2a22** that has only indole *N*-methylated. Thus, *N*-methylation in indole could have somewhat stronger effect (**2a21** vs. **2a27**).

In addition, the strongest inhibitor **4a22** was selected to identify its binding mode and interactions in the ATP-binding site of TrkA. The molecular docking study is described in Supplementary material.

In general, the IC_{50} values obtained with biochemical assays were lower compared to cellular assays. However, the relative activity remained similar with the strongest inhibitors being **2a22** and **4a22** and the IC_{50} 's above the measurement range for **2a33** and **2a41**. The differences in measurements of cellular and biochemical assays could have resulted from the solubility of the compounds. However, the aqueous solubility at room temperature of compounds **2a22**, **2a25**, and **4a22** did not differ significantly, it was determined as 9.7 ± 0.3 , 7.8 ± 0.2 , and 3.3 ± 0.3 μ M (i.e. 3.7 ± 0.1 , 3.2 ± 0.1 , and 1.3 ± 0.1 μ g/mL), respectively, showing that all compounds were soluble at the tested concentrations. It is also possible that the differences in the IC_{50} values measured by cellular and biochemical assays could yield from other reasons, for example specificity among intracellular interaction partners and cell permeability properties of the compounds. In addition, six compounds with the highest inhibition rates against TrkA were characterized biochemically against TrkB and TrkC. The results show that these compounds exhibit no significant selectivity of TrkA over TrkB and TrkC (Table 2). The tendency of correlation between functional groups and compound activity to inhibit TrkB and TrkC is similar to the correlation previously described for TrkA measurements.

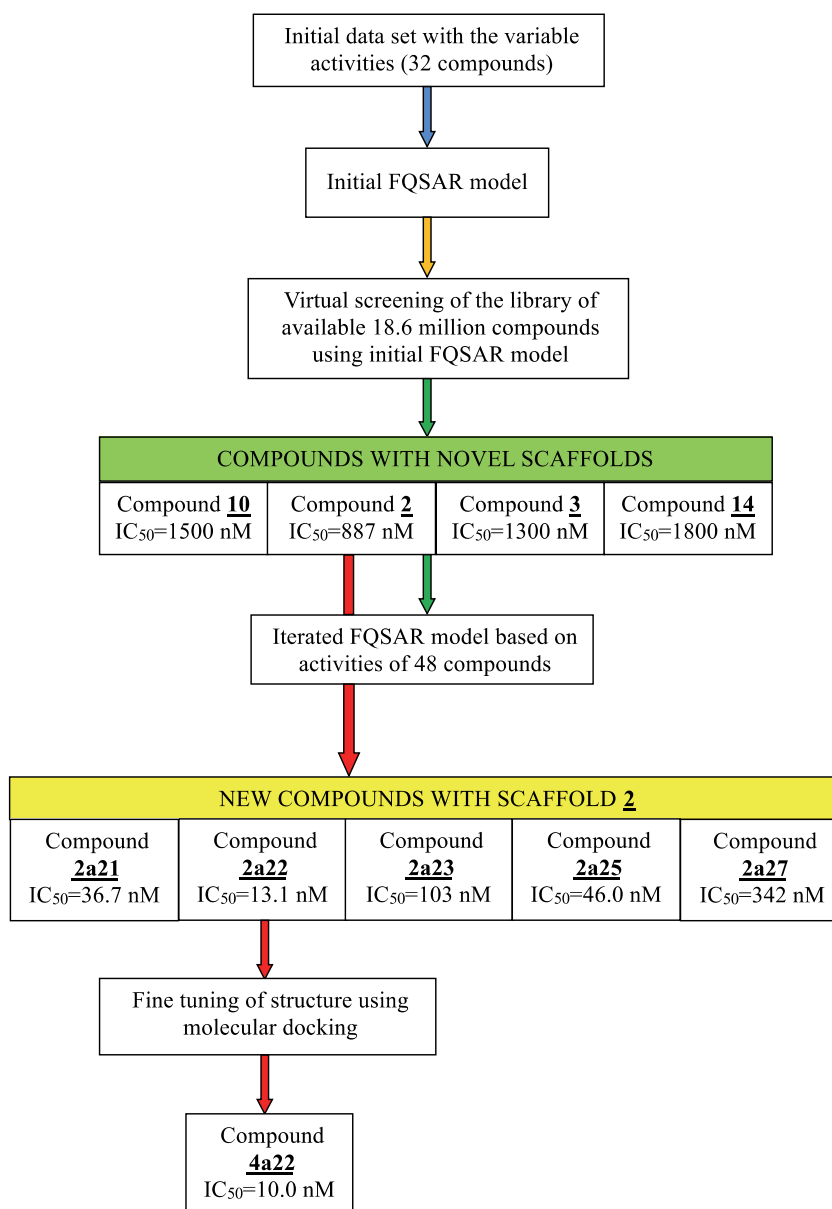
2.4. Comparison of biochemical and predicted IC_{50} values

In this study, the training set was constructed using the modeling data set and included 40 compounds from the final QSAR model. The external test set was based on compound **2** and its 10 derivatives with measured biochemical values. The correlation between biochemically measured and predicted IC_{50} 's for the both sets is rather satisfactory ($R^2 = 0.770$ and 0.751 , respectively; Fig. 4A).

Williams graph (Fig. 4B) illustrates which points deviate because of descriptors and which points because of experimental values. According to leverage value h of descriptors, one compound (entry 9 in Table S1) deviates significantly because of its extreme values of descriptors D2 and D3 (entry 8 in Table S4). Other compounds stay within the critical area determined by a vertical line at 0.375. Compounds of the external test set belong to the applicability domain, i.e. they are structurally similar to the training set. According to the standardized residual r' for biochemically measured data, all compounds deviate more than 2.5 units from the correlation line are considered to be strong deviations. One compound (entry 18 and 17 in Tables S1 and S4, respectively) from the training set is quite close to this critical point. In case of the external test set, the results are somewhat underestimated, which is probably due to the different method to predict IC_{50} 's for the training set (obtained directly by the QSARModel) and the external test set (descriptors obtained by FQSARModel were used in the full-molecular best MLR QSAR model).

2.5. Compounds **2a22**, **2a25**, and **4a22** are potent inhibitors of both TrkA and TrkB in cellular context

According to experimental results with the PC-12/luc/Elk1 cell



Scheme 1. The flowchart of the development of low-nanomolar TrkA inhibitors (IC₅₀'s are measured by cellular assays).

line, three compounds – **2a22**, **2a25**, and **4a22** were selected for further testing by western blot using antibodies specific for phosphorylated TrkA, TrkB, and their downstream kinases. Compounds **2a22** and **4a22** were two of the most efficient new inhibitors tested. Compound **2a25** was chosen, as it has been shown not to suppress Syk activity, whereas **2a21**, **2a22**, **4a22** as well as **2a23** were reported as Syk inhibitors [56]. The compounds were tested on PC-12 and MG87/TrkB/luc/Elk1 cells that express TrkA and TrkB,

respectively. The cells were treated concurrently with NGF or BDNF and the compounds at three different concentrations. The levels of phosphorylated kinases were assessed using respective antibodies and further quantification of western blot signals. The phosphorylation of TrkA and TrkB was effectively inhibited by all of the tested compounds with statistically significant reduction in activity at concentration of 1 μ M. The phosphorylation of downstream kinases Akt and Erk1/2 was observed to be diminished likewise compared

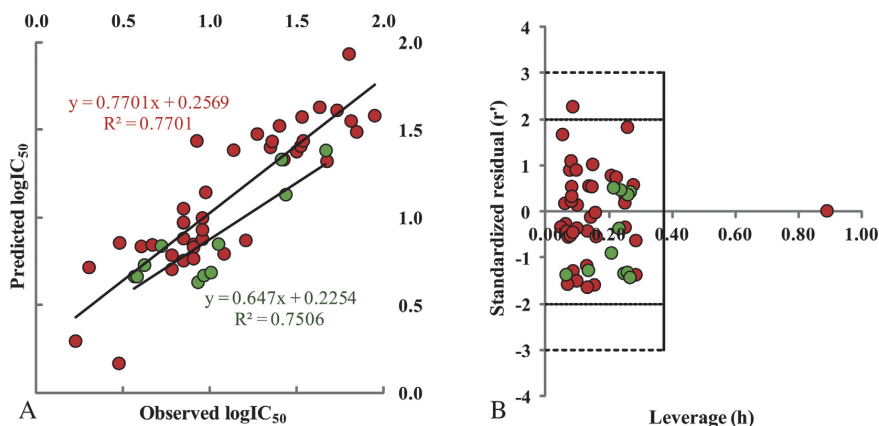
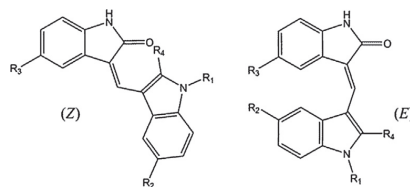


Fig. 4. Graphical characterization of the QSAR model. (A) Correlation of observed (biochemical assay) and predicted $\log IC_{50}$ for the training set (red points) and the external test set (green points). (B) Williams plot for verifying the applicability domain of the QSAR model, showing the relationship between standardized residuals (r') and leverages (h). (For interpretation of the references to colour in this figure legend, the reader is referred to the web version of this article.)

Table 2

Observed and predicted IC_{50} values for (Z)-3-(5-methoxy-1H-indol-3-yl)methylene)-2-oxindole (**2**) and its derivatives.



Comp. (Isomer)	R_1	R_2	R_3	R_4	IC_{50} (nM) Cellular assays		IC_{50} (nM) Biochemical assays			IC_{50} (nM) Predicted ^a
					TrkA	TrkB	TrkA	TrkB	TrkC	
2 (Z)	H	OCH ₃	H	H	887	—	27.21	—	—	13.45
2a21 (Z)	CH ₃	H	SO ₂ NH ₂	H	36.7	—	4.17	7.62	6.86	5.34
2a22 (Z)	CH ₃	OCH ₃	SO ₂ NH ₂	H	13.1	110.95	3.78	3.92	4.10	4.59
2a27 (Z)	H	H	SO ₂ NH ₂	H	342	—	11.14	—	—	7.03
2a31 (E)	H	H	H	H	2760	—	46.34	—	—	24.04
2a33 (Z)	H	H	H	CH ₃	N/A	—	>1·10 ⁻⁵ M	—	—	23.65
2a41 (E)	H	H	H	Cl	N/A	—	>1·10 ⁻⁵ M	—	—	28.86
2a42 (Z)	CH ₃	H	H	H	998	—	25.7	—	—	21.35
2a23 (Z)	H	OCH ₃	SO ₂ NH ₂	H	103	—	8.49	8.53	8.82	4.25
2a25 (Z)	CH ₃	OCH ₃	SO ₂ N(CH ₃) ₂	H	46.0	141.83	10.09	15.25	11.67	4.83
3a23 (Z)	H	OH	SO ₂ NH ₂	H	366	—	5.22	—	—	6.85
3a25 (Z)	CH ₃	OH	SO ₂ N(CH ₃) ₂	H	92.8	—	9.17	13.45	9.72	4.65
4a22 (Z)	CH ₃	OCH ₃	SO ₂ NH(CH ₃)	H	10.0	41.07	3.66	4.52	4.25	4.59

^a 2D structures (above) were converted into 3D structures and preoptimized by molecular mechanics MM+ field using HyperChem 8.0. To keep the corresponding isomers, no conformational search by FQSARModel was carried out. Descriptors obtained by FQSARModel were used in the best MLR QSAR model.

to the positive control NGF or BDNF (Fig. 5). These results are consistent with the biochemical IC_{50} results obtained for the Trk family kinases, which showed no selectivity of these compounds in inhibiting TrkA over TrkB and TrkC (Table 2). However, luciferase assays performed with PC-12/luc/Elk1 and MG87/TrkB/luc/Elk1 cell lines indicate that the given compounds are more potent inhibitors of TrkA than of TrkB in given cellular contexts (Table 2). This is most probably caused by the use of different cell lines to assay the inhibition of TrkA (PC-12/luc/Elk1) and TrkB (MG87/TrkB/luc/Elk1) that possibly can have different off-target proteins for the tested compounds, as well as slightly dissimilar membrane properties that can affect the influx of these chemicals. Additionally, in these two

distinct cellular systems the activity of the Trk proteins may be incomparable due to their different concentration or interaction partners that can affect their behavior. For this reason, most probably there is no big selectivity of these compounds for the Trk kinases which is expected, as the ATP-binding pockets of Trk proteins are highly similar.

2.6. Compounds **2a22**, **2a25**, and **4a22** do not affect the viability of cortical neurons or MG87/TrkB/luc/Elk1 cells

Activation of Trk kinases by neurotrophins has been implicated to be involved in the survival of neuronal cells [1]. For this reason,

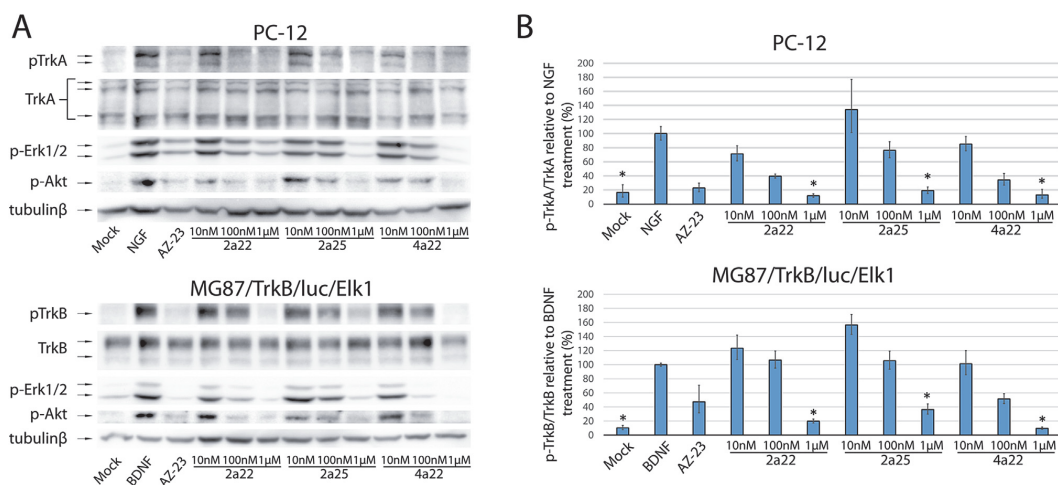


Fig. 5. Compounds 2a22, 2a25, and 4a22 inhibit phosphorylation of TrkA and TrkB and activation of their downstream intracellular targets. (A) PC-12 or MG87/TrkB/luc/Elk1 cells were treated with 2a22, 2a25, and 4a22 at different concentrations concurrently with 50 ng/mL of neurotrophins NGF (for PC-12 cells) or BDNF (for MG87/TrkB/luc/Elk1 cells) for 5 min. Equal amount of lysates were analyzed using western blotting and the indicated antibodies. Neurotrophin alone was used as a positive control, 5 nM of AZ-23 as a positive control and “mock” corresponds to DMSO-treated cells. Representative blots of three independent experiments are shown. (B) Quantified western blot signal ratios of phospho-Trk to total Trk were log-transformed, mean-centered, and autoscaled for ANOVA analysis. For graphical representation, the data was back-transformed and normalized to neurotrophin-treated cell lysate signals. Mean \pm SEM data is shown and asterisks indicate statistical significance according to Dunnett’s post-hoc test comparing means with neurotrophin-treated cell lysate data mean ($n = 3$, $p < 0.05$).

we tested if Trk inhibitors 2a22, 2a25, and 4a22 can attenuate the viability of neurons. Rat cortical cells were treated with these compounds at different concentrations for 24 h. No reduction in the number of viable neurons even at 1 μ M concentration was observed (Fig. 6A).

To test the effect of these compounds on the viability of rapidly dividing cells, 2a22, 2a25, and 4a22 were applied at different concentrations to the growth medium of TrkB-expressing MG87/TrkB/luc/Elk1 cells for 24 h, after which the cellular ATP content was quantified. Similarly to the experiment with cortical neurons, no effect of these compounds on cell viability was seen (Fig. 6B).

2.7. Kinase profiling of 6 potent compounds

A selection of 48 kinases representing the human kinome (Fig. S3) was used for *in vitro* kinase profiling to determine the activity of 6 potent TrkA inhibitors that were selected based on the PC-12/luc/Elk1 luciferase assay results (IC_{50} ’s around 100 nM or lower). The compounds used were 2a21, 2a22, 2a23, 2a25, 3a25, and 4a22 at 100 nM and 1 μ M concentrations (Table 3). According to the results, at concentration of 100 nM all compounds were relatively TrkA specific inhibiting only up to 3 off-target kinases, while reducing the activity of TrkA by at least 82% at 100 nM concentration and 94% at 1 μ M concentration. At 100 nM, 2a25 was able to inhibit only TrkA. 2a23, 3a25, and 4a22 were reducing the activity at least by 50% of only one kinase in addition to the Trk kinases at 100 nM. Kinases that were inhibited by most of the compounds at 1 μ M concentration included Aurora-B, CAMKK2, CHK2, IRAK4, LCK, and MAP3K11.

As compounds 2a21, 2a22, 4a22, and 2a23 have been described as Syk inhibitors [56], it was initially a surprise that these compounds failed to inhibit Syk at significant levels in our experiments. However, a recent extensive analysis of kinase inhibitors, which also addressed some Syk inhibitors, including the compound named here as 2a21, concluded that three of the tested “Syk

inhibitors” had extremely different selectivity among a wide range of kinases and only one of these three compounds was a potent Syk inhibitor [57]. It is noteworthy that our results highly correlate with the results of this study – at 1 μ M concentration of 2a21 Gao et al. reported 38% residual activity of Syk and 1% residual activity of TrkA, compared to our results of 47% and 2%, respectively. Thus, 2a21 together with some other compounds described here by us (especially 2a22 and 4a22) are potent and selective Trk inhibitors with no significant effect on Syk.

3. Conclusions

Based on our virtual screening for new scaffolds, (Z)-3-((5-methoxy-1H-indol-3-yl)methylene)-2-oxindole (2) was identified as a potential TrkA receptor antagonist by means of the combination of full-molecular QSAR and fragment-based QSAR, which were used to predict IC_{50} values. Subsequently, several derivatives of 2 were searched from databases, designed according to SAR (3a23, 3a25), synthesized (2a23, 2a25, 3a23, 3a25, 4a22), and final 13 compounds were tested in cellular assays as well as *in vitro* using biochemical methods. Compounds 2a22 and 4a22 were two of the most efficient new inhibitors tested. Six compounds (2a21, 2a22, 2a23, 2a25, 3a25, 4a22) with the highest inhibition rates against TrkA were also characterized biochemically for TrkB and TrkC inhibition. No significant selectivity of TrkA over TrkB and TrkC was exhibited by any of the compounds tested. Compounds 2a22, 2a25, and 4a22 did not influence the viability of cortical neurons or dividing MG87/TrkB/luc/Elk1 cells and are therefore good candidates for testing in animal models of neuropathic pain.

4. Experimental section

4.1. Data set and methodology

The data on known indole-like TrkA inhibitors were collected

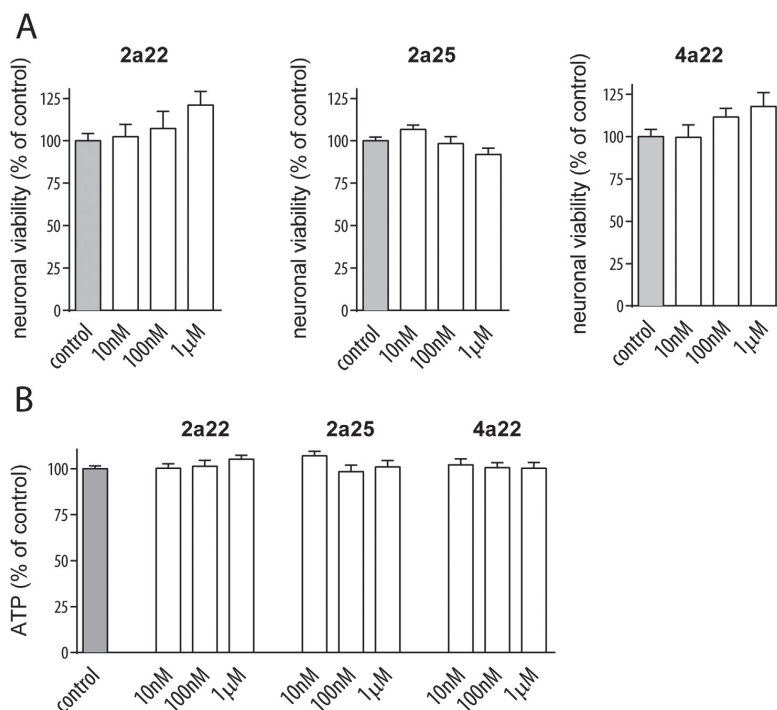


Fig. 6. Compounds **2a22**, **2a25**, and **4a22** do not have effect on cell viability. (A) Primary cortical neurons were treated with **2a22**, **2a25**, and **4a22** at different concentrations for 24 h, after which the number of survived neurons were counted. The average of different measurements \pm SEM is shown ($n = 2$ with 4–6 technical replicates). (B) MG87/TrkB/luc/Elk1 cells were treated with **2a22**, **2a25**, and **4a22** at different concentrations for 24 h and the cellular ATP content was quantified using CellTiter-Glo[®] Luminescent Cell Viability Assay. The average of different measurements \pm SEM is shown ($n = 2$ with 4–6 technical replicates).

from ChEMBL database [44], using keywords “Nerve growth factor receptor TrkA, Homo sapiens, Homologous protein/Protein, Assay Type B (i.e. biochemical assays)”. The data set consisted of 11 oxindoles and aza-oxindoles [35], 24 3,5-disubstituted 7-azaindoles [36], and 14 oxindole amides and ureas [37] (Fig. 1 and Table S1) but one oxindole and one 7-azaindole were discarded because of too high IC_{50} values (4700 and 3167 nM, respectively). The IC_{50} 's of other compounds were in the range 1.67–160 nM. In the further treatment, the IC_{50} values were transformed into $\log IC_{50}$ units.

The two-dimensional molecular structures of the aforementioned compounds were converted into the three-dimensional structures and preoptimized by built-in minimizer using Maestro 9.3 [58]. Conformational search was carried out by the CMol3D program of QSARModel [33] (version 5.0) for the known indole-like compounds, where random conformations were constructed by means of Stochastic Proximity Embedding algorithm [59] followed by optimization based on MMFF94s force field [60] to improve their quality. Thereafter, all geometries were optimized as random vacuum conformer with the minimum potential energy using MOPAC 6.0 [61]. The quantum-mechanical semiempirical calculation in the form of the AM1 [62] energy minimization was subsequently applied, using the Polak-Ribiere Conjugate Gradient (PRCG) optimization method with a gradient 0.01 kcal/Å as a stop criterion. The following keywords were used for the optimization procedure: AM1 VECTORS BONDS PI POLAR PRECISE ENPART EF MMOCK NOINTER GRAPH GNORM = 0.05 XYZ.

The essence of the FQSARModel program is an efficient and

rapid generation of totally new compounds from a training set (compounds are fragmented into linearly connected structural fragments) and automatic prediction of a studied property [34]. In case of the series of compound **2**, FQSARModel (version 1.0) was used for the prediction of IC_{50} values. As conformational search was not carried out by CMol3D program to keep the corresponding isomers, a somewhat better correlation was obtained when the three-dimensional structures of compound **2** and its derivatives were preoptimized by molecular mechanics MM+ field using HyperChem 8.0 [63]. Methodology of the geometry optimization in FQSARModel is the same as in the QSARModel. The final step in the FQSAR algorithm is the calculation of descriptors to obtain a descriptor-compounds matrix. The corresponding descriptors were used in the best MLR QSAR model (Equation (3) in Table 1) to calculate the IC_{50} values for the series of compound **2**.

4.2. Biological assays and methods

4.2.1. Generation of stable cell line with a sensitive reporter-gene system to monitor TrkA activity

PC-12 (rat adrenal pheochromocytoma cell line) cells were transfected using LipoD293[™] DNA In Vitro Transfection Reagent (SigmaGen) with 1 µg of pFA2-Elk1 plasmid and 4 µg of pFR-LUC plasmid (PathDetect Elk1 *trans*-Reporting System; Agilent Technologies). pFA2-Elk1 plasmid codes for the fusion protein consisting of GAL4-dbd (DNA-binding domain) followed by Elk1 transcription factor and contains Geneticin G418 resistance gene neomycin. pFR-LUC plasmid codes for GAL4 upstream activation

Table 3

Biochemical profiling of 6 compounds at two concentrations, each against 48 protein kinases, average of duplicate measurements. Results are presented as percentage of residual activity.

Comp.	Residual activity ≤ 50%											
	2a21		2a22		2a23		2a25		3a25		4a22	
	0.1	1	0.1	1	0.1	1	0.1	1	0.1	1	0.1	1
Assay conc. (μM)												
AKT1 aa106-480	92	97	92	96	115	101	101	93	104	105	93	98
AMPK-alpha1 aa1-550	83	56	94	89	101	72	98	91	103	87	104	88
Aurora-B	59	42	79	50	95	48	85	71	43	11	74	76
BTK	111	119	117	107	100	91	89	89	95	107	97	73
CAMK1D	106	90	84	97	97	94	99	94	100	103	90	80
CAMKK2	62	25	53	19	83	31	76	30	73	25	56	50
CHK2	9	5	35	39	59	12	100	99	94	92	93	75
CK1-delta	88	82	87	84	92	79	89	86	88	87	89	91
CK2-alpha1	102	96	101	94	90	84	98	90	97	89	105	100
DYRK1A	122	114	101	99	105	96	98	94	101	101	89	95
EEF2K	99	103	101	102	107	112	99	86	97	106	103	92
EPHA2	99	90	98	89	110	98	106	89	111	98	100	84
ERBB4	94	101	101	87	94	60	103	85	110	95	98	42
GSK3-beta	104	92	93	83	103	79	98	97	99	92	90	90
HIPK2	112	103	108	81	124	84	109	85	120	96	106	102
IGF1-R	105	107	105	100	98	97	94	79	102	95	96	60
IRAK4 (untagged)	6	3	12	20	45	9	91	83	68	52	59	37
JAK2	85	67	90	86	91	67	88	72	78	55	89	87
JNK1	121	94	110	95	103	87	103	100	105	97	103	112
LCK	64	50	65	32	72	61	81	64	62	33	45	41
MAP3K11	36	12	34	38	66	25	84	37	80	51	76	55
MAP3K7/MAP3K7IP1	85	63	93	89	93	64	106	88	101	92	104	95
MARK3	93	88	96	90	101	93	93	97	103	96	100	87
MEK1 wt	67	59	82	71	87	72	104	97	107	98	104	93
MST2	91	62	86	84	101	64	101	104	98	83	95	77
MYLK	97	90	94	90	94	83	94	91	91	84	92	90
NEK6	111	109	106	98	117	108	100	100	104	103	99	97
p38-alpha	107	104	106	100	102	93	95	97	97	96	102	99
PAK4	74	78	77	68	93	82	96	99	95	90	84	91
PDK1	90	70	93	75	98	66	99	84	94	83	92	123
PIM1	105	93	96	88	103	79	104	97	102	95	94	88
PKA	94	87	91	91	88	84	91	98	94	103	91	83
PKC-alpha	106	94	91	102	104	87	93	95	96	103	101	103
PKC-mu	95	91	90	91	95	72	89	92	99	89	92	93
PLK1	102	91	93	93	93	95	83	93	93	91	92	87
PRK2	94	78	98	89	96	81	108	94	91	89	90	86
RIPK2	102	84	100	97	96	48	104	95	94	89	108	100
ROCK2	76	55	99	87	101	61	92	89	79	69	94	79
RPS6KA5	99	93	103	95	93	95	105	108	106	107	96	88
S6K	90	81	92	92	88	70	87	85	87	92	96	83
SGK1	81	55	80	75	85	49	90	80	87	81	94	81
SRC (GST-HIS-tag)	124	108	113	91	107	74	93	70	79	68	92	73
SRPK1	116	101	106	99	114	93	111	95	109	94	105	101
SYK aa1-635	69	47	75	69	86	35	102	91	107	91	95	56
TBK1	75	58	79	55	96	62	100	79	96	81	97	93
TRK-A	3	2	3	1	6	0	18	6	10	2	4	3
TTK	104	85	109	96	101	80	102	106	104	96	99	86
VEGF-R1	82	81	94	85	96	76	96	93	100	93	91	59

sequence (UAS) followed by luciferase reporter gene. A puromycin resistance gene was introduced to the pFR-LUC plasmid using Bst1107I and NdeI restriction enzymes from pGL4.22[luc2CP/Puro] (Promega). The selection of transfected cells was initiated two days after the transfection with addition of 300 μg/mL of G418 (Sigma) and 0.75 μg/mL of puromycin (Sigma-Aldrich) and continued for about one and a half months until distinct cell colonies could be picked, plated, and tested for responsiveness to NGF. Generated cell line, called hereafter PC-12/luc/Elk1, was maintained in Dulbecco's Modified Eagle's Medium (DMEM; PAA Laboratories), containing 6% fetal bovine serum (FBS; PAA Laboratories), 6% horse serum (HS; PAA Laboratories), 1% penicillin/streptomycin (PS; Gibco), 300 μg/mL of Geneticin G418, and 0.75 μg/mL of puromycin. MG87/TrkB/

luc/Elk1 and MG87/par/luc/Elk1 [64] were maintained in Minimum Essential Media (MEM; PAA Laboratories), including 10% FBS, 1% PS, 2 μg/mL Blasticidin (PAA Laboratories), and 500 μg/mL G418. PC-12 cells were maintained in DMEM, containing 6% FBS, 6% HS, and 1% PS.

4.2.2. Determination of the Z'-factor of the PC-12/luc/Elk1 cell-line

PC-12/luc/Elk1 cells were plated one day before the assay on 96-well plates in 25,000 cell per well. Next day the growth media was changed to 50 ng/mL of NGF (Peprotech) together with 0.1% dimethyl sulfoxide (DMSO; Sigma-Aldrich; negative control) or to 50 ng/mL of NGF together with 5 nM of a known TrkA inhibitor AZ-23 [41] (Axon Medchem; positive control) in 100 μL of DMEM,

containing 6% HS, 6% FBS, and 1% PS. Three time points were chosen to be tested (24 h, 18 h, and 6 h) with 16 wells per effector per time point. After 24 h, 18 h or 6 h the growth media was removed and 20 μ L of Steady Glo Assay Reagent (Promega) was added to each well. The plate was subjected to 10 min of shaking and, thereafter, analyzed using TECAN plate reader. The results were used to calculate the Z'-factor with the Equation (4)

$$Z' = 1 - \frac{(3\sigma_+ + 3\sigma_-)}{|\mu_+ - \mu_-|} \quad (4)$$

where σ_+ and σ_- are the standard deviations of the positive and negative control, and μ_+ and μ_- their means [40].

4.2.3. Determination of IC_{50} of compounds in cellular context

Based on our virtual screening for new scaffolds, one potential compound (Z)-3-((5-methoxy-1H-indol-3-yl)methylene)-2-oxindole (**2**) was selected for further research. Compound **2** and its seven derivatives were purchased, five new predicted active compounds were synthesized by us (Table S2). The IC_{50} 's of the compounds were determined using cellular and biochemical assays. In the cellular assays, using PC-12/luc/Elk1 and MG87/TrkB/luc/Elk1 cells, the compounds were assessed in gradual dilutions of the compounds in triplets together with NGF or BDNF (Peprotech), respectively. TrkA inhibition was determined using same methodology as for measuring the Z'-factor with 18 h treatment time. The MG87/TrkB/luc/Elk1 cells were plated one day prior to the experiment, 15,000 cells per well on a 96-well plate. BDNF (50 ng/mL) together with 0.1% DMSO was used as the negative control and BDNF with 5 nM of AZ-23 [41] as the positive control in 100 μ L of MEM, containing 10% FBS and 1% PS. Thereafter, the assay was conducted likewise as with PC-12/luc/Elk1 cells.

Based on cellular assays, the statistical calculations for determining IC_{50} values were performed using R statistical programming software. Percent inhibition values for each compound together with log transformed drug concentrations were fitted to 4 parameter non-linear logistic model, which was used to calculate IC_{50} values for each compound. The formula used for calculation of percent inhibition for treatments was

$$\frac{X_{max} - X_i}{X_{max}} \quad (5)$$

where X_i – luciferase signal in the presence of compound together with NGF or BDNF (inhibitory activity), X_{max} – luciferase signal in DMSO and NGF or BDNF treated cells (normal activity).

The biochemical kinase assays were custom ordered from ProQinase, Germany.

4.2.4. Western blotting

The PC-12 and MG87/TrkB/luc/Elk1 cells were plated on 6-well plates one day prior to the assay. Cells were treated for 5 min with compounds and simultaneously with 50 ng/mL of NGF (PC-12 cells) or BDNF (MG87/TrkB/luc/Elk1 cells). 0.1% of DMSO was used to determine the base level, 0.1% of DMSO concurrently with 50 ng/mL of NGF or BDNF served as a negative control and 0.1% of DMSO concurrently with 5 nM of AZ-23 as a positive control. Thereafter, western blotting was performed as described previously [65]. Antibodies used included: rabbit anti-TrkA (#06-574; 1:1000) from Millipore, rabbit anti phospho-TrkA (#9141; 1:1000), rabbit anti phospho-TrkA/TrkB (#4619; 1:1000), rabbit anti-TrkB (#4603; 1:1000), and rabbit anti phospho-Akt (#4058; 1:3000) from Cell Signaling; mouse anti phospho-Erk1/2 (#sc-7383; 1:1000) from Santa Cruz and anti-tubulin β clone E7 (1:1000) from Prof. Michael Klymkovskiy.

Western blot signals were quantified using ImageQuant TL software from GE Healthcare Life Sciences. Phospho-Trk to total Trk ratios were log-transformed, mean-centered, and autoscaled. ANOVA analysis and Dunnett's test of this data was performed using Prism (GraphPad).

4.2.5. Cell viability assessment

Primary cultures of rat cortical cells were prepared from neonatal Wistar rats as described earlier [66]. Neurons were grown in NeurobasalTMA medium supplemented with B27 with phenol red on poly-L-lysine-coated 35-mm glass-bottomed dishes. Culture media and supplements were obtained from Invitrogen. For viability measurements neurons were first transfected with neuronal marker, pAAV-hSyn-DsRedExpress obtained from Addgene (Cambridge, MA) allowing better to assess the morphology of individual neurons. Briefly, the conditioned medium was replaced with 100 μ L Opti-MEM 1 medium, containing 2% Lipofectamine 2000 and 1–2 μ g of total DNA. Neurons were incubated for 3–4 h, after which fresh medium was added. 3 days later the neurons were treated with **2a22**, **2a25**, and **4a22** at different concentrations for 24 h, after which the neuronal number was counted from 8 to 12 dishes per treatment group (at least 50 randomly chosen fields from each dish).

For measurement of ATP content, the MG87/TrkB/luc/Elk1 cells were grown on 96-well white plates, treated with **2a22**, **2a25**, and **4a22** at different concentrations for 24 h and the cellular ATP content was quantified using CellTiter-Glo[®] Luminescent Cell Viability Assay (Promega, Sweden) according to manufacturer's recommendations. ATP was measured at least from 8 different wells per each treatment condition.

4.3. Preparation procedure

All reactions were carried out based on a literature procedure [67]. Full assignment of ¹H chemical shifts is based on the 1D and 2D FT NMR spectra on a 400 MHz instrument. The HR mass spectra were recorded by using Agilent Technologies 6540 UHD Accurate-Mass Q-TOF LC/MS spectrometer by using ESI ionization.

4.3.1. Synthesis of (Z)-3-((5-methoxy-1H-indol-3-yl)methylene)-2-oxindole-5-sulfonamide (**2a23**)

2-oxindole-5-sulfonamide (47 mg, 0.22 mmol) and 5-methoxy-1H-indole-3-carbaldehyde (42 mg, 0.24 mmol) were suspended in absolute ethanol (0.44 mL) and piperidine (6.5 μ L, 0.066 mmol) was added. Mixture was heated to 70 °C for 2 h. Additional amount of ethanol (0.44 mL) was added and mixture heated for further 3 h. Reaction was allowed to cool to ambient temperature and product that precipitated was filtered out as yellow-brown solid (74 mg, 91%) (d.r = 7.5:1 (Z/E)). ¹H NMR (400 MHz, DMSO-*d*₆) δ 12.03 (s, 1H), 10.90 (s, 1H), 9.48 (s, 1H), 8.35 (d, *J* = 1.8 Hz, 1H), 8.28 (s, 1H), 7.75 (d, *J* = 2.4 Hz, 1H), 7.63 (dd, *J* = 8.2, 1.8 Hz, 1H), 7.42 (d, *J* = 8.7 Hz, 1H), 7.15 (s, 2H), 6.97 (d, *J* = 8.1 Hz, 1H), 6.88 (dd, *J* = 8.7, 2.4 Hz, 1H), 3.89 (s, 3H). HRMS (ESI): calcd. for [M+H]⁺ (C₁₈H₁₆N₃O₄S)⁺ requires *m/z* 370.0856, found 370.0857; [M+Na]⁺ 392.0675, found 392.0672.

4.3.2. Synthesis of (Z)-3-((5-hydroxy-1H-indol-3-yl)methylene)-2-oxindole-5-sulfonamide (**3a23**)

2-oxindole-5-sulfonamide (47 mg, 0.22 mmol) and 5-hydroxy-1H-indole-3-carbaldehyde (39 mg, 0.24 mmol) were suspended in absolute ethanol (0.88 mL) and piperidine (6.5 μ L, 0.066 mmol) was added. Mixture was heated to 70 °C for 3 h and then allowed to cool to ambient temperature. Product precipitated as brown solid and was filtered out and dried in vacuum (65 mg, 83%) (d.r = 6:1 (Z/E)). ¹H NMR (400 MHz, DMSO-*d*₆) δ 11.95 (s, 1H), 10.87 (s, 1H), 9.38 (s, 1H), 9.04 (s, 1H), 8.26 (d, *J* = 1.8 Hz, 1H), 8.11 (s, 1H), 7.60 (dd, *J* = 8.1,

1.8 Hz, 1H), 7.46 (d, $J = 2.2$ Hz, 1H), 7.33 (d, $J = 8.5$ Hz, 1H), 7.13 (s, 2H), 6.96 (d, $J = 8.2$ Hz, 1H), 6.77 (dd, $J = 8.6, 2.3$ Hz, 1H). HRMS (ESI): calcd. for $[M+H]^+$ ($C_{17}H_{14}N_3O_4S$)⁺ requires m/z 356.0700, found 356.0702; $[M+Na]^+$ 378.0519, found 378.0511.

4.3.3. Synthesis of (Z)-3-((5-methoxy-1-methyl-1H-indol-3-yl)methylene)-N,N-dimethyl-2-oxindole-5-sulfonamide (2a25)

N,N-dimethyl-2-oxindole-5-sulfonamide (48 mg, 0.20 mmol) and 5-methoxy-1-methyl-1H-indole-3-carbaldehyde (42 mg, 0.22 mmol) were suspended in absolute ethanol (0.8 mL) and piperidine (6 μ L, 0.060 mmol) was added. Mixture was heated to 70 °C for 4 h and then cooled to ambient temperature. Product precipitated and was filtered out and dried in vacuum to yield 71 mg of product (86%) as yellow solid (d.r = 20:1 (Z/E)). ¹H NMR (400 MHz, DMSO-*d*₆) δ 11.01 (s, 1H), 9.49 (s, 1H), 8.39 (s, 1H), 8.32 (d, $J = 1.8$ Hz, 1H), 7.90 (d, $J = 2.4$ Hz, 1H), 7.60–7.46 (m, 2H), 7.05 (d, $J = 8.2$ Hz, 1H), 6.98 (dd, $J = 8.8, 2.4$ Hz, 1H), 3.94 (s, 3H), 3.91 (s, 3H), 2.65 (s, 6H). HRMS (ESI): calcd. for $[M+H]^+$ ($C_{21}H_{22}N_3O_4S$)⁺ requires m/z 412.1326, found 412.1322; $[M+Na]^+$ 434.1145, found 434.1141.

4.3.4. Synthesis of (Z)-3-((5-hydroxy-1-methyl-1H-indol-3-yl)methylene)-N,N-dimethyl-2-oxindole-5-sulfonamide (3a25)

N,N-dimethyl-2-oxindole-5-sulfonamide (48 mg, 0.20 mmol) and 5-hydroxy-1-methyl-1H-indole-3-carbaldehyde (39 mg, 0.22 mmol) were suspended in absolute ethanol (0.8 mL) and piperidine (6 μ L, 0.06 mmol) was added. Mixture was heated to 70 °C for 4 h and then cooled to ambient temperature. Product precipitated and was filtered out and dried in vacuum to yield 51 mg of product (64%) as yellow solid (d.r = 20:1 (Z/E)). ¹H NMR (400 MHz, DMSO-*d*₆) δ 10.96 (s, 1H), 9.38 (s, 1H), 9.10 (s, 1H), 8.36–8.24 (m, 2H), 7.67 (d, $J = 2.3$ Hz, 1H), 7.50 (dd, $J = 8.2, 1.8$ Hz, 1H), 7.38 (d, $J = 8.8$ Hz, 1H), 7.02 (d, $J = 8.1$ Hz, 1H), 6.83 (dd, $J = 8.7, 2.3$ Hz, 1H), 3.89 (s, 3H), 2.63 (s, 6H). HRMS (ESI): calcd. for $[M+H]^+$ ($C_{20}H_{20}N_3O_4S$)⁺ requires m/z 398.1169, found 398.1165; $[M+Na]^+$ 420.0988, found 420.0987.

4.3.5. Synthesis of (Z)-3-((5-methoxy-1-methyl-1H-indol-3-yl)methylene)-N-methyl-2-oxindole-5-sulfonamide (4a22)

N-methyl-2-oxindole-5-sulfonamide (36 mg, 0.16 mmol) and 5-methoxy-1-methyl-1H-indole-3-carbaldehyde (33 mg, 0.18 mmol) were suspended in absolute ethanol (0.64 mL) and piperidine (4.8 μ L, 0.05 mmol) was added. Mixture was heated to 70 °C for 4 h and then cooled to ambient temperature. Product precipitated and was filtered out and dried in vacuum to yield 47 mg of product (74%) as yellow solid (d.r = 20:1 (Z/E)). ¹H NMR (400 MHz, DMSO-*d*₆) δ 10.95 (s, 1H), 9.45 (s, 1H), 8.31 (d, $J = 2.9$ Hz, 2H), 7.83 (d, $J = 2.4$ Hz, 1H), 7.56 (dd, $J = 8.2, 1.8$ Hz, 1H), 7.50 (d, $J = 8.8$ Hz, 1H), 7.17 (q, $J = 5.1$ Hz, 1H), 7.00 (d, $J = 8.1$ Hz, 1H), 6.95 (dd, $J = 8.9, 2.4$ Hz, 1H), 3.92 (s, 3H), 3.90 (s, 3H), 2.44 (d, $J = 5.0$ Hz, 3H). HRMS (ESI): calcd. for $[M+H]^+$ ($C_{20}H_{20}N_3O_4S$)⁺ requires m/z 398.1169, found 398.1165; $[M+Na]^+$ 420.0988, found 420.0988.

4.4. Solubility measurements

The solubility of three compounds, such as **2a22**, **2a25**, and **4a22**, was studied using Agilent 1200 Series LC system equipped with a diode array detector (DAD) and Kinetex C18 (2.6 μ m, 2.1 \times 100 mm) column. The mobile phase comprised of acetonitrile/water and the separation was performed with gradient elution (30/70) with 10 min, at flow rate of 0.2 mL/min and at 30 °C. Absorbances of compounds were measured at 210 nm and peak areas were used for the quantitative analysis. Standard samples for calibration curve were prepared as follows: each compound was dissolved in methanol (at conc. 30 μ g/mL) for 60 min using ultrasonic

bath and diluted as required for the analysis. Calibration curves were performed in the range of 3–30 μ g/mL for each compound. Saturated aqueous solutions of above mentioned compounds were prepared as follows: 30 μ g/mL of each compound was dissolved in deionized water using ultrasonic bath for 60 min, centrifuged for 3 min using Starstedt MC 6 centrifuge (6000 rpm), and used for quantitative analysis by RP-HPLC-DAD. All HPLC measurements were performed triplicate and the average relative uncertainty was 3.2%.

Acknowledgements

We thank Maxim Bepalov and Mart Saarma for MG87/TrkB/luc/Elk1 and MG87/par/luc/Elk1 cell lines. The authors also thank Dr. Ivar Järving from Department of Chemistry, Tallinn University of Technology for performing the HRMS analysis. This work was supported by (i) the EU European Regional Development Fund through the Center of Excellence in Chemical Biology (Project No. 3.2.0101.08-0017), Center of Excellence in Molecular Cell Engineering (Project No. 2014-2020.4.01.15-0013), and Center of Excellence for Genomics and Translational Medicine (Project No. 2014-2020.4.01.15-0012), Estonia; (ii) Estonian Ministry of Education and Research (SF0140031As0); (iii) Estonian Research Council (IUT19-18 and IUT19-32, PUT95 and PUT582); (iv) National R&D program “Biotechnology” (AR12171, SLOKT12236T); (v) Estonian Academy of Sciences.

Appendix A. Supplementary data

Supplementary data related to this article can be found at <http://dx.doi.org/10.1016/j.ejmech.2016.06.003>.

References

- [1] E.J. Huang, L.F. Reichardt, Trk receptors: roles in neuronal signal transduction, *Annu. Rev. Biochem.* 72 (2003) 609–642.
- [2] E.J. Huang, L.F. Reichardt, Neurotrophins: roles in neuronal development and function, *Annu. Rev. Neurosci.* 24 (2001) 677–736.
- [3] H.-H. Zhang, X.-Q. Zhang, Q.-S. Xue, Yan-Luo, J.-L. Huang, S. Zhang, H.-J. Shao, H. Lu, W.-Y. Wang, B.-W. Yu, The BDNF/TrkB signaling pathway is involved in heat hyperalgesia mediated by Cdk5 in rats, *PLoS One* 9 (2014) e85536.
- [4] N. Khan, M.T. Smith, Neurotrophins and neuropathic pain: role in pathobiology, *Mol. Basel Switz.* 20 (2015) 10657–10688.
- [5] E. Einarsdottir, A. Carlsson, J. Minde, G. Toolanen, O. Svensson, G. Solders, G. Holmgren, D. Holmberg, M. Holmberg, A mutation in the nerve growth factor beta gene (NGFB) causes loss of pain perception, *Hum. Mol. Genet.* 13 (2004) 799–805.
- [6] L. McKelvey, G.D. Shorten, G.W. O’Keefe, Nerve growth factor-mediated regulation of pain signalling and proposed new intervention strategies in clinical pain management, *J. Neurochem.* 124 (2013) 276–289 (and references therein).
- [7] A. Nakagawara, Trk receptor tyrosine kinases: a bridge between cancer and neural development, *Cancer Lett.* 169 (2001) 107–114.
- [8] T. Wang, D. Yu, M.L. Lamb, Trk kinase inhibitors as new treatments for cancer and pain, *Expert Opin. Ther. Pat.* 19 (2009) 305–319.
- [9] M.B. Schneider, J. Standop, A. Ulrich, W. Wittel, H. Friess, A. Andrén-Sandberg, P.M. Pour, Expression of nerve growth factors in pancreatic neural tissue and pancreatic cancer, *J. Histochem. Cytochem.* 49 (2001) 1205–1210.
- [10] Y. Zhang, C. Dang, Q. Ma, Y. Shimahara, Expression of nerve growth factor receptors and their prognostic value in human pancreatic cancer, *Oncol. Rep.* 14 (2005) 161–171.
- [11] D. Liu, Y. Zhang, C. Dang, Q. Ma, W. Lee, W. Chen, siRNA directed against TrkA sensitizes human pancreatic cancer cells to apoptosis induced by gemcitabine through an inactivation of PI3K/Akt-dependent pathway, *Oncol. Rep.* 18 (2007) 673–677.
- [12] J. Ma, Y. Jiang, Y. Jiang, Y. Sun, X. Zhao, Expression of nerve growth factor and tyrosine kinase receptor A and correlation with perineural invasion in pancreatic cancer, *J. Gastroenterol. Hepatol.* 23 (2008) 1852–1859.
- [13] A.T. Weeraratna, J.T. Arnold, D.J. George, A. DeMarzo, J.T. Isaacs, Rational basis for Trk inhibition therapy for prostate cancer, *Prostate* 45 (2000) 140–148.
- [14] C. Festuccia, P. Muzi, G.L. Gravina, D. Millimaggi, S. Speca, V. Dolo, E. Ricevuto, C. Vicentini, M. Bologna, Tyrosine kinase inhibitor CEP-701 blocks the NTRK1/NGF receptor and limits the invasive capability of prostate cancer cells in vitro, *Int. J. Oncol.* 30 (2007) 193–200.

- [15] A.G. Papatsoris, D. Liolitsa, C. Deliveliotis, Manipulation of the nerve growth factor network in prostate cancer, *Expert Opin. Investig. Drugs* 16 (2007) 303–309.
- [16] C. Lagadec, S. Meignan, E. Adriaenssens, B. Foveau, E. Vanhecke, R. Romon, R.A. Toillon, B. Ombrore, H. Hondermarck, X. Le Bourhis, TrkA overexpression enhances growth and metastasis of breast cancer cells, *Oncogene* 28 (2009) 1960–1970.
- [17] W. Jin, G.M. Kim, M.S. Kim, M.H. Lim, C. Yun, J. Jeong, J.-S. Nam, S.-J. Kim, TrkC plays an essential role in breast tumor growth and metastasis, *Carcinogenesis* 31 (2010) 1939–1947.
- [18] D.B. Cornelio, C.B. de Farias, D.S. Prusch, T.E. Heinen, R.P. Dos Santos, A.L. Abujamra, G. Schwartzmann, R. Roesler, Influence of GRPR and BDNF/TrkB signaling on the viability of breast and gynecologic cancer cells, *Mol. Clin. Oncol.* 1 (2013) 148–152.
- [19] B. Davidson, R. Reich, P. Lazarovici, J.M. Nesland, M. Skrede, B. Risberg, C.G. Tropé, V.A. Flørenes, Expression and activation of the nerve growth factor receptor TrkA in serous ovarian carcinoma, *Clin. Cancer Res.* 9 (2003) 2248–2259.
- [20] X. Campos, Y. Muñoz, A. Selman, R. Yazigi, L. Moyano, C. Weinstein-Oppenheimer, H.E. Lara, C. Romero, Nerve growth factor and its high-affinity receptor TrkA participate in the control of vascular endothelial growth factor expression in epithelial ovarian cancer, *Gynecol. Oncol.* 104 (2007) 168–175.
- [21] V.A. Flørenes, G.M. Maelandsmo, R. Holm, R. Reich, P. Lazarovici, B. Davidson, Expression of activated TrkA protein in melanocytic tumors: relationship to cell proliferation and clinical outcome, *Am. J. Clin. Pathol.* 122 (2004) 412–420.
- [22] A. Greco, E. Roccatto, M.A. Pierotti, Trk oncogenes in papillary thyroid carcinoma, *Cancer Treat. Res.* 122 (2005) 207–219.
- [23] A. Tacconelli, A.R. Farina, L. Cappabianca, G. DeSantis, A. Tessitore, A. Vetuschi, R. Sferra, N. Rucci, B. Argenti, I. Screpanti, A. Gulino, A.R. Mackay, TrkA alternative splicing: a regulated tumor-promoting switch in human neuroblastoma, *Cancer Cell* 6 (2004) 347–360.
- [24] A. Schramm, J.H. Schulte, K. Astrahantseff, O. Apostolov, V.V. Limpt, H. Sieverts, S. Kuhfittig-Kulle, P. Pfeiffer, R. Versteeg, A. Eggert, Biological effects of TrkA and TrkB receptor signaling in neuroblastoma, *Cancer Lett.* 228 (2005) 143–153.
- [25] S. Douma, T. van Laar, J. Zevenhoven, R. Meuwissen, E. van Garderen, D.S. Peeper, Suppression of anoikis and induction of metastasis by the neurotrophic receptor TrkB, *Nature* 430 (2004) 1034–1039.
- [26] M. Takahashi, S. Hayashi, A. Kakita, K. Wakabayashi, M. Fukuda, S. Kameyama, R. Tanaka, H. Takahashi, H. Nawa, Patients with temporal lobe epilepsy show an increase in brain-derived neurotrophic factor protein and its correlation with neuropeptide Y, *Brain Res.* 818 (1999) 579–582.
- [27] F. Boulle, G. Kenis, M. Cazorla, M. Hamon, H.W.M. Steinbusch, L. Lanfumey, D.L.A. van den Hove, TrkB inhibition as a therapeutic target for CNS-related disorders, *Prog. Neurobiol.* 98 (2012) 197–206.
- [28] J.O. McNamara, H.E. Scharfman, Temporal lobe epilepsy and the BDNF receptor, TrkB, in: J.L. Noebels, M. Avoli, M.A. Rogawski, R.W. Olsen, A.V. Delgado-Escueta (Eds.), *Jasper's Basic Mechanisms of the Epilepsies*, fourth ed., National Center for Biotechnology Information, US, Bethesda, MD, 2012.
- [29] G. Liu, B. Gu, X.P. He, R.B. Joshi, H.D. Wackerle, R.M. Rodriguez, W.C. Wetsel, J.O. McNamara, Transient inhibition of TrkB kinase after status epilepticus prevents development of temporal lobe epilepsy, *Neuron* 79 (2013) 31–38.
- [30] J. Budini, T. Bellettini-Santos, F. Mina, M.L. Garcez, A.I. Zugno, The involvement of BDNF, NGF and GDNF in aging and Alzheimer's disease, *Aging Dis.* 6 (2015) 331–341.
- [31] C.-J. Xu, J.-L. Wang, W.-L. Jin, The emerging therapeutic role of NGF in Alzheimer's disease, *Neurochem. Res.* (2016), <http://dx.doi.org/10.1007/s11064-016-1829-9>.
- [32] C. McCarthy, E. Walker, Tropomyosin receptor kinase inhibitors: a patent update 2009–2013, *Expert Opin. Ther. Pat.* 24 (2014) 731–744.
- [33] A.R. Katritzky, M. Kuanar, S. Slavov, C.D. Hall, M. Karelson, I. Kahn, D.A. Dobchev, Quantitative correlations of physical and chemical properties with chemical structure; utility for prediction, *Chem. Rev.* 110 (2010) 5714–5789.
- [34] M. Karelson, D.A. Dobchev, G. Karelson, T. Tamm, K. Tamm, A. Nikonov, M. Mutso, A. Merits, Fragment-based development of HCV protease inhibitors for the treatment of hepatitis C, *Curr. Comput. Aided Drug Des.* 8 (2012) 55–61.
- [35] E.R. Wood, L. Kuyper, K.G. Petrov, R.N. Hunter III, P.A. Harris, K. Lackey, Discovery and in vitro evaluation of potent TrkA kinase inhibitors: oxindole and aza-oxindoles, *Bioorg. Med. Chem. Lett.* 14 (2004) 953–957.
- [36] S. Hong, J. Kim, J.H. Seo, K.H. Jung, S.-S. Hong, S. Hong, Design, synthesis, and evaluation of 3,5-disubstituted 7-azaindoles as Trk inhibitors with anticancer and antiangiogenic activities, *J. Med. Chem.* 55 (2012) 5337–5349.
- [37] P. Albaugh, Y. Fan, Y. Mi, F. Sun, F. Adrian, N. Li, Y. Jia, Y. Sarkisova, A. Kreuzsch, T. Hood, M. Lu, G. Liu, S. Huang, Z. Liu, J. Loren, T. Tuntland, D.S. Karanewsky, H.M. Seidel, V. Molteni, Discovery of GNF-5837, a selective Trk inhibitor with efficacy in rodent cancer tumor models, *ACS Med. Chem. Lett.* 3 (2012) 140–145.
- [38] M. Karelson, *Molecular Descriptors in QSAR/QSPR*, Wiley & Sons, New York, 2000.
- [39] M. Karelson, G. Karelson, T. Tamm, I. Tulp, J. Jänes, K. Tamm, A. Lomaka, D. Savchenko, D. Dobchev, QSAR study of pharmacological permeabilities, *Arkiv* (2009) 218–238.
- [40] J.H. Zhang, T.D.Y. Chung, K.R. Oldenburg, A simple statistical parameter for use in evaluation and validation of high throughput screening assays, *J. Biomol. Screen* 4 (1999) 67–73.
- [41] K. Thress, T. Macintyre, H. Wang, D. Whitston, Z.-Y. Liu, E. Hoffmann, T. Wang, J.L. Brown, K. Webster, C. Omer, P.E. Zage, L. Zeng, P.A. Zweidler-McKay, Identification and preclinical characterization of AZ-23, a novel, selective, and orally bioavailable inhibitor of the Trk kinase pathway, *Mol. Cancer Ther.* 8 (2009) 1818–1827.
- [42] J.J. Irwin, T. Sterling, M.M. Mysinger, E.S. Bolstad, R.G. Coleman, ZINC: a free tool to discover chemistry for biology, *J. Chem. Inf. Model* 52 (2012) 1757–1768.
- [43] <http://www.molport.com/shop/index>; MolPort, Lacplesa iela 41, Rīga, LV-1011, Latvia.
- [44] <http://www.ebi.ac.uk/chembl/>.
- [45] F. Carta, C.T. Supuran, Diuretics with carbonic anhydrase inhibitory action: a patent and literature review (2005–2013), *Expert Opin. Ther. Pat.* 23 (2013) 681–691.
- [46] Z. Chen, Z.C. Wang, X.Q. Yan, P.F. Wang, X.Y. Lu, L.W. Chen, H.L. Zhu, H.W. Zhang, Design, synthesis, biological evaluation and molecular modeling of dihydropyrazole sulphonamide derivatives as potential COX-1/COX-2 inhibitors, *Bioorg. Med. Chem. Lett.* 25 (2015) 1947–1951.
- [47] S. Barbey, L. Goossens, T. Taverne, J. Cornet, V. Choessel, C. Rouaud, G. Gimeno, S. Yannic-Arnoult, C. Michaux, C. Charlier, R. Houssin, J.P. Henichart, Synthesis and activity of a new methoxytetrahydropryan derivative as dual cyclooxygenase-2/5-lipoxygenase inhibitor, *Bioorg. Med. Chem. Lett.* 12 (2002) 779–782.
- [48] J.H. Cui, J. Ju, M.H. Yoon, Pharmacology of cannabinoid receptor agonists and a cyclooxygenase-2 inhibitor in rat bone tumor pain, *Pharmacology* 92 (2013) 150–157.
- [49] J.J. Chen, K.C. Hung, K. Lu, S.W. Yu, C.C. Chang, C.C. Liu, J. Spielberger, P.Y. Ku, P.H. Tan, The pre-emptive analgesic effect of a cyclooxygenase-2 inhibitor in a rat model of acute postoperative pain, *Anesthesia* 67 (2012) 1225–1231.
- [50] J.A. Baron, R.S. Sandler, R.S. Bresalier, H. Quan, R. Riddell, A. Lanis, J.A. Bolognese, B. Oxenius, K. Horgan, S. Loftus, D.G. Morton, A randomized trial of rofecoxib for the chemoprevention of colorectal adenomas, *Gastroenterology* 131 (2006) 1674–1682.
- [51] M. Vera, E. Barcia, S. Negro, P. Marcianes, L. Garcia-Garcia, K. Slowing, A. Fernández-Carballido, New celecoxib multiparticulate systems to improve glioblastoma treatment, *Int. J. Pharm.* 473 (2014) 518–527.
- [52] X. Pang, Z. Liu, G. Zhai, Advances in non-peptidomimetic HIV protease inhibitors, *Curr. Med. Chem.* 21 (2014) 1997–2011.
- [53] I. Usach, V. Melis, J.-E. Peris, Non-nucleoside reverse transcriptase inhibitors: a review on pharmacokinetics, pharmacodynamics, safety and tolerability, *J. Int. AIDS Soc.* 16 (2013) 18567.
- [54] D.A. Smith (Ed.), *Metabolism, Pharmacokinetics, and Toxicity of Functional Groups: Impact of Chemical Building Blocks on ADMET*, RSC, London, 2010.
- [55] T.B. Vree, *Clinical Pharmacokinetics of Sulfonamides and Their Metabolites*, An Encyclopedia, Karger, Basel, 1987.
- [56] J.Y.Q. Lai, P.J. Cox, R. Patel, S. Sadiq, D.J. Aldous, S. Thurairatnam, K. Smith, D. Wheeler, S. Jagpal, S. Parveen, G. Fenton, T.K.P. Harrison, C. McCarthy, P. Bamborough, Potent small molecule inhibitors of spleen tyrosine kinase (Syk), *Bioorg. Med. Chem. Lett.* 13 (2003) 3111–3114.
- [57] Y. Gao, S.P. Davies, M. Augustin, A. Woodward, U.A. Patel, R. Kovelman, K.J. Harvey, A broad activity screen in support of a chemogenomic map for kinase signalling research and drug discovery, *Biochem. J.* 451 (2013) 313–328.
- [58] Schrödinger Release, Maestro, Version 9.3, Schrödinger, LLC, New York, NY, 2012, 2012.
- [59] H. Xu, D. Izrailev, D.K. Agrafiotis, Conformational sampling by self-organization, *J. Chem. Inf. Comput. Sci.* 43 (2003) 1186–1191.
- [60] T.A. Halgren, MMFF VI, MMFF94s option for energy minimization studies, *J. Comput. Chem.* 20 (1999) 720–729.
- [61] J.J.P. Stewart, MOPAC program package 6.0, QCPE No. 455, 1990.
- [62] M.J.S. Dewar, E.G. Zoebisch, E.F. Healy, J.J.P. Stewart, Development and use of quantum mechanical molecular models. 76. AM1: a new general purpose quantum mechanical molecular model, *J. Am. Chem. Soc.* 107 (1985) 3902–3909.
- [63] HyperChem 8.0, Molecular modeling package, Hypercube Software, Gainesville, FL.
- [64] Y.A. Sidorova, K. Mätilä, M. Paveliev, M. Lindahl, E. Piranen, J. Milbrandt, U. Arumäe, M. Saarma, M.M. Bespalov, Persephin signaling through GFR α 1: the potential for the treatment of Parkinson's disease, *Mol. Cell. Neurosci.* 44 (2010) 223–232.
- [65] M. Sepp, K. Kannike, A. Eesmaa, M. Urb, T. Timmsku, Functional diversity of human basic helix-loop-helix transcription factor TCF4 isoforms generated by alternative 5' exon usage and splicing, *PLoS One* 6 (2011) e22138.
- [66] P. Wareski, A. Vaarmann, V. Choubey, D. Safulina, J. Liiv, M. Kuum, A. Kaasik, PGC-1 α and PGC-1 β regulate mitochondrial density in neurons, *J. Biol. Chem.* 284 (2009) 21379–21385.
- [67] G. Wang, X. Liu, T. Huang, Y. Kuang, L. Lin, X. Feng, Asymmetric catalytic 1,3-dipolar cycloaddition reaction of nitrile imines for the synthesis of chiral spiro-pyrazoline-oxindoles, *Org. Lett.* 15 (2013) 76–79.

SUPPLEMENTARY MATERIAL

Indole-like Trk receptor antagonists

Jaana Tammiku-Taul ^{a,b,1}, Rahel Park ^{c,1,2}, Kaur Jaanson ^c, Kristi Luberg ^c, Dimitar A. Dobchev ^b, Dzmitry Kananovich ^b, Artur Noole ^b, Merle Mandel ^d, Allen Kaasik ^d, Margus Lopp ^b, Tõnis Timmusk ^{c,*}, Mati Karelson ^{a,b,*}

^a *University of Tartu, Institute of Chemistry, Ravila 14A, Tartu 50411, Estonia*

^b *Tallinn University of Technology, Department of Chemistry, Akadeemia 15, Tallinn 12618, Estonia*

^c *Tallinn University of Technology, Department of Gene Technology, Akadeemia 15, Tallinn 12618, Estonia*

^d *University of Tartu, Institute of Biomedicine and Translational Medicine, Department of Pharmacology, Ravila 19, Tartu 50411, Estonia*

AUTHOR INFORMATION

Corresponding Author

* *E-mail addresses:* tonis.timmusk@ttu.ee (T. Timmusk), mati.karelson@ut.ee (M. Karelson)

Author Contributions

¹ These authors contributed equally to this work.

² Present address: Laboratory for Genetics and Genomics, Centre of Microbial and Plant Genetics (CMPG), Department of Microbial and Molecular Systems, KU Leuven, Gaston Geenslaan 1, 3001 Leuven (Heverlee), Belgium; VIB Laboratory of Systems Biology, Gaston Geenslaan 1, 3001 Leuven (Heverlee), Belgium.

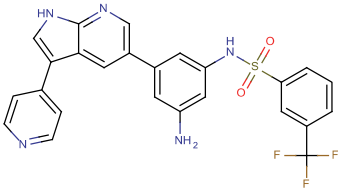
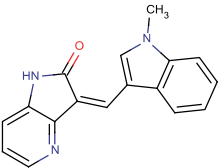
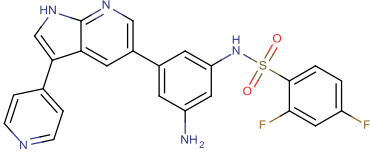
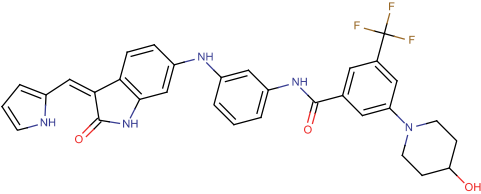
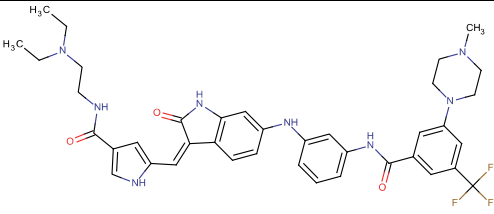
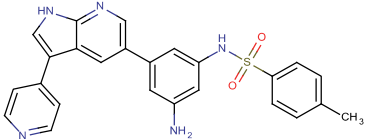
Contents

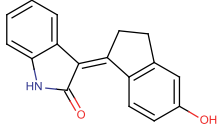
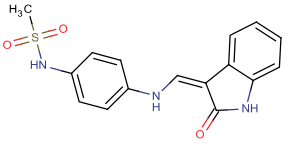
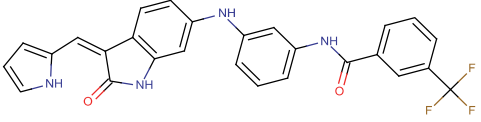
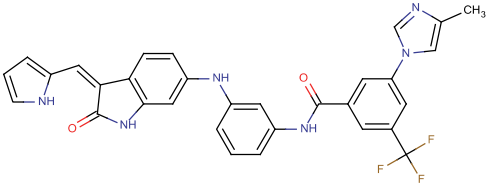
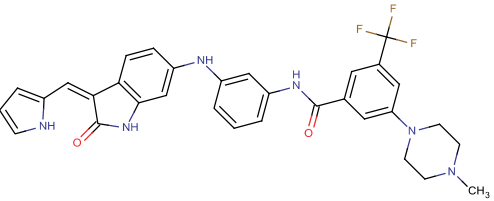
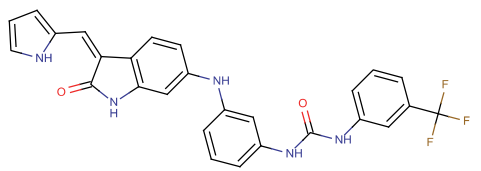
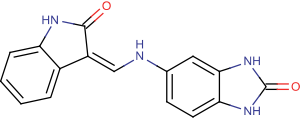
1. Molecular data set	3
2. Experimental technology	10
3. Data for Williams graph	12
4. Molecular docking.....	14
5. Kinase profiling.....	17
6. References	18

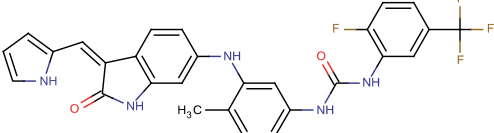
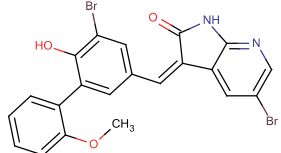
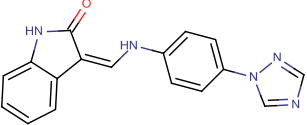
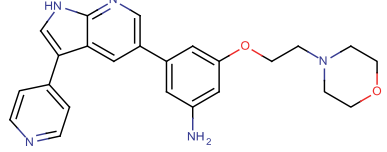
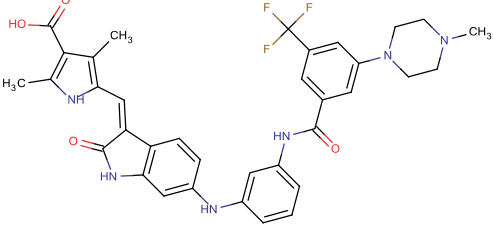
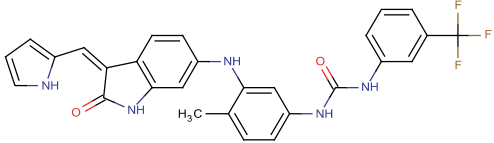
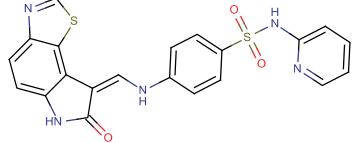
1. Molecular data set

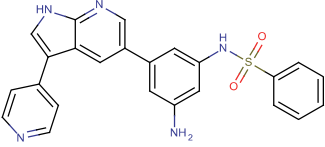
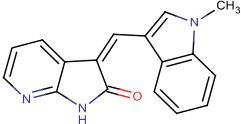
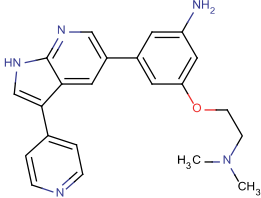
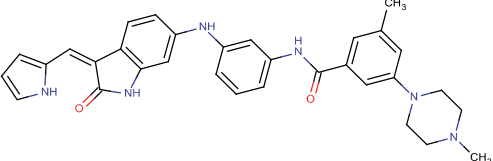
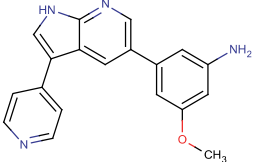
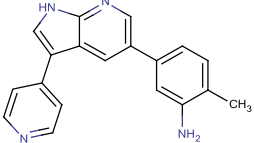
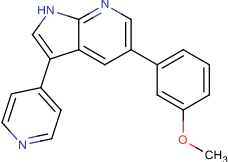
Table S1

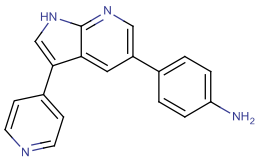
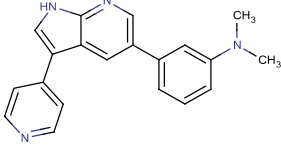
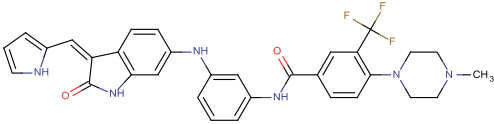
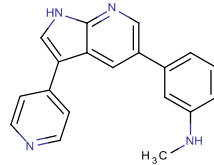
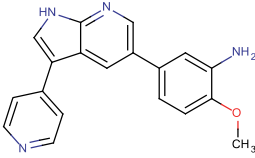
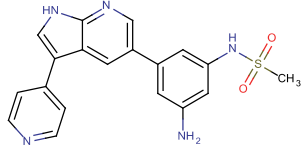
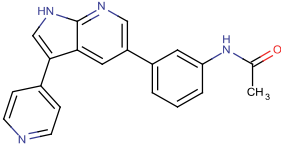
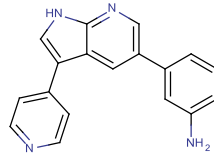
Molecular data set (47 compounds) and the corresponding IC_{50} (in units nM) and $\log IC_{50}$ values.

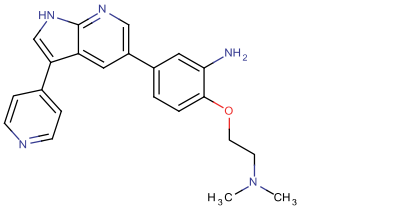
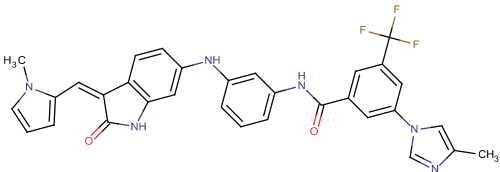
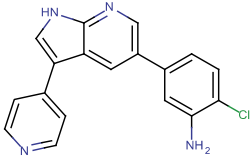
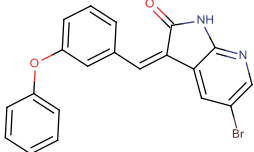
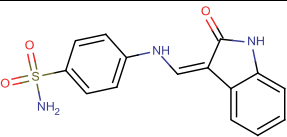
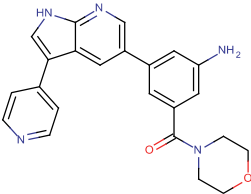
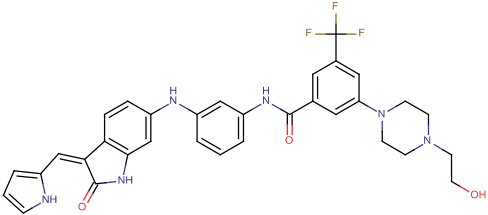
No.	ChEMBL ID	Structure	IC_{50}^a	$\log IC_{50}$	Ref.
1	CHEMBL2152288		1.67	0.223	[1]
2	CHEMBL176544		2.00	0.301	[2]
3	CHEMBL2152287		2.97	0.473	[1]
4	CHEMBL2037213		3.00	0.477	[3]
5	CHEMBL2037221		4.00	0.602	[3]
6	CHEMBL2152286		4.62	0.665	[1]

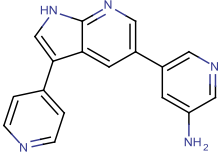
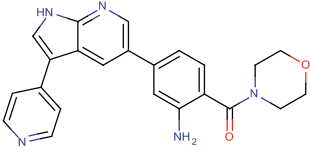
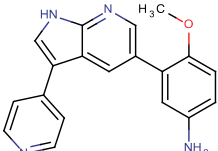
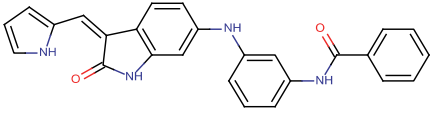
7 ^b	CHEMBL2152289		5.41	0.733	[1]
8	CHEMBL175321		6.00	0.778	[2]
9	CHEMBL1794058		6.00	0.778	[2]
10	CHEMBL2037208		7.00	0.845	[3]
11	CHEMBL2037209		7.00	0.845	[3]
12	CHEMBL2037211		7.00	0.845	[3]
13	CHEMBL2037224		7.00	0.845	[3]
14	CHEMBL1794057		7.00	0.845	[2]

15	CHEMBL2037226		8.00	0.903	[3]
16	CHEMBL176857		8.00	0.903	[2]
17	CHEMBL1794056		8.00	0.903	[2]
18	CHEMBL2152283		8.36	0.922	[1]
19	CHEMBL2037222		9.00	0.954	[3]
20	CHEMBL2037225		9.00	0.954	[3]
21	CHEMBL1276446		9.00	0.954	[2]

22	CHEMBL2152285		9.40	0.973	[1]
23	CHEMBL172179		12.00	1.079	[2]
24	CHEMBL2152282		13.63	1.134	[1]
25	CHEMBL2037210		16.00	1.204	[3]
26	CHEMBL2152280		18.60	1.270	[1]
27	CHEMBL2152277		22.20	1.346	[1]
28	CHEMBL2152272		22.70	1.356	[1]

29	CHEMBL2152274		25.02	1.398	[1]
30	CHEMBL2152271		26.47	1.423	[1]
31 ^b	CHEMBL2037212		27.00	1.431	[3]
32	CHEMBL2152270		31.40	1.497	[1]
33	CHEMBL2152275		33.20	1.521	[1]
34	CHEMBL2152284		33.75	1.528	[1]
35	CHEMBL2152273		34.30	1.535	[1]
36	CHEMBL2152264		42.70	1.630	[1]

37	CHEMBL2152279		47.00	1.672	[1]
38 ^b	CHEMBL2037217		49.00	1.690	[3]
39	CHEMBL2152276		53.70	1.730	[1]
40 ^b	CHEMBL369490		61.00	1.785	[2]
41	CHEMBL1794059		63.00	1.799	[2]
42	CHEMBL2152281		64.70	1.811	[1]
43 ^b	CHEMBL2037214		68.00	1.833	[3]

44	CHEMBL2152269		69.60	1.843	[1]
45	CHEMBL2152278		88.60	1.947	[1]
46 ^b	CHEMBL2152290		110.30	2.043	[1]
47 ^b	CHEMBL2037194		160.00	2.204	[3]

^a IC₅₀'s were determined in biochemical assays.

^b Identified outliers from the final QSAR model.

2. Experimental technology

Table S2

Experimentally tested compounds.

Compound (ChEMBL ID)	Provider (catalogue ID)	Concentrations used to determine the IC₅₀ of TrkA signaling (PC- 12/luc/Elk1 cells)	Concentrations used to determine the IC₅₀ of TrkB signaling (MG87/TrkB/luc/Elk1 cells)
AZ-23 (CHEMBL457614)	Axon Medchem (1610)	5 nM; 2.5 nM; 1 nM; 0.5 nM; 0.1 nM	
2 (CHEMBL1214654)	Key Organics (1X-0886)	5 μM; 1 μM; 500 nM; 5 nM; 2.5 nM	
2a21 (CHEMBL104279)	Millipore (574711)	500 nM; 50 nM; 25 nM; 5 nM; 2.5 nM; 1 nM	
2a41 (CHEMBL261425)	Millipore (217695)	-	
2a31 (CHEMBL190134)	Molport (002-894-472)	50 μM; 5 μM; 2.5 μM; 1 μM; 500 nM; 50 nM	
2a33 (CHEMBL382707)	Molport (001-807-694)	-	
2a42 (CHEMBL471375)	Molport (005-910-302)	5 μM; 2.5 μM; 1 μM; 500 nM; 250 nM; 50 nM	
2a27 (CHEMBL321955)	Santa Cruz (sc-206507)	1 μM; 500 nM; 250 nM; 50 nM; 5 nM; 1 nM	
2a22 (CHEMBL104333)	Otava (7070707050)	50 nM; 25 nM; 5 nM; 2.5 nM	1 μM; 300 nM; 100 nM; 30 nM; 10 nM; 3 nM
2a23 (CHEMBL106226)	In-house synthesis	5 μM; 1 μM; 100 nM; 10 nM; 5 nM; 1 nM	
2a25 (CHEMBL322153)	In-house synthesis	5 μM; 1 μM; 100 nM; 10 nM; 5 nM; 1 nM	1 μM; 300 nM; 100 nM; 30 nM; 10 nM; 3 nM
3a23 (-)	In-house synthesis	5 μM; 1 μM; 100 nM; 10 nM; 5 nM; 1 nM	
3a25 (-)	In-house synthesis	5 μM; 1 μM; 100 nM; 10 nM; 5 nM; 1 nM	
4a22 (CHEMBL104519)	In-house synthesis	5 μM; 1 μM; 100 nM; 50 nM; 10 nM; 5 nM; 1 nM	300 nM; 100 nM; 30 nM; 10 nM; 3 nM; 1 nM

Table S3Calculated IC₅₀ values on TrkA signaling measured in PC-12/luc/Elk1 cells.

Compound (isomer) ^a	Count	IC ₅₀ (nM)			logIC ₅₀ (nM)		pIC ₅₀	
		Geom. mean	Geom. SD +	Geom. SD -	Mean	SD	Mean	SD
AZ-23	1	0.26	-	-	-0.585	-	9.585	-
2 (Z)	1	886.53	-	-	2.948	-	6.052	-
2a21 (Z)	2	36.70	8.33	6.79	1.565	0.089	7.435	0.089
2a22 (Z)	6	13.07	1.33	1.20	1.116	0.042	7.884	0.042
2a27 (Z)	1	341.76	-	-	2.534	-	6.466	-
2a31 (E)	1	2760.22	-	-	3.441	-	5.559	-
2a42 (Z)	1	998.49	-	-	2.999	-	6.001	-
2a23 (Z)	2	102.57	0.18	0.18	2.011	0.001	6.989	0.001
2a25 (Z)	4	45.99	7.09	6.14	1.663	0.062	7.337	0.062
3a23 (Z)	1	365.69	-	-	2.563	-	6.437	-
3a25 (Z)	2	92.82	3.79	3.65	1.968	0.017	7.032	0.017
4a22 (Z)	4	9.98	3.94	2.82	0.999	0.144	8.001	0.144

^a After several months, a mixture of isomers was detected in a repeated measurement.

3. Data for Williams graph

Table S4

Data set (T – training; E – external test), descriptors (D1 – Lowest atomic state energy (AM1) for C atoms; D2 – Lowest atomic state energy (AM1) for H atoms; D3 – Max electrophilic reactivity index (AMI) for C atoms; D4 – Molecular volume / XYZ box (AM1)) and parameters for the model (leverage value (h); standardized residual (r'); predicted (Pred.) and observed (Obs.) $\log[C_{50}]$; difference of predicted and observed values (Diff.); standard deviation (s^2)).

ID	Data set	D1	D2	D3	D4	h	r'	Pred.	Obs.	Diff.	s^2
1	T	-104.595	-7.455	0.033	0.205	0.252	0.314	0.294	0.223	0.071	5.01E-03
2	T	-103.263	-7.719	0.028	0.415	0.258	1.834	0.714	0.301	0.413	1.70E-01
3	T	-104.590	-7.428	0.035	0.223	0.285	-1.363	0.166	0.473	-0.307	9.41E-02
4	T	-103.443	-7.790	0.029	0.257	0.053	1.675	0.854	0.477	0.377	1.42E-01
5	T	-103.545	-7.941	0.031	0.148	0.148	1.029	0.834	0.602	0.232	5.36E-02
6	T	-104.507	-7.724	0.017	0.297	0.207	0.789	0.842	0.665	0.177	3.15E-02
7	T	-103.410	-7.640	0.028	0.417	0.251	-0.335	0.703	0.778	-0.075	5.68E-03
8	T	-103.147	-9.882	0.004	0.368	0.890	0.023	0.783	0.778	0.005	2.75E-05
9	T	-103.423	-7.466	0.032	0.241	0.082	0.548	0.968	0.845	0.123	1.52E-02
10	T	-103.636	-7.768	0.034	0.157	0.131	-0.411	0.752	0.845	-0.093	8.57E-03
11	T	-103.426	-7.924	0.031	0.186	0.099	0.149	0.879	0.845	0.034	1.13E-03
12	T	-103.426	-7.445	0.030	0.251	0.076	0.907	1.049	0.845	0.204	4.16E-02
13	T	-103.151	-7.500	0.032	0.301	0.136	0.561	0.971	0.845	0.126	1.59E-02
14	T	-103.425	-7.767	0.031	0.241	0.062	-0.258	0.845	0.903	-0.058	3.37E-03
15	T	-103.569	-7.824	0.029	0.244	0.047	-0.329	0.829	0.903	-0.074	5.47E-03
16	T	-104.050	-7.491	0.020	0.431	0.285	-0.619	0.764	0.903	-0.139	1.94E-02
17	T	-103.457	-7.799	0.019	0.255	0.085	2.280	1.435	0.922	0.513	2.63E-01
18	T	-103.407	-7.924	0.031	0.190	0.098	-0.351	0.875	0.954	-0.079	6.23E-03
19	T	-103.454	-7.808	0.028	0.213	0.060	0.186	0.996	0.954	0.042	1.75E-03
20	T	-104.402	-7.413	0.023	0.236	0.142	-0.114	0.928	0.954	-0.026	6.57E-04
21	T	-104.516	-7.446	0.017	0.232	0.223	0.752	1.142	0.973	0.169	2.87E-02
22	T	-103.402	-7.734	0.029	0.316	0.086	-1.279	0.791	1.079	-0.288	8.29E-02

23	T	-103.372	-7.945	0.019	0.252	0.080	1.105	1.383	1.134	0.249	6.18E-02
24	T	-103.424	-7.918	0.031	0.188	0.098	-1.493	0.868	1.204	-0.336	1.13E-01
25	T	-103.368	-7.817	0.019	0.250	0.096	0.908	1.474	1.270	0.204	4.18E-02
26	T	-103.350	-7.806	0.018	0.307	0.081	0.235	1.399	1.346	0.053	2.79E-03
27	T	-103.349	-7.810	0.019	0.268	0.082	0.339	1.432	1.356	0.076	5.82E-03
28	T	-103.351	-7.474	0.019	0.331	0.146	0.548	1.521	1.398	0.123	1.52E-02
29	T	-103.352	-7.874	0.019	0.298	0.066	-0.417	1.329	1.423	-0.094	8.79E-03
30	T	-103.350	-7.888	0.019	0.278	0.071	-0.544	1.375	1.497	-0.122	1.50E-02
31	T	-103.351	-7.830	0.018	0.292	0.077	-0.513	1.405	1.521	-0.116	1.33E-02
32	T	-104.146	-7.453	0.011	0.277	0.250	0.195	1.572	1.528	0.044	1.93E-03
33	T	-103.501	-7.626	0.020	0.266	0.085	-0.442	1.436	1.535	-0.099	9.89E-03
34	T	-103.351	-7.475	0.018	0.297	0.156	-0.012	1.627	1.630	-0.003	7.46E-06
35	T	-103.350	-7.949	0.018	0.304	0.069	-1.566	1.320	1.672	-0.352	1.24E-01
36	T	-103.350	-7.427	0.019	0.301	0.159	-0.533	1.610	1.730	-0.120	1.44E-02
37	T	-103.222	-7.495	0.015	0.279	0.277	0.586	1.931	1.799	0.132	1.74E-02
38	T	-103.349	-7.756	0.019	0.225	0.129	-1.166	1.549	1.811	-0.262	6.88E-02
39	T	-103.371	-7.431	0.019	0.342	0.153	-1.583	1.487	1.843	-0.356	1.27E-01
40	T	-103.348	-7.771	0.018	0.237	0.131	-1.634	1.579	1.947	-0.368	1.35E-01
4a22	E	-104.429	-7.853	0.025	0.133	0.267	0.436	0.662	0.563	0.098	9.63E-03
2a22	E	-104.430	-7.828	0.026	0.135	0.260	0.373	0.661	0.577	0.084	7.03E-03
2a21	E	-104.427	-7.730	0.025	0.141	0.237	0.476	0.727	0.620	0.107	1.15E-02
3a23	E	-104.435	-7.495	0.026	0.147	0.214	0.524	0.836	0.718	0.118	1.39E-02
2a23	E	-104.434	-7.828	0.026	0.144	0.247	-1.333	0.629	0.929	-0.300	9.00E-02
3a25	E	-104.433	-7.837	0.025	0.138	0.258	-1.311	0.667	0.962	-0.295	8.70E-02
2a25	E	-104.432	-7.837	0.025	0.133	0.266	-1.420	0.684	1.004	-0.320	1.02E-01
2a27	E	-104.429	-7.490	0.026	0.152	0.207	-0.889	0.847	1.047	-0.200	4.01E-02
2a42	E	-103.171	-7.742	0.029	0.133	0.232	-0.358	1.329	1.410	-0.081	6.49E-03
2	E	-103.263	-7.756	0.027	0.244	0.064	-1.359	1.129	1.435	-0.306	9.36E-02
2a31	E	-103.175	-7.473	0.026	0.240	0.134	-1.266	1.381	1.666	-0.285	8.12E-02

4. Molecular docking

A conformational search of **4a22** for *Z* isomers was carried out with MacroModel of Maestro version 9.3 [4], using MMFFs force field in water solution [5]. Geometry optimizations of the obtained conformers in the gas phase were performed with Gaussian 09 program package [6], using CAM B3LYP [7] functional and 6-31+G* basis set. Frequency analysis was used to confirm whether the structure is a minimum (NImag = 0).

The crystal structure of TrkA was downloaded from Protein Data Bank (ID: 4AOJ) with resolution 2.75 Å measured by X-ray diffraction. The protein consisted of a homotrimer of Chain A, Chain B, and Chain C, thus, only Chain A was used. Water molecules were not removed.

AutoDock 4.2.1 [8] was used for the docking studies. All hydrogens were added to the protein. The potential binding partner groups for **4a22** to the TrkA receptor were taken from a previous study [9] and are shown in Table S5. The calculated grid maps had dimensions of 41×41×41 points with spacing of 0.375 Å. Number of Genetic Algorithm was set to 50 runs, other docking parameters were default settings. Genetic Algorithm with Local Search, i.e. Lamarckian GA was used as the docking algorithm.

Table S5
Studied binding partner groups in the TrkA receptor.

Binding site in TrkA	x-coordinate	y-coordinate	z-coordinate
Phe589 O	89.268	60.592	29.925
Glu590 O	91.100	57.741	29.914
Met592 NH	94.271	56.489	30.879
Met592 CB	94.621	54.173	30.106
Met592 O	96.815	55.675	29.636
Asp596 NH	98.905	52.333	24.858
Asp596 O	100.215	49.964	24.769
Arg599 O	105.214	48.998	24.434
Gly667 NH	90.110	50.125	24.146

All obtained conformers of **4a22** were used in the docking procedure. The most preferable binding partner was carbonyl oxygen of Met592 for *Z* isomer. The best corresponding docking score (i.e. AutoDock estimated binding energy) was -9.59 kcal/mol (estimated inhibition constant $K_i = 92.84$ nM) in case of not the lowest-energy conformer, embedded in the pocket (Fig. S1) used in the previous study with AZ-23 [9].

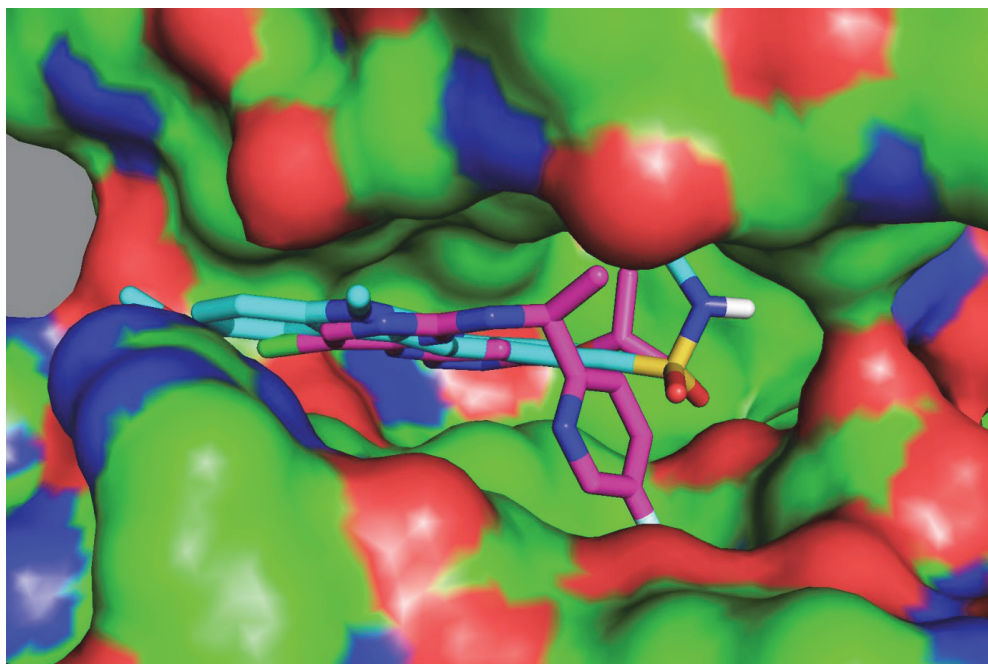


Fig. S1. Side-view with ligands sandwiched in the pocket (**4a22** is shown in cyan and AZ-23 in pink). Protein is in surface representation.

Compound **4a22** binds through the oxindole motif, forming hydrogen bonds to the backbone atoms of residues Glu590 (carbonyl oxygen), Tyr591 (amide NH), and Met592 (amide NH). The sulfonamide group has electrostatic interactions with zwitterion of Lys544 and carbonyl oxygen of Gly667. Indole moiety interacts with the carbonyl oxygen of Leu516 and amine group (NH₂) of Arg599. Besides, the hydrogens in methoxy substituent form additional hydrogen bonds with the backbone carbonyl oxygen of Leu516, hydroxyl group of Tyr591, and carbonyl oxygen of Arg593. All corresponding hydrogen bond (HB) lengths and electrostatic interactions are given in Table S6 and shown in Fig. S2.

Table S6Proposed binding partners for **4a22** (Z) in the TrkA ATP-binding site.

Length, Å	Interaction between atoms	Type of interaction [10]
2.7	oxindole, NH...O, Glu590	moderate HB
3.3	oxindole, NH...NH, Tyr591	weak HB
2.0	oxindole, HN...HN, Met592	strong HB
2.7	oxindole, O...HN, Met592	moderate HB
3.6	sulfonamide, NH...NH ₃ ⁺ , Lys544	weak HB
2.5	sulfonamide, O...O, Gly667	mostly electrostatic
2.9	sulfonamide, O...O, Gly667	mostly electrostatic
3.1	sulfonamide, S...O, Gly667	mostly electrostatic
3.1	indole, H ₃ C-N...O, Leu516	mostly electrostatic
3.5	indole, H ₃ C-N...H ₂ N, Arg599	weak HB
2.9	indole, N-CH ₃ ...O, Leu516	moderate HB
3.2	indole, O-CH ₃ ...OH, Tyr591	moderate HB
3.0	indole, O-CH ₃ ...O, Arg593	moderate HB
2.5	indole, H ₃ C-O...O, Arg593	mostly electrostatic

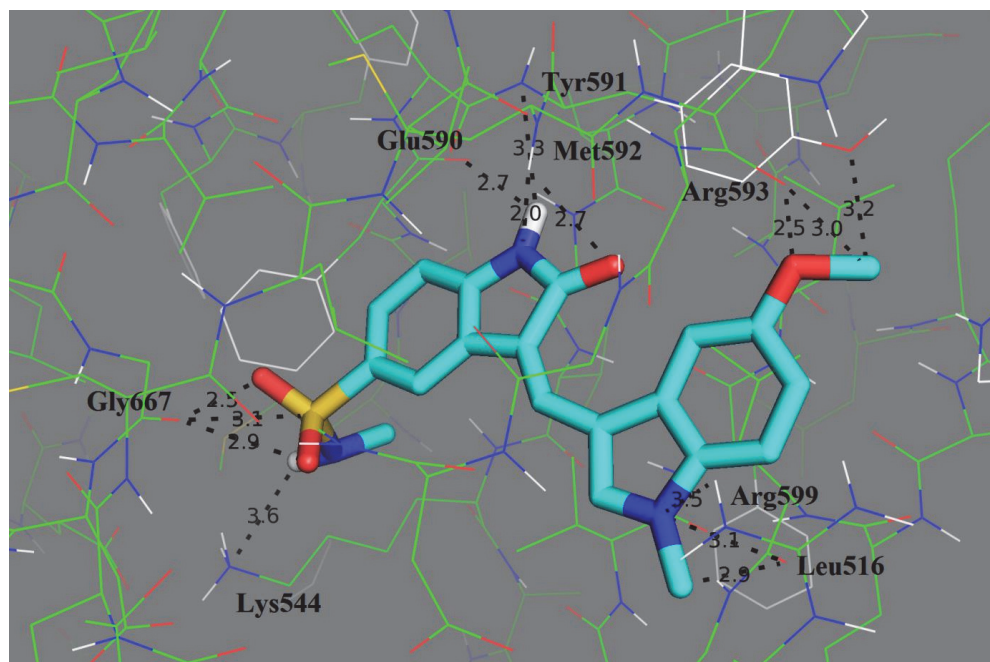


Fig. S2. Calculated binding mode of **4a22** in the ATP-binding site of TrkA (PDB ID: 4AOJ). Hydrogen bonds and electrostatic interactions with corresponding lengths in Å are shown with dashed lines.

5. Kinase profiling

Free software of Cell Signaling Technology, Inc. [11] was used to portray the position on the human kinase tree, and inhibition rate by compound **4a22**, of 48 kinases used *in vitro* kinase profiling experiment. Fig. S3 illustrates how effective is the compound **4a22** at 100 nM concentration to inhibit the tested kinases. Similar results were obtained for compounds **2a21**, **2a22**, **2a23**, **2a25**, and **3a25** (see Table 3). As a wide spectrum of human kinases is represented, it can be concluded that these compounds are relatively specific for TrkA.

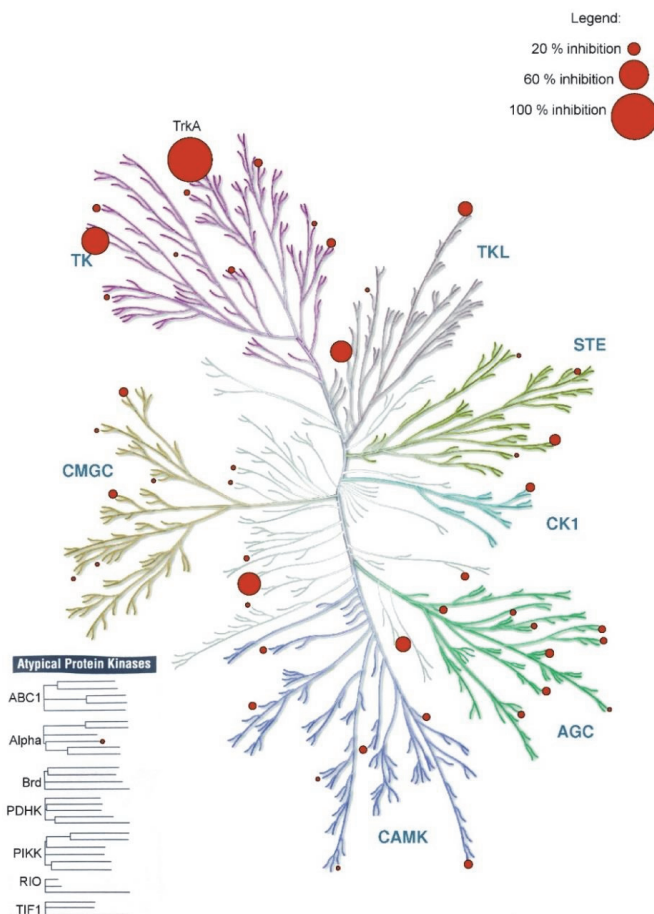


Fig. S3. Enzymes used for kinase profiling represent a wide spectrum of human kinases. Red circles highlight the positions of tested proteins in the human kinase tree. The size of the circle depicts the level of inhibition by **4a22** at 100 nM concentration. Illustration reproduced courtesy of Cell Signaling Technology, Inc. (www.cellsignal.com).

6. References

- [1] S. Hong, J. Kim, J.H. Seo, K.H. Jung, S.-S. Hong, S. Hong, Design, synthesis, and evaluation of 3,5-disubstituted 7-azaindoles as Trk inhibitors with anticancer and antiangiogenic activities, *J. Med. Chem.* 55 (2012) 5337-5349.
- [2] E.R. Wood, L. Kuyper, K.G. Petrov, R.N. Hunter III, P.A. Harris, K. Lackey, Discovery and in vitro evaluation of potent TrkA kinase inhibitors: oxindole and aza-oxindoles, *Bioorg. Med. Chem. Lett.* 14 (2004) 953-957.
- [3] P. Albaugh, Y. Fan, Y. Mi, F. Sun, F. Adrian, N. Li, Y. Jia, Y. Sarkisova, A. Kreuzsch, T. Hood, M. Lu, G. Liu, S. Huang, Z. Liu, J. Loren, T. Tuntland, D.S. Karanewsky, H.M. Seidel, V. Molteni, Discovery of GNF-5837, a selective Trk inhibitor with efficacy in rodent cancer tumor models, *ACS Med. Chem. Lett.* 3 (2012) 140-145.
- [4] Schrödinger Release 2012, Maestro, version 9.3, Schrödinger, LLC, New York, NY, 2012.
- [5] A. Cheng, S.A. Best, K.M. Merz, Jr., C.H. Reynolds, GB/SA water model for the Merck molecular force field (MMFF), *J. Mol. Graphics Modell.* 18 (2000) 273-282.
- [6] Gaussian 09, Revision C.01, M.J. Frisch, G.W. Trucks, H.B. Schlegel, G.E. Scuseria, M.A. Robb, J.R. Cheeseman, G. Scalmani, V. Barone, B. Mennucci, G.A. Petersson, H. Nakatsuji, M. Caricato, X. Li, H.P. Hratchian, A.F. Izmaylov, J. Bloino, G. Zheng, J.L. Sonnenberg, M. Hada, M. Ehara, K. Toyota, R. Fukuda, J. Hasegawa, M. Ishida, T. Nakajima, Y. Honda, O. Kitao, H. Nakai, T. Vreven, J.A. Montgomery, Jr., J.E. Peralta, F. Ogliaro, M. Bearpark, J.J. Heyd, E. Brothers, K.N. Kudin, V.N. Staroverov, T. Keith, R. Kobayashi, J. Normand, K. Raghavachari, A. Rendell, J.C. Burant, S.S. Iyengar, J. Tomasi, M. Cossi, N. Rega, J.M. Millam, M. Klene, J.E. Knox, J.B. Cross, V. Bakken, C. Adamo, J. Jaramillo, R. Gomperts, R.E. Stratmann, O. Yazyev, A.J. Austin, R. Cammi, C. Pomelli, J.W. Ochterski, R.L. Martin, K. Morokuma, V.G. Zakrzewski, G.A. Voth, P. Salvador, J.J. Dannenberg, S. Dapprich, A.D. Daniels, O. Farkas, J.B. Foresman, J.V. Ortiz, J. Cioslowski, D.J. Fox, Gaussian, Inc., Wallingford CT, 2010.
- [7] T. Yanai, D. Tew, N. Handy, A new hybrid exchange-correlation functional using the Coulomb-attenuating method (CAM-B3LYP), *Chem. Phys. Lett.* 393 (2004) 51-57.
- [8] G.M. Morris, R. Huey, W. Lindstrom, M.F. Sanner, R.K. Belew, D.S. Goodsell, A.J. Olson, Autodock4 and AutoDockTools4: automated docking with selective receptor flexibility, *J. Comput. Chem.* 16 (2009) 2785-2791.
- [9] T. Wang, M.L. Lamb, M.H. Block, A.M. Davies, Y. Han, E. Hoffmann, S. Ioannidis, J.A. Josey, Z.-Y. Liu, P.D. Lyne, T. MacIntyre, P.J. Mohr, C.A. Omer, T. Sjögren, K. Thress, B. Wang, H. Wang, D. Yu, H.-J. Zhang, Discovery of disubstituted imidazo[4,5-b]pyridines and purines as potent TrkA inhibitors, *ACS Med. Chem. Lett.* 3 (2012) 705-709.
- [10] G.A. Jeffrey, An introduction to hydrogen bonding, Oxford University Press, 1997.
- [11] Cell Signaling Technology, Inc., www.cellsignal.com

CURRICULUM VITAE

Name: Kristi Luberg (born Tamm)

Date and place of birth: 28.11.1982, Tallinn, Estonia

E-mail address: kristi.luberg@gmail.com

Education

2007–... Tallinn University of Technology, doctoral studies in chemistry and gene technology

2005–2007 University of Tartu, MSc in molecular and cell biology

2004–2004 Uppsala University, exchange student

2001–2005 University of Tartu, BSc in transgenic technology, cum laude

Language competence

Estonian native

English fluent

Russian basic

German basic

French basic

Special courses and conferences

2016: Society for Neuroscience Annual Meeting 2016, San Diego, USA

2016: Behavioural phenotyping of rodent disease models - potential and pitfalls, Tartu / Pühajärve, Estonia

2010: NGF 2010: Neurotrophic Factors in Health and Disease, Helsinki, Finland

2009: FEBS Practical and Lecture Course. Sofia School of Protein Science. From basic research to drug design, Sofia, Bulgaria

2008: 8th EMBL Transcription Meeting, Heidelberg, Germany

Employment

2007–... Tallinn University of Technology, Department of Gene Technology, engineer

2007–2015 Competence Center for Cancer Research, engineer

2005–2007 Estonian Biocentre, specialist

Supervised dissertations

- Rahel Park, Master's thesis, 2013, "TrkA alternative splicing and localization of putative intracellular fragments of TrkA and TrkB", Tallinn University of Technology, Department of Gene Technology.
- Elina Aleksejeva, Master's thesis, 2012, "Characterization of TrkA protein isoforms", Tallinn University of Technology, Department of Gene Technology.

- Elina Aleksejeva, Bachelor's thesis, 2010, "Cloning and characterization of novel TrkA isoforms", Tallinn University of Technology Department of Gene Technology.
- Rahel Park, Bachelor's thesis, 2009, "Human TrkA gene structure and alternative splicing ", Tallinn University of Technology, Department of Gene Technology.

Publications

Tammiku-Taul, J.*, Park, R.*, Jaanson, K., **Luberg, K.**, Dobchev, D.A., Kananovich, D., Noole, A., Mandel, M., Kaasik, A., Lopp, M., Timmusk, T., and Karelson, M. (2016). Indole-like Trk receptor antagonists. *Eur. J. Med. Chem.* 121, 541–552.

Luberg, K.*, Park, R.*, Aleksejeva, E.*, and Timmusk, T. (2015). Novel transcripts reveal a complex structure of the human TRKA gene and imply the presence of multiple protein isoforms. *BMC Neurosci.* 16, 78.

Luberg, K., Wong, J., Weickert, C.S., and Timmusk, T. (2010). Human TrkB gene: novel alternative transcripts, protein isoforms and expression pattern in the prefrontal cerebral cortex during postnatal development. *J. Neurochem.* 113, 952–964.

Tamm, K., Merits, A., and Sarand, I. (2008). Mutations in the nuclear localization signal of nsP2 influencing RNA synthesis, protein expression and cytotoxicity of Semliki Forest virus. *J. Gen. Virol.* 89, 676–686.

* Authors contributed equally

Inventions

A method for creating a viral genomic library, a viral genomic library and a kit for creating the same; Owners: Tartu Ülikool; Authors: Kai Rausalu, Valeria Lulla, Liis Karo-Astover, **Kristi Luberg**, Liane Viru, Inga Sarand, Andres Merits, Anna Iofik; Priority number: P200700047; Priority date: 31.08.2007.

ELULOOKIRJELDUS

Nimi: Kristi Luberg (sündinud Tamm)
Sünniaeg ja -koht: 28.11.1982, Tallinn, Estonia
E-posti aadress: kristi.luberg@gmail.com

Hariduskäik

2007–... Tallinna Tehnikaülikool, keemia ja geenitehnoloogia doktorantuur
2005–2007 Tartu Ülikool, MSc kraad molekulaarse ja rakubioloogia erialal
2004–2004 Uppsala Ülikool, vahetusüliõpilane
2001–2005 Tartu Ülikool, BSc kraad transgeense tehnoloogia erialal, *cum laude*

Keeleoskus

eesti	emakeel
inglise	kõrgtase
vene	algtase
saksa	algtase
prantsuse	algtase

Kursused ja konverentsid

2016: Society for Neuroscience Annual Meeting 2016, San Diego, USA
2016: Behavioural phenotyping of rodent disease models - potential and pitfalls, Tartu / Pühajärve, Eesti
2010: NGF 2010: Neurotrophic Factors in Health and Disease, Helsingi, Soome
2009: FEBS Practical and Lecture Course. Sofia School of Protein Science. From basic research to drug design, Sofia, Bulgaaria
2008: 8th EMBL Transcription Meeting, Heidelberg, Saksamaa

Teenistuskäik

2007–... Tallinna Tehnikaülikool, Geenitehnoloogia instituut, insener
2007–2015 Vähiuuringute Tehnoloogia Arenduskeskus AS, insener
2005–2007 Eesti Biokeskus, spetsialist

Juhendatud lõputööd

- Rahel Park, magistritöö, 2013, "TrkA alternative splicing and localization of putative intracellular fragments of TrkA and TrkB", Tallinna Tehnikaülikool, Geenitehnoloogia instituut.
- Elina Aleksejeva, magistritöö, 2012, "Characterization of TrkA protein isoforms", Tallinna Tehnikaülikool, Geenitehnoloogia instituut.
- Elina Aleksejeva, bakalaureusetöö, 2010, "Cloning and characterization of novel TrkA isoforms", Tallinna Tehnikaülikool, Geenitehnoloogia instituut.

- Rahel Park, bakalaureusetöö, 2009, "Human TrkA gene structure and alternative splicing ", Tallinna Tehnikaülikool, Geenitehnoloogia instituut.

Publikatsioonid

Tammiku-Taul, J.*, Park, R.*, Jaanson, K., **Luberg, K.**, Dobchev, D.A., Kananovich, D., Noole, A., Mandel, M., Kaasik, A., Lopp, M., Timmusk, T., and Karelson, M. (2016). Indole-like Trk receptor antagonists. *Eur. J. Med. Chem.* 121, 541–552.

Luberg, K.*, Park, R.*, Aleksejeva, E.*, and Timmusk, T. (2015). Novel transcripts reveal a complex structure of the human TRKA gene and imply the presence of multiple protein isoforms. *BMC Neurosci.* 16, 78.

Luberg, K., Wong, J., Weickert, C.S., and Timmusk, T. (2010). Human TrkB gene: novel alternative transcripts, protein isoforms and expression pattern in the prefrontal cerebral cortex during postnatal development. *J. Neurochem.* 113, 952–964.

Tamm, K., Merits, A., and Sarand, I. (2008). Mutations in the nuclear localization signal of nsP2 influencing RNA synthesis, protein expression and cytotoxicity of Semliki Forest virus. *J. Gen. Virol.* 89, 676–686.

* Autorid panustasid võrdselt

Patentsed leiutised

A method for creating a viral genomic library, a viral genomic library and a kit for creating the same; omanikud: Tartu Ülikool; autorid: Kai Rausalu, Valeria Lulla, Liis Karo-Astover, **Kristi Luberg**, Liane Viru, Inga Sarand, Andres Merits, Anna Iofik; Priority number: P200700047; Priority date: 31.08.2007.

**DISSERTATIONS DEFENDED AT
TALLINN UNIVERSITY OF TECHNOLOGY ON
NATURAL AND EXACT SCIENCES**

1. **Olav Kongas**. Nonlinear Dynamics in Modeling Cardiac Arrhythmias. 1998.
2. **Kalju Vanatalu**. Optimization of Processes of Microbial Biosynthesis of Isotopically Labeled Biomolecules and Their Complexes. 1999.
3. **Ahto Buldas**. An Algebraic Approach to the Structure of Graphs. 1999.
4. **Monika Drews**. A Metabolic Study of Insect Cells in Batch and Continuous Culture: Application of Chemostat and Turbidostat to the Production of Recombinant Proteins. 1999.
5. **Eola Valdre**. Endothelial-Specific Regulation of Vessel Formation: Role of Receptor Tyrosine Kinases. 2000.
6. **Kalju Lott**. Doping and Defect Thermodynamic Equilibrium in ZnS. 2000.
7. **Reet Koljak**. Novel Fatty Acid Dioxygenases from the Corals *Plexaura homomalla* and *Gersemia fruticosa*. 2001.
8. **Anne Paju**. Asymmetric oxidation of Prochiral and Racemic Ketones by Using Sharpless Catalyst. 2001.
9. **Marko Vendelin**. Cardiac Mechanoenergetics *in silico*. 2001.
10. **Pearu Peterson**. Multi-Soliton Interactions and the Inverse Problem of Wave Crest. 2001.
11. **Anne Menert**. Microcalorimetry of Anaerobic Digestion. 2001.
12. **Toomas Tiivel**. The Role of the Mitochondrial Outer Membrane in *in vivo* Regulation of Respiration in Normal Heart and Skeletal Muscle Cell. 2002.
13. **Olle Hints**. Ordovician Scolecodonts of Estonia and Neighbouring Areas: Taxonomy, Distribution, Palaeoecology, and Application. 2002.
14. **Jaak Nõlvak**. Chitinozoan Biostratigraphy in the Ordovician of Baltoscandia. 2002.
15. **Liivi Kluge**. On Algebraic Structure of Pre-Operad. 2002.
16. **Jaanus Lass**. Biosignal Interpretation: Study of Cardiac Arrhythmias and Electromagnetic Field Effects on Human Nervous System. 2002.
17. **Janek Peterson**. Synthesis, Structural Characterization and Modification of PAMAM Dendrimers. 2002.
18. **Merike Vaher**. Room Temperature Ionic Liquids as Background Electrolyte Additives in Capillary Electrophoresis. 2002.
19. **Valdek Mikli**. Electron Microscopy and Image Analysis Study of Powdered Hardmetal Materials and Optoelectronic Thin Films. 2003.
20. **Mart Viljus**. The Microstructure and Properties of Fine-Grained Cermets. 2003.
21. **Signe Kask**. Identification and Characterization of Dairy-Related *Lactobacillus*. 2003.
22. **Tiiu-Mai Laht**. Influence of Microstructure of the Curd on Enzymatic and Microbiological Processes in Swiss-Type Cheese. 2003.
23. **Anne Kuusksalu**. 2–5A Synthetase in the Marine Sponge *Geodia cydonium*. 2003.
24. **Sergei Bereznev**. Solar Cells Based on Polycrystalline Copper-Indium Chalcogenides and Conductive Polymers. 2003.

25. **Kadri Kriis**. Asymmetric Synthesis of C₂-Symmetric Bimorpholines and Their Application as Chiral Ligands in the Transfer Hydrogenation of Aromatic Ketones. 2004.
26. **Jekaterina Reut**. Polypyrrole Coatings on Conducting and Insulating Substrates. 2004.
27. **Sven Nõmm**. Realization and Identification of Discrete-Time Nonlinear Systems. 2004.
28. **Olga Kijatkina**. Deposition of Copper Indium Disulphide Films by Chemical Spray Pyrolysis. 2004.
29. **Gert Tamberg**. On Sampling Operators Defined by Rogosinski, Hann and Blackman Windows. 2004.
30. **Monika Übner**. Interaction of Humic Substances with Metal Cations. 2004.
31. **Kaarel Adamberg**. Growth Characteristics of Non-Starter Lactic Acid Bacteria from Cheese. 2004.
32. **Imre Vallikivi**. Lipase-Catalysed Reactions of Prostaglandins. 2004.
33. **Merike Peld**. Substituted Apatites as Sorbents for Heavy Metals. 2005.
34. **Vitali Syritski**. Study of Synthesis and Redox Switching of Polypyrrole and Poly(3,4-ethylenedioxythiophene) by Using *in-situ* Techniques. 2004.
35. **Lee Põllumaa**. Evaluation of Ecotoxicological Effects Related to Oil Shale Industry. 2004.
36. **Riina Aav**. Synthesis of 9,11-Secosterols Intermediates. 2005.
37. **Andres Braunbrück**. Wave Interaction in Weakly Inhomogeneous Materials. 2005.
38. **Robert Kitt**. Generalised Scale-Invariance in Financial Time Series. 2005.
39. **Juss Pavelson**. Mesoscale Physical Processes and the Related Impact on the Summer Nutrient Fields and Phytoplankton Blooms in the Western Gulf of Finland. 2005.
40. **Olari Ilison**. Solitons and Solitary Waves in Media with Higher Order Dispersive and Nonlinear Effects. 2005.
41. **Maksim Säkki**. Intermittency and Long-Range Structurization of Heart Rate. 2005.
42. **Enli Kiipli**. Modelling Seawater Chemistry of the East Baltic Basin in the Late Ordovician–Early Silurian. 2005.
43. **Igor Golovtsov**. Modification of Conductive Properties and Processability of Polyparaphenylene, Polypyrrole and polyaniline. 2005.
44. **Katrin Laos**. Interaction Between Furcellaran and the Globular Proteins (Bovine Serum Albumin β -Lactoglobulin). 2005.
45. **Arvo Mere**. Structural and Electrical Properties of Spray Deposited Copper Indium Disulphide Films for Solar Cells. 2006.
46. **Sille Ehala**. Development and Application of Various On- and Off-Line Analytical Methods for the Analysis of Bioactive Compounds. 2006.
47. **Maria Kulp**. Capillary Electrophoretic Monitoring of Biochemical Reaction Kinetics. 2006.
48. **Anu Aaspõllu**. Proteinases from *Vipera lebetina* Snake Venom Affecting Hemostasis. 2006.
49. **Lyudmila Chekulayeva**. Photosensitized Inactivation of Tumor Cells by Porphyrins and Chlorins. 2006.

50. **Merle Uudsemaa**. Quantum-Chemical Modeling of Solvated First Row Transition Metal Ions. 2006.
51. **Tagli Pitsi**. Nutrition Situation of Pre-School Children in Estonia from 1995 to 2004. 2006.
52. **Angela Ivask**. Luminescent Recombinant Sensor Bacteria for the Analysis of Bioavailable Heavy Metals. 2006.
53. **Tiina Lõugas**. Study on Physico-Chemical Properties and Some Bioactive Compounds of Sea Buckthorn (*Hippophae rhamnoides* L.). 2006.
54. **Kaja Kasemets**. Effect of Changing Environmental Conditions on the Fermentative Growth of *Saccharomyces cerevisiae* S288C: Auxo-accelerostat Study. 2006.
55. **Ildar Nisamedtinov**. Application of ^{13}C and Fluorescence Labeling in Metabolic Studies of *Saccharomyces* spp. 2006.
56. **Alar Leibak**. On Additive Generalisation of Voronoï's Theory of Perfect Forms over Algebraic Number Fields. 2006.
57. **Andri Jagomägi**. Photoluminescence of Chalcopyrite Tellurides. 2006.
58. **Tõnu Martma**. Application of Carbon Isotopes to the Study of the Ordovician and Silurian of the Baltic. 2006.
59. **Marit Kauk**. Chemical Composition of CuInSe_2 Monograin Powders for Solar Cell Application. 2006.
60. **Julia Kois**. Electrochemical Deposition of CuInSe_2 Thin Films for Photovoltaic Applications. 2006.
61. **Ilona Oja Açıık**. Sol-Gel Deposition of Titanium Dioxide Films. 2007.
62. **Tiia Anmann**. Integrated and Organized Cellular Bioenergetic Systems in Heart and Brain. 2007.
63. **Katrin Trummal**. Purification, Characterization and Specificity Studies of Metalloproteinases from *Vipera lebetina* Snake Venom. 2007.
64. **Gennadi Lessin**. Biochemical Definition of Coastal Zone Using Numerical Modeling and Measurement Data. 2007.
65. **Enno Pais**. Inverse problems to determine non-homogeneous degenerate memory kernels in heat flow. 2007.
66. **Maria Borissova**. Capillary Electrophoresis on Alkylimidazolium Salts. 2007.
67. **Karin Valmsen**. Prostaglandin Synthesis in the Coral *Plexaura homomalla*: Control of Prostaglandin Stereochemistry at Carbon 15 by Cyclooxygenases. 2007.
68. **Kristjan Piirimäe**. Long-Term Changes of Nutrient Fluxes in the Drainage Basin of the Gulf of Finland – Application of the PolFlow Model. 2007.
69. **Tatjana Dedova**. Chemical Spray Pyrolysis Deposition of Zinc Sulfide Thin Films and Zinc Oxide Nanostructured Layers. 2007.
70. **Katrin Tomson**. Production of Labelled Recombinant Proteins in Fed-Batch Systems in *Escherichia coli*. 2007.
71. **Cecilia Sarmiento**. Suppressors of RNA Silencing in Plants. 2008.
72. **Vilja Mardla**. Inhibition of Platelet Aggregation with Combination of Antiplatelet Agents. 2008.
73. **Maie Bachmann**. Effect of Modulated Microwave Radiation on Human Resting Electroencephalographic Signal. 2008.
74. **Dan Hüvonen**. Terahertz Spectroscopy of Low-Dimensional Spin Systems. 2008.

75. **Ly Villo**. Stereoselective Chemoenzymatic Synthesis of Deoxy Sugar Esters Involving *Candida antarctica* Lipase B. 2008.
76. **Johan Anton**. Technology of Integrated Photoelasticity for Residual Stress Measurement in Glass Articles of Axisymmetric Shape. 2008.
77. **Olga Volobujeva**. SEM Study of Selenization of Different Thin Metallic Films. 2008.
78. **Artur Jõgi**. Synthesis of 4'-Substituted 2,3'-dideoxynucleoside Analogues. 2008.
79. **Mario Kadastik**. Doubly Charged Higgs Boson Decays and Implications on Neutrino Physics. 2008.
80. **Fernando Pérez-Caballero**. Carbon Aerogels from 5-Methylresorcinol-Formaldehyde Gels. 2008.
81. **Sirje Vaask**. The Comparability, Reproducibility and Validity of Estonian Food Consumption Surveys. 2008.
82. **Anna Menaker**. Electrosynthesized Conducting Polymers, Polypyrrole and Poly(3,4-ethylenedioxythiophene), for Molecular Imprinting. 2009.
83. **Lauri Ilson**. Solitons and Solitary Waves in Hierarchical Korteweg-de Vries Type Systems. 2009.
84. **Kaia Ernits**. Study of In₂S₃ and ZnS Thin Films Deposited by Ultrasonic Spray Pyrolysis and Chemical Deposition. 2009.
85. **Veljo Sinivee**. Portable Spectrometer for Ionizing Radiation "Gammamapper". 2009.
86. **Jüri Virkepu**. On Lagrange Formalism for Lie Theory and Operadic Harmonic Oscillator in Low Dimensions. 2009.
87. **Marko Piirsoo**. Deciphering Molecular Basis of Schwann Cell Development. 2009.
88. **Kati Helmja**. Determination of Phenolic Compounds and Their Antioxidative Capability in Plant Extracts. 2010.
89. **Merike Sõmera**. Sobemoviruses: Genomic Organization, Potential for Recombination and Necessity of P1 in Systemic Infection. 2010.
90. **Kristjan Laes**. Preparation and Impedance Spectroscopy of Hybrid Structures Based on CuIn₃Se₅ Photoabsorber. 2010.
91. **Kristin Lippur**. Asymmetric Synthesis of 2,2'-Bimorpholine and its 5,5'-Substituted Derivatives. 2010.
92. **Merike Luman**. Dialysis Dose and Nutrition Assessment by an Optical Method. 2010.
93. **Mihhail Berezovski**. Numerical Simulation of Wave Propagation in Heterogeneous and Microstructured Materials. 2010.
94. **Tamara Aid-Pavlidis**. Structure and Regulation of BDNF Gene. 2010.
95. **Olga Bragina**. The Role of Sonic Hedgehog Pathway in Neuro- and Tumorigenesis. 2010.
96. **Merle Randrüüt**. Wave Propagation in Microstructured Solids: Solitary and Periodic Waves. 2010.
97. **Marju Laars**. Asymmetric Organocatalytic Michael and Aldol Reactions Mediated by Cyclic Amines. 2010.
98. **Maarja Grossberg**. Optical Properties of Multinary Semiconductor Compounds for Photovoltaic Applications. 2010.

99. **Alla Maloverjan**. Vertebrate Homologues of Drosophila Fused Kinase and Their Role in Sonic Hedgehog Signalling Pathway. 2010.
100. **Priit Pruunsild**. Neuronal Activity-Dependent Transcription Factors and Regulation of Human *BDNF* Gene. 2010.
101. **Tatjana Knjazeva**. New Approaches in Capillary Electrophoresis for Separation and Study of Proteins. 2011.
102. **Atanas Katerski**. Chemical Composition of Sprayed Copper Indium Disulfide Films for Nanostructured Solar Cells. 2011.
103. **Kristi Timmo**. Formation of Properties of CuInSe_2 and $\text{Cu}_2\text{ZnSn}(\text{S},\text{Se})_4$ Monograin Powders Synthesized in Molten KI. 2011.
104. **Kert Tamm**. Wave Propagation and Interaction in Mindlin-Type Microstructured Solids: Numerical Simulation. 2011.
105. **Adrian Popp**. Ordovician Proetid Trilobites in Baltoscandia and Germany. 2011.
106. **Ove Pärn**. Sea Ice Deformation Events in the Gulf of Finland and This Impact on Shipping. 2011.
107. **Germo Väli**. Numerical Experiments on Matter Transport in the Baltic Sea. 2011.
108. **Andrus Seiman**. Point-of-Care Analyser Based on Capillary Electrophoresis. 2011.
109. **Olga Katargina**. Tick-Borne Pathogens Circulating in Estonia (Tick-Borne Encephalitis Virus, *Anaplasma phagocytophilum*, *Babesia* Species): Their Prevalence and Genetic Characterization. 2011.
110. **Ingrid Sumeri**. The Study of Probiotic Bacteria in Human Gastrointestinal Tract Simulator. 2011.
111. **Kairit Zovo**. Functional Characterization of Cellular Copper Proteome. 2011.
112. **Natalja Makarytsheva**. Analysis of Organic Species in Sediments and Soil by High Performance Separation Methods. 2011.
113. **Monika Mortimer**. Evaluation of the Biological Effects of Engineered Nanoparticles on Unicellular Pro- and Eukaryotic Organisms. 2011.
114. **Kersti Tepp**. Molecular System Bioenergetics of Cardiac Cells: Quantitative Analysis of Structure-Function Relationship. 2011.
115. **Anna-Liisa Peikolainen**. Organic Aerogels Based on 5-Methylresorcinol. 2011.
116. **Leeli Amon**. Palaeoecological Reconstruction of Late-Glacial Vegetation Dynamics in Eastern Baltic Area: A View Based on Plant Macrofossil Analysis. 2011.
117. **Tanel Peets**. Dispersion Analysis of Wave Motion in Microstructured Solids. 2011.
118. **Liina Kaupmees**. Selenization of Molybdenum as Contact Material in Solar Cells. 2011.
119. **Allan Olsper**. Properties of VPg and Coat Protein of Sobemoviruses. 2011.
120. **Kadri Koppel**. Food Category Appraisal Using Sensory Methods. 2011.
121. **Jelena Gorbatšova**. Development of Methods for CE Analysis of Plant Phenolics and Vitamins. 2011.
122. **Karin Viipsi**. Impact of EDTA and Humic Substances on the Removal of Cd and Zn from Aqueous Solutions by Apatite. 2012.

123. **David Schryer**. Metabolic Flux Analysis of Compartmentalized Systems Using Dynamic Isotopologue Modeling. 2012.
124. **Ardo Illaste**. Analysis of Molecular Movements in Cardiac Myocytes. 2012.
125. **Indrek Reile**. 3-Alkylcyclopentane-1,2-Diones in Asymmetric Oxidation and Alkylation Reactions. 2012.
126. **Tatjana Tamberg**. Some Classes of Finite 2-Groups and Their Endomorphism Semigroups. 2012.
127. **Taavi Liblik**. Variability of Thermohaline Structure in the Gulf of Finland in Summer. 2012.
128. **Priidik Lagemaa**. Operational Forecasting in Estonian Marine Waters. 2012.
129. **Andrei Errapart**. Photoelastic Tomography in Linear and Non-linear Approximation. 2012.
130. **Külliki Krabbi**. Biochemical Diagnosis of Classical Galactosemia and Mucopolysaccharidoses in Estonia. 2012.
131. **Kristel Kaseleht**. Identification of Aroma Compounds in Food using SPME-GC/MS and GC-Olfactometry. 2012.
132. **Kristel Kodar**. Immunoglobulin G Glycosylation Profiling in Patients with Gastric Cancer. 2012.
133. **Kai Rosin**. Solar Radiation and Wind as Agents of the Formation of the Radiation Regime in Water Bodies. 2012.
134. **Ann Tiiman**. Interactions of Alzheimer's Amyloid-Beta Peptides with Zn(II) and Cu(II) Ions. 2012.
135. **Olga Gavrilova**. Application and Elaboration of Accounting Approaches for Sustainable Development. 2012.
136. **Olesja Bondarenko**. Development of Bacterial Biosensors and Human Stem Cell-Based *In Vitro* Assays for the Toxicological Profiling of Synthetic Nanoparticles. 2012.
137. **Katri Muska**. Study of Composition and Thermal Treatments of Quaternary Compounds for Monograin Layer Solar Cells. 2012.
138. **Ranno Nahku**. Validation of Critical Factors for the Quantitative Characterization of Bacterial Physiology in Accelerostat Cultures. 2012.
139. **Petri-Jaan Lahtvee**. Quantitative Omics-level Analysis of Growth Rate Dependent Energy Metabolism in *Lactococcus lactis*. 2012.
140. **Kerti Orumets**. Molecular Mechanisms Controlling Intracellular Glutathione Levels in Baker's Yeast *Saccharomyces cerevisiae* and its Random Mutagenized Glutathione Over-Accumulating Isolate. 2012.
141. **Loreida Timberg**. Spice-Cured Sprats Ripening, Sensory Parameters Development, and Quality Indicators. 2012.
142. **Anna Mihhalevski**. Rye Sourdough Fermentation and Bread Stability. 2012.
143. **Liisa Arike**. Quantitative Proteomics of *Escherichia coli*: From Relative to Absolute Scale. 2012.
144. **Kairi Otto**. Deposition of In₂S₃ Thin Films by Chemical Spray Pyrolysis. 2012.
145. **Mari Sepp**. Functions of the Basic Helix-Loop-Helix Transcription Factor TCF4 in Health and Disease. 2012.
146. **Anna Suhhova**. Detection of the Effect of Weak Stressors on Human Resting Electroencephalographic Signal. 2012.
147. **Aram Kazarjan**. Development and Production of Extruded Food and Feed Products Containing Probiotic Microorganisms. 2012.

148. **Rivo Uiboupin**. Application of Remote Sensing Methods for the Investigation of Spatio-Temporal Variability of Sea Surface Temperature and Chlorophyll Fields in the Gulf of Finland. 2013.
149. **Tiina Kriščiunaite**. A Study of Milk Coagulability. 2013.
150. **Tuuli Levandi**. Comparative Study of Cereal Varieties by Analytical Separation Methods and Chemometrics. 2013.
151. **Natalja Kabanova**. Development of a Microcalorimetric Method for the Study of Fermentation Processes. 2013.
152. **Himani Khanduri**. Magnetic Properties of Functional Oxides. 2013.
153. **Julia Smirnova**. Investigation of Properties and Reaction Mechanisms of Redox-Active Proteins by ESI MS. 2013.
154. **Mervi Sepp**. Estimation of Diffusion Restrictions in Cardiomyocytes Using Kinetic Measurements. 2013.
155. **Kersti Jääger**. Differentiation and Heterogeneity of Mesenchymal Stem Cells. 2013.
156. **Victor Alari**. Multi-Scale Wind Wave Modeling in the Baltic Sea. 2013.
157. **Taavi Päll**. Studies of CD44 Hyaluronan Binding Domain as Novel Angiogenesis Inhibitor. 2013.
158. **Allan Niidu**. Synthesis of Cyclopentane and Tetrahydrofuran Derivatives. 2013.
159. **Julia Geller**. Detection and Genetic Characterization of *Borrelia* Species Circulating in Tick Population in Estonia. 2013.
160. **Irina Stulova**. The Effects of Milk Composition and Treatment on the Growth of Lactic Acid Bacteria. 2013.
161. **Jana Holmar**. Optical Method for Uric Acid Removal Assessment During Dialysis. 2013.
162. **Kerti Ausmees**. Synthesis of Heterobicyclo[3.2.0]heptane Derivatives via Multicomponent Cascade Reaction. 2013.
163. **Minna Varikmaa**. Structural and Functional Studies of Mitochondrial Respiration Regulation in Muscle Cells. 2013.
164. **Indrek Koppel**. Transcriptional Mechanisms of BDNF Gene Regulation. 2014.
165. **Kristjan Pilt**. Optical Pulse Wave Signal Analysis for Determination of Early Arterial Ageing in Diabetic Patients. 2014.
166. **Andres Anier**. Estimation of the Complexity of the Electroencephalogram for Brain Monitoring in Intensive Care. 2014.
167. **Toivo Kallaste**. Pyroclastic Sanidine in the Lower Palaeozoic Bentonites – A Tool for Regional Geological Correlations. 2014.
168. **Erki Kärber**. Properties of ZnO-nanorod/In₂S₃/CuInS₂ Solar Cell and the Constituent Layers Deposited by Chemical Spray Method. 2014.
169. **Julia Lehner**. Formation of Cu₂ZnSnS₄ and Cu₂ZnSnSe₄ by Chalcogenisation of Electrochemically Deposited Precursor Layers. 2014.
170. **Peep Pitk**. Protein- and Lipid-rich Solid Slaughterhouse Waste Anaerobic Co-digestion: Resource Analysis and Process Optimization. 2014.
171. **Kaspar Valgepea**. Absolute Quantitative Multi-omics Characterization of Specific Growth Rate-dependent Metabolism of *Escherichia coli*. 2014.
172. **Artur Noole**. Asymmetric Organocatalytic Synthesis of 3,3'-Disubstituted Oxindoles. 2014.
173. **Robert Tsanev**. Identification and Structure-Functional Characterisation of the Gene Transcriptional Repressor Domain of Human Gli Proteins. 2014.

174. **Dmitri Kartofelev**. Nonlinear Sound Generation Mechanisms in Musical Acoustic. 2014.
175. **Sigrid Hade**. GIS Applications in the Studies of the Palaeozoic Graptolite Argillite and Landscape Change. 2014.
176. **Agne Velthut-Meikas**. Ovarian Follicle as the Environment of Oocyte Maturation: The Role of Granulosa Cells and Follicular Fluid at Pre-Ovulatory Development. 2014.
177. **Kristel Hälvin**. Determination of B-group Vitamins in Food Using an LC-MS Stable Isotope Dilution Assay. 2014.
178. **Mailis Päre**. Characterization of the Oligoadenylate Synthetase Subgroup from Phylum Porifera. 2014.
179. **Jekaterina Kazantseva**. Alternative Splicing of *TAF4*: A Dynamic Switch between Distinct Cell Functions. 2014.
180. **Jaanus Suurväli**. Regulator of G Protein Signalling 16 (RGS16): Functions in Immunity and Genomic Location in an Ancient MHC-Related Evolutionarily Conserved Synteny Group. 2014.
181. **Ene Viiard**. Diversity and Stability of Lactic Acid Bacteria During Rye Sourdough Propagation. 2014.
182. **Kristella Hansen**. Prostaglandin Synthesis in Marine Arthropods and Red Algae. 2014.
183. **Helike Lõhelaid**. Allene Oxide Synthase-lipoxygenase Pathway in Coral Stress Response. 2015.
184. **Normunds Stivrīnš**. Postglacial Environmental Conditions, Vegetation Succession and Human Impact in Latvia. 2015.
185. **Mary-Liis Kütt**. Identification and Characterization of Bioactive Peptides with Antimicrobial and Immunoregulating Properties Derived from Bovine Colostrum and Milk. 2015.
186. **Kazbulat Šogenov**. Petrophysical Models of the CO₂ Plume at Prospective Storage Sites in the Baltic Basin. 2015.
187. **Taavi Raadik**. Application of Modulation Spectroscopy Methods in Photovoltaic Materials Research. 2015.
188. **Reio Pöder**. Study of Oxygen Vacancy Dynamics in Sc-doped Ceria with NMR Techniques. 2015.
189. **Sven Siir**. Internal Geochemical Stratification of Bentonites (Altered Volcanic Ash Beds) and its Interpretation. 2015.
190. **Kaur Jaanson**. Novel Transgenic Models Based on Bacterial Artificial Chromosomes for Studying BDNF Gene Regulation. 2015.
191. **Niina Karro**. Analysis of ADP Compartmentation in Cardiomyocytes and Its Role in Protection Against Mitochondrial Permeability Transition Pore Opening. 2015.
192. **Piret Laht**. B-plexins Regulate the Maturation of Neurons Through Microtubule Dynamics. 2015.
193. **Sergei Žari**. Organocatalytic Asymmetric Addition to Unsaturated 1,4-Dicarbonyl Compounds. 2015.
194. **Natalja Buhhalko**. Processes Influencing the Spatio-temporal Dynamics of Nutrients and Phytoplankton in Summer in the Gulf of Finland, Baltic Sea. 2015.
195. **Natalia Maticiu**. Mechanism of Changes in the Properties of Chemically Deposited CdS Thin Films Induced by Thermal Annealing. 2015.

196. **Mario Öeren**. Computational Study of Cyclohexylhemicucurbiturils. 2015.
197. **Mari Kalda**. Mechanoenergetics of a Single Cardiomyocyte. 2015.
198. **Ieva Grudzinska**. Diatom Stratigraphy and Relative Sea Level Changes of the Eastern Baltic Sea over the Holocene. 2015.
199. **Anna Kazantseva**. Alternative Splicing in Health and Disease. 2015.
200. **Jana Kazarjan**. Investigation of Endogenous Antioxidants and Their Synthetic Analogues by Capillary Electrophoresis. 2016.
201. **Maria Safonova**. SnS Thin Films Deposition by Chemical Solution Method and Characterization. 2016.
202. **Jekaterina Mazina**. Detection of Psycho- and Bioactive Drugs in Different Sample Matrices by Fluorescence Spectroscopy and Capillary Electrophoresis. 2016.
203. **Karin Rosenstein**. Genes Regulated by Estrogen and Progesterone in Human Endometrium. 2016.
204. **Aleksei Tretjakov**. A Macromolecular Imprinting Approach to Design Synthetic Receptors for Label-Free Biosensing Applications. 2016.
205. **Mati Danilson**. Temperature Dependent Electrical Properties of Kesterite Monograin Layer Solar Cells. 2016.
206. **Kaspar Kevvai**. Applications of ¹⁵N-labeled Yeast Hydrolysates in Metabolic Studies of *Lactococcus lactis* and *Saccharomyces Cerevisiae*. 2016.
207. **Kadri Aller**. Development and Applications of Chemically Defined Media for Lactic Acid Bacteria. 2016.
208. **Gert Preegel**. Cyclopentane-1,2-dione and Cyclopent-2-en-1-one in Asymmetric Organocatalytic Reactions. 2016.
209. **Jekaterina Služenikina**. Applications of Marine Scatterometer Winds and Quality Aspects of their Assimilation into Numerical Weather Prediction Model HIRLAM. 2016.
210. **Erkki Kask**. Study of Kesterite Solar Cell Absorbers by Capacitance Spectroscopy Methods. 2016.
211. **Jürgen Arund**. Major Chromophores and Fluorophores in the Spent Dialysate as Cornerstones for Optical Monitoring of Kidney Replacement Therapy. 2016.
212. **Andrei Šamarin**. Hybrid PET/MR Imaging of Bone Metabolism and Morphology. 2016.
213. **Kairi Kasemets**. Inverse Problems for Parabolic Integro-Differential Equations with Instant and Integral Conditions. 2016.
214. **Edith Soosaar**. An Evolution of Freshwater Bulge in Laboratory Scale Experiments and Natural Conditions. 2016.
215. **Peeter Laas**. Spatiotemporal Niche-Partitioning of Bacterioplankton Community across Environmental Gradients in the Baltic Sea. 2016.
216. **Margus Voolma**. Geochemistry of Organic-Rich Metalliferous Oil Shale/Black Shale of Jordan and Estonia. 2016.
217. **Karin Ojamäe**. The Ecology and Photobiology of Mixotrophic Alveolates in the Baltic Sea. 2016.
218. **Anne Pink**. The Role of CD44 in the Control of Endothelial Cell Proliferation and Angiogenesis. 2016.
219. **Kristiina Kreek**. Metal-Doped Aerogels Based on Resorcinol Derivatives. 2016.
220. **Kaia Kukk**. Expression of Human Prostaglandin H Synthases in the Yeast *Pichia pastoris*. 2016.

221. **Martin Laasmaa**. Revealing Aspects of Cardiac Function from Fluorescence and Electrophysiological Recordings. 2016.
222. **Eeva-Gerda Kobrin**. Development of Point of Care Applications for Capillary Electrophoresis. 2016.
223. **Villu Kikas**. Physical Processes Controlling the Surface Layer Dynamics in the Stratified Gulf of Finland: An Application of Ferrybox Technology. 2016.
224. **Maris Skudra**. Features of Thermohaline Structure and Circulation in the Gulf of Riga. 2017.
225. **Sirje Sildever**. Influence of Physical-Chemical Factors on Community and Populations of the Baltic Sea Spring Bloom Microalgae. 2017.
226. **Nicolae Spalatu**. Development of CdTe Absorber Layer for Thin-Film Solar Cells. 2017.